

**BUKTI KORESPONDENSI**  
**ARTIKEL JURNAL INTERNASIONAL BEREPUTASI**

Judul artikel	:	Iron (II) impregnated double-shelled hollow mesoporous silica as acid-base bifunctional catalyst for the conversion of low-quality oil to methyl esters
Jurnal	:	Renewable Energy (Elsevier, Q1, impact factor: 9.0)
Penulis	:	Stefanus Kevin Suryajaya ( <i>first author</i> ) Yohanes Ricky Mulyono Shella Permatasari Santoso Maria Yuliana ( <i>corresponding author</i> ) Alfin Kurniawan Aning Ayucitra Yueting Sun Sandy Budi Hartono Felycia Edi Soetaredjo Suryadi Ismadji

No	Perihal	Tanggal
1	Bukti konfirmasi submit artikel dan artikel yang disubmit	18 Agustus 2020
2	Bukti konfirmasi review dan hasil review pertama	24 November 2020
3	Bukti konfirmasi submit revisi pertama, respon kepada reviewer, dan artikel yang diresubmit	3 Desember 2020
4	Bukti konfirmasi review dan hasil review kedua	20 Januari 2021
5	Bukti konfirmasi submit revisi kedua, respon kepada reviewer, dan artikel yang diresubmit	21 Januari 2021
6	Bukti konfirmasi artikel accepted	22 Januari 2021
7	Bukti konfirmasi artikel published online	31 Januari 2021



Maria Yuliana &lt;mariayuliana@ukwms.ac.id&gt;

## Submission Confirmation

1 message

**Renewable Energy** <eesserver@eesmail.elsevier.com>

Tue, Aug 18, 2020 at 10:22 AM

Reply-To: Renewable Energy &lt;rene@elsevier.com&gt;

To: mariayuliana@ukwms.ac.id, maria\_yuliana\_liauw@yahoo.com

Cc: sstefanuskevin@gmail.com, rickymulyono96@gmail.com, shella\_p5@yahoo.com, alfin\_kur@yahoo.com, aayucitra@yahoo.com, y.sun.9@bham.ac.uk, sandy@ukwms.ac.id, felyciae@yahoo.com, suryadiismadji@yahoo.com

\*\*\* Automated email sent by the system \*\*\*

Ms. Ref. No.:

Title: IRON (II) IMPREGNATED DOUBLE-SHELLED HOLLOW MESOPOROUS SILICA AS ACID-BASE BIFUNCTIONAL CATALYST FOR THE CONVERSION OF LOW-QUALITY OIL TO METHYL ESTERS

Article Type: Research Paper

Journal: Renewable Energy

Dear Dr. Maria Yuliana,

We have received your article "IRON (II) IMPREGNATED DOUBLE-SHELLED HOLLOW MESOPOROUS SILICA AS ACID-BASE BIFUNCTIONAL CATALYST FOR THE CONVERSION OF LOW-QUALITY OIL TO METHYL ESTERS" for consideration for publication in Renewable Energy.

Your manuscript will be given a reference number once an editor has been assigned.

To track the status of your paper, please do the following:

1. Go to this URL: <https://ees.elsevier.com/rene/>

2. Enter these login details:

Your username is: [mariayuliana@ukwms.ac.id](mailto:mariayuliana@ukwms.ac.id)

If you need to retrieve password details, please go to:

[http://ees.elsevier.com/rene/automail\\_query.asp](http://ees.elsevier.com/rene/automail_query.asp)

3. Click [Author Login]

This takes you to the Author Main Menu.

4. Click [Submissions Being Processed]

Our reviewers will endeavour to review your paper at the earliest opportunity although it may take several weeks to let you know the outcome. Thank you for your patience.

Thank you for your interest in Renewable Energy.

Kind regards,

Elsevier Editorial System  
Renewable Energy

\*\*\*\*\*

Please note that the editorial process varies considerably from journal to journal. To view a sample editorial process, please click here:

[http://help.elsevier.com/app/answers/detail/p/7923/a\\_id/160](http://help.elsevier.com/app/answers/detail/p/7923/a_id/160)

For further assistance, please visit our customer support site at <http://help.elsevier.com/app/answers/list/p/7923>. Here you can search for solutions on a range of topics, find answers to frequently asked questions and learn more about EES via interactive tutorials. You will also find our 24/7 support contact details should you need any further assistance from one of

4/7/23, 9:16 PM

Universitas Katolik Widya Mandala Surabaya Mail - Submission Confirmation

our customer support representatives.

Manuscript Number:

Title: IRON (II) IMPREGNATED DOUBLE-SHELLED HOLLOW MESOPOROUS SILICA AS ACID-BASE BIFUNCTIONAL CATALYST FOR THE CONVERSION OF LOW-QUALITY OIL TO METHYL ESTERS

Article Type: Research Paper

Keywords: bifunctional catalyst; biodiesel; renewable energy; hollow mesoporous silica; iron impregnation; amine functionalization

Corresponding Author: Dr. Maria Yuliana, Ph.D.

Corresponding Author's Institution: Widya Mandala Catholic University Surabaya

First Author: Stefanus K Suryajaya

Order of Authors: Stefanus K Suryajaya; Yohanes R Mulyono; Shella P Santoso; Maria Yuliana, Ph.D.; Alfin Kurniawan; Aning Ayucitra; Yueting Sun; Sandy B Hartono; Felycia E Soetaredjo; Suryadi Ismadji

Abstract: To promote the use of low-quality oils in producing biodiesel, a bifunctional acid-base catalyst Fe/DS-HMS-NH<sub>2</sub> is fabricated using the two-step condensation technique. The obtained Fe/DS-HMS-NH<sub>2</sub> is of a doubled shell structure in spherical shape with a uniform size of 156 nm. Its hollow core (with a diameter of 86 nm) and two spatial shells with different active sites enables the esterification and transesterification reactions to be accomplished in a one-pot synthesis. The influences of four independent reaction variables on the yield of fatty acid methyl esters YF was studied, including catalyst loading  $m_c$ , reaction time  $t$ , reaction temperature  $T$ , and the methanol to degummed palm oil mass ratio  $rm/o$ . The highest yield was obtained at 85.36% (w/w) when  $m_c = 6\%$  (w/w),  $t = 4.5$  h,  $T = 60$  °C, and  $rm/o = 6:1$ . The Fe/DS-HMS-NH<sub>2</sub> shows a good recyclability with  $YF > 80\%$  (w/w) up to three reaction cycles.

Suggested Reviewers: Liang Sun Lee  
t3100206@ncu.edu.tw

Chun Hui Zhou  
chunhui09clay@yahoo.com.cn

Jaka Sunarso  
jsunarso@swinburne.edu.my

# **IRON (II) IMPREGNATED DOUBLE-SHELLED HOLLOW MESOPOROUS SILICA AS ACID-BASE BIFUNCTIONAL CATALYST FOR THE CONVERSION OF LOW-QUALITY OIL TO METHYL ESTERS**

Stefanus Kevin Suryajaya<sup>1,a</sup>, Yohanes Ricky Mulyono<sup>1,a</sup>, Shella Permatasari Santoso<sup>1,2</sup>, Maria Yuliana<sup>1\*</sup>, Alfin Kurniawan<sup>3</sup>, Aning Ayucitra<sup>1</sup>, Yueting Sun<sup>4</sup>, Sandy Budi Hartono<sup>1</sup>, Felycia Edi Soetaredjo<sup>1,2</sup>, Suryadi Ismadji<sup>1,2</sup>

<sup>1</sup> Department of Chemical Engineering, Widya Mandala Catholic University Surabaya, Kalijudan 37, Surabaya 60114, Indonesia

<sup>2</sup> Department of Chemical Engineering, National Taiwan University of Science and Technology, 43, Keelung Rd., Sec. 4, Taipei 10607, Taiwan

<sup>3</sup> Department of Chemistry, National Sun Yat-Sen University, Kaohsiung 80424, Taiwan

<sup>4</sup> Department of Mechanical Engineering, University of Birmingham, Edgbaston, Birmingham B15 2TT, United Kingdom

<sup>a</sup> These authors contributed equally to this work

\*Corresponding authors: Tel. (62) 31 3891264; Fax. (62) 31 3891267; Email address: [mariayuliana@ukwms.ac.id](mailto:mariayuliana@ukwms.ac.id) (M. Yuliana)



Widya Mandala Catholic University Surabaya  
Engineering Faculty

**CHEMICAL ENGINEERING DEPARTMENT**

Jl. Kalijudan 37 Surabaya 60114; Phone: +62 313893933 Fax: +62 31 3891267

Website: <http://www.ukwms.ac.id>

---

August 18, 2020

**Professor Soteris Kalogirou**

Editor-in-Chief

*Renewable Energy*

Dear Professor Kalogirou,

On behalf of my co-author, I am writing to submit the manuscript for publication consideration in *Renewable Energy*. The details of the manuscript are as follows:

**Title of Manuscript: IRON (II) IMPREGNATED DOUBLE-SHELLED HOLLOW MESOPOROUS SILICA AS ACID-BASE BIFUNCTIONAL CATALYST FOR THE CONVERSION OF LOW-QUALITY OIL TO METHYL ESTERS**

**Authors:** Stefanus Kevin Suryajaya ([sstefanuskevin@gmail.com](mailto:sstefanuskevin@gmail.com)), Yohanes Ricky Mulyono ([rickymulyono96@gmail.com](mailto:rickymulyono96@gmail.com)), Shella Permatasari Santoso ([shella\\_p5@yahoo.com](mailto:shella_p5@yahoo.com)), Maria Yuliana, Alfin Kurniawan ([alfin\\_kur@yahoo.com](mailto:alfin_kur@yahoo.com)), Aning Ayucitra ([aayucitra@yahoo.com](mailto:aayucitra@yahoo.com)), Yueting Sun ([y.sun.9@bham.ac.uk](mailto:y.sun.9@bham.ac.uk)), Sandy Budi Hartono ([sandy@ukwms.ac.id](mailto:sandy@ukwms.ac.id)), Felycia Edi Soetaredjo ([felyciae@yahoo.com](mailto:felyciae@yahoo.com)), Suryadi Ismadji ([suryadiismadji@yahoo.com](mailto:suryadiismadji@yahoo.com))

**Corresponding author:**

Maria Yuliana; Department of Chemical Engineering; Widya Mandala Catholic University Surabaya; Kalijudan 37, Surabaya 60114, Indonesia

Tel: (62) 31 3891264; Fax. (62) 31 3891267;

E-mail: [mariayuliana@ukwms.ac.id](mailto:mariayuliana@ukwms.ac.id)

**Keywords:** *bifunctional catalyst; biodiesel; renewable energy; hollow mesoporous silica; iron impregnation; amine functionalization*

**Word counts:** 4749 words (excluding abstract, references, tables and figures)

**Rationale of the manuscript:**

This manuscript provides an innovative solution to the pressing energy challenges, specifically in Indonesia. We propose a technology to develop a novel bifunctional acid-base catalyst, iron (II) impregnated double-shelled hollow mesoporous silica (Fe/DS-HMS-NH<sub>2</sub>), to convert low-quality oil to biodiesel (FAME) in a one-pot synthesis. The catalytic activity, stability, reusability of



Widya Mandala Catholic University Surabaya

Engineering Faculty

**CHEMICAL ENGINEERING DEPARTMENT**

Jl. Kalijudan 37 Surabaya 60114; Phone: +62 313893933 Fax: +62 31 3891267

Website: <http://www.ukwms.ac.id>

---

Fe/DS-HMS-NH<sub>2</sub> are discussed in the manuscript. The catalytic route for the in-situ esterification/transesterification of low-quality oil using this bifunctional catalyst is also presented. We believe that our findings are consistent with the journal scope and able to give a significant contribution to the scientific advancement, particularly in the field of renewable energy.

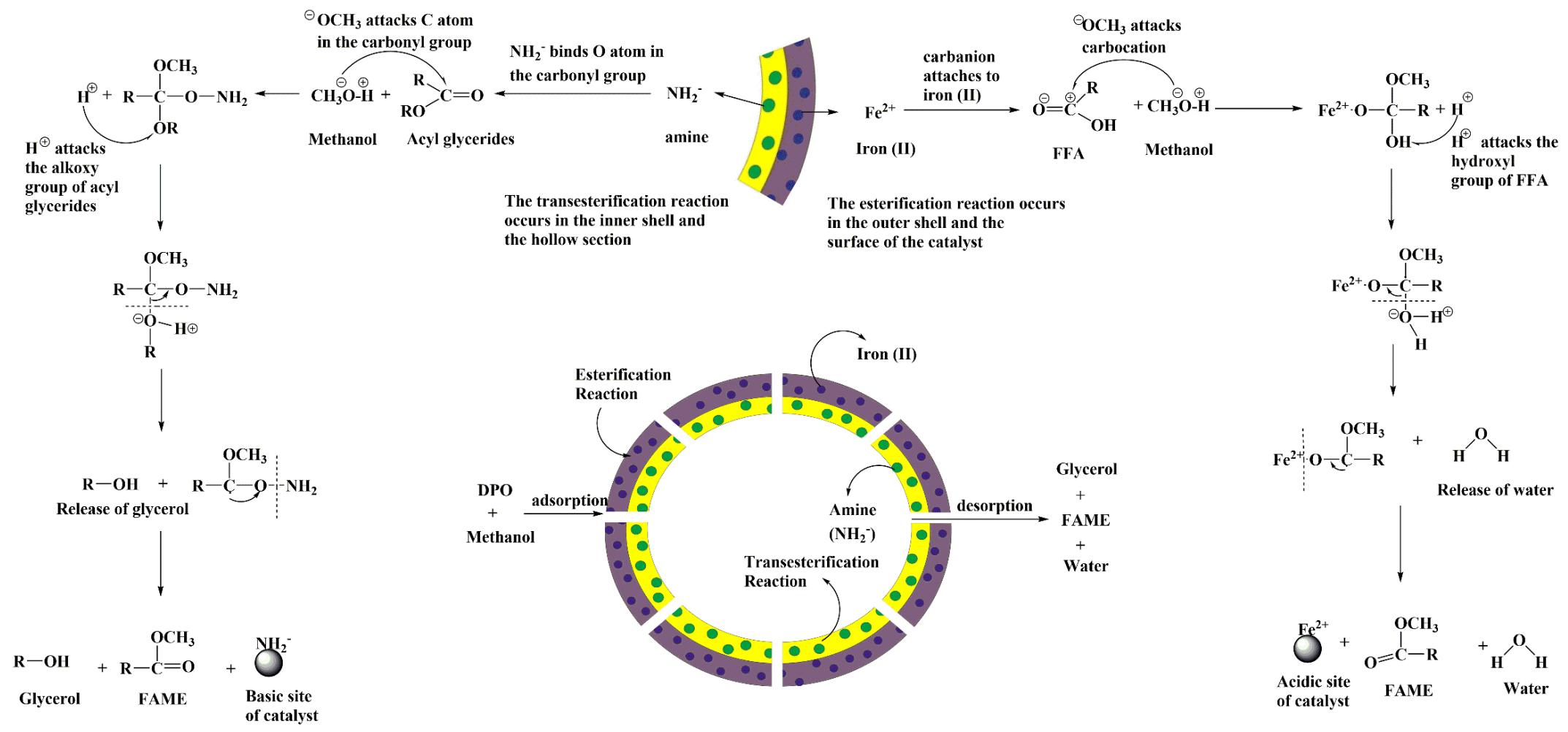
We ensure that the submitted manuscript is entirely original work of the authors. All authors have mutually agreed that this manuscript should be submitted to *Renewable Energy*. We also guarantee that the article has not received prior publication and is not under consideration for publication elsewhere. We know of no conflicts of interest associated with this publication and there has been no significant financial supports for this work that could have influenced its outcome. Furthermore, we have read, understood and adhered to the Ethical Guidelines, and we have strictly prepared the manuscript in accordance with the journal guidelines.

Thank you for your consideration. I am looking forward to hearing from your positive response.

Sincerely yours,

Maria Yuliana

# Graphical Abstract



## \*Highlights

- A novel acid-base bifunctional catalyst, Fe/DS-HMS-NH<sub>2</sub>, has been fabricated
- Fe/DS-HMS-NH<sub>2</sub> has been successfully employed to convert low-quality oil to FAME
- 85.36% of FAME yield was achieved from low-quality oil using Fe/DS-HMS-NH<sub>2</sub>
- The fuel properties of the final FAME product conform to ASTM D6751
- Fe/DS-HMS-NH<sub>2</sub> shows a good recyclability with FAME yield > 80% up to the third run

## 1 Abstract

2 To promote the use of low-quality oils in producing biodiesel, a bifunctional acid-base  
3 catalyst Fe/DS-HMS-NH<sub>2</sub> is fabricated using the two-step condensation technique. The obtained  
4 Fe/DS-HMS-NH<sub>2</sub> is of a doubled shell structure in spherical shape with a uniform size of 156 nm.  
5 Its hollow core (with a diameter of 86 nm) and two spatial shells with different active sites  
6 enables the esterification and transesterification reactions to be accomplished in a one-pot  
7 synthesis. The influences of four independent reaction variables on the yield of fatty acid methyl  
8 esters  $Y_F$  was studied, including catalyst loading  $m_c$ , reaction time  $t$ , reaction temperature  $T$ , and  
9 the methanol to degummed palm oil mass ratio  $r_{m/o}$ . The highest yield was obtained at 85.36%  
10 (w/w) when  $m_c = 6\%$  (w/w),  $t = 4.5$  h,  $T = 60$  °C, and  $r_{m/o} = 6:1$ . The Fe/DS-HMS-NH<sub>2</sub> shows a  
11 good recyclability with  $Y_F > 80\%$  (w/w) up to three reaction cycles.

12 *Keywords: bifunctional catalyst; biodiesel; renewable energy; hollow mesoporous silica; iron*  
13 *impregnation; amine functionalization*

14 **1. Introduction<sup>1</sup>**

15 The global fuel demand is growing rapidly as it undergoes an extensive  
16 urbanization. Our heavy reliance on fossil fuel brings the risk of unstable market price and  
17 reduced fuel availability. The gas emission from fossil fuel combustion also causes  
18 environmental concerns. Therefore, developing an alternative fuel that is biodegradable,  
19 sustainable and with a low carbon emission is the most significant energy and environmental  
20 challenge for us in the coming decades [1,2].

21 Since 2006, the Indonesian government has been committed to reducing carbon  
22 emissions by replacing fossil fuels with biodiesel [3]. It is also declared that the use of  
23 biodiesel in diesel blend will be increased from B20 to B30 starting from 2020 [4], with a  
24 strategy to boost the domestic use of palm oil and lower down energy imports. Usually,  
25 biodiesel is obtained through the conventional transesterification process of refined oil [5].  
26 The acyl glycerides in the oil react with the alcohol in the presence of a basic homogeneous  
27 catalyst to produce biodiesel as the main product and glycerine as a by-product [6,7], while

---

1

FFA	Free fatty acids
FAME	Fatty acid methyl esters
RPO	Refined palm oil
DPO	Degummed palm oil
CPO	Crude palm oil
SS-HMS-NH <sub>2</sub>	Single-shelled hollow mesoporous silica
DS-HMS-NH <sub>2</sub>	Double-shelled hollow mesoporous silica
Fe/DS-HMS-NH <sub>2</sub>	Iron (II) impregnated double-shelled hollow mesoporous silica

28 the free fatty acids (FFA) in the oil are saponified by the basic catalyst to form soap [8,9].  
29 The latter is unfavorable as it complicates the separation process and reduces biodiesel  
30 conversion. For this reason, currently the biodiesel feedstock is restricted to high-quality oils,  
31 with the requirement that FFA and water content should be lower than 0.1% (w/w).

32 Indonesia is one of the largest palm oil producers, with an annual production of  
33 approximately 40 million tons [10,11]. However, almost all of the manufacturers in the  
34 country have to use refined palm oil (RPO) as the raw material; the technologies of utilizing  
35 non-refined oil are to be developed [12]. This study aims to replace RPO with degummed  
36 palm oil (DPO) to simplify the procedure of biodiesel preparation. With similar content of  
37 FFA and moisture as the crude palm oil (CPO), DPO is classified as a low-quality oil, along  
38 with industrial fats, oils and greases (FOG), and other crude/waste lipids [13,14].

39 Some technical routes of converting low-quality oils into biodiesel have been  
40 studied, including the two steps acidic esterification followed by basic transesterification  
41 [15], noncatalytic transesterification using alcohol under subcritical [16] and supercritical  
42 conditions [17], enzymatic transesterification [18] and solid-catalyzed transesterification  
43 [19–24]. Berchmans and Hirata (2008) found that adding the acid esterification steps to  
44 remove FFA prior to alkaline transesterification improves the yield of biodiesel. However,  
45 this additional procedure prolongs the processing time, corrodes the equipment, and  
46 increases the production and maintenance costs [25]. Similar drawbacks also apply to the  
47 enzyme-catalyzed transesterification, which requires complicated processes for catalyst  
48 extraction with inefficient operating expenditures [26–28]. Although the noncatalytic  
49 transesterification has gained wide attention due to its sustainability and environmentally  
50 benign nature, it is still far from industrial applications due to its extreme processing  
51 conditions such as high temperature and pressure [29,30].

52           On the other hand, the use of heterogeneous catalysts that contain multiple types of  
53 active sites is promising for the preparation of biodiesel from low-quality oils and has been  
54 attracting a growing interest in recent years [31,32]. Compared with the homogenous  
55 catalyst, using the heterogeneous catalyst has the advantage of easier separation, tolerance to  
56 impurities (i.e., FFA, water and other minor compounds), and good reusability which means  
57 minimal waste and toxic water production [8,9,23,33–35] and environmentally friendly [36].  
58 Various solid catalysts and their modifications have been reported, such as zirconia [37],  
59 silica impregnated with zinc stearate (ZS/Si) [38], heterogeneous KF/ZnO catalyst [23],  
60 heterogeneous Zn/I<sub>2</sub> catalyst [22]. Despite their insensitivity to impurities, these catalysts  
61 solely act as the mono functional catalysts, depending on their acidity nature and have the  
62 following disadvantages during the conversion of low-quality oils to biodiesel: (1) the  
63 reaction carried out in the presence of an acidic heterogeneous catalyst is slow, and at the  
64 same time, requires large amount of alcohol [32], meanwhile (2) the basic heterogeneous  
65 catalysts usually result in a lower biodiesel yield and purity, since this type of catalyst leaves  
66 the FFA unreacted during the reaction.

67           In this paper, we prepared and characterized a new class of heterogeneous catalyst,  
68 the double-shelled hollow mesoporous silica impregnated with divalent iron metal (Fe/DS-  
69 HMS-NH<sub>2</sub>), to be used as an acid-base bifunctional catalyst in the production of biodiesel  
70 from DPO. This catalyst enables a simple process of converting DPO to biodiesel by  
71 combining the two processes of esterification and transesterification into a single-stage  
72 process. This is achieved by having double active surface layers that facilitate the two  
73 reactions to run simultaneously.

74           Mesoporous silica is selected here due to its easy fabrication and modification, as  
75 well as its high stability at different conditions [39,40]. The primary (inner) shell of the

76 Fe/DS-HMS-NH<sub>2</sub> was fabricated by reacting the ammonium solution, tetraethyl  
77 orthosilicate (TEOS) as the silica precursor and cetyltrimethylammonium bromide (CTAB)  
78 as the soft template; meanwhile, the formation of the outer shell was induced by the co-  
79 condensation reaction of the primary shell. Then a hollow mesoporous silica was obtained  
80 by high-temperature calcination to remove the surfactant and open the hollow cavity, which  
81 significantly increases the pore volume. The outer silica was then impregnated with the  
82 divalent iron (Fe (II)), which is selected as the impregnated metals due to its nature as a  
83 strong Lewis acid, and its ability to change the oxidation level and activate the substance  
84 during the process [41].

85 The synthesis, characterization and catalytic activity of the Fe/DS-HMS-NH<sub>2</sub> will  
86 be investigated in this paper. Its performance as an acid-base bifunctional catalyst for  
87 biodiesel preparation from DPO will be examined at various conditions, including catalyst  
88 loading  $m_c$  (% , w/w), reaction temperature  $T$  (°C), reaction time  $t$  (h), and the mass ratio of  
89 methanol to DPO  $r_{m/o}$ . The existence of two active shells is expected to increase the catalytic  
90 activity [42] and reduce processing time [43]. We will also show that the Fe/DS-HMS-NH<sub>2</sub>  
91 can be regenerated and reused, which is regarded as an important feature for heterogeneous  
92 catalysts [42,44,45] as it will reduce the cost for production and pollutant discharges  
93 [42,43,46]. The recyclability of the catalyst will be investigated at the operating condition  
94 giving the highest yield of fatty acid methyl esters (FAME)  $Y_F$ .

95

## 96 **2. Materials and methods**

### 97 **2.1 Materials**

98 CPO was collected from the local manufacturer in Indonesia. Prior to use, CPO was  
99 degummed using 1% (w/w) phosphoric acid (PA, 85% purity) at a temperature of 80 – 90°C

100 for 30 min to reduce the phosphorus content. Several important characteristics of the  
101 degummed CPO (i.e., DPO), namely free fatty acid content, acid value, saponification value,  
102 and moisture content were analyzed in accordance with the standard method of AOCS Ca  
103 5a-40, Cd 3d-63, Cd 3d-25, and Ca 2e-84, respectively.

104 3-aminopropyl-triethoxysilane (APTES) was purchased from Fisher Scientific  
105 (Pittsburgh, USA), while other chemicals required for the fabrication of Fe/DS-HMS,  
106 namely iron (II) sulfate heptahydrate ( $\text{FeSO}_4 \cdot 7\text{H}_2\text{O}$ , 99.99% purity), tetraethylorthosilicate  
107 (TEOS), cetyltrimethylammonium bromide (CTAB), ethanol (98% purity), methanol (99.9%  
108 purity), hydrochloric acid (HCl, 37% purity), ammonium hydroxide solution ( $\text{NH}_4\text{OH}$ , 25%  
109 purity), and n-hexane (95% purity) were obtained from Merck (Merck, Germany). The  
110 FAMES standard (47885 U) containing 37 components FAME mix was procured from  
111 Supelco (Bellefonte, PA, USA). Ultra-high purity nitrogen gas (> 99.0% purity) was  
112 purchased from Aneka Gas Industry Pty. Ltd., Indonesia. All chemicals used in this study  
113 were of analytical grade and required no further purification.

114

## 115 **2.2 Preparation of DS-HMS-NH<sub>2</sub>**

116 In a typical synthesis, 0.14 g of CTAB, 20 ml of ethanol, 50 ml of deionized water  
117 and 1 ml of  $\text{NH}_4\text{OH}$  solution were simultaneously introduced into a glass beaker and mixed  
118 for 15 minutes at room temperature. Then 1 ml of TEOS was slowly added into the above  
119 solution and kept stirring for 24 hours. The precipitates were collected through  
120 centrifugation at 4500 rpm for 30 min, triplicate ethanol washing, and drying at 120 °C  
121 overnight. After the calcination at 550°C for 6 h, the single shelled hollow mesoporous silica  
122 (SS-HMS-NH<sub>2</sub>) was obtained.

123           The outer shell of the particle was fabricated using a multilevel scheme based on SS-  
124 HMS-NH<sub>2</sub>. In a typical synthesis, 0.5 g CTAB, 18 ml deionized water, and 50 ml of ethanol  
125 were introduced into a beaker glass. Meanwhile, 0.063 g of SS-HMS-NH<sub>2</sub> was added into a  
126 mixture of 4 ml deionized water and 8.5 ml of 25% (w/w) NH<sub>4</sub>OH solution. The above two  
127 solutions were then combined and stirred for 15 min at 250 rpm, after which 100 μl TEOS  
128 and 21 μl APTES were slowly added into it and the mixture was kept stirring for 24 h to  
129 allow the condensation reaction of silica. Finally, the solid product was collected by  
130 centrifugation at 4500 rpm for 15 min, which was then repeatedly washed with 60 ml of  
131 ethanol and 4 ml of HCl, and oven-dried at 120°C. The dried product was calcined at 550 °C  
132 for 6 h to obtain double-shelled hollow mesoporous silica (DS-HMS-NH<sub>2</sub>).

133

### 134 **2.3 Iron (II) impregnation onto DS-HMS-NH<sub>2</sub> surface**

135           The impregnation of divalent iron onto the DS-HMS-NH<sub>2</sub> surface was achieved as  
136 follows to fabricate Fe/DS-HMS-NH<sub>2</sub> catalysts. In a typical synthesis, 0.1 g DS-HMS-NH<sub>2</sub>  
137 was mixed with 50 ml of deionized water under sonication for 30 minutes at room  
138 temperature. Meanwhile, two separate solutions were prepared: (1) 5 mg of FeSO<sub>4</sub>·7H<sub>2</sub>O  
139 was dissolved in 50 ml of deionized water, and (2) 0.2 g of CTAB was dissolved in 10 ml  
140 ethanol. Solution (1) and (2) were then added into the DS-HMS-NH<sub>2</sub> solution and stirred for  
141 12 hours at ambient conditions. The Fe/DS-HMS-NH<sub>2</sub> precipitates were separated by a  
142 centrifugation at 4500 rpm for 15 min, and then dried at 120 °C for 12 h and calcined at 550 °C  
143 for 5 hours to obtain the Fe/DS-HMS-NH<sub>2</sub> powder.

144

### 145 **2.4. Catalytic activity of Fe/DS-HMS-NH<sub>2</sub> at various reaction conditions**

146 The *in-situ* esterification/transesterification reactions from DPO to FAME were  
147 carried out in a glass flask equipped with a reflux condenser and external heater under  
148 constant magnetic stirring (250 rpm) at various conditions. Specifically, the influence of four  
149 reaction parameters were investigated due to their relevance to industrial applications:  
150 catalyst loading  $m_c$  (% , w/w), reaction temperature  $T$  (°C), reaction time  $t$  (h), and the mass  
151 ratio of methanol to DPO  $r_{m/o}$ . To determine the amount of Fe/DS-HMS-NH<sub>2</sub> catalyst that  
152 produces the maximum FAME yield  $Y_F$ , a few reactions were carried out with different  
153 amounts of Fe/DS-HMS-NH<sub>2</sub> ( $m_c = 2\%$ ,  $4\%$ ,  $6\%$ ,  $8\%$ , w/w) at the following condition:  $T =$   
154  $60$  °C,  $t = 4.5$  h and  $r_{m/o} = 10:1$ . Once the optimum catalyst loading is obtained, the catalytic  
155 activity of Fe/DS-HMS-NH<sub>2</sub> was investigated within an experimental matrix defined by  $T =$   
156  $40$  °C,  $50$  °C,  $60$  °C,  $t = 0.5$  h,  $2.5$  h,  $4.5$  h, and  $r_{m/o} = 2:1$ ,  $6:1$ ,  $10:1$ . The experimental runs  
157 were designed in a random order using face centered-central composite design (CCF-CCD)  
158 as listed in Table 1. All the experimental runs were conducted with the same procedure.

159 **Table 1**

160 After the reaction completed, Fe/DS-HMS-NH<sub>2</sub> catalyst was recovered by  
161 centrifugation at 4500 rpm for 15 min, and calcination at 550 °C for 5 h. The liquid product  
162 was subjected to a two-stage liquid-liquid extraction using methanol and n-hexane  
163 sequentially for purification. Then the FAME-rich phase was separated from the by-products  
164 (i.e., glycerol, excess methanol, soap, and the other unwanted materials) and evaporated  
165 under vacuum to obtain the final FAME product. As an evaluation of the catalytic activity  
166 of Fe/DS-HMS-NH<sub>2</sub>, the yield of FAME was calculated by the following equation:

$$Y_F (\%, \text{ w/w}) = \frac{m_F p_F}{m_S} \times 100 \quad (1)$$

167           Where  $m_F$  is the mass of the final FAME product (g),  $p_F$  is the FAME purity (% w/w)  
168           obtained from equation (2) shown in the next section, and  $m_S$  is the total mass of the DPO  
169           (g).

170

## 171 **2.5 Characterization of Fe/DS-HMS-NH<sub>2</sub> catalyst and FAME**

172           The characterization of Fe/DS-HMS-NH<sub>2</sub> was conducted using field-emission  
173           scanning electron microscopy with energy dispersive X-Ray spectroscopy (FESEM/EDX),  
174           transmission electron microscopy (TEM), nitrogen sorption, and thermogravimetric analysis  
175           (TGA). The FESEM/EDX images were taken on a JEOL JSM-6500 F (Jeol Ltd., Japan)  
176           running at 15 kV with a working distance of 12.4 mm, while TEM was carried out on JEOL  
177           JEM-2100 with an accelerating voltage of 200 kV. Nitrogen sorption analysis was  
178           conducted at 77 K on a Micrometrics ASAP 2010 Sorption Analyzer. The sample was  
179           degassed at 423 K prior to analysis. To determine the thermal stability and volatile  
180           component fraction of the Fe/DS-HMS-NH<sub>2</sub> catalyst, a TGA analysis was performed using  
181           TG/DTA Diamond instrument (Perkin-Elmer, Japan).

182           The purity of FAME ( $p_F$ ) in the final product was analyzed using a gas  
183           chromatograph (Shimadzu GC-2014) equipped with a split/splitless injector and a flame  
184           ionization detector (FID). The stationary phase used for separation was the narrow bore non-  
185           polar DB-WAX column (30 m × 0.25 mm ID × 0.25 μm film thickness, Agilent Technology,  
186           CA), and the temperature profile for the analysis was in accordance with the study  
187           conducted by Harijaya et al. (2019) [47]. Methyl heptadecanoate (MH) was used as an  
188           internal standard, while an external FAME reference (47885 U, containing 37 components  
189           FAME standard mix) was used to obtain the FAME compositional profile.  $p_F$  is calculated  
190           by the following equation:

$$p_F (\%, w/w) = \left( \frac{\sum A_F - A_{MH}}{A_{MH}} \right) \left( \frac{V_{MH} C_{MH}}{m_F} \right) \times 100 \quad (2)$$

191 Where  $\sum A_F$  is the total peak area of FAME,  $A_{MH}$  is the corresponding area of methyl  
192 heptadecanoate (MH) peak,  $V_{MH}$  is the volume of MH solution (ml),  $C_{MH}$  is the actual  
193 concentration of MH solution (g/ml), and  $m_F$  is the actual mass of the final FAME product  
194 (g).

## 195 **2.6 Recyclability of Fe/DS-HMS-NH<sub>2</sub>**

196 Fe/DS-HMS-NH<sub>2</sub> was repeatedly used for the transesterification process at the  
197 operating condition where the maximum yield of FAME was obtained. The recyclability of  
198 Fe/DS-HMS-NH<sub>2</sub> was determined by the number of repetitions until when the yield became  
199 lower than 80% (w/w). The purity and yield of FAME were analyzed according to the  
200 procedures in section 2.4-2.5. All experiments were carried out in triplicates to verify the  
201 results.

202

## 203 **3. Result and Discussions**

### 204 **3.1 The mechanism scheme of Fe/DS-HMS-NH<sub>2</sub> fabrication**

205 The Fe/DS-HMS-NH<sub>2</sub> was synthesized by a two-step co-condensation technique.  
206 The mechanism scheme in Figure 1 illustrates the fabrication route: (1) firstly, TEOS and  
207 CTAB undergo a co-condensation reaction along with the ammonium solution; (2) then  
208 CTAB, the soft template of the core, is removed by calcination, and the SS-HMS-NH<sub>2</sub> is  
209 thus formed; (3) TEOS, APTES, and CTAB undergo another co-condensation reaction on  
210 the outer surface of the SS-HMS-NH<sub>2</sub> spheres; (4) DS-HMS-NH<sub>2</sub> nanosphere is obtained by  
211 removing CTAB and APTES in calcination; (5) the divalent iron (Fe (II)) was incorporated

212 onto the surface of DS-HMS-NH<sub>2</sub> by a traditional wet impregnation technique, and the  
213 Fe/DS-HMS-NH<sub>2</sub> nanosphere is obtained.

### 214 **Figure 1**

215

### 216 **3.2 Characterization of Fe/DS-HMS-NH<sub>2</sub> catalysts**

217 Figure 2a, c–d present the SEM and TEM images of the Fe/DS-HMS-NH<sub>2</sub>  
218 catalyst synthesized by the co-condensation technique. The catalyst is spherical with a  
219 uniform size at *ca.* 156 nm (Figure 2a). Notably, Fe/DS-HMS-NH<sub>2</sub> is composed of two shell  
220 layers, indicated by the darker color of the inner shell in Figure 2c-d. Its hollow-core  
221 structure is clearly presented with the diameter of 86 nm (Figure 2d). The shell thicknesses  
222 of the inner and outer layer of Fe/DS-HMS-NH<sub>2</sub>, are 22 nm and 13 nm, respectively. The  
223 impregnation of Fe (II) on the surface of the silica layer was successful, evidenced from the  
224 EDX result showing a percentage of 2.87% (Figure 2b). Based on the fabrication procedure,  
225 it was reasonable to consider that the Fe (II) sites and basic amino sites were spatially  
226 isolated and located in different shells.

227 The textural properties of Fe/DS-HMS-NH<sub>2</sub> analyzed by the nitrogen sorption are  
228 presented in Table 2 and Figure 2e. The nitrogen adsorption and desorption isotherm of the  
229 catalyst exhibits a typical type-IV isotherm, indicating the presence of a mesoporous  
230 structure with worm-like capillary pores molded by the CTAB micelles. The pore size of the  
231 mesoporous structure is found to be 2.43 nm (Figure 2e (inset)). A steep increase of the  
232 nitrogen adsorption amount at  $p/p^0$  close to unity also suggests that there are macropores  
233 structure within the particle, corresponding to the hollow core. Similar adsorption and  
234 desorption profile also pointed out that the pores are highly accessible. The specific surface

235 area  $S_{\text{BET}}$  obtained in this study was 782.84 m<sup>2</sup>/g, lower than the value 1100 – 1350 m<sup>2</sup>/g for  
236 a similar double shelled hollow mesoporous silica [42]. Such a discrepancy was likely due  
237 to the reason that it was strongly influenced by the shell thickness. Zhou et al. (2014)  
238 reported that when the thickness of hollow mesoporous silica nanoparticles (HMSN)  
239 increases from 46 nm to 82 nm, the surface area of HMSN particles was declined from 986  
240 m<sup>2</sup>/g to 614 m<sup>2</sup>/g [48]. Zhou et al. (2014) and Cao et al. (2011) also observed that an  
241 increase in the particle mass due to the addition of TEOS and CTAB in the synthesis of the  
242 second shell lowers the surface area, since the amount of TEOS during the fabrication is  
243 directly proportional to the thickness of the shell [48,49]. Meanwhile, the pore volume of  
244 Fe/DS-HMS-NH<sub>2</sub> (0.64 cm<sup>3</sup>/g) was found to be slightly higher than that reported by You et  
245 al. (2018) (0.61 cm<sup>3</sup>/g) [42]. Based on its textural analysis, Fe/DS-HMS-NH<sub>2</sub> possesses  
246 comparable specific surface area and pore volume with those of existing heterogeneous  
247 catalysts which usually range from 200 – 1300 cm<sup>2</sup>/g and 0.18 – 1.68 cm<sup>3</sup>/g respectively  
248 [42,50–52].

## 249 **Table 2**

250 To demonstrate the feasibility of Fe/DS-HMS-NH<sub>2</sub> for the reactions at an elevated  
251 temperature, its thermal stability was investigated. The TGA profile in Figure 2f shows a 20%  
252 decrease in weight up to the temperature of 100°C, attributed to the removal of free moisture  
253 content. Further heating up to 800 °C does not significantly decrease the mass of Fe/DS-  
254 HMS-NH<sub>2</sub>, suggesting that the catalyst is stable at high temperatures [53]. Therefore, our  
255 Fe/DS-HMS-NH<sub>2</sub> can be considered as a promising heterogeneous catalyst for the *in-situ*  
256 esterification/transesterification reaction.

257 **Figure 2**

258

259 **3.3 The catalytic activity of Fe/DS-HMS-NH<sub>2</sub> in the *in-situ* esterification/transesterification**  
260 **of DPO**

261 The characteristics of DPO as the raw material for biodiesel preparation are  
262 presented in Table 3. As homogenous catalysts are sensitive to impurities, the conversion of  
263 DPO to FAME for biodiesel production usually requires two reaction steps, namely acid-  
264 catalyzed esterification to lower the FFA content by converting them into FAME, and basic  
265 catalyzed transesterification to convert the acyl glycerides into FAME. However,  
266 heterogeneous catalysts can have good tolerance towards the FFA and water content in the  
267 lipid materials [31]; for Fe/DS-HMS-NH<sub>2</sub>, its two spatial shells with different active sites  
268 can facilitate the above two reactions in a one-pot process, and therefore efficient  
269 conversion from DPO to FAME is achieved in a single step.

270 **Table 3**

271 Figure 3 presents the FAME yield obtained at various Fe/DS-HMS-NH<sub>2</sub> loadings  
272 at the condition of  $T = 60\text{ }^{\circ}\text{C}$ ,  $t = 4.5\text{ h}$  and  $r_{m/o} = 10:1$ . The results indicate that the yield of  
273 FAME is proportional to the number of active sites offered by the Fe/DS-HMS-NH<sub>2</sub> [54,55];  
274 therefore  $Y_F$  increases with  $m_c$  when the latter is within 6% (w/w). This agrees well with  
275 previous work on biodiesel production using different catalysts [45,54,55]. A maximum  
276 yield 85.24% (w/w) is obtained when the catalyst loading  $m_c = 6\%$  (w/w). Further increase  
277 of the Fe/DS-HMS-NH<sub>2</sub> results in a reduced yield of FAME, which is probably due to the  
278 aggregation and inconsistent dispersity of the catalyst in the reaction system of an enhanced  
279 viscosity [56–60].

280 **Figure 3**

281 At a constant catalyst loading  $m_c = 6\%$  (w/w), Figure 4 and Table 1 present the  
282 FAME yield  $Y_F$  at various reaction time  $t$ , temperature  $T$ , and mass ratio of methanol to DPO  
283  $r_{m/o}$ . The maximum  $Y_F = 85.36\%$  (w/w) (with a purity of 97.89% (w/w)) is obtained at the  
284 condition of  $T = 60\text{ }^\circ\text{C}$ ,  $t = 4.5\text{ h}$ ,  $r_{m/o} = 6:1$ . The reaction time  $t$  was the most significant  
285 factor, followed by  $r_{m/o}$  and  $T$ , which is supported by the Pareto chart of the standardized  
286 effect in Figure 5 showing that  $t$ ,  $r_{m/o}$ , and the two-way interaction between  $t$  and  $T$  are the  
287 three significant parameters in the reaction system.

288 **Figure 4**

289 **Figure 5**

290 The effect of reaction temperature on the production of biodiesel using Fe/DS-  
291 HMS-NH<sub>2</sub> is shown in Figure 4a–b. An increased reaction temperature contributes to a  
292 higher yield, with the maximum achieved at 60°C, which is related to the fact that both  
293 esterification and transesterification reaction are endothermic and reversible [61,62]. At a  
294 higher reaction temperature, the kinetic energy and mobility of reactant molecules increase,  
295 promoting the collisions between the molecules and Fe/DS-HMS-NH<sub>2</sub> particles which then  
296 increases the reaction rate constant and shift the reaction towards the product [61,63–65].  
297 Moreover, the mass transfer of the reactant molecules through the boundary layer of Fe/DS-  
298 HMS-NH<sub>2</sub> is also accelerated at an elevated temperature, resulting in the faster diffusion of  
299 the reactants into the pore of catalyst; hence, improving the FAME yield.

300 Specifically, Figures 4a and c show a significant increase of the FAME yield by  
301 extending the duration of the biodiesel synthesis from 0.5 h to 4.5 h, at a constant  
302 temperature or mass ratio of methanol to DPO. Longer reaction time provides sufficient  
303 time for the reactants to reach the active sites of Fe/DS-HMS-NH<sub>2</sub> through adsorption and

304 diffusion, and convert DPO into FAME [66]. Meanwhile, prolonged duration of reaction  
305 also gives the catalyst more time to adsorb the reactant and desorb the reaction product [52].  
306 Wei et al. (2009) also mentioned that adsorption and desorption of reactants from the  
307 catalyst is the rate-determining step in the overall reaction [67]. Therefore, allowing longer  
308 contact between the reactant molecules and the catalyst ensures high conversions of FFA  
309 and acyl glycerides to FAME.

310 Stochiometrically, three moles of methanol are required to react with one mole of  
311 triglycerides in the transesterification reaction, while one mole of methanol is needed to  
312 react with one mole of free fatty acids in the esterification reaction [68,69]. Both reactions  
313 are known to be reversible; thus, the amount of methanol in the two reactions is usually  
314 provided in excess to shift the reaction equilibrium to the product side. As seen from Figure  
315 4b–c, having excess methanol from  $r_{m/o} = 2:1$  to  $r_{m/o} = 6:1$  contributes to a higher FAME  
316 yield, while further addition up to  $r_{m/o} = 10:1$  has no improvement. While most studies agree  
317 that excess methanol is desirable to allow more frequent interactions between the lipid and  
318 methanol triggering the formation of FAME, Pangestu et al. (2019) found that excess  
319 methanol may also accelerate the production of glycerol despite the higher yield of FAME  
320 [52]. As the esterification and transesterification are both reversible, a higher concentration  
321 of glycerol in the reaction system may induce a reverse reaction to the reactant side, creating  
322 an equilibrium between the products and reactants [52]. Hayyan et al. (2011) also reported  
323 that an excessive amount of methanol causes higher solubility of glycerol in the FAME  
324 phase that could lead to a complicated separation between biodiesel and glycerol [70].  
325 Moreover, from the techno-economic viewpoint, the higher mass ratio of methanol to DPO  
326 also increases the material and processing cost [47,70]. Therefore, it can be concluded that  
327 the optimum level is  $r_{m/o} = 6:1$ .

328 The fuel properties of the final FAME product are presented in Table 4. The  
329 measurement results indicate that the product resulted in this study has a comparable  
330 combustion and flow properties with those of the commercial biodiesel. The calorific value  
331 (45.143 MJ/kg) is also within the range required in the common petrodiesel (42-46 MJ/kg).

332 **Table 4**

333

### 334 **3.4 Recyclability of Fe/DS-HMS-NH<sub>2</sub>**

335 An important feature of using heterogeneous catalysts for biodiesel preparation is  
336 its recyclability. In order to determine the recyclability of Fe/DS-HMS-NH<sub>2</sub>, several  
337 reaction cycles were conducted in series using the operating condition of  $m_c = 6\%$  (w/w),  $T$   
338  $= 60\text{ }^\circ\text{C}$ ,  $t = 4.5\text{ h}$ ,  $r_{m/o} = 6:1$ . Fe/DS-HMS-NH<sub>2</sub> was recovered following the method  
339 described in section 2.4, while fresh methanol and DPO were used in every cycle. The  
340 catalytic ability of the recycled Fe/DS-HMS-NH<sub>2</sub> for *in-situ* esterification/transesterification  
341 process is presented in Figure 6. The result indicates that recycled Fe/DS-HMS-NH<sub>2</sub> can  
342 maintain a high yield of FAME above 80% (w/w) until the third cycle, close to the yield of  
343 fresh catalyst 85.36% (w/w). The purity of FAME for the first three cycles are 97.89%,  
344 97.66% and 98.01% (w/w) respectively, higher than the commercial purity (96.5%, w/w).  
345 These results indicate that the catalytic activity of Fe/DS-HMS-NH<sub>2</sub> is maintained at a high  
346 level after regeneration. A significant drop in catalytic ability is observed from the forth  
347 cycle in Figure 6; similar performance has been reported for some other heterogeneous  
348 catalysts where three cycles seem to be an average number in term of their recyclability  
349 [71,72]. The catalytic deactivation of Fe/DS-HMS-NH<sub>2</sub> is generally due to the pore  
350 blockage caused by the contact between active sites on the catalyst surface and the  
351 deactivation-induced components, namely free glycerol, acyl glycerides, and biodiesel.

352 Moreover, the high content of FFA in DPO also plays an important role in the deactivation  
353 of Fe/DS-HMS-NH<sub>2</sub> catalyst because FFA tends to neutralize the basic sites in the inner  
354 shell of Fe/DS-HMS-NH<sub>2</sub> [73], resulting in the generation of amine-carboxylate that induces  
355 the formation of emulsion.

### 356 **Figure 6**

### 357

### 358 **3.5 The reaction mechanism of the *in-situ* esterification/transesterification of DPO using**

### 359 **Fe/DS-HMS-NH<sub>2</sub>**

360 In the preparation of biodiesel from DPO, Fe/DS-HMS-NH<sub>2</sub> acts as both acid and  
361 base catalysts to facilitate the esterification of FFA and the transesterification of acyl  
362 glycerides. The main steps for the reaction mechanism catalyzed by Fe/DS-HMS-NH<sub>2</sub> are  
363 the nucleophilic attack [74–76] and electron delocalisation [74] as depicted in Figure 7. The  
364 detailed description is as follows:

365 **Step 1:** Acyl glycerides, FFA and methanol enter the surface of catalyst through the  
366 adsorption process to reach the outer shell impregnated by the divalent iron. In this step,  
367 FFA undergoes the electron delocalization to form a carbocation and a carbanion, where the  
368 latter binds to the iron embedded on the catalyst.

369 **Step 2:** The reaction continues as the methoxide anion of methanol attacks the carbocation,  
370 whereas the hydronium cation attaches to the hydroxyl group of FFA to form water.

371 **Step 3:** Through the electron delocalization of the carbon atom, the water is released from  
372 the complex with FAME and the iron-embedded catalyst, followed by the release of FAME  
373 from the catalyst.

374 **Step 4:** The reaction continues when the acyl glycerides and methanol diffuse further to the  
375 amine-functionalized inner shell. The oxygen atom in the carbonyl group of acyl glycerides  
376 readily binds to the amine active sites.

377 **Step 5:** Subsequently, the methoxide anion of the methanol attacks the carbon atom in the  
378 carbonyl group of acyl glycerides, while the protonated  $H^+$  binds to the alkoxy group (RO-)  
379 of the acyl glycerides to form a complex of amine-functionalized catalyst with FAME and  
380 glycerol.

381 **Step 6:** Again, through the delocalization of oxygen in the complex, the glycerol and amine-  
382 functionalized catalyst are successively released from the complex.

383 **Step 7:** All three products, including FAME, glycerol, and water are then desorbed to the  
384 surface of the Fe/DS-HMS-NH<sub>2</sub> catalyst.

385 **Figure 7**

386

## 387 **Conclusions**

388 Fe/DS-HMS-NH<sub>2</sub> is synthesized through the two-step condensation technique and  
389 successfully employed as a heterogeneous catalyst for preparing biodiesel from DPO, a lipid  
390 source with significant FFA and moisture content. The obtained Fe/DS-HMS-NH<sub>2</sub> has a  
391 uniform spherical shape with a particle size of 156 nm and hollow diameter of 86 nm. It is  
392 composed of two spatial silica shells with different active sites, and their thickness are 22  
393 nm for the inner shell and 13 nm for the outer shell. Fe/DS-HMS-NH<sub>2</sub> has a specific surface  
394 area of 782.84 m<sup>2</sup>/g with a pore volume of 0.64 cm<sup>3</sup>/g, comparable with the existing solid  
395 catalysts. In the *in-situ* esterification/transesterification process using the Fe/DS-HMS-NH<sub>2</sub>  
396 catalyst, reaction time  $t$  is the variable with most significant influence on the yield of FAME  
397  $Y_F$ , followed by the reaction temperature  $T$  and the mass ratio of methanol to DPO  $r_{m/o}$ . The

398 maximum  $Y_F$  is 85.36% (w/w), obtained at the following conditions:  $T = 60^\circ\text{C}$ ,  $t = 4.5$  h, and  
399  $r_{m/o} = 6:1$ , with a catalyst loading of 6% (w/w). Notably, Fe/DS-HMS-NH<sub>2</sub> catalyst shows a  
400 good recyclability, with the yield staying above 80% for three reaction cycles. Therefore,  
401 Fe/DS-HMS-NH<sub>2</sub> is a promising heterogeneous catalyst to obtain biodiesel from DPO or  
402 other lipid materials with high FFA and water content.

403

#### 404 **Acknowledgments**

405 The authors acknowledge the funding supports from Widya Mandala Catholic University  
406 Surabaya, through the research grant no. 2263/WM01/N/2020. We also thank Professor  
407 Chun-Hu Chen, National Sun Yat Sen University, and Taiwan Tech (National Taiwan  
408 University of Science and Technology) for providing the facility for the catalyst  
409 characterizations.

#### 410 **REFERENCES**

- 411 [1] P. Agung, D. Hartono, A.A. Awirya, Pengaruh Urbanisasi Terhadap Konsumsi Energi  
412 Dan Emisi CO<sub>2</sub>: Analisis Provinsi di Indonesia, *J. Ekon. Kuantitatif Terap.* (2017).  
413 <https://doi.org/10.24843/jekt.2017.v10.i01.p02>.
- 414 [2] A. Fitriyatus, A. Fauzi, B. Juanda, Prediction of Fuel Supply and Consumption in  
415 Indonesia with System Dynamics Model, *J. Ekon. Dan Pembang. Indones.* 17 (2018) 118–  
416 137.
- 417 [3] F.T.R. Silalahi, T.M. Simatupang, M.P. Siallagan, Biodiesel produced from palm oil in  
418 Indonesia: Current status and opportunities, *AIMS Energy.* 8 (2020) 81–101.  
419 <https://doi.org/10.3934/energy.2020.1.81>.
- 420 [4] F. Nangoy, B.C. Munthe, Indonesia President wants B30 in use by Jan 2020: cabinet

- 421 secretary, Reuters. (2019).
- 422 [5] J.M. Marchetti, A summary of the available technologies for biodiesel production based  
423 on a comparison of different feedstock's properties, *Process Saf. Environ. Prot.* 90 (2012)  
424 157–163. <https://doi.org/10.1016/j.psep.2011.06.010>.
- 425 [6] A. Haryanto, U. Silviana, S. Triyono, S. Prabawa, Produksi Biodiesel Dari  
426 Transesterifikasi Minyak Jelantah Dengan Bantuan Gelombang Mikro: Pengaruh  
427 Intensitas Daya Dan Waktu Reaksi Terhadap Rendemen Dan Karakteristik Biodiesel, 35  
428 (2015) 235.
- 429 [7] I. Istadi, P. Purwanto, Advanced Chemical Reactor Technologies for Biodiesel Production  
430 from Vegetable Oils - A Review, *Bull. Chem. React. Eng. Catal.* 11 (2016) 406–430.
- 431 [8] N. Fadilah, *Tinjauan Pustaka Katalis*, (2017).
- 432 [9] M.K. Lam, K.T. Lee, A.R. Mohamed, Homogeneous, heterogeneous and enzymatic  
433 catalysis for transesterification of high free fatty acid oil (waste cooking oil) to biodiesel:  
434 A review, *Biotechnol. Adv.* 28 (2010) 500–518.  
435 <https://doi.org/10.1016/j.biotechadv.2010.03.002>.
- 436 [10] I. Mukherjee, B.K. Sovacool, Palm oil-based biofuels and sustainability in southeast Asia:  
437 A review of Indonesia, Malaysia, and Thailand, 37 (2014) 1–12.
- 438 [11] S. Mekhilef, S. Siga, R. Saidur, A review on palm oil biodiesel as a source of renewable  
439 fuel, *Renew. Sustain. Energy Rev.* 15 (2011) 1937–1949.  
440 <https://doi.org/10.1016/j.rser.2010.12.012>.
- 441 [12] M.M. Gui, K.T. Lee, S. Bhatia, Feasibility of Edible Oil vs. Non-edible Oil vs. Waste  
442 Edible Oil as Biodiesel Feedstock, (2008). <https://doi.org/10.1016/j.energy.2008.06.002>.
- 443 [13] Haryono, S. Fairus, Y. Sari, I. Rakhmawati, Pengolahan Minyak Goreng Kelapa Sawit  
444 Bekas menjadi Biodiesel Studi Kasus: Minyak Goreng Bekas dari KFC Dago Bandung,

- 445 (2010).
- 446 [14] S. Hernanda, S. Bahri, Yusnimar, Pembuatan Biodiesel dari Limbah Ikan Baung dengan  
447 Katalis Padat Lempung, (n.d.).
- 448 [15] K. Suwannakarn, E. Lotero, K. Ngaosuwan, J.G. Goodwin Jr, Simultaneous free fatty acid  
449 esterification and triglyceride transesterification using a solid acid catalyst with in situ  
450 removal of water and unreacted methanol, 48 (2009) 2810–2818.
- 451 [16] Y.A. Tsigie, L.H. Huynh, S. Ismadji, A.M. Engida, Y.H. Ju, In situ biodiesel production  
452 from wet *Chlorella vulgaris* under subcritical condition, Chem. Eng. J. 213 (2012) 104–  
453 108. <https://doi.org/10.1016/j.cej.2012.09.112>.
- 454 [17] P.D. Patil, V.G. Gude, A. Mannarswamy, P. Cooke, N. Nirmalakhandan, P. Lammers, S.  
455 Deng, Comparison of direct transesterification of algal biomass under supercritical  
456 methanol and microwave irradiation conditions, Fuel. 97 (2012) 822–831.  
457 <https://doi.org/10.1016/j.fuel.2012.02.037>.
- 458 [18] A. Kumari, P. Mahapatra, V.K. Garlapati, R. Banerjee, Enzymatic transesterification of  
459 *Jatropha* oil, Biotechnol Biofuels. 2 (2009) 1. <https://doi.org/10.1186/1754-6834-2-1>.
- 460 [19] I.A. Musa, The effects of alcohol to oil molar ratios and the type of alcohol on biodiesel  
461 production using transesterification process, Egypt. J. Pet. 25 (2016) 21–31.  
462 <https://doi.org/https://doi.org/10.1016/j.ejpe.2015.06.007>.
- 463 [20] W. Fanny, S. Subagjo, T. Prakoso, PENGEMBANGAN KATALIS KALSIUM OKSIDA  
464 UNTUK SINTESIS BIODIESEL, Indones. J. Chem. Eng. 11 (2012) 66–73.
- 465 [21] W. Xie, X. Yang, M. Fan, Novel solid base catalyst for biodiesel production: Mesoporous  
466 SBA-15 silica immobilized with 1,3-dicyclohexyl-2-octylguanidine, Renew. Energy. 80  
467 (2015) 230–237. <https://doi.org/10.1016/j.renene.2015.02.014>.
- 468 [22] H. Li, W. Xie, Transesterification of Soybean Oil to Biodiesel with Zn/I<sub>2</sub> Catalyst, Catal.

- 469 Letters. 107 (2006) 25–30. <https://doi.org/10.1007/s10562-005-9727-9>.
- 470 [23] W. Xie, X. %J C.L. Huang, Synthesis of biodiesel from soybean oil using heterogeneous  
471 KF/ZnO catalyst, 107 (2006) 53–59.
- 472 [24] W. Xie, H. Li, Alumina-supported potassium iodide as a heterogeneous catalyst for  
473 biodiesel production from soybean oil, *J. Mol. Catal. A Chem.* 255 (2006) 1–9.  
474 <https://doi.org/https://doi.org/10.1016/j.molcata.2006.03.061>.
- 475 [25] H.J. Berchmans, S. Hirata, Biodiesel production from crude *Jatropha curcas* L. seed oil  
476 with a high content of free fatty acids, *Bioresour Technol.* 99 (2008) 1716–1721.  
477 <https://doi.org/10.1016/j.biortech.2007.03.051>.
- 478 [26] R. Sivaramakrishnan, A. Incharoensakdi, Microalgae as feedstock for biodiesel production  
479 under ultrasound treatment - A review, *Bioresour Technol.* 250 (2018) 877–887.  
480 <https://doi.org/10.1016/j.biortech.2017.11.095>.
- 481 [27] H. Taher, S. Al-Zuhair, A.H. Al-Marzouqi, Y. Haik, M.M. Farid, A review of enzymatic  
482 transesterification of microalgal oil-based biodiesel using supercritical technology, *Enzym.*  
483 *Res.* 2011 (2011) 468292. <https://doi.org/10.4061/2011/468292>.
- 484 [28] A. Gog, M. Roman, M. Toşa, C. Paizs, F.D. Irimie, Biodiesel production using enzymatic  
485 transesterification - Current state and perspectives, *Renew. Energy.* 39 (2012) 10–16.  
486 <https://doi.org/10.1016/j.renene.2011.08.007>.
- 487 [29] Joelianingsih, H. Maeda, S. Hagiwara, H. Nabetani, Y. Sagara, T.H. Soerawidjaya, A.H.  
488 Tambunan, K. Abdullah, Biodiesel fuels from palm oil via the non-catalytic  
489 transesterification in a bubble column reactor at atmospheric pressure: A kinetic study,  
490 *Renew. Energy.* 33 (2008) 1629–1636. <https://doi.org/10.1016/j.renene.2007.08.011>.
- 491 [30] T. Pinnarat, P.E. Savage, Noncatalytic esterification of oleic acid in ethanol, *J. Supercrit.*  
492 *Fluids.* 53 (2010) 53–59.

- 493 [31] R. Mat, R.A. Samsudin, M. Mohamed, A. Johari, Solid catalysts and their application in  
494 biodiesel production, *Bull. Chem. React. Eng. Catal.* 7 (2012) 142–149.  
495 <https://doi.org/10.9767/bcrec.7.2.3047.142-149>.
- 496 [32] S.M. Coman, V.I. Parvulescu, Heterogeneous Catalysis for Biodiesel Production, *Role*  
497 *Catal. Sustain. Prod. Bio-Fuels Bio-Chemicals.* (2013) 93–136.  
498 <https://doi.org/10.1016/B978-0-444-56330-9.00004-8>.
- 499 [33] W. Suryaputra, I. Winata, N. Indraswati, S. Ismadji, Waste capiz (*Amusium cristatum*)  
500 shell as a new heterogeneous catalyst for biodiesel production, *Renew. Energy.* 50 (2013)  
501 795–799. <https://doi.org/10.1016/j.renene.2012.08.060>.
- 502 [34] E. Crabbe, C. Nolasco-Hipolito, G. Kobayashi, K. Sonomoto, A. Ishizaki, Biodiesel  
503 production from crude palm oil and evaluation of butanol extraction and fuel properties,  
504 *Process Biochem.* 37 (2001) 65–71. [https://doi.org/10.1016/S0032-9592\(01\)00178-9](https://doi.org/10.1016/S0032-9592(01)00178-9).
- 505 [35] P.L. Boey, G.P. Maniam, S.A. Hamid, Performance of calcium oxide as a heterogeneous  
506 catalyst in biodiesel production: A review, *Chem. Eng. J.* 168 (2011) 15–22.  
507 <https://doi.org/10.1016/j.cej.2011.01.009>.
- 508 [36] A.A. Refaat, A.A. Refaat, Archive of SID Different techniques for the production of  
509 biodiesel from waste vegetable oil, *Int. J. Environ. Sci. Tech.* 7 (2010) 183–213.
- 510 [37] W.N.N.W. Omar, N.A.S. Amin, Biodiesel production from waste cooking oil over  
511 alkaline modified zirconia catalyst, 92 (2011) 2397–2405.
- 512 [38] N. Pal, M. Paul, A. Bhaumik, Highly ordered Zn-doped mesoporous silica: An efficient  
513 catalyst for transesterification reaction, *J. Solid State Chem.* 184 (2011) 1805–1812.  
514 <https://doi.org/10.1016/j.jssc.2011.05.033>.
- 515 [39] M. Hartmann, Ordered Mesoporous Materials for Bioadsorption and Biocatalysis, *Chem.*  
516 *Mater.* 17 (2005) 4577–4593. <https://doi.org/10.1021/cm0485658>.

- 517 [40] J.Y. Ying, C.P. Mehnert, M.S. Wong, Synthesis and Applications of Supramolecular-  
518 Templated Mesoporous Materials, *Angew. Chemie Int. Ed.* 38 (1999) 56–77.  
519 [https://doi.org/https://doi.org/10.1002/\(SICI\)1521-3773\(19990115\)38:1/2<56::AID-  
520 ANIE56>3.0.CO;2-E](https://doi.org/10.1002/(SICI)1521-3773(19990115)38:1/2<56::AID-ANIE56>3.0.CO;2-E).
- 521 [41] J. Santos, J. Phillips, J.A. Dumesic, Metal-support interactions between iron and titania for  
522 catalysts prepared by thermal decomposition of iron pentacarbonyl and by impregnation,  
523 81 (1983) 147–167.
- 524 [42] C. You, C. Yu, X. Yang, Y. Li, H. Huo, Z. Wang, Y. Jiang, X. Xu, K. Lin, Double-shelled  
525 hollow mesoporous silica nanosphere as acid-base bifunctional catalyst for cascade  
526 reactions, *New J. Chem.* 42 (2018) 4095–4101. <https://doi.org/10.1039/C7NJ04670G>.
- 527 [43] S.S. Park, C. Ha, Hollow mesoporous functional hybrid materials: fascinating platforms  
528 for advanced applications, 28 (2018) 1703814.
- 529 [44] P.L. Boey, G.P. Maniam, S.A. Hamid, Biodiesel production via transesterification of palm  
530 olein using waste mud crab (*Scylla serrata*) shell as a heterogeneous catalyst, *Bioresour.  
531 Technol.* 100 (2009) 6362–6368. <https://doi.org/10.1016/j.biortech.2009.07.036>.
- 532 [45] C. Samart, P. Sreetongkittikul, C. Sookman, Heterogeneous catalysis of transesterification  
533 of soybean oil using KI/mesoporous silica, *Fuel Process. Technol.* 90 (2009) 922–925.  
534 <https://doi.org/10.1016/j.fuproc.2009.03.017>.
- 535 [46] D.D. Bala, M. Misra, D. Chidambaram, Solid-acid catalyzed biodiesel production, part I:  
536 biodiesel synthesis from low quality feedstock, *J. Clean. Prod.* 142 (2017) 4169–4177.  
537 <https://doi.org/10.1016/j.jclepro.2016.02.128>.
- 538 [47] F.H. Santosa, L. Laysandra, F.E. Soetaredjo, S.P. Santoso, S. Ismadji, M. Yuliana, A  
539 facile noncatalytic methyl ester production from waste chicken tallow using single step  
540 subcritical methanol: Optimization study, *Int. J. Energy Res.* 43 (2019) 8852–8863.

- 541 <https://doi.org/10.1002/er.4844>.
- 542 [48] X. Zhou, X. Cheng, W. Feng, K. Qiu, L. Chen, W. Nie, Z. Yin, X. Mo, H. Wang, C. He,  
543 Synthesis of hollow mesoporous silica nanoparticles with tunable shell thickness and pore  
544 size using amphiphilic block copolymers as core templates, *Dalt. Trans.* 43 (2014) 11834–  
545 11842. <https://doi.org/10.1039/c4dt01138d>.
- 546 [49] S. Cao, Z. Zhao, X. Jin, W. Sheng, S. Li, Y. Ge, M. Dong, W. Wu, L. Fang, Unique  
547 double-shelled hollow silica microspheres: Template-guided self-assembly, tunable pore  
548 size, high thermal stability, and their application in removal of neutral red, *J. Mater. Chem.*  
549 21 (2011) 19124–19131. <https://doi.org/10.1039/c1jm13011k>.
- 550 [50] N.B. Klinghoffer, M.J. Castaldi, A. Nzihou, Catalyst Properties and Catalytic Performance  
551 of Char from Biomass Gasification, *Ind. Eng. Chem. Res.* 51 (2012) 13113–13122.  
552 <https://doi.org/10.1021/ie3014082>.
- 553 [51] M. Zakeri, A. Samimi, M. Shafiee Afarani, A. Salehirad, Effects of Porosity and Pore Size  
554 Distribution on Mechanical Strength Reliability of Industrial Scale Catalyst during  
555 Preparation and Catalytic Test Steps, *Part. Sci. Technol.* (2016).  
556 <https://doi.org/10.1080/02726351.2016.1220437>.
- 557 [52] T. Pangestu, Y. Kurniawan, F.E. Soetaredjo, S.P. Santoso, W. Irawaty, M. Yuliana, S.B.  
558 Hartono, S. Ismadji, The synthesis of biodiesel using copper based metal-organic  
559 framework as a catalyst, *J. Environ. Chem. Eng.* 7 (2019) 103277.  
560 <https://doi.org/10.1016/j.jece.2019.103277>.
- 561 [53] N. Rahmat, N. Sadon, M.A. Yusof, Thermogravimetric Analysis (TGA) Profile at  
562 Different Calcination Conditions for Synthesis of PTES-SBA-15, *Am. J. Appl. Sci.* 14  
563 (2017) 938–944. <https://doi.org/10.3844/ajassp.2017.938.944>.
- 564 [54] Y.Y. Margaretha, H.S. Prastyo, A. Ayucitra, S. Ismadji, Calcium oxide from pomacea sp.

565 shell as a catalyst for biodiesel production, *Int. J. Energy Environ. Eng.* 3 (2012) 1–9.  
566 <https://doi.org/10.1186/2251-6832-3-33>.

567 [55] A.M. Dekhoda, A.H. West, N. Ellis, Biochar based solid acid catalyst for biodiesel  
568 production, *Appl. Catal. A Gen.* 382 (2010) 197–204.  
569 <https://doi.org/10.1016/j.apcata.2010.04.051>.

570 [56] H.R. Ong, M.R. Khan, M.N.K. Chowdhury, A. Yousuf, C.K. Cheng, Synthesis and  
571 characterization of CuO/C catalyst for the esterification of free fatty acid in rubber seed oil,  
572 *Fuel*. 120 (2014) 195–201. <https://doi.org/https://doi.org/10.1016/j.fuel.2013.12.015>.

573 [57] J. Cai, Q.Y. Zhang, F.F. Wei, J.S. Huang, Y.M. Feng, H.T. Ma, Y. Zhang, Preparation of  
574 Copper (II) Containing Phosphomolybdic Acid Salt as Catalyst for the Synthesis of  
575 Biodiesel by Esterification, *J Oleo Sci.* 67 (2018) 427–432.  
576 <https://doi.org/10.5650/jos.ess17208>.

577 [58] G. Baskar, S. Soumiya, Production of biodiesel from castor oil using iron (II) doped zinc  
578 oxide nanocatalyst, *Renew. Energy.* 98 (2016) 101–107.  
579 <https://doi.org/https://doi.org/10.1016/j.renene.2016.02.068>.

580 [59] C. Samart, C. Chaiya, P. Reubroycharoen, Biodiesel production by methanolysis of  
581 soybean oil using calcium supported on mesoporous silica catalyst, *Energy Convers.*  
582 *Manag.* 51 (2010) 1428–1431. <https://doi.org/10.1016/j.enconman.2010.01.017>.

583 [60] B. Gurunathan, A. Ravi, Biodiesel production from waste cooking oil using copper doped  
584 zinc oxide nanocomposite as heterogeneous catalyst, *Bioresour. Technol.* 188 (2015) 124–  
585 127. <https://doi.org/https://doi.org/10.1016/j.biortech.2015.01.012>.

586 [61] M. Farooq, A. Ramli, Biodiesel production from low FFA waste cooking oil using  
587 heterogeneous catalyst derived from chicken bones, *Renew. Energy.* 76 (2015) 362–368.  
588 <https://doi.org/10.1016/j.renene.2014.11.042>.

- 589 [62] R. Alenezi, G.A. Leeke, J.M. Winterbottom, R.C.D. Santos, A.R. Khan, Esterification  
590 kinetics of free fatty acids with supercritical methanol for biodiesel production, *Energy*  
591 *Convers. Manag.* 51 (2010) 1055–1059. <https://doi.org/10.1016/j.enconman.2009.12.009>.
- 592 [63] M. Canakci, J. Van Gerpen, Biodiesel production via acid catalysis, *Trans. Am. Soc.*  
593 *Agric. Eng.* 42 (1999) 1203–1210. <https://doi.org/10.13031/2013.13285>.
- 594 [64] M. Farooq, A. Ramli, D. Subbarao, Biodiesel production from waste cooking oil using  
595 bifunctional heterogeneous solid catalysts, *J. Clean. Prod.* 59 (2013) 131–140.  
596 <https://doi.org/10.1016/j.jclepro.2013.06.015>.
- 597 [65] S. Liu, Y. Wang, J.H. Oh, J.L. Herring, Fast biodiesel production from beef tallow with  
598 radio frequency heating, *Renew. Energy.* 36 (2011) 1003–1007.  
599 <https://doi.org/10.1016/j.renene.2010.09.015>.
- 600 [66] I. Amalia Kartika, M. Yani, D. Ariono, P. Evon, L. Rigal, Biodiesel production from  
601 jatropha seeds: Solvent extraction and in situ transesterification in a single step, *Fuel.* 106  
602 (2013) 111–117. <https://doi.org/10.1016/j.fuel.2013.01.021>.
- 603 [67] Z. Wei, C. Xu, B. Li, Application of waste eggshell as low-cost solid catalyst for biodiesel  
604 production, *Bioresour. Technol.* 100 (2009) 2883–2885.  
605 <https://doi.org/10.1016/j.biortech.2008.12.039>.
- 606 [68] A. Demirbas, Biodiesel from waste cooking oil via base-catalytic and supercritical  
607 methanol transesterification, *Energy Convers. Manag.* 50 (2009) 923–927.  
608 <https://doi.org/10.1016/j.enconman.2008.12.023>.
- 609 [69] I.A. Reşitoğlu, A. Keskin, M. Gürü, The optimization of the esterification reaction in  
610 biodiesel production from trap grease, *Energy Sources, Part A Recover. Util. Environ. Eff.*  
611 34 (2012) 1238–1248. <https://doi.org/10.1080/15567031003792395>.
- 612 [70] A. Hayyan, F.S. Mjalli, M.A. Hashim, M. Hayyan, I.M. AlNashef, S.M. Al-Zahrani, M.A.

613 Al-Saadi, Ethanesulfonic acid-based esterification of industrial acidic crude palm oil for  
614 biodiesel production, *Bioresour Technol.* 102 (2011) 9564–9570.  
615 <https://doi.org/10.1016/j.biortech.2011.07.074>.

616 [71] S.L. Lee, Y.C. Wong, Y.P. Tan, S.Y. Yew, Transesterification of palm oil to biodiesel by  
617 using waste obtuse horn shell-derived CaO catalyst, *Energy Convers. Manag.* 93 (2015)  
618 282–288. <https://doi.org/10.1016/j.enconman.2014.12.067>.

619 [72] W. Xie, T. Wang, Biodiesel production from soybean oil transesterification using tin  
620 oxide-supported WO<sub>3</sub> catalysts, *Fuel Process. Technol.* 109 (2013) 150–155.  
621 <https://doi.org/10.1016/j.fuproc.2012.09.053>.

622 [73] M. Kouzu, J.S. Hidaka, Transesterification of vegetable oil into biodiesel catalyzed by  
623 CaO: A review, *Fuel.* 93 (2012) 1–12. <https://doi.org/10.1016/j.fuel.2011.09.015>.

624 [74] D.M. Marinković, M. V. Stanković, A. V. Veličković, J.M. Avramović, M.R. Miladinović,  
625 O.O. Stamenković, V.B. Veljković, D.M. Jovanović, Calcium oxide as a promising  
626 heterogeneous catalyst for biodiesel production: Current state and perspectives, *Renew.*  
627 *Sustain. Energy Rev.* 56 (2016) 1387–1408. <https://doi.org/10.1016/j.rser.2015.12.007>.

628 [75] A.K. Endalew, Y. Kiros, R. Zanzi, Inorganic heterogeneous catalysts for biodiesel  
629 production from vegetable oils, *Biomass and Bioenergy.* 35 (2011) 3787–3809.  
630 <https://doi.org/10.1016/j.biombioe.2011.06.011>.

631 [76] S. Sharma, V. Saxena, A. Baranwal, P. Chandra, L.M. Pandey, Engineered nanoporous  
632 materials mediated heterogeneous catalysts and their implications in biodiesel production ,  
633 *Mater. Sci. Energy.* 1 (2018) 11–21.  
634 <https://doi.org/10.1016/j.mset.2018.05.002>.

635  
636

637

**Table 1.** Experimental matrix at the optimum catalyst loading  $m_c = 6\%$  (w/w)

Run	Input Parameters			$Y_F$ (% w/w)
	$T$ (°C)	$t$ (h)	$r_{m/o}$	
1	60	4.5	10:1	85.24
2	40	0.5	10:1	40.27
3	40	2.5	6:1	55.09
4	50	4.5	6:1	75.15
5	50	2.5	10:1	60.07
6	40	0.5	2:1	35.19
7	40	4.5	10:1	70.22
8	50	2.5	2:1	67.03
9	60	4.5	2:1	80.11
10	50	2.5	6:1	65.16
11	50	2.5	6:1	66.96
12	50	2.5	6:1	65.87
13	50	0.5	6:1	65.01
14	60	4.5	6:1	85.36
15	50	2.5	6:1	63.21
16	60	0.5	10:1	70.01
17	50	2.5	6:1	63.20
18	50	2.5	6:1	67.18
19	60	0.5	2:1	69.09
20	40	4.5	2:1	59.11

638

639

640

**Table 2.** Textural properties of Fe/DS-HMS-NH<sub>2</sub>.

Material	$S_{\text{BET}}$ (cm <sup>2</sup> /g)	Pore volume (cm <sup>3</sup> /g)	Pore size (nm)
Fe/DS-HMS-NH <sub>2</sub>	782.84	0.64	2.43

641

642

**Table 3.** Characteristics of DPO.

Parameter	Value
FFA (% w/w)	5.54
Moisture Content (% w/w)	0.20
Saponification Value (mg KOH/g DPO)	234.08
Acid Value (mg KOH/g DPO)	12.04
Molecular weight (g/mol)	756.62

643

644

645

**Table 4.** Fuel properties of the final FAME product

Properties	Methods	Unit	Final FAME product	ASTM D6751
Kinematic viscosity (at 40°C)	ASTM D445	mm <sup>2</sup> /s	2.64	1.9 – 6.0
Flashpoint	ASTM D93	°C	164.2	93 min
Cetane number	ASTM D613	-	55.7	47 min
Acid value	ASTM D664	mg KOH/g	0.24	0.5 max
Calorific value	ASTM D240	MJ/kg	45.143	-

646

647

648

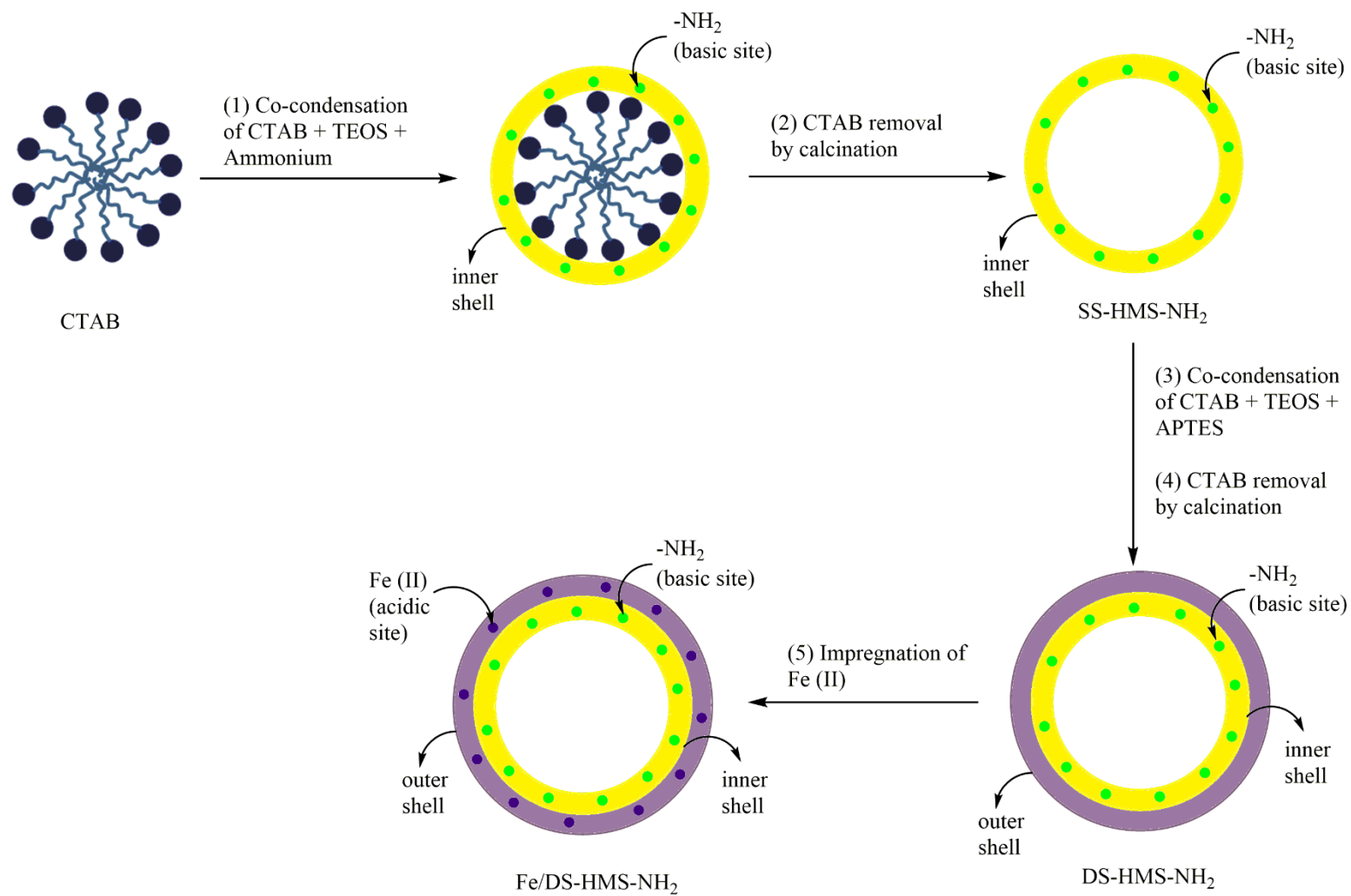
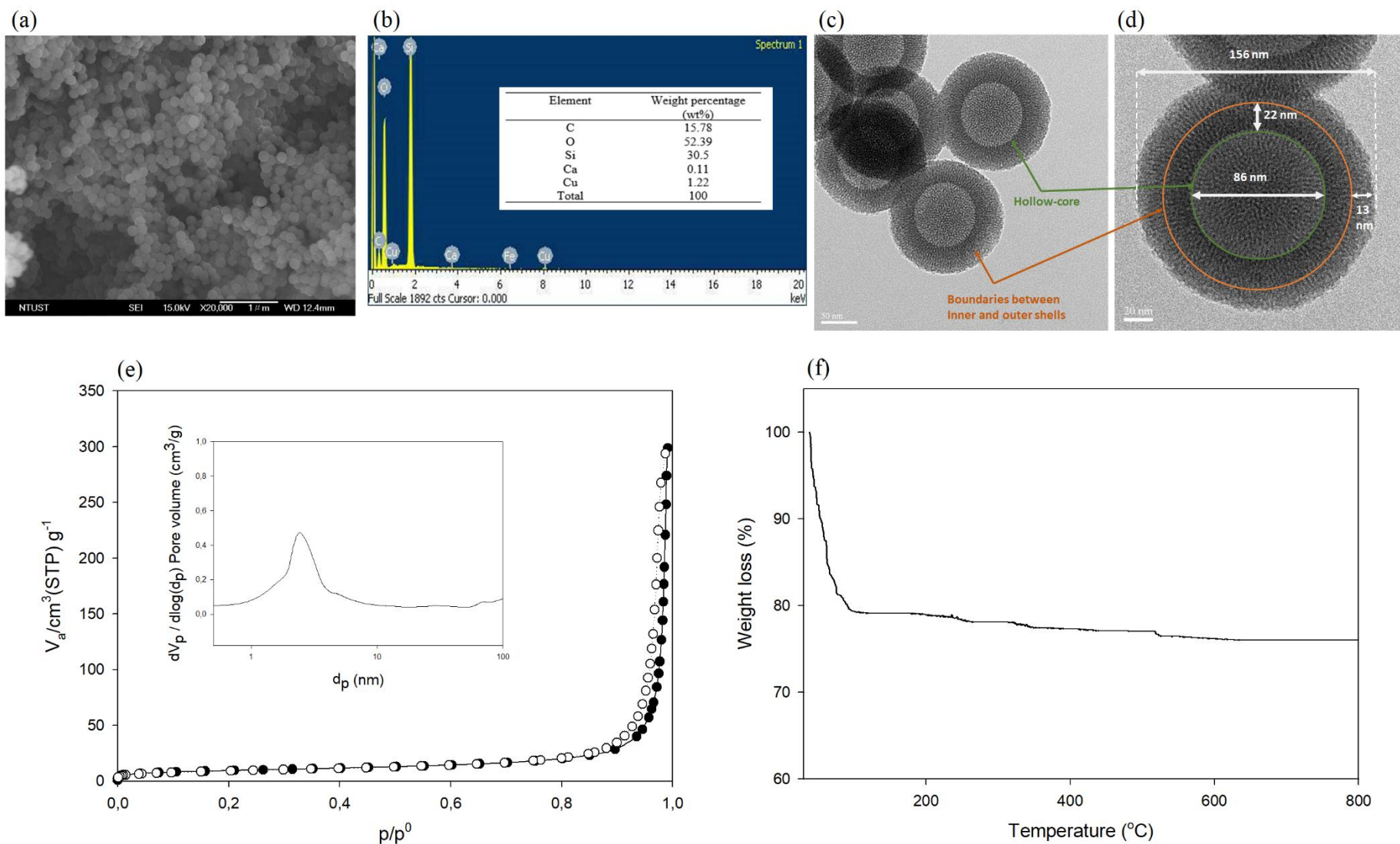


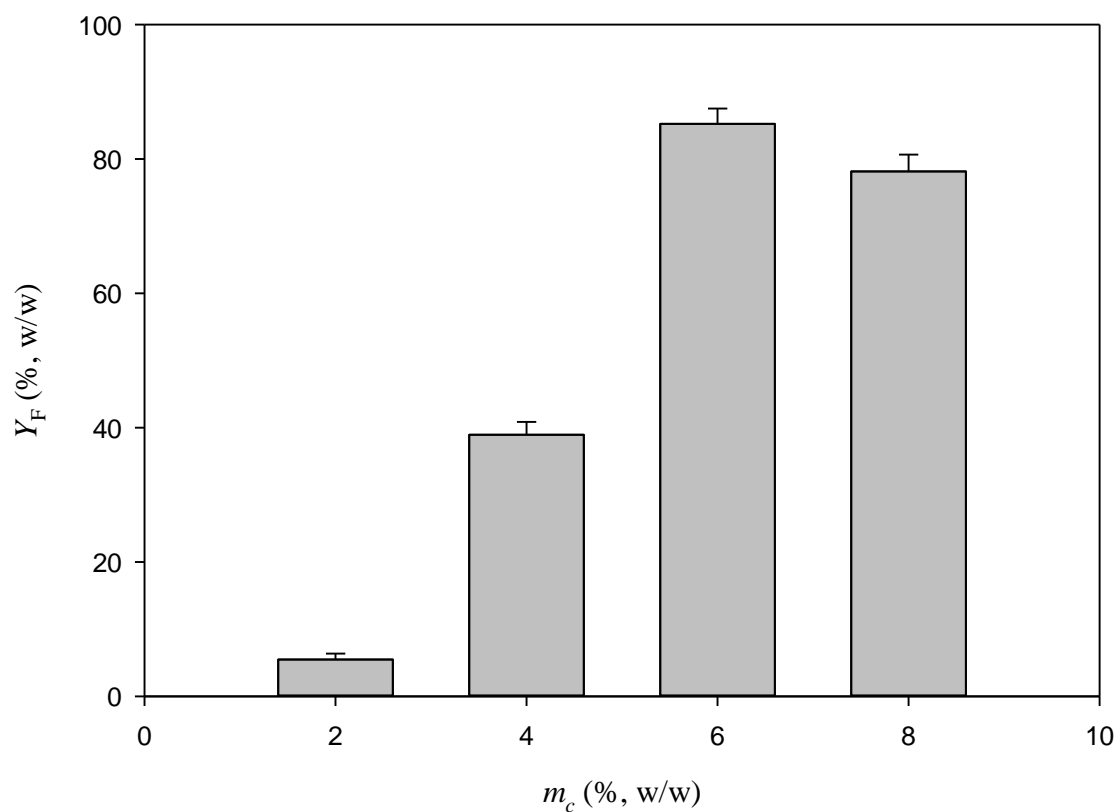
**Figure 1.** The mechanism scheme of Fe/DS-HMS-NH<sub>2</sub> fabrication.

649  
650

651

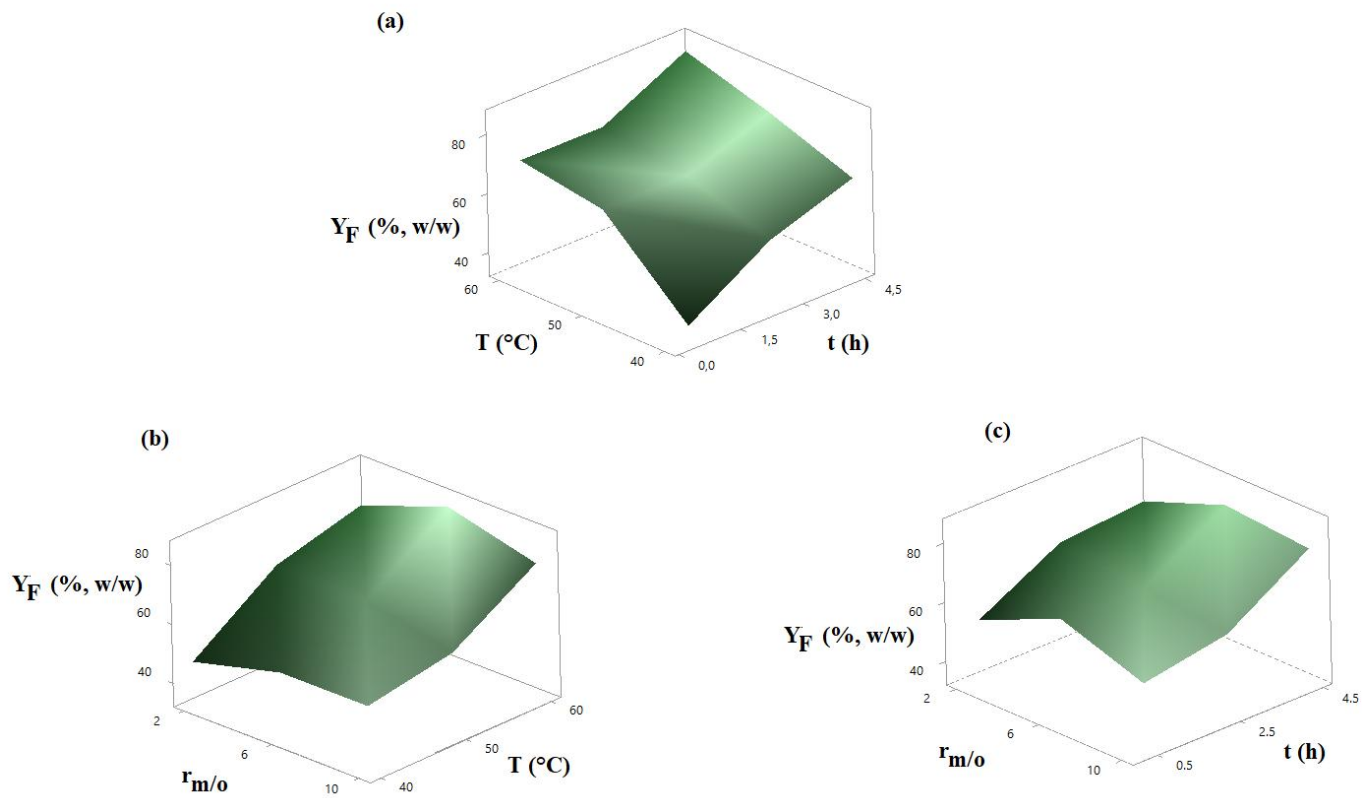


653 **Figure 2.** (a) SEM image, (b) Elemental composition, (c) – (d) TEM images at various magnifications, (e) BJH pore size distribution  
 654 curve, (e) Nitrogen adsorption-desorption isotherm with BJH pore size distribution curve (inset), (f) Thermogravimetric profile of the  
 655 Fe/DS-HMS-NH<sub>2</sub> catalyst.



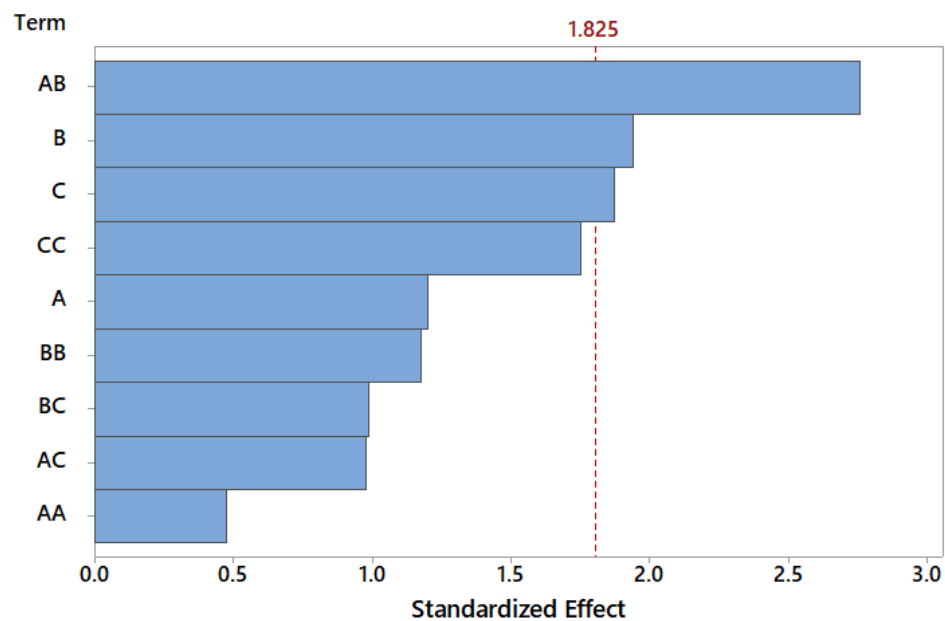
656  
657  
658  
659  
660  
661

**Figure 3.** The yield of FAME at various Fe/DS-HMS-NH<sub>2</sub> loadings with the reaction condition of  $T = 60$  °C,  $t = 4.5$  h and  $r_{m/o} = 10:1$ .



663 **Figure 4.** The FAME yield  $Y_F$  (% w/w) at various (a)  $T$  and  $t$ , (b)  $T$  and  $r_{m/o}$ , and (c)  $t$  and  $r_{m/o}$ .  
 664

665



666

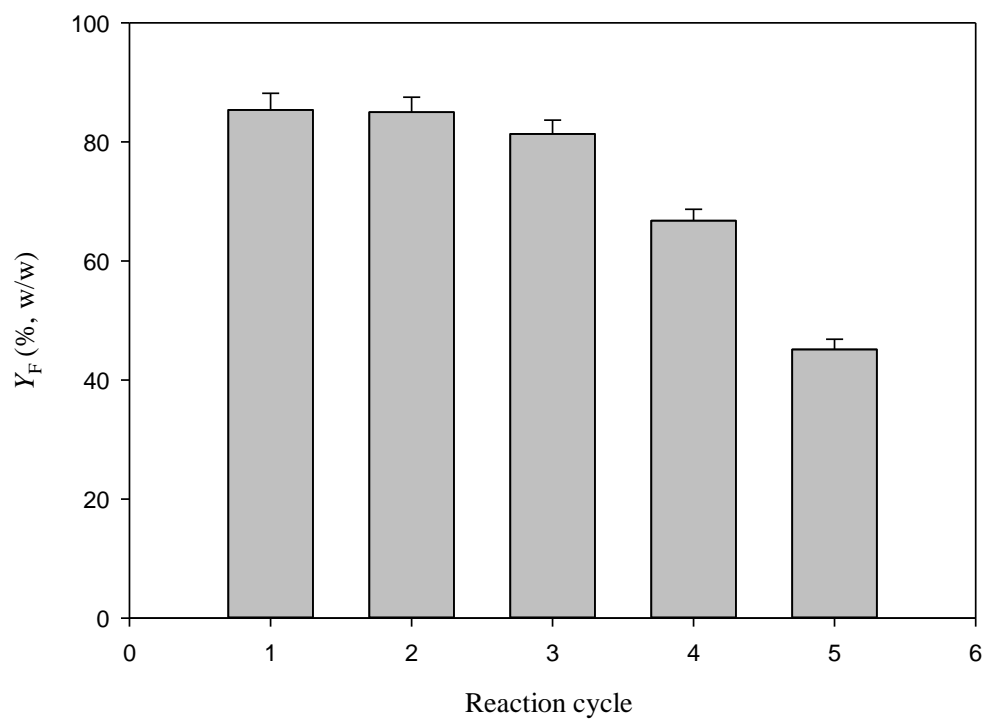
667

**Figure 5.** Pareto chart of the standardized effect for the biodiesel preparation with Fe/DS-HMS-NH<sub>2</sub>, using  $Y_F$  as the response at a 95% confidence interval where  $A = T$ ,  $B = t$ ,  $C = r_{m/o}$ .

668

669

670



671

672

673

674

**Figure 6.** Recyclability of Fe/DS-HMS-NH<sub>2</sub> in the *in-situ* esterification/transesterification of DPO.

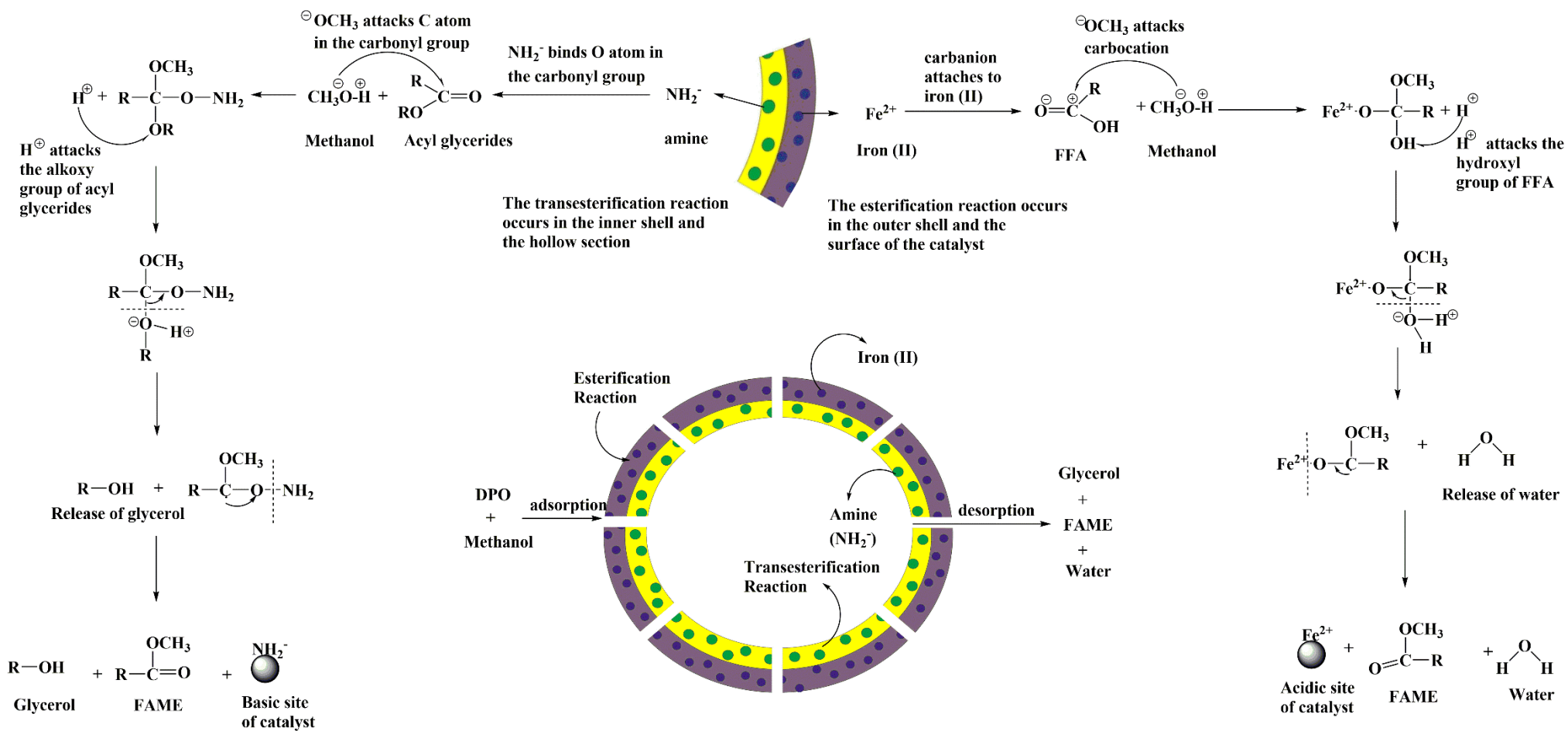


**Figure 7.** The reaction mechanism of the *in-situ* esterification/transesterification of DPO using Fe/DS-HMS-NH<sub>2</sub>.

**Declaration of interests**

The authors declare that they have no known competing financial interests or personal relationships that could have appeared to influence the work reported in this paper.

The authors declare the following financial interests/personal relationships which may be considered as potential competing interests:

## CREDIT AUTHOR STATEMENT

- Stefanus Kevin Suryajaya - Conceptualization, methodology, investigation, software, writing – original draft
- Yohanes Ricky Mulyono - Conceptualization, methodology, investigation, software, writing – original draft
- Shella Permatasari Santoso - Conceptualization, data curation, supervision
- Maria Yuliana - Conceptualization, resources, visualization, writing-review and editing, supervision
- Alfin Kurniawan - Investigation, resources
- Aning Ayucitra - Investigation, validation
- Yueting Sun - Writing-review and editing
- Sandy Budi Hartono - Software, validation
- Felycia Edi Soetaredjo - Resources, visualization
- Suryadi Ismadji - Resources, validation



Maria Yuliana &lt;mariayuliana@ukwms.ac.id&gt;

---

**Your Submission RENE-D-20-04164**

1 message

---

**Renewable Energy** <em@editorialmanager.com>  
Reply-To: Renewable Energy <rene@elsevier.com>  
To: Maria Yuliana <mariayuliana@ukwms.ac.id>

Tue, Nov 24, 2020 at 1:08 PM

Ms. Ref. No.: RENE-D-20-04164

Title: IRON (II) IMPREGNATED DOUBLE-SHELLED HOLLOW MESOPOROUS SILICA AS ACID-BASE BIFUNCTIONAL CATALYST FOR THE CONVERSION OF LOW-QUALITY OIL TO METHYL ESTERS

Renewable Energy

Dear Dr. Yuliana,

The review of your paper is now complete; the Reviewers' reports are below. We kindly ask you to revise the paper considering the Reviewers' remarks and suggestions presented below. When this process is completed, the paper may be acceptable for publication in RENEWABLE ENERGY.

Once you have revised the paper accordingly, please submit it together with a detailed description of your response to these comments. Please, also include a separate copy of the revised paper in which you have marked the revisions made.

The revision will be due by: 24/12/2020

To submit a revision, please go to <https://www.editorialmanager.com/rene/> and login as an Author.

Your username is: [mariayuliana@ukwms.ac.id](mailto:mariayuliana@ukwms.ac.id)

If you need to retrieve password details, please go to: <https://www.editorialmanager.com/rene/l.asp?i=1071530&l=E0QOM3JG>

NOTE: Upon submitting your revised manuscript, please upload the source files for your article. For additional details regarding acceptable file formats, please refer to the Guide for Authors at: <http://www.elsevier.com/journals/renewable-energy/0960-1481/guide-for-authors>

When submitting your revised paper, we ask that you include the following items:

Manuscript, Marked manuscript and Figure Source Files (mandatory)

We cannot accommodate PDF manuscript files for production purposes. We also ask that when submitting your revision you follow the journal formatting guidelines. Figures and tables may be embedded within the source file for the submission as long as they are of sufficient resolution for Production. For any figure that cannot be embedded within the source file (such as \*.PSD Photoshop files), the original figure needs to be uploaded separately. Refer to the Guide for Authors for additional information.

<http://www.elsevier.com/journals/renewable-energy/0960-1481/guide-for-authors>

Highlights (mandatory)

Highlights consist of a short collection of bullet points that convey the core findings of the article and should be submitted in a separate file in the online submission system. Please use 'Highlights' in the file name and include 3 to 5 bullet points (maximum 85 characters, including spaces, per bullet point). See the following website for more information

<http://www.elsevier.com/highlights>

On your Main Menu page, you will find a folder entitled "Submissions Needing Revision". Your submission record will be presented here.

Please note that this journal offers a new, free service called AudioSlides: brief, webcast-style presentations that are shown next to published articles on ScienceDirect (see also <http://www.elsevier.com/audioslides>). If your paper is accepted for publication, you will automatically receive an invitation to create an AudioSlides presentation.

Effective peer review is essential to uphold the quality and validity of individual articles, but also the overall integrity of the journal. We would like to remind you that for every article considered for publication, there are usually at least 2 reviews required for each review round, and it is critical that scientists wishing to publish their research also be willing to provide reviews to similarly enable the peer review of papers by other authors. Please accept any review assignment within your expertise area(s) we may address to you and undertake reviewing in the manner in which you would hope your own paper to be reviewed.

Renewable Energy features the Interactive Plot Viewer, see: <http://www.elsevier.com/interactiveplots>. Interactive Plots provide easy access to the data behind plots. To include one with your article, please prepare a .csv file with your plot data and test it online at <http://authortools.elsevier.com/interactiveplots/verification> before submission as supplementary material.

Renewable Energy features the Interactive Plot Viewer, see: <http://www.elsevier.com/interactiveplots>. Interactive Plots provide easy access to the data behind plots. To include one with your article, please prepare a .csv file with your plot data and test it online at <http://authortools.elsevier.com/interactiveplots/verification> before submission as supplementary material.

#### MethodsX file (optional)

If you have customized (a) research method(s) for the project presented in your Renewable Energy article, you are invited to submit this part of your work as MethodsX article alongside your revised research article. MethodsX is an independent journal that publishes the work you have done to develop research methods to your specific needs or setting. This is an opportunity to get full credit for the time and money you may have spent on developing research methods, and to increase the visibility and impact of your work.

How does it work?

- 1) Fill in the MethodsX article template: <https://www.elsevier.com/MethodsX-template>
- 2) Place all MethodsX files (including graphical abstract, figures and other relevant files) into a .zip file and upload this as a 'Method Details (MethodsX)' item alongside your revised Renewable Energy manuscript. Please ensure all of your relevant MethodsX documents are zipped into a single file.
- 3) If your Renewable Energy research article is accepted, your MethodsX article will automatically be transferred to MethodsX, where it will be reviewed and published as a separate article upon acceptance. MethodsX is a fully Open Access journal, the publication fee is only 520 US\$.

Questions? Please contact the MethodsX team at [methodsx@elsevier.com](mailto:methodsx@elsevier.com). Example MethodsX articles can be found here: <http://www.sciencedirect.com/science/journal/22150161>

Include interactive data visualizations in your publication and let your readers interact and engage more closely with your research. Follow the instructions here: <https://www.elsevier.com/authors/author-services/data-visualization> to find out about available data visualization options and how to include them with your article.

Thank you very much for expressing your interest in RENEWABLE ENERGY.

#### MethodsX file (optional)

We invite you to submit a method article alongside your research article. This is an opportunity to get full credit for the time and money you have spent on developing research methods, and to increase the visibility and impact of your work. If your research article is accepted, your method article will be automatically transferred over to the open access journal, MethodsX, where it will be editorially reviewed and published as a separate method article upon acceptance. Both articles will be linked on ScienceDirect. Please use the MethodsX template available here when preparing your article: <https://www.elsevier.com/MethodsX-template>. Open access fees apply.

Sincerely,

Soteris Kalogirou, D.Sc.  
Editor-in-Chief  
Renewable Energy

#### Data in Brief (optional):

We invite you to convert your supplementary data (or a part of it) into an additional journal publication in Data in Brief, a multi-disciplinary open access journal. Data in Brief articles are a fantastic way to describe supplementary data and associated metadata, or full raw datasets deposited in an external repository, which are otherwise unnoticed. A Data in Brief article (which will be reviewed, formatted, indexed, and given a DOI) will make your data easier to find, reproduce, and cite.

You can submit to Data in Brief via the Renewable Energy submission system when you upload your revised Renewable Energy manuscript. To do so, complete the template and follow the co-submission instructions found here: [www.elsevier.com/dib-template](http://www.elsevier.com/dib-template). If your Renewable Energy manuscript is accepted, your Data in Brief submission will automatically be transferred to Data in Brief for editorial review and publication.

Please note: an open access Article Publication Charge (APC) is payable by the author or research funder to cover the costs associated with publication in Data in Brief and ensure your data article is immediately and permanently free to access by all. For the current APC see: [www.elsevier.com/journals/data-in-brief/2352-3409/open-access-journal](http://www.elsevier.com/journals/data-in-brief/2352-3409/open-access-journal)

Please contact the Data in Brief editorial office at [dib-me@elsevier.com](mailto:dib-me@elsevier.com) or visit the Data in Brief homepage ([www.journals.elsevier.com/data-in-brief/](http://www.journals.elsevier.com/data-in-brief/)) if you have questions or need further information.

.....  
 Note: While submitting the revised manuscript, please double check the author names provided in the submission so that authorship related changes are made in the revision stage. If your manuscript is accepted, any authorship change will involve approval from co-authors and respective editor handling the submission and this may cause a significant delay in publishing your manuscript.  
 .....

Reviewers' comments:

%ATTACH\_FOR\_REVIEWER\_DEEP\_LINK INSTRUCTIONS%

Subject Editor:

Further to Reviewers comments:

- The Graphical Abstract is too detailed - impossible to understand when reduced;
- Authors cited lists of 3 or more references without proper justification of their relevance. Authors must rearrange text or add at least a few words/a single sentence to justify why each reference must be cited.
- Authors must define how FAME yield was calculated.
- Biodiesel characterization must be provided.
- Figures and Tables must be embeded in the text.
- Ref. [6] - add language and title in English; reference is incomplete; similarly for Ref. [8], [14]
- Check other references that are incomplete - missing journal, volume, etc.

Reviewer #1: The present manuscript titled with IRON (II) IMPREGNATED DOUBLE-SHELLED HOLLOW MESOPOROUS SILICA AS ACID-BASE BIFUNCTIONAL CATALYST FOR THE CONVERSION OF LOW-QUALITY OIL TO METHYL ESTERS" is a novel work performed by the authors and they explained well about the process efficiency and final compound out puts. Strongly agreeing to acceptance of the present manuscript with minor changes.

1. Introduction required changes.....Its too lengthy, and there is no any connection between the paragraphs.
2. Present aim of the manuscript or research work should always comes as last paragraph of introduction.
3. Conclusion needs to be framed with future applications in concern with industrial orientation or application to field

Reviewer #2: This study reports a novel acid-base bifunctional catalyst Fe/DS-HMS-NH<sub>2</sub> for the production of FAME from the low-quality oil. This novel catalyst enables the esterification and transesterification reactions to take place in a single step, with a high yield of FAME of 85.36% achieved. Overall, this manuscript is well written. I recommend the acceptance of this manuscript with minor revisions.

I have some technical comments for the authors to address.

1. The Graphic Abstract needs to be revised to a small size.
2. Please provide the compositional profile of FAME product after reaction.
3. What was the conversion of FFA after reaction? Please provide the content of FFA in the final product.
4. The purity of FAME was calculated based on the peak area of FAME. How accurate is this method for the quantification of the FAME yield?
5. Provide the errors for the results in Table 1.
6. A significant reduction in the catalyst ability can be found after only 3 cycles. Is there any method to regenerate the catalyst?
7. The authors need to benchmark the performance of the new catalyst with other existing or commercial catalysts in the literature.

For further assistance, please visit our customer support site at <http://help.elsevier.com/app/answers/list/p/7923> Here you

can search for solutions on a range of topics, find answers to frequently asked questions and learn more about EM via interactive tutorials. You will also find our 24/7 support contact details should you need any further assistance from one of our customer support representatives.

---

In compliance with data protection regulations, you may request that we remove your personal registration details at any time. (Use the following URL: <https://www.editorialmanager.com/rene/login.asp?a=r>). Please contact the publication office if you have any questions.



Maria Yuliana &lt;mariayuliana@ukwms.ac.id&gt;

---

**Submission Confirmation for RENE-D-20-04164R1**

1 message

---

**Renewable Energy** <em@editorialmanager.com>  
Reply-To: Renewable Energy <rene@elsevier.com>  
To: Maria Yuliana <mariayuliana@ukwms.ac.id>

Thu, Dec 3, 2020 at 12:20 PM

Ms. Ref. No.: RENE-D-20-04164R1  
Title: IRON (II) IMPREGNATED DOUBLE-SHELLED HOLLOW MESOPOROUS SILICA AS ACID-BASE BIFUNCTIONAL CATALYST FOR THE CONVERSION OF LOW-QUALITY OIL TO METHYL ESTERS  
Article Type: Research Paper  
Journal: Renewable Energy

Dear Dr. Maria Yuliana,

This message is to acknowledge that we have received your revised manuscript for reconsideration for publication in Renewable Energy.

You may check the status of your manuscript by logging into the Editorial Manager as an author at <https://www.editorialmanager.com/rene/>.

Thank you for submitting your work to Renewable Energy.

Kind regards,

Editorial Manager  
Renewable Energy

\*\*\*\*\*

For further assistance, please visit our customer support site at <http://help.elsevier.com/app/answers/list/p/7923>. Here you can search for solutions on a range of topics, find answers to frequently asked questions and learn more about EM via interactive tutorials. You will also find our 24/7 support contact details should you need any further assistance from one of our customer support representatives.

---

In compliance with data protection regulations, you may request that we remove your personal registration details at any time. (Use the following URL: <https://www.editorialmanager.com/rene/login.asp?a=r>). Please contact the publication office if you have any questions.

## Renewable Energy

# IRON (II) IMPREGNATED DOUBLE-SHELLED HOLLOW MESOPOROUS SILICA AS ACID-BASE BIFUNCTIONAL CATALYST FOR THE CONVERSION OF LOW-QUALITY OIL TO METHYL ESTERS

--Manuscript Draft--

<b>Manuscript Number:</b>	RENE-D-20-04164R1
<b>Article Type:</b>	Research Paper
<b>Keywords:</b>	bifunctional catalyst; biodiesel; renewable energy; hollow mesoporous silica; iron impregnation; amine functionalization
<b>Corresponding Author:</b>	Maria Yuliana, Ph.D. Widya Mandala Catholic University Surabaya: Universitas Katolik Widya Mandala Surabaya Surabaya, East Java INDONESIA
<b>First Author:</b>	Stefanus Kevin Suryajaya
<b>Order of Authors:</b>	Stefanus Kevin Suryajaya Yohanes Ricky Mulyono Shella Permatasari Santoso Maria Yuliana, Ph.D. Alfin Kurniawan Aning Ayucitra Yueting Sun Sandy Budi Hartono Felycia Edi Soetaredjo Suryadi Ismadji
<b>Abstract:</b>	<p>To promote the use of low-quality oils in producing biodiesel, a bifunctional acid-base catalyst Fe/DS-HMS-NH<sub>2</sub> is fabricated using the two-step condensation technique. The obtained Fe/DS-HMS-NH<sub>2</sub> is of a doubled shell structure in spherical shape with a uniform size of 156 nm. Its hollow core (with a diameter of 86 nm) and two spatial shells with different active sites enables the esterification and transesterification reactions to be accomplished in a one-pot synthesis. The influences of four independent reaction variables on the yield of fatty acid methyl esters YF was studied, including catalyst loading <math>m_c</math>, reaction time <math>t</math>, reaction temperature <math>T</math>, and the methanol to degummed palm oil mass ratio <math>m/o</math>. The highest yield was obtained at 85.36% (w/w) when <math>m_c = 6\%</math> (w/w), <math>t = 4.5</math> h, <math>T = 60</math> oC, and <math>m/o = 6:1</math>. The Fe/DS-HMS-NH<sub>2</sub> shows a good recyclability with YF &gt; 80% (w/w) up to three reaction cycles.</p>

# **IRON (II) IMPREGNATED DOUBLE-SHELLED HOLLOW MESOPOROUS SILICA AS ACID-BASE BIFUNCTIONAL CATALYST FOR THE CONVERSION OF LOW-QUALITY OIL TO METHYL ESTERS**

Stefanus Kevin Suryajaya<sup>1,a</sup>, Yohanes Ricky Mulyono<sup>1,a</sup>, Shella Permatasari Santoso<sup>1,2</sup>, Maria Yuliana<sup>1\*</sup>, Alfin Kurniawan<sup>3</sup>, Aning Ayucitra<sup>1</sup>, Yueting Sun<sup>4</sup>, Sandy Budi Hartono<sup>1</sup>, Felycia Edi Soetaredjo<sup>1,2</sup>, Suryadi Ismadji<sup>1,2</sup>

<sup>1</sup> Department of Chemical Engineering, Widya Mandala Catholic University Surabaya, Kalijudan 37, Surabaya 60114, Indonesia

<sup>2</sup> Department of Chemical Engineering, National Taiwan University of Science and Technology, 43, Keelung Rd., Sec. 4, Taipei 10607, Taiwan

<sup>3</sup> Department of Chemistry, National Sun Yat-Sen University, Kaohsiung 80424, Taiwan

<sup>4</sup> Department of Mechanical Engineering, University of Birmingham, Edgbaston, Birmingham B15 2TT, United Kingdom

<sup>a</sup> These authors contributed equally to this work

\*Corresponding authors: Tel. (62) 31 3891264; Fax. (62) 31 3891267; Email address: [mariayuliana@ukwms.ac.id](mailto:mariayuliana@ukwms.ac.id) (M. Yuliana)



Widya Mandala Catholic University Surabaya  
Engineering Faculty  
**CHEMICAL ENGINEERING DEPARTMENT**  
Jl. Kalijudan 37 Surabaya 60114; Phone: +62 313893933 Fax: +62 31 3891267  
Website: <http://www.ukwms.ac.id>

---

December 2, 2020

**Professor Soteris Kalogirou**

Editor-in-Chief

*Renewable Energy*

Dear Professor Kalogirou,

On behalf of my co-author, I am writing to submit the revised manuscript for publication consideration in *Renewable Energy*. The details of the manuscript are as follows:

Title of Manuscript: **IRON (II) IMPREGNATED DOUBLE-SHELLED HOLLOW MESOPOROUS SILICA AS ACID-BASE BIFUNCTIONAL CATALYST FOR THE CONVERSION OF LOW-QUALITY OIL TO METHYL ESTERS**

Authors: Stefanus Kevin Suryajaya ([sstefanuskevin@gmail.com](mailto:sstefanuskevin@gmail.com)), Yohanes Ricky Mulyono ([rickymulyono96@gmail.com](mailto:rickymulyono96@gmail.com)), Shella Permatasari Santoso ([shella\\_p5@yahoo.com](mailto:shella_p5@yahoo.com)), Maria Yuliana, Alfin Kurniawan ([alfin\\_kur@yahoo.com](mailto:alfin_kur@yahoo.com)), Aning Ayucitra ([aayucitra@yahoo.com](mailto:aayucitra@yahoo.com)), Yueting Sun ([y.sun.9@bham.ac.uk](mailto:y.sun.9@bham.ac.uk)), Sandy Budi Hartono ([sandy@ukwms.ac.id](mailto:sandy@ukwms.ac.id)), Felycia Edi Soetaredjo ([felyciae@yahoo.com](mailto:felyciae@yahoo.com)), Suryadi Ismadji ([suryadiismadji@yahoo.com](mailto:suryadiismadji@yahoo.com))

Corresponding author:

Maria Yuliana; Department of Chemical Engineering; Widya Mandala Catholic University Surabaya; Kalijudan 37, Surabaya 60114, Indonesia

Tel: (62) 31 3891264; Fax. (62) 31 3891267;

E-mail: [mariayuliana@ukwms.ac.id](mailto:mariayuliana@ukwms.ac.id)

Keywords: *bifunctional catalyst; biodiesel; renewable energy; hollow mesoporous silica; iron impregnation; amine functionalization*

Word counts: 4798 words (excluding abstract, references, tables and figures)

We greatly appreciate the constructive comments and suggestions given by the editor and reviewers. We have addressed the major concerns of the reviewers and revised the manuscript accordingly. We also know of no conflicts of interest associated with this publication and there has been no significant financial support for this work that could have influenced its outcome. Furthermore, we have strictly prepared the manuscript in accordance with the journal and ethical guidelines.



Widya Mandala Catholic University Surabaya

Engineering Faculty

**CHEMICAL ENGINEERING DEPARTMENT**

Jl. Kalijudan 37 Surabaya 60114; Phone: +62 313893933 Fax: +62 31 3891267

Website: <http://www.ukwms.ac.id>

---

Thank you for your consideration. I am looking forward to hearing from your positive response.

Sincerely yours,

A handwritten signature in blue ink, consisting of a tall, thin vertical stroke followed by a series of loops and a horizontal line at the bottom.

Maria Yuliana



Widya Mandala Catholic University Surabaya  
Engineering Faculty  
**CHEMICAL ENGINEERING DEPARTMENT**  
Jl. Kalijudan 37 Surabaya 60114; Phone: +62 313893933 Fax: +62 31  
3891267  
Website: <http://www.ukwms.ac.id>

---

Journal: *Renewable Energy*

Title: **Iron (II) impregnated double-shelled hollow mesoporous silica as acid-base bifunctional catalyst for the conversion of low-quality oil to methyl esters**

Dear Editor,

We appreciate your useful comments and suggestions on our manuscript. We have modified the manuscript accordingly, and detailed corrections are listed below:

Subject Editor

- 1) The Graphical Abstract is too detailed - impossible to understand when reduced  
*Response: We have modified the graphical abstract, so that it does not give a very detailed information, but instead, provides only a concept of the research.*
- 2) Authors cited lists of 3 or more references without proper justification of their relevance. Authors must rearrange text or add at least a few words/a single sentence to justify why each reference must be cited.  
*Response: Every reference has been properly cited and justified in the manuscript (p.3 line 30-36; p.12 line 224-228; p.14 line 258-260; p.14 line 261-p.15 line 266).*
- 3) Authors must define how FAME yield was calculated.  
*Response: The calculation of FAME yield has been defined in equation (1) (p.8 line 142)*
- 4) Biodiesel characterization must be provided.  
*Response: We have added the procedures for biodiesel characterization in section 2.5 (p.8 line 157 – p.9 line 171). Meanwhile, the results are presented in p.19 line 332-347 and Table 4.*
- 5) Figures and Tables must be embedded in the text.  
*Response: We have embedded the Figures and Tables in the text.*
- 6) Ref. [6] - add language and title in English; reference is incomplete; similarly for Ref. [8], [14]  
*Response: We have added the English title for reference [1]. This reference has been also completed with the journal name, year, volume, and doi link, as seen in p.25 line 433-436. The authors have also agreed to remove several non-English references from the manuscript.*



Widya Mandala Catholic University Surabaya  
Engineering Faculty

**CHEMICAL ENGINEERING DEPARTMENT**

Jl. Kalijudan 37 Surabaya 60114; Phone: +62 313893933 Fax: +62 31  
3891267

Website: <http://www.ukwms.ac.id>

---

7) Check other references that are incomplete - missing journal, volume, etc.

*Response: We have revised the other incomplete references.*

#### *Reviewer #1*

1) The present manuscript titled with IRON (II) IMPREGNATED DOUBLE-SHELLED HOLLOW MESOPOROUS SILICA AS ACID-BASE BIFUNCTIONAL CATALYST FOR THE CONVERSION OF LOW-QUALITY OIL TO METHYL ESTERS" is a novel work performed by the authors and they explained well about the process efficiency and final compound out puts. Strongly agreeing to acceptance of the present manuscript with minor changes.

*Response: We are grateful for the reviews provided by the reviewer. The comments are especially encouraging for the authors. The detailed responses to the comments are provided below.*

2) Introduction required changes. It is too lengthy, and there is no any connection between the paragraphs.

*Response: We have modified the introduction part, as seen in p.2-4 (line 14-69).*

3) Present aim of the manuscript or research work should always come as the last paragraph of introduction.

*Response: We have moved the objectives of the study in the last paragraph of the introduction (p.4 line 57-69).*

4) Conclusion needs to be framed with future applications in concern with industrial orientation or application to field.

*Response: We have added a remark regarding this in p.24 line 421-424.*

#### *Reviewer #2*

1) This study reports a novel acid-base bifunctional catalyst Fe/DS-HMS-NH<sub>2</sub> for the production of FAME from the low-quality oil. This novel catalyst enables the esterification and transesterification reactions to take place in a single step, with a high yield of FAME of 85.36% achieved. Overall, this manuscript is well written. I recommend the acceptance of this manuscript with minor revisions. I have some technical comments for the authors to address.

*Response: The authors appreciate the reviewer's comments and have incorporated much of the feedback into the manuscript. We give a point-by-point reply to your comments below.*



- 2) The Graphic Abstract needs to be revised to a small size.

*Response: We have revised the graphical abstract to a smaller size.*

- 3) Please provide the compositional profile of FAME product after reaction.

*Response: We have provided the compositional profile of the final FAME product in p.19 line 338-347.*

- 4) What was the conversion of FFA after reaction? Please provide the content of FFA in the final product.

*Response: The content of FFA in the final product corresponds directly to the acid value (AV). AOCS Ca 5a-40 stated that to convert AC to FFA, we have to divide the AV by 1.99. As the AV of the final FAME product is measured at 0.24 (presented in Table 4, p.19), the amount of FFA is found to be 0.12% (w/w). We have also measured the FFA content in the glycerol phase, and it is observed at 1.13% (w/w). As the respective yields of FAME and glycerol are 85.36% (w/w) and 12.3% (w/w), the conversion of FFA after reaction is calculated to be 95.6%.*

- 5) The purity of FAME was calculated based on the peak area of FAME. How accurate is this method for the quantification of the FAME yield?

*Response: The purity of FAME is calculated based on (1) the total peak area of FAME and (2) the peak area of internal standard with a known concentration, as shown in equation (2) (p.9 line 167). This calculation is in accordance to the standard method of EN 14103, with little modifications.*

- 6) Provide the errors for the results in Table 1.

*Response: We have provided the error for  $Y_F$  in Table 1 (p.7)*

- 7) A significant reduction in the catalyst ability can be found after only 3 cycles. Is there any method to regenerate the catalyst?

*Response: In the present research, thermal treatment (high temperature calcination) is used to regenerate the catalyst. However, as stated in the conclusions, the authors will consider performing an in-depth evaluation to find a suitable technique for catalyst regeneration, in order to extend the catalyst lifetime. Several techniques currently discussed include (1) alcohol washing, (2) ultrasonic vibration, and (3) calcination under nitrogen condition.*

- 8) The authors need to benchmark the performance of the new catalyst with other existing or commercial catalysts in the literature.

*Response: We have compared the performance of Fe/DS-HMS-NH<sub>2</sub> with the existing catalysts reported in literatures, as seen in p.15 line 274-p.16 line 281.*



Widya Mandala Catholic University Surabaya  
Engineering Faculty

**CHEMICAL ENGINEERING DEPARTMENT**

Jl. Kalijudan 37 Surabaya 60114; Phone: +62 313893933 Fax: +62 31  
3891267

Website: <http://www.ukwms.ac.id>

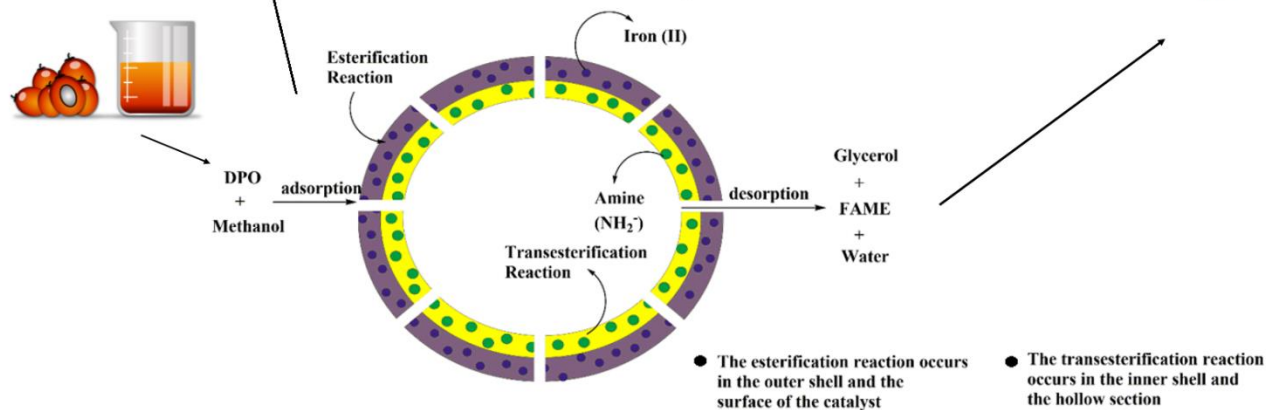
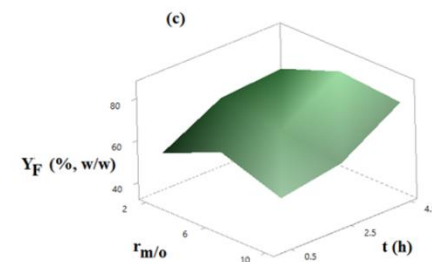
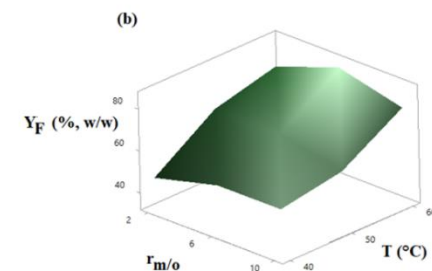
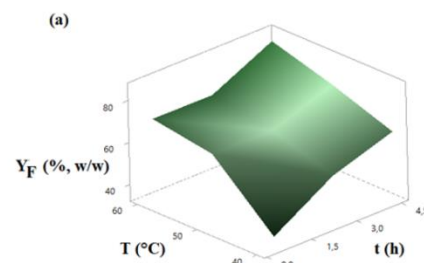
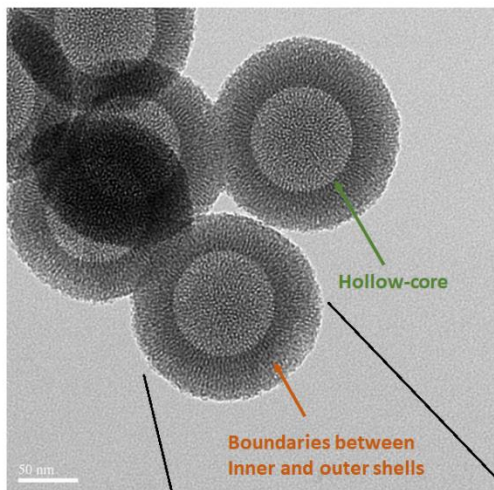
---

The manuscript has been resubmitted to your journal. We look forward to your positive response.

Sincerely yours,

A handwritten signature in blue ink, consisting of a large, stylized 'M' followed by a smaller 'i' and a horizontal line.

Maria Yuliana



- A novel acid-base bifunctional catalyst, Fe/DS-HMS-NH<sub>2</sub>, has been fabricated
- Fe/DS-HMS-NH<sub>2</sub> has been successfully employed to convert low-quality oil to FAME
- 85.36% of FAME yield was achieved from low-quality oil using Fe/DS-HMS-NH<sub>2</sub>
- The fuel properties of the final FAME product conform to ASTM D6751
- Fe/DS-HMS-NH<sub>2</sub> shows a good recyclability with FAME yield > 80% up to the third run

**1 Abstract**

2 To promote the use of low-quality oils in producing biodiesel, a bifunctional acid-base  
3 catalyst Fe/DS-HMS-NH<sub>2</sub> is fabricated using the two-step condensation technique. The obtained  
4 Fe/DS-HMS-NH<sub>2</sub> is of a doubled shell structure in spherical shape with a uniform size of 156 nm.  
5 Its hollow core (with a diameter of 86 nm) and two spatial shells with different active sites enables  
6 the esterification and transesterification reactions to be accomplished in a one-pot synthesis. The  
7 influences of four independent reaction variables on the yield of fatty acid methyl esters  $Y_F$  was  
8 studied, including catalyst loading  $m_c$ , reaction time  $t$ , reaction temperature  $T$ , and the methanol to  
9 degummed palm oil mass ratio  $r_{m/o}$ . The highest yield was obtained at 85.36% (w/w) when  $m_c =$   
10 6% (w/w),  $t = 4.5$  h,  $T = 60$  °C, and  $r_{m/o} = 6:1$ . The Fe/DS-HMS-NH<sub>2</sub> shows a good recyclability  
11 with  $Y_F > 80\%$  (w/w) up to three reaction cycles.

12 *Keywords: bifunctional catalyst; biodiesel; renewable energy; hollow mesoporous silica; iron*  
13 *impregnation; amine functionalization*

14 **1. Introduction<sup>1</sup>**

15           The global fuel demand is growing rapidly as it undergoes an extensive urbanization.  
16       Our heavy reliance on fossil fuel brings the risk of unstable market price and reduced fuel  
17       availability. The gas emission from fossil fuel combustion also causes environmental concerns.  
18       Therefore, developing an alternative fuel that is biodegradable, sustainable and with a low  
19       carbon emission is the most significant energy and environmental challenge for us in the  
20       coming decades [1,2]. Since 2006, the Indonesian government has been committed to reducing  
21       carbon emissions by replacing fossil fuels with biodiesel [3]. It is also declared that the use of  
22       biodiesel in diesel blend will be increased from B20 to B30 starting from 2020 [4], with a  
23       strategy to boost the domestic use of palm oil and lower down energy imports. Usually,  
24       biodiesel is obtained through the conventional transesterification process of refined oil [5].  
25       However, the technologies of utilizing non-refined oil, specifically the low-quality oil, have  
26       currently attracted extensive interests and are being developed. Various types of low-quality  
27       oil have been studied to produce high-quality biodiesel using sundry of technical routes,  
28       including the two steps acidic esterification followed by basic transesterification [6],

---

1

FFA	Free fatty acids
FAME	Fatty acid methyl esters
DPO	Degummed palm oil
CPO	Crude palm oil
SS-HMS-NH <sub>2</sub>	Single-shelled hollow mesoporous silica
DS-HMS-NH <sub>2</sub>	Double-shelled hollow mesoporous silica
Fe/DS-HMS-NH <sub>2</sub>	Iron (II) impregnated double-shelled hollow mesoporous silica

29 noncatalytic transesterification using alcohol under subcritical [7] and supercritical conditions  
30 [8], enzymatic transesterification [9] and solid-catalyzed transesterification [10]. Among the  
31 available routes, the use of heterogeneous (solid) catalysts has been attracting a growing  
32 interest in recent years, as it has the advantage of easier separation, tolerance to impurities  
33 (i.e., FFA, water and other minor compounds), and good reusability [11] which means  
34 minimal waste and toxic water production [12] and environmentally friendly [13]. Boey et al.  
35 (2011) and Lam et al. (2010) also stated that heterogeneous catalysts lower the product  
36 contamination level, and reduce the corrosion problem [14,15]. Various solid catalysts and  
37 their modifications have been reported, such as zirconia [16], silica impregnated with zinc  
38 stearate (ZS/Si) [17], heterogeneous KF/ZnO catalyst [18], heterogeneous Zn/I<sub>2</sub> catalyst [12].  
39 However, despite their insensitivity to impurities, these catalysts solely act as the mono  
40 functional catalysts, depending on their acidity nature and have the following disadvantages  
41 during the conversion of low-quality oil to biodiesel: (1) the reaction carried out in the  
42 presence of an acidic heterogeneous catalyst is slow, and at the same time, requires large  
43 amount of alcohol [19], meanwhile (2) the basic heterogeneous catalysts usually result in a  
44 lower biodiesel yield and purity, since this type of catalyst leaves the FFA unreacted during  
45 the reaction.

46 In this paper, we prepared and characterized a new class of heterogeneous catalyst,  
47 the double-shelled hollow mesoporous silica impregnated with divalent iron metal (Fe/DS-  
48 HMS-NH<sub>2</sub>), to be used as an acid-base bifunctional catalyst in the production of biodiesel  
49 from a low-quality oil. This catalyst enables a simple process of converting low-quality oil to  
50 biodiesel by combining the two processes of esterification and transesterification into a single-  
51 stage process. This is achieved by having double active surface layers that facilitate the two  
52 reactions to run simultaneously. The primary (inner) shell is designed to promote the

53 transesterification reaction by adding  $\text{-NH}_2$  as the basic site, while the outer layer is  
54 impregnated with the divalent iron (Fe (II)), which is selected as the impregnated metals due  
55 to its nature as a strong Lewis acid, and its ability to change the oxidation level and activate  
56 the substance during the process [20].

57 The synthesis, characterization and catalytic activity of the Fe/DS-HMS-NH<sub>2</sub> will be  
58 investigated in this paper. Its performance as an acid-base bifunctional catalyst for biodiesel  
59 preparation will be examined at various conditions, including catalyst loading  $m_c$  (% , w/w),  
60 reaction temperature  $T$  (°C), reaction time  $t$  (h), and the mass ratio of methanol to oil  $r_{m/o}$ . In  
61 this present research, degummed palm oil (DPO) is selected as the lipid material. With similar  
62 content of FFA and moisture as the crude palm oil (CPO), DPO is also classified as a low-  
63 quality oil, along with industrial fats, oils and greases, and other crude/waste lipids. Therefore,  
64 it is considered as a suitable raw material to determine the catalytic ability of Fe/DS-HMS-  
65 NH<sub>2</sub> in converting both FFA and triglycerides in DPO into biodiesel. We will also show that  
66 the Fe/DS-HMS-NH<sub>2</sub> can be regenerated and reused, which is regarded as an important feature  
67 for heterogeneous catalysts as it will reduce the cost for production and pollutant discharges  
68 [21,22]. The recyclability of the catalyst will be investigated at the operating condition giving  
69 the highest yield of fatty acid methyl esters (FAME)  $Y_F$ .

70

## 71 **2. Materials and methods**

### 72 **2.1 Materials**

73 CPO was collected from the local manufacturer in Indonesia. Prior to use, CPO was  
74 degummed using 1% (w/w) phosphoric acid (PA, 85% purity) at a temperature of 80 – 90°C  
75 for 30 min to reduce the phosphorus content. Several important characteristics of the  
76 degummed CPO (i.e., DPO), namely free fatty acid content, acid value, saponification value,

77 and moisture content were analyzed in accordance with the standard method of AOCS Ca 5a-  
78 40, Cd 3d-63, Cd 3d-25, and Ca 2e-84, respectively.

79 3-aminopropyl-triethoxysilane (APTES) was purchased from Fisher Scientific  
80 (Pittsburgh, USA), while other chemicals required for the fabrication of Fe/DS-HMS, namely  
81 iron (II) sulfate heptahydrate ( $\text{FeSO}_4 \cdot 7\text{H}_2\text{O}$ , 99.99% purity), tetraethylorthosilicate (TEOS),  
82 cetyltrimethylammonium bromide (CTAB), ethanol (98% purity), methanol (99,9% purity),  
83 hydrochloric acid (HCl, 37% purity), ammonium hydroxide solution ( $\text{NH}_4\text{OH}$ , 25% purity),  
84 and n-hexane (95% purity) were obtained from Merck (Merck, Germany). The FAMES  
85 standard (47885 U) containing 37 components FAME mix was procured from Supelco  
86 (Bellefonte, PA, USA). Ultra-high purity nitrogen gas (> 99.0% purity) was purchased from  
87 Aneka Gas Industry Pty. Ltd., Indonesia. All chemicals used in this study were of analytical  
88 grade and required no further purification.

89

## 90 **2.2 Preparation of DS-HMS-NH<sub>2</sub>**

91 In a typical synthesis, 0.14 g of CTAB, 20 ml of ethanol, 50 ml of deionized water and  
92 1 ml of  $\text{NH}_4\text{OH}$  solution were simultaneously introduced into a glass beaker and mixed for 15  
93 minutes at room temperature. Then 1 ml of TEOS was slowly added into the above solution  
94 and kept stirring for 24 hours. The precipitates were collected through centrifugation at 4500  
95 rpm for 30 min, triplicate ethanol washing, and drying at 120 °C overnight. After the  
96 calcination at 550°C for 6 h, the single shelled hollow mesoporous silica (SS-HMS-NH<sub>2</sub>) was  
97 obtained.

98 The outer shell of the particle was fabricated using a multilevel scheme based on SS-  
99 HMS-NH<sub>2</sub>. In a typical synthesis, 0.5 g CTAB, 18 ml deionized water, and 50 ml of ethanol  
100 were introduced into a beaker glass. Meanwhile, 0.063 g of SS-HMS-NH<sub>2</sub> was added into a

101 mixture of 4 ml deionized water and 8.5 ml of 25% (w/w)  $\text{NH}_4\text{OH}$  solution. The above two  
102 solutions were then combined and stirred for 15 min at 250 rpm, after which 100  $\mu\text{l}$  TEOS  
103 and 21  $\mu\text{l}$  APTES were slowly added into it and the mixture was kept stirring for 24 h to allow  
104 the condensation reaction of silica. Finally, the solid product was collected by centrifugation  
105 at 4500 rpm for 15 min, which was then repeatedly washed with 60 ml of ethanol and 4 ml of  
106 HCl, and oven-dried at 120°C. The dried product was calcined at 550 °C for 6 h to obtain  
107 double-shelled hollow mesoporous silica (DS-HMS-NH<sub>2</sub>).

108

### 109 **2.3 Iron (II) impregnation onto DS-HMS-NH<sub>2</sub> surface**

110 The impregnation of divalent iron onto the DS-HMS-NH<sub>2</sub> surface was achieved as  
111 follows to fabricate Fe/DS-HMS-NH<sub>2</sub> catalysts. In a typical synthesis, 0.1 g DS-HMS-NH<sub>2</sub>  
112 was mixed with 50 ml of deionized water under sonication for 30 minutes at room temperature.  
113 Meanwhile, two separate solutions were prepared: (1) 5 mg of  $\text{FeSO}_4 \cdot 7\text{H}_2\text{O}$  was dissolved in  
114 50 ml of deionized water, and (2) 0.2 g of CTAB was dissolved in 10 ml ethanol. Solution (1)  
115 and (2) were then added into the DS-HMS-NH<sub>2</sub> solution and stirred for 12 hours at ambient  
116 conditions. The Fe/DS-HMS-NH<sub>2</sub> precipitates were separated by a centrifugation at 4500 rpm  
117 for 15 min, and then dried at 120 °C for 12 h and calcined at 550 °C for 5 hours to obtain the  
118 Fe/DS-HMS-NH<sub>2</sub> powder.

119

### 120 **2.4. Catalytic activity of Fe/DS-HMS-NH<sub>2</sub> at various reaction conditions**

121 The *in-situ* esterification/transesterification reactions from DPO to FAME were carried  
122 out in a glass flask equipped with a reflux condenser and external heater under constant  
123 magnetic stirring (250 rpm) at various conditions. Specifically, the influence of four reaction  
124 parameters were investigated due to their relevance to industrial applications: catalyst loading

125  $m_c$  (% , w/w), reaction temperature  $T$  ( $^{\circ}\text{C}$ ), reaction time  $t$  (h), and the mass ratio of methanol  
 126 to DPO  $r_{m/o}$ . To determine the amount of Fe/DS-HMS-NH<sub>2</sub> catalyst that produces the  
 127 maximum FAME yield  $Y_F$ , a few reactions were carried out with different amounts of Fe/DS-  
 128 HMS-NH<sub>2</sub> ( $m_c = 2\%$ ,  $4\%$ ,  $6\%$ ,  $8\%$ , w/w) at the following condition:  $T = 60$   $^{\circ}\text{C}$ ,  $t = 4.5$  h and  
 129  $r_{m/o} = 10:1$ . Once the optimum catalyst loading is obtained, the catalytic activity of Fe/DS-  
 130 HMS-NH<sub>2</sub> was investigated within an experimental matrix defined by  $T = 40$   $^{\circ}\text{C}$ ,  $50$   $^{\circ}\text{C}$ ,  $60$   $^{\circ}\text{C}$ ,  
 131  $t = 0.5$  h,  $2.5$  h,  $4.5$  h, and  $r_{m/o} = 2:1$ ,  $6:1$ ,  $10:1$ . The experimental runs were designed in a  
 132 random order using face centered-central composite design (CCF-CCD) as listed in Table 1.  
 133 All the experimental runs were conducted with the same procedure.

134 **Table 1.** Experimental matrix at the optimum catalyst loading  $m_c = 6\%$  (w/w)

Run	Input Parameters			$Y_F$ (% , w/w)
	$T$ ( $^{\circ}\text{C}$ )	$t$ (h)	$r_{m/o}$	
1	60	4.5	10:1	85.24 $\pm$ 1.19
2	40	0.5	10:1	40.27 $\pm$ 0.58
3	40	2.5	6:1	55.09 $\pm$ 0.76
4	50	4.5	6:1	75.15 $\pm$ 0.65
5	50	2.5	10:1	60.07 $\pm$ 0.44
6	40	0.5	2:1	35.19 $\pm$ 0.92
7	40	4.5	10:1	70.22 $\pm$ 1.01
8	50	2.5	2:1	67.03 $\pm$ 0.51
9	60	4.5	2:1	80.11 $\pm$ 0.68
10	50	2.5	6:1	65.16 $\pm$ 0.47
11	50	2.5	6:1	66.96 $\pm$ 0.73
12	50	2.5	6:1	65.87 $\pm$ 0.79
13	50	0.5	6:1	65.01 $\pm$ 0.37
14	60	4.5	6:1	85.36 $\pm$ 0.62
15	50	2.5	6:1	63.21 $\pm$ 0.42
16	60	0.5	10:1	70.01 $\pm$ 0.56
17	50	2.5	6:1	63.20 $\pm$ 0.69
18	50	2.5	6:1	67.18 $\pm$ 0.45
19	60	0.5	2:1	69.09 $\pm$ 0.53
20	40	4.5	2:1	59.11 $\pm$ 0.78

135  
 136 After the reaction completed, Fe/DS-HMS-NH<sub>2</sub> catalyst was recovered by  
 137 centrifugation at 4500 rpm for 15 min, and calcination at 550  $^{\circ}\text{C}$  for 5 h. The liquid product

138 was subjected to a two-stage liquid-liquid extraction using methanol and n-hexane  
139 sequentially for purification. Then the FAME-rich phase was separated from the by-products  
140 (i.e., glycerol, excess methanol, soap, and the other unwanted materials) and evaporated under  
141 vacuum to obtain the final FAME product. As an evaluation of the catalytic activity of Fe/DS-  
142 HMS-NH<sub>2</sub>, the yield of FAME was calculated by the following equation:

$$Y_F (\%, \text{ w/w}) = \frac{m_F p_F}{m_s} \times 100 \quad (1)$$

143 Where  $m_F$  is the mass of the final FAME product (g),  $p_F$  is the FAME purity (% w/w)  
144 obtained from equation (2) shown in the next section, and  $m_s$  is the total mass of the DPO (g).  
145

## 146 **2.5 Characterization of Fe/DS-HMS-NH<sub>2</sub> catalyst and FAME**

147 The characterization of Fe/DS-HMS-NH<sub>2</sub> was conducted using field-emission  
148 scanning electron microscopy with energy dispersive X-Ray spectroscopy (FESEM/EDX),  
149 transmission electron microscopy (TEM), nitrogen sorption, and thermogravimetric analysis  
150 (TGA). The FESEM/EDX images were taken on a JEOL JSM-6500 F (Jeol Ltd., Japan)  
151 running at 15 kV with a working distance of 12.4 mm, while TEM was carried out on JEOL  
152 JEM-2100 with an accelerating voltage of 200 kV. Nitrogen sorption analysis was conducted  
153 at 77 K on a Micrometrics ASAP 2010 Sorption Analyzer. The sample was degassed at 423  
154 K prior to analysis. To determine the thermal stability and volatile component fraction of the  
155 Fe/DS-HMS-NH<sub>2</sub> catalyst, a TGA analysis was performed using TG/DTA Diamond  
156 instrument (Perkin-Elmer, Japan).

157 The final FAME product characteristics, including its kinematic viscosity (at 40°C),  
158 flashpoint, cetane number, acid value and calorific value were determined according to the  
159 standard methods of ASTM D445, ASTM D93, ASTM D613, ASTM D664, and ASTM D240,  
160 respectively. The purity of FAME ( $p_F$ ) in the final product was analyzed using a gas

161 chromatograph (Shimadzu GC-2014) equipped with a split/splitless injector and a flame  
162 ionization detector (FID). The stationary phase used for separation was the narrow bore non-  
163 polar DB-WAX column (30 m × 0.25 mm ID × 0.25 μm film thickness, Agilent Technology,  
164 CA), and the temperature profile for the analysis was in accordance with the study conducted  
165 by Harijaya et al. (2019) [23]. Methyl heptadecanoate (MH) was used as an internal standard,  
166 while an external FAME reference (47885 U, containing 37 components FAME standard mix)  
167 was used to obtain the FAME compositional profile.  $p_F$  is calculated by the following equation:

$$p_F (\%, w/w) = \left( \frac{\sum A_F - A_{MH}}{A_{MH}} \right) \left( \frac{V_{MH} C_{MH}}{m_F} \right) \times 100 \quad (2)$$

168 Where  $\sum A_F$  is the total peak area of FAME,  $A_{MH}$  is the corresponding area of methyl  
169 heptadecanoate (MH) peak,  $V_{MH}$  is the volume of MH solution (ml),  $C_{MH}$  is the actual  
170 concentration of MH solution (g/ml), and  $m_F$  is the actual mass of the final FAME product  
171 (g).

172

## 173 **2.6 Recyclability of Fe/DS-HMS-NH<sub>2</sub>**

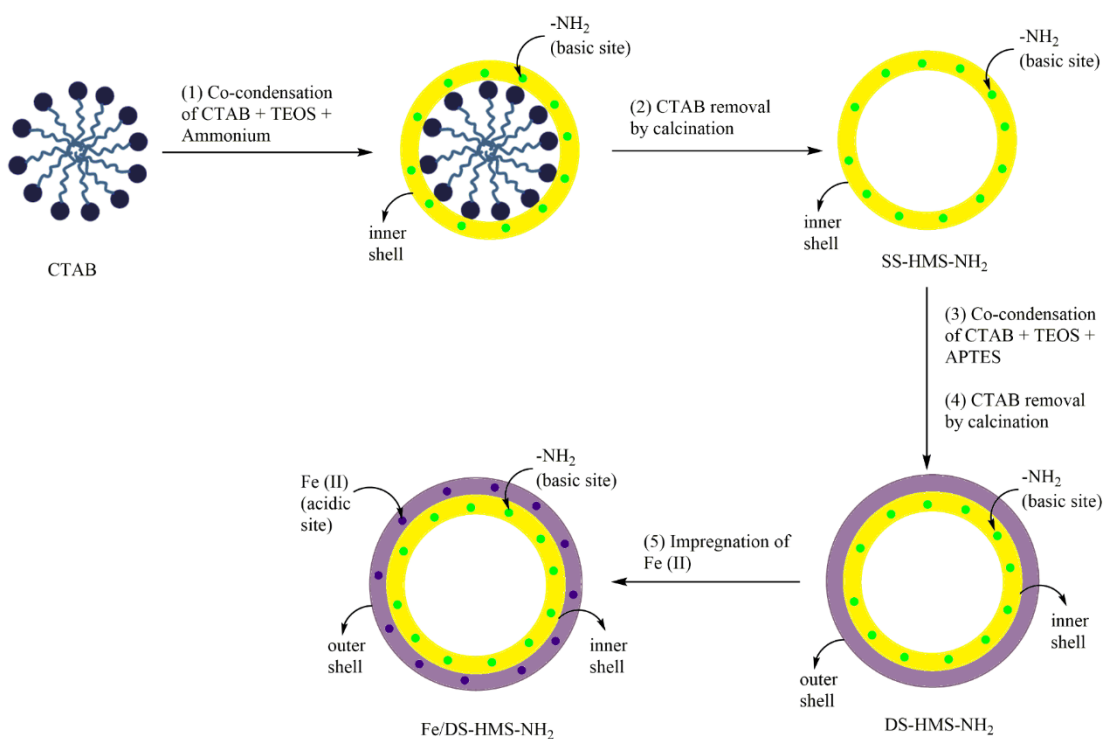
174 Fe/DS-HMS-NH<sub>2</sub> was repeatedly used for the transesterification process at the  
175 operating condition where the maximum yield of FAME was obtained. The recyclability of  
176 Fe/DS-HMS-NH<sub>2</sub> was determined by the number of repetitions until when the yield became  
177 lower than 80% (w/w). The purity and yield of FAME were analyzed according to the  
178 procedures in section 2.4-2.5. All experiments were carried out in triplicates to verify the  
179 results.

180

## 181 **3. Result and Discussions**

### 182 **3.1 The mechanism scheme of Fe/DS-HMS-NH<sub>2</sub> fabrication**

183 The Fe/DS-HMS-NH<sub>2</sub> was synthesized by a two-step co-condensation technique.  
184 The mechanism scheme in Figure 1 illustrates the fabrication route: (1) firstly, TEOS and  
185 CTAB undergo a co-condensation reaction along with the ammonium solution; (2) then  
186 CTAB, the soft template of the core, is removed by calcination, and the SS-HMS-NH<sub>2</sub> is thus  
187 formed; (3) TEOS, APTES, and CTAB undergo another co-condensation reaction on the outer  
188 surface of the SS-HMS-NH<sub>2</sub> spheres; (4) DS-HMS-NH<sub>2</sub> nanosphere is obtained by removing  
189 CTAB and APTES in calcination; (5) the divalent iron (Fe (II)) was incorporated onto the  
190 surface of DS-HMS-NH<sub>2</sub> by a traditional wet impregnation technique, and the Fe/DS-HMS-  
191 NH<sub>2</sub> nanosphere is obtained.



192  
193 **Figure 1.** The mechanism scheme of Fe/DS-HMS-NH<sub>2</sub> fabrication.

194  
195 **3.2 Characterization of Fe/DS-HMS-NH<sub>2</sub> catalysts**

196 Figure 2a, c–d present the SEM and TEM images of the Fe/DS-HMS-NH<sub>2</sub> catalyst  
197 synthesized by the co-condensation technique. The catalyst is spherical with a uniform size at  
198 *ca.* 156 nm (Figure 2a). Notably, Fe/DS-HMS-NH<sub>2</sub> is composed of two shell layers, indicated  
199 by the darker color of the inner shell in Figure 2c-d. Its hollow-core structure is clearly  
200 presented with the diameter of 86 nm (Figure 2d). The shell thicknesses of the inner and outer  
201 layer of Fe/DS-HMS-NH<sub>2</sub>, are 22 nm and 13 nm, respectively. The impregnation of Fe (II) on  
202 the surface of the silica layer was successful, evidenced from the EDX result showing a  
203 percentage of 2.87% (Figure 2b). Based on the fabrication procedure, it was reasonable to  
204 consider that the Fe (II) sites and basic amino sites were spatially isolated and located in  
205 different shells.

206 The textural properties of Fe/DS-HMS-NH<sub>2</sub> analyzed by the nitrogen sorption are  
207 presented in Table 2 and Figure 2e. The nitrogen adsorption and desorption isotherm of the  
208 catalyst exhibits a typical type-IV isotherm, indicating the presence of a mesoporous structure  
209 with worm-like capillary pores molded by the CTAB micelles. The pore size of the  
210 mesoporous structure is found to be 2.43 nm (Figure 2e (inset)). A steep increase of the  
211 nitrogen adsorption amount at  $p/p^0$  close to unity also suggests that there are macropores  
212 structure within the particle, corresponding to the hollow core. Similar adsorption and  
213 desorption profile also pointed out that the pores are highly accessible. The specific surface  
214 area  $S_{\text{BET}}$  obtained in this study was 782.84 m<sup>2</sup>/g, lower than the value 1100 – 1350 m<sup>2</sup>/g for  
215 a similar double shelled hollow mesoporous silica [22]. Such a discrepancy was likely due to  
216 the reason that it was strongly influenced by the shell thickness. Zhou et al. (2014) reported  
217 that when the thickness of hollow mesoporous silica nanoparticles (HMSN) increases from  
218 46 nm to 82 nm, the surface area of HMSN particles was declined from 986 m<sup>2</sup>/g to 614 m<sup>2</sup>/g

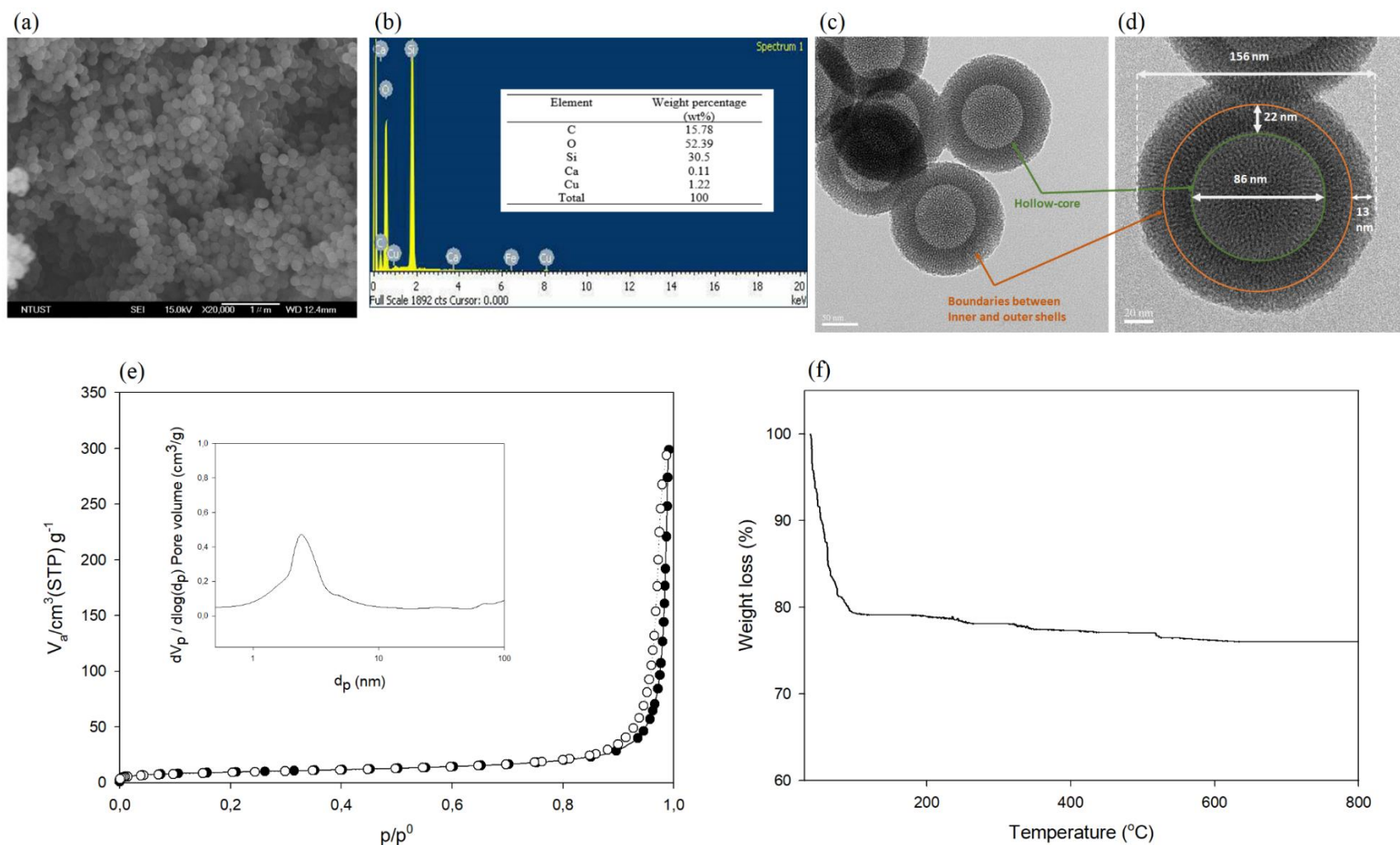
219 [24]. Zhou et al. (2014) and Cao et al. (2011) also observed that an increase in the particle  
 220 mass due to the addition of TEOS and CTAB in the synthesis of the second shell lowers the  
 221 surface area, since the amount of TEOS during the fabrication is directly proportional to the  
 222 thickness of the shell [24,25]. Meanwhile, the pore volume of Fe/DS-HMS-NH<sub>2</sub> (0.64 cm<sup>3</sup>/g)  
 223 was found to be slightly higher than that reported by You et al. (2018) (0.61 cm<sup>3</sup>/g) [22].  
 224 Based on its textural analysis, Fe/DS-HMS-NH<sub>2</sub> possesses comparable specific surface area  
 225 and pore volume with those of existing heterogeneous catalysts (i.e., HMS-Al@MS-NH<sub>2</sub> [22],  
 226 char-based catalyst [26],  $\gamma$ -alumina industrial-grade catalyst [27], and copper-based metal-  
 227 organic framework [28]), which usually range from 200 – 1300 cm<sup>2</sup>/g and 0.18 – 1.68 cm<sup>3</sup>/g  
 228 respectively.

229 **Table 2.** Textural properties of Fe/DS-HMS-NH<sub>2</sub>.

Material	$S_{\text{BET}}$ (cm <sup>2</sup> /g)	Pore volume (cm <sup>3</sup> /g)	Pore size (nm)
Fe/DS-HMS-NH <sub>2</sub>	782.84	0.64	2.43

230 To demonstrate the feasibility of Fe/DS-HMS-NH<sub>2</sub> for the reactions at an elevated  
 231 temperature, its thermal stability was investigated. The TGA profile in Figure 2f shows a 20%  
 232 decrease in weight up to the temperature of 100°C, attributed to the removal of free moisture  
 233 content. Further heating up to 800 °C does not significantly decrease the mass of Fe/DS-HMS-  
 234 NH<sub>2</sub>, suggesting that the catalyst is stable at high temperatures [29]. Therefore, our Fe/DS-  
 235 HMS-NH<sub>2</sub> can be considered as a promising heterogeneous catalyst for the *in-situ*  
 236 esterification/transesterification reaction.

237



239 **Figure 2.** (a) SEM image, (b) Elemental composition, (c) – (d) TEM images at various magnifications, (c) BJH pore size distribution  
 240 curve, (e) Nitrogen adsorption-desorption isotherm with BJH pore size distribution curve (inset), (f) Thermogravimetric profile of the  
 241 Fe/DS-HMS-NH<sub>2</sub> catalyst.

242 **3.3 The catalytic activity of Fe/DS-HMS-NH<sub>2</sub> in the *in-situ* esterification/transesterification**  
243 **of DPO**

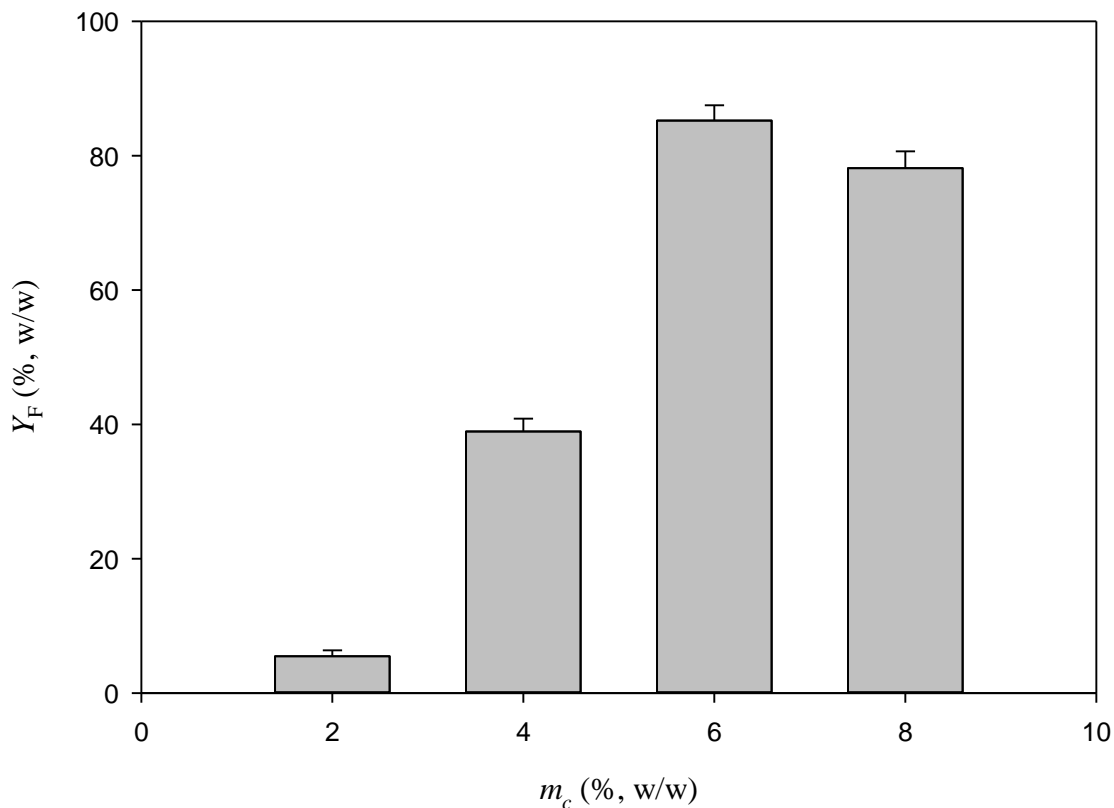
244 The characteristics of DPO as the raw material for biodiesel preparation are  
245 presented in Table 3. As homogenous catalysts are sensitive to impurities, the conversion of  
246 DPO to FAME for biodiesel production usually requires two reaction steps, namely acid-  
247 catalyzed esterification to lower the FFA content by converting them into FAME, and basic  
248 catalyzed transesterification to convert the acyl glycerides into FAME. However,  
249 heterogeneous catalysts can have good tolerance towards the FFA and water content in the  
250 lipid materials [10]; for Fe/DS-HMS-NH<sub>2</sub>, its two spatial shells with different active sites can  
251 facilitate the above two reactions in a one-pot process, and therefore efficient conversion from  
252 DPO to FAME is achieved in a single step.

253 **Table 3.** Characteristics of DPO.

Parameter	Value
FFA (% w/w)	5.54
Moisture Content (% w/w)	0.20
Saponification Value (mg KOH/g DPO)	234.08
Acid Value (mg KOH/g DPO)	12.04
Molecular weight (g/mol)	756.62

254  
255 Figure 3 presents the FAME yield obtained at various Fe/DS-HMS-NH<sub>2</sub> loadings  
256 at the condition of  $T = 60$  °C,  $t = 4.5$  h and  $r_{m/o} = 10:1$ . The results indicate that the yield of  
257 FAME is proportional to the number of active sites offered by the Fe/DS-HMS-NH<sub>2</sub> [30,31];  
258 therefore  $Y_F$  increases with  $m_c$  when the latter is within 6% (w/w). This agrees well with  
259 previous work on biodiesel production using different solid catalysts, e.g., pomacea sp. shell-  
260 based CaO [30], sulfonated biochar [31], and KI/mesoporous silica [32]. A maximum yield  
261 85.24% (w/w) is obtained when the catalyst loading  $m_c = 6\%$  (w/w). Further increase of the  
262 Fe/DS-HMS-NH<sub>2</sub> results in a reduced yield of FAME, which is probably due to the

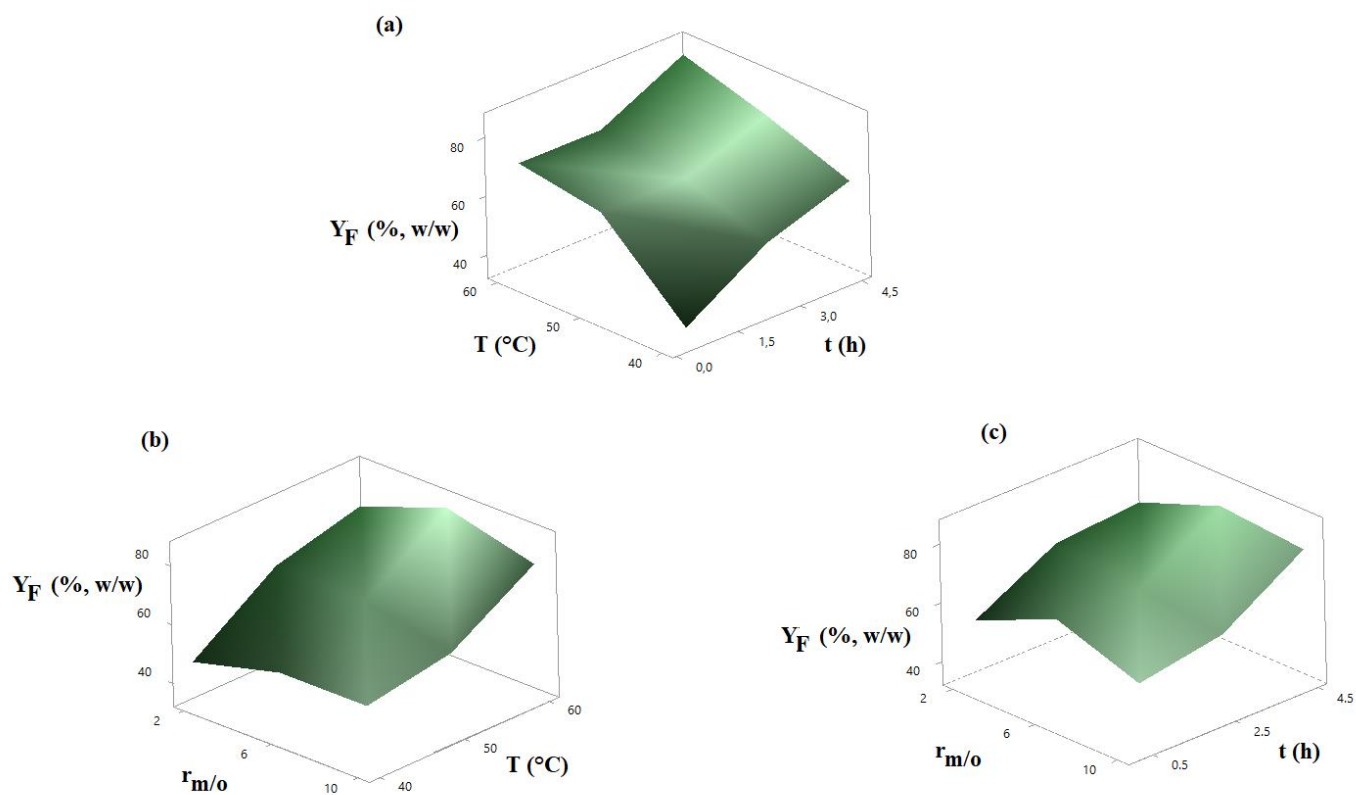
263 aggregation and inconsistent dispersity of the catalyst in the reaction system of an enhanced  
264 viscosity [33,34]. Cai et al. (2018) and Samart et al. (2010) also mentioned that excess catalyst  
265 may also disturbed the mixing between the reactants, due to stronger adsorption of the  
266 reactants to the catalyst [35,36].



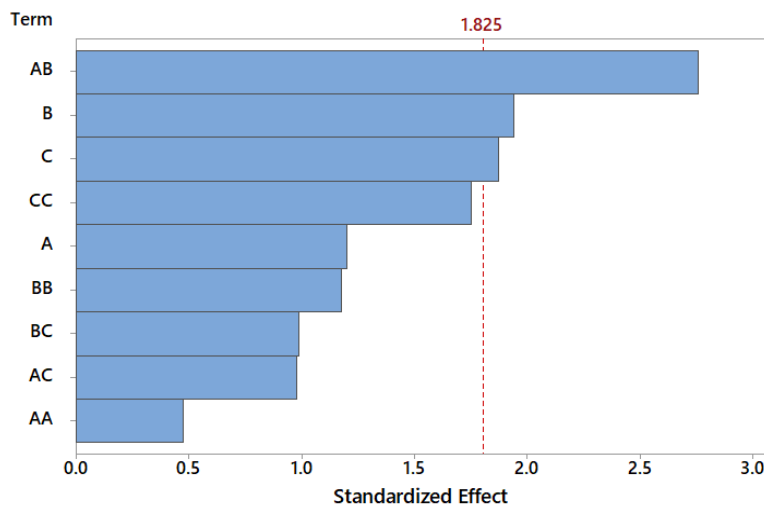
267 **Figure 3.** The yield of FAME at various Fe/DS-HMS-NH<sub>2</sub> loadings with the reaction  
268 condition of  $T = 60$  °C,  $t = 4.5$  h and  $r_{m/o} = 10:1$ .  
269  
270

271 At a constant catalyst loading  $m_c = 6\%$  (w/w), Figure 4 and Table 1 present the  
272 FAME yield  $Y_F$  at various reaction time  $t$ , temperature  $T$ , and mass ratio of methanol to DPO  
273  $r_{m/o}$ . The maximum  $Y_F = 85.36\%$  (w/w) (with a purity of 97.89% (w/w)) is obtained at the  
274 condition of  $T = 60$  °C,  $t = 4.5$  h,  $r_{m/o} = 6:1$ . This result indicates that Fe/DS-HMS-NH<sub>2</sub> is  
275 superior, specifically in terms of reaction time and temperature, compared with the existing  
276 catalysts reported in the literatures. Pal et al. (2011) mentioned that 94% (w/w) FAME yield

277 was achieved only after 24 h reaction using 7% Zn-doped mesoporous silica as the catalyst  
278 loading [17]. Long reaction time (8 h) were also reported by Xie and Li (2006) using alumina-  
279 supported KI [37]. Meanwhile, Omar and Amin (2011) stated that the transesterification of  
280 waste cooking oil over alkaline/zirconia catalyst requires high temperature (115.5°C) to  
281 achieve 79.7% (w/w) FAME yield [16].



283 **Figure 4.** The FAME yield  $Y_F$  (% , w/w) at various (a)  $T$  and  $t$ , (b)  $T$  and  $r_{m/o}$ , and (c)  $t$  and  $r_{m/o}$ .  
284



285  
286  
287  
288  
289

**Figure 5.** Pareto chart of the standardized effect for the biodiesel preparation with Fe/DS-HMS-NH<sub>2</sub>, using  $Y_F$  as the response at a 95% confidence interval where  $A = T$ ,  $B = t$ ,  $C = r_{m/o}$ .

290

Based on the experimental results, the reaction time  $t$  was the most significant factor,

291

followed by  $r_{m/o}$  and  $T$ , which is supported by the Pareto chart of the standardized effect in

292

Figure 5 showing that  $t$ ,  $r_{m/o}$ , and the two-way interaction between  $t$  and  $T$  are the three

293

significant parameters in the reaction system. The effect of reaction temperature on the

294

production of biodiesel using Fe/DS-HMS-NH<sub>2</sub> is shown in Figure 4a–b. An increased

295

reaction temperature contributes to a higher yield, with the maximum achieved at 60°C, which

296

is related to the fact that both esterification and transesterification reaction are endothermic

297

and reversible [38,39]. At a higher reaction temperature, the kinetic energy and mobility of

298

reactant molecules increase, promoting the collisions between the molecules and Fe/DS-

299

HMS-NH<sub>2</sub> particles which then increases the reaction rate constant and shift the reaction

300

towards the product [38,40]. Moreover, the mass transfer of the reactant molecules through

301

the boundary layer of Fe/DS-HMS-NH<sub>2</sub> is also accelerated at an elevated temperature,

302

resulting in the faster diffusion of the reactants into the pore of catalyst; hence, improving the

303

FAME yield.

304                   Specifically, Figures 4a and c show a significant increase of the FAME yield by  
305 extending the duration of the biodiesel synthesis from 0.5 h to 4.5 h, at a constant temperature  
306 or mass ratio of methanol to DPO. Longer reaction time provides sufficient time for the  
307 reactants to reach the active sites of Fe/DS-HMS-NH<sub>2</sub> through adsorption and diffusion, and  
308 convert DPO into FAME [41]. Meanwhile, prolonged duration of reaction also gives the  
309 catalyst more time to adsorb the reactant and desorb the reaction product [28]. Wei et al. (2009)  
310 also mentioned that adsorption and desorption of reactants from the catalyst is the rate-  
311 determining step in the overall reaction [42]. Therefore, allowing longer contact between the  
312 reactant molecules and the catalyst ensures high conversions of FFA and acyl glycerides to  
313 FAME.

314                   Stoichiometrically, three moles of methanol are required to react with one mole of  
315 triglycerides in the transesterification reaction, while one mole of methanol is needed to react  
316 with one mole of free fatty acids in the esterification reaction [43,44]. Both reactions are  
317 known to be reversible; thus, the amount of methanol in the two reactions is usually provided  
318 in excess to shift the reaction equilibrium to the product side. As seen from Figure 4b–c,  
319 having excess methanol from  $r_{m/o} = 2:1$  to  $r_{m/o} = 6:1$  contributes to a higher FAME yield,  
320 while further addition up to  $r_{m/o} = 10:1$  has no improvement. While most studies agree that  
321 excess methanol is desirable to allow more frequent interactions between the lipid and  
322 methanol triggering the formation of FAME, Pangestu et al. (2019) found that excess  
323 methanol may also accelerate the production of glycerol despite the higher yield of FAME  
324 [28]. As the esterification and transesterification are both reversible, a higher concentration  
325 of glycerol in the reaction system may induce a reverse reaction to the reactant side, creating  
326 an equilibrium between the products and reactants [28]. Hayyan et al. (2011) also reported  
327 that an excessive amount of methanol causes higher solubility of glycerol in the FAME phase

328 that could lead to a complicated separation between biodiesel and glycerol [45]. Moreover,  
 329 from the techno-economic viewpoint, the higher mass ratio of methanol to DPO also increases  
 330 the material and processing cost [23,45]. Therefore, it can be concluded that the optimum  
 331 level is  $r_{m/o} = 6:1$ .

332 The fuel properties of the final FAME product are presented in Table 4. The  
 333 measurement results indicate that the product resulted in this study has a comparable  
 334 combustion and flow properties with those of the commercial biodiesel. The calorific value  
 335 (45.143 MJ/kg) is also within the range required in the common petrodiesel (42-46 MJ/kg).

336 **Table 4.** Fuel properties of the final FAME product

Properties	Methods	Unit	Final FAME product	ASTM D6751
Kinematic viscosity (at 40°C)	ASTM D445	mm <sup>2</sup> /s	2.64	1.9 – 6.0
Flashpoint	ASTM D93	°C	164.2	93 min
Cetane number	ASTM D613	-	55.7	47 min
Acid value	ASTM D664	mg KOH/g	0.24	0.5 max
Calorific value	ASTM D240	MJ/kg	45.143	-

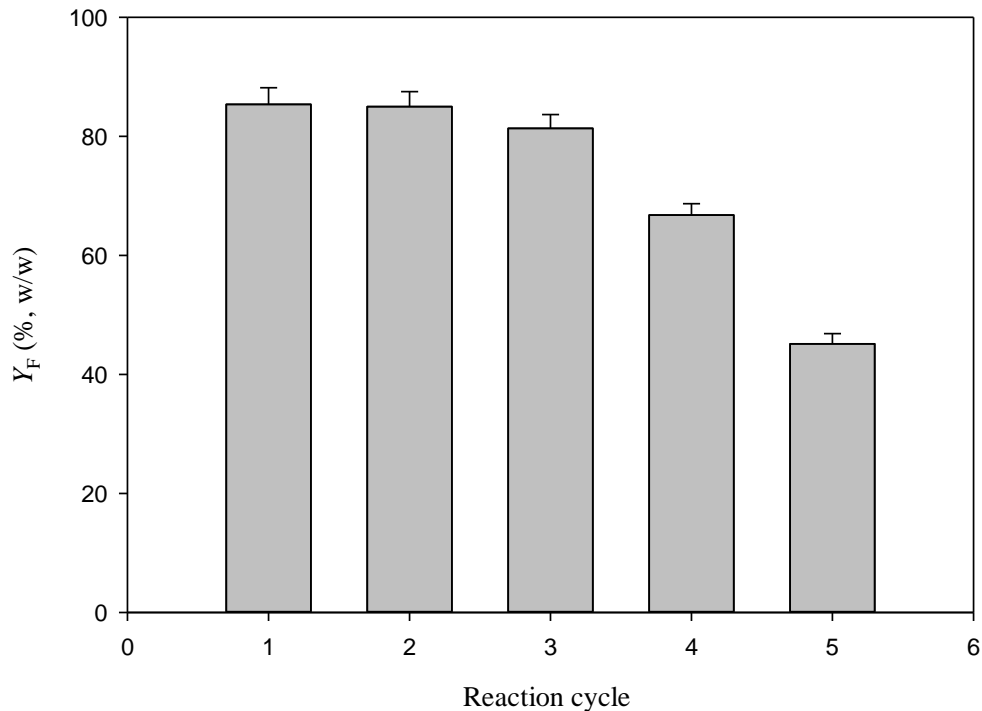
337

338 Meanwhile, its compositional profile is obtained by comparing the methyl ester  
 339 peaks in the chromatogram with those in the external FAME standard (47885 U, containing  
 340 37 components FAME standard mix). The 12 identified peaks are 3.05% myristoleic acid  
 341 methyl ester (C14:1), 2.37% cis-10-pentadecanoic acid methyl ester (C15:1), 35.78% palmitic  
 342 acid methyl ester (C16:0), 8.13% palmitoleic acid methyl ester (C16:1), 8.36% stearic acid  
 343 methyl ester (C18:0), 32.57% oleic acid methyl ester (C18:1n9c), 3.05% elaidic acid methyl  
 344 ester (C18:1n9t), 1.17% cis-8,11,14-eicosatrienoic acid methyl ester (C20:3n6), 2.48%  
 345 arachidonic acid methyl ester (C20:4n6), 0.52% cis-5,8,11,14,17-eicosapentaenoic acid  
 346 methyl ester (C20:5n3), 1.07% erucic acid methyl ester (C22:1n9), 1.45 % cis-13,16-  
 347 docosadienoic acid methyl ester (C22:2).

348

### 349 **3.4 Recyclability of Fe/DS-HMS-NH<sub>2</sub>**

350           An important feature of using heterogeneous catalysts for biodiesel preparation is  
351 its recyclability. In order to determine the recyclability of Fe/DS-HMS-NH<sub>2</sub>, several reaction  
352 cycles were conducted in series using the operating condition of  $m_c = 6\%$  (w/w),  $T = 60\text{ }^\circ\text{C}$ ,  $t$   
353  $= 4.5\text{ h}$ ,  $r_{m/o} = 6:1$ . Fe/DS-HMS-NH<sub>2</sub> was recovered following the method described in section  
354 2.4, while fresh methanol and DPO were used in every cycle. The catalytic ability of the  
355 recycled Fe/DS-HMS-NH<sub>2</sub> for *in-situ* esterification/transesterification process is presented in  
356 Figure 6. The result indicates that recycled Fe/DS-HMS-NH<sub>2</sub> can maintain a high yield of  
357 FAME above 80% (w/w) until the third cycle, close to the yield of fresh catalyst 85.36%  
358 (w/w). The purity of FAME for the first three cycles are 97.89%, 97.66% and 98.01% (w/w)  
359 respectively, higher than the commercial purity (96.5%, w/w). These results indicate that the  
360 catalytic activity of Fe/DS-HMS-NH<sub>2</sub> is maintained at a high level after regeneration. A  
361 significant drop in catalytic ability is observed from the forth cycle in Figure 6; similar  
362 performance has been reported for some other heterogeneous catalysts where three cycles  
363 seem to be an average number in term of their recyclability [46,47]. The catalytic deactivation  
364 of Fe/DS-HMS-NH<sub>2</sub> is generally due to the pore blockage caused by the contact between  
365 active sites on the catalyst surface and the deactivation-induced components, namely free  
366 glycerol, acyl glycerides, and biodiesel. Moreover, the high content of FFA in DPO also plays  
367 an important role in the deactivation of Fe/DS-HMS-NH<sub>2</sub> catalyst because FFA tends to  
368 neutralize the basic sites in the inner shell of Fe/DS-HMS-NH<sub>2</sub> [48], resulting in the  
369 generation of amine-carboxylate that induces the formation of emulsion.



370

371 **Figure 6.** Recyclability of Fe/DS-HMS-NH<sub>2</sub> in the *in-situ* esterification/transesterification  
 372 of DPO.

373

374 **3.5 The reaction mechanism of the *in-situ* esterification/transesterification of DPO using**  
 375 **Fe/DS-HMS-NH<sub>2</sub>**

376 In the preparation of biodiesel from DPO, Fe/DS-HMS-NH<sub>2</sub> acts as both acid and  
 377 base catalysts to facilitate the esterification of FFA and the transesterification of acyl  
 378 glycerides. The main steps for the reaction mechanism catalyzed by Fe/DS-HMS-NH<sub>2</sub> are the  
 379 formation of nucleophilic alkoxides, the nucleophilic attack on the electrophilic part of the  
 380 carbonyl group of the triglycerides, and electron delocalisation [49,50] as depicted in Figure  
 381 7. The detailed description is as follows:

382 **Step 1:** Acyl glycerides, FFA and methanol enter the surface of catalyst through the  
 383 adsorption process to reach the outer shell impregnated by the divalent iron. In this step, FFA

384 undergoes the electron delocalization to form a carbocation and a carbanion, where the latter  
385 binds to the iron embedded on the catalyst.

386 **Step 2:** The reaction continues as the methoxide anion of methanol attacks the carbocation,  
387 whereas the hydronium cation attaches to the hydroxyl group of FFA to form water.

388 **Step 3:** Through the electron delocalization of the carbon atom, the water is released from the  
389 complex with FAME and the iron-embedded catalyst, followed by the release of FAME from  
390 the catalyst.

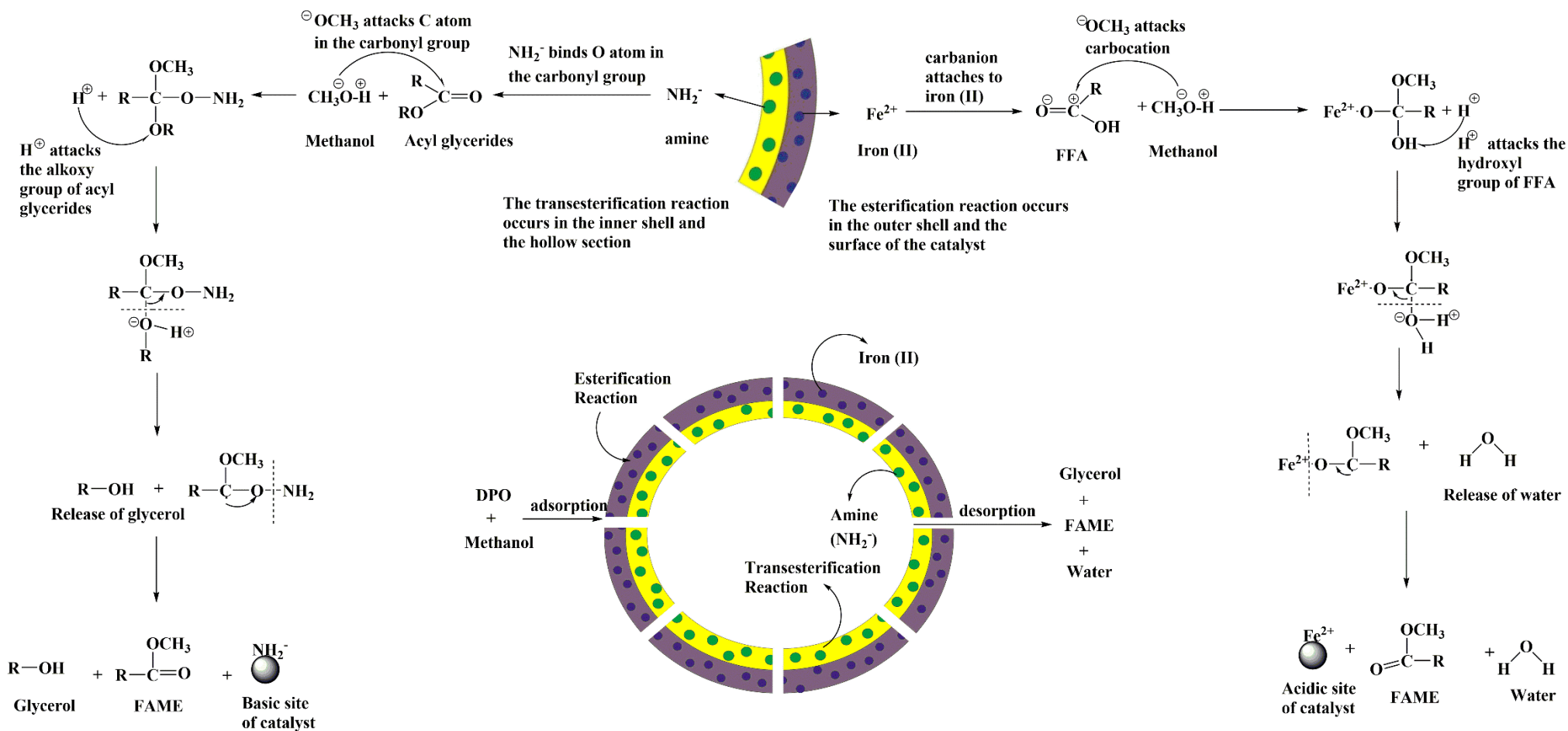
391 **Step 4:** The reaction continues when the acyl glycerides and methanol diffuse further to the  
392 amine-functionalized inner shell. The oxygen atom in the carbonyl group of acyl glycerides  
393 readily binds to the amine active sites.

394 **Step 5:** Subsequently, the methoxide anion of the methanol attacks the carbon atom in the  
395 carbonyl group of acyl glycerides, while the protonated  $H^+$  binds to the alkoxy group (RO-)  
396 of the acyl glycerides to form a complex of amine-functionalized catalyst with FAME and  
397 glycerol.

398 **Step 6:** Again, through the delocalization of oxygen in the complex, the glycerol and amine-  
399 functionalized catalyst are successively released from the complex.

400 **Step 7:** All three products, including FAME, glycerol, and water are then desorbed to the  
401 surface of the Fe/DS-HMS-NH<sub>2</sub> catalyst.

402



404 **Figure 7.** The reaction mechanism of the *in-situ* esterification/transesterification of DPO using Fe/DS-HMS-NH<sub>2</sub>.

405

## 406 **Conclusions**

407 Fe/DS-HMS-NH<sub>2</sub> is synthesized through the two-step condensation technique and  
408 successfully employed as a heterogeneous catalyst for preparing biodiesel from DPO, a lipid  
409 source with significant FFA and moisture content. The obtained Fe/DS-HMS-NH<sub>2</sub> has a  
410 uniform spherical shape with a particle size of 156 nm and hollow diameter of 86 nm. It is  
411 composed of two spatial silica shells with different active sites, and their thickness are 22 nm  
412 for the inner shell and 13 nm for the outer shell. Fe/DS-HMS-NH<sub>2</sub> has a specific surface area  
413 of 782.84 m<sup>2</sup>/g with a pore volume of 0.64 cm<sup>3</sup>/g, comparable with the existing solid catalysts.  
414 In the *in-situ* esterification/transesterification process using the Fe/DS-HMS-NH<sub>2</sub> catalyst,  
415 reaction time  $t$  is the variable with most significant influence on the yield of FAME  $Y_F$ ,  
416 followed by the reaction temperature  $T$  and the mass ratio of methanol to DPO  $r_{m/o}$ . The  
417 maximum  $Y_F$  is 85.36% (w/w), obtained at the following conditions:  $T = 60^\circ\text{C}$ ,  $t = 4.5$  h, and  
418  $r_{m/o} = 6:1$ , with a catalyst loading of 6% (w/w). Notably, Fe/DS-HMS-NH<sub>2</sub> catalyst shows a  
419 good recyclability, with the yield staying above 80% for three reaction cycles. Therefore,  
420 Fe/DS-HMS-NH<sub>2</sub> is a promising heterogeneous catalyst to obtain biodiesel from DPO or other  
421 lipid materials with high FFA and water content. Further study on (1) the extension of the  
422 catalyst lifetime by creating a technique suitable for its regeneration, and also (2) the design  
423 of a plausible route between the current research and its industrial application should be the  
424 main focus for future research expansion.

425

## 426 **Acknowledgments**

427 The authors acknowledge the funding supports from Widya Mandala Catholic University  
428 Surabaya, through the research grant no. 2263/WM01/N/2020. We also thank Professor  
429 Chun-Hu Chen, National Sun Yat Sen University, and Taiwan Tech (National Taiwan

430 University of Science and Technology) for providing the facility for the catalyst  
431 characterizations.

## 432 REFERENCES

- 433 [1] P. Agung, D. Hartono, A.A. Awirya, Pengaruh Urbanisasi Terhadap Konsumsi Energi Dan  
434 Emisi CO<sub>2</sub>: Analisis Provinsi di Indonesia (The Effect of Urbanization on Energy  
435 Consumption and CO<sub>2</sub> Emissions: An Analysis of Provinces in Indonesia), *J. Ekon.*  
436 *Kuantitatif Terap.* 1 (2017) 9–17. <https://doi.org/10.24843/jekt.2017.v10.i01.p02>.
- 437 [2] A. Fitriyatus, A. Fauzi, B. Juanda, Prediction of Fuel Supply and Consumption in Indonesia  
438 with System Dynamics Model, *J. Ekon. Dan Pembang. Indones.* 17 (2018) 118–137.
- 439 [3] F.T.R. Silalahi, T.M. Simatupang, M.P. Siallagan, Biodiesel produced from palm oil in  
440 Indonesia: Current status and opportunities, *AIMS Energy.* 8 (2020) 81–101.  
441 <https://doi.org/10.3934/energy.2020.1.81>.
- 442 [4] F. Nangoy, B.C. Munthe, Indonesia President wants B30 in use by Jan 2020: cabinet  
443 secretary, Reuters. (2019).
- 444 [5] J.M. Marchetti, A summary of the available technologies for biodiesel production based on  
445 a comparison of different feedstock's properties, *Process Saf. Environ. Prot.* 90 (2012) 157–  
446 163. <https://doi.org/10.1016/j.psep.2011.06.010>.
- 447 [6] K. Suwannakarn, E. Lotero, K. Ngaosuwan, J.G. Goodwin Jr, Simultaneous free fatty acid  
448 esterification and triglyceride transesterification using a solid acid catalyst with in situ  
449 removal of water and unreacted methanol, *Ind. Eng. Chem. Res.* 48 (2009) 2810–2818.  
450 <https://doi.org/https://doi.org/10.1021/ie800889w>.
- 451 [7] Y.A. Tsigie, L.H. Huynh, S. Ismadji, A.M. Engida, Y.H. Ju, In situ biodiesel production  
452 from wet *Chlorella vulgaris* under subcritical condition, *Chem. Eng. J.* 213 (2012) 104–108.  
453 <https://doi.org/10.1016/j.cej.2012.09.112>.

- 454 [8] P.D. Patil, V.G. Gude, A. Mannarswamy, P. Cooke, N. Nirmalakhandan, P. Lammers, S.  
455 Deng, Comparison of direct transesterification of algal biomass under supercritical  
456 methanol and microwave irradiation conditions, *Fuel*. 97 (2012) 822–831.  
457 <https://doi.org/10.1016/j.fuel.2012.02.037>.
- 458 [9] A. Kumari, P. Mahapatra, V.K. Garlapati, R. Banerjee, Enzymatic transesterification of  
459 *Jatropha* oil, *Biotechnol Biofuels*. 2 (2009) 1. <https://doi.org/10.1186/1754-6834-2-1>.
- 460 [10] R. Mat, R.A. Samsudin, M. Mohamed, A. Johari, Solid catalysts and their application in  
461 biodiesel production, *Bull. Chem. React. Eng. Catal.* 7 (2012) 142–149.  
462 <https://doi.org/10.9767/bcrec.7.2.3047.142-149>.
- 463 [11] W. Suryaputra, I. Winata, N. Indraswati, S. Ismadji, Waste capiz (*Amusium cristatum*) shell  
464 as a new heterogeneous catalyst for biodiesel production, *Renew. Energy*. 50 (2013) 795–  
465 799. <https://doi.org/10.1016/j.renene.2012.08.060>.
- 466 [12] H. Li, W. Xie, Transesterification of Soybean Oil to Biodiesel with Zn/I<sub>2</sub> Catalyst, *Catal.*  
467 *Letters*. 107 (2006) 25–30. <https://doi.org/10.1007/s10562-005-9727-9>.
- 468 [13] A.A. Refaat, A.A. Refaat, Archive of SID Different techniques for the production of  
469 biodiesel from waste vegetable oil, *Int. J. Environ. Sci. Tech.* 7 (2010) 183–213.
- 470 [14] P.L. Boey, G.P. Maniam, S.A. Hamid, Performance of calcium oxide as a heterogeneous  
471 catalyst in biodiesel production: A review, *Chem. Eng. J.* 168 (2011) 15–22.  
472 <https://doi.org/10.1016/j.cej.2011.01.009>.
- 473 [15] M.K. Lam, K.T. Lee, A.R. Mohamed, Homogeneous, heterogeneous and enzymatic  
474 catalysis for transesterification of high free fatty acid oil (waste cooking oil) to biodiesel: A  
475 review, *Biotechnol. Adv.* 28 (2010) 500–518.  
476 <https://doi.org/10.1016/j.biotechadv.2010.03.002>.
- 477 [16] W.N.N.W. Omar, N.A.S. Amin, Biodiesel production from waste cooking oil over alkaline

478 modified zirconia catalyst, *Fuel Process. Technol.* 92 (2011) 2397–2405.  
479 <https://doi.org/10.1016/j.fuproc.2011.08.009>.

480 [17] N. Pal, M. Paul, A. Bhaumik, Highly ordered Zn-doped mesoporous silica: An efficient  
481 catalyst for transesterification reaction, *J. Solid State Chem.* 184 (2011) 1805–1812.  
482 <https://doi.org/10.1016/j.jssc.2011.05.033>.

483 [18] W. Xie, X. Huang, Synthesis of biodiesel from soybean oil using heterogeneous KF/ZnO  
484 catalyst, *Catal. Letters.* 107 (2006) 53–59. [https://doi.org/https://doi.org/10.1007/s10562-](https://doi.org/https://doi.org/10.1007/s10562-005-9731-0)  
485 [005-9731-0](https://doi.org/https://doi.org/10.1007/s10562-005-9731-0).

486 [19] S.M. Coman, V.I. Parvulescu, Heterogeneous Catalysis for Biodiesel Production, Role  
487 *Catal. Sustain. Prod. Bio-Fuels Bio-Chemicals.* (2013) 93–136.  
488 <https://doi.org/10.1016/B978-0-444-56330-9.00004-8>.

489 [20] J. Santos, J. Phillips, J.A. Dumesic, Metal-support interactions between iron and titania for  
490 catalysts prepared by thermal decomposition of iron pentacarbonyl and by impregnation, *J.*  
491 *Catal.* 81 (1983) 147–167. [https://doi.org/10.1016/0021-9517\(83\)90154-9](https://doi.org/10.1016/0021-9517(83)90154-9).

492 [21] D.D. Bala, M. Misra, D. Chidambaram, Solid-acid catalyzed biodiesel production, part I:  
493 biodiesel synthesis from low quality feedstock, *J. Clean. Prod.* 142 (2017) 4169–4177.  
494 <https://doi.org/10.1016/j.jclepro.2016.02.128>.

495 [22] C. You, C. Yu, X. Yang, Y. Li, H. Huo, Z. Wang, Y. Jiang, X. Xu, K. Lin, Double-shelled  
496 hollow mesoporous silica nanosphere as acid-base bifunctional catalyst for cascade  
497 reactions, *New J. Chem.* 42 (2018) 4095–4101. <https://doi.org/10.1039/C7NJ04670G>.

498 [23] F.H. Santosa, L. Laysandra, F.E. Soetaredjo, S.P. Santoso, S. Ismadji, M. Yuliana, A facile  
499 noncatalytic methyl ester production from waste chicken tallow using single step subcritical  
500 methanol: Optimization study, *Int. J. Energy Res.* 43 (2019) 8852–8863.  
501 <https://doi.org/10.1002/er.4844>.

- 502 [24] X. Zhou, X. Cheng, W. Feng, K. Qiu, L. Chen, W. Nie, Z. Yin, X. Mo, H. Wang, C. He,  
503 Synthesis of hollow mesoporous silica nanoparticles with tunable shell thickness and pore  
504 size using amphiphilic block copolymers as core templates, *Dalt. Trans.* 43 (2014) 11834–  
505 11842. <https://doi.org/10.1039/c4dt01138d>.
- 506 [25] S. Cao, Z. Zhao, X. Jin, W. Sheng, S. Li, Y. Ge, M. Dong, W. Wu, L. Fang, Unique double-  
507 shelled hollow silica microspheres: Template-guided self-assembly, tunable pore size, high  
508 thermal stability, and their application in removal of neutral red, *J. Mater. Chem.* 21 (2011)  
509 19124–19131. <https://doi.org/10.1039/c1jm13011k>.
- 510 [26] N.B. Klinghoffer, M.J. Castaldi, A. Nzihou, Catalyst Properties and Catalytic Performance  
511 of Char from Biomass Gasification, *Ind. Eng. Chem. Res.* 51 (2012) 13113–13122.  
512 <https://doi.org/10.1021/ie3014082>.
- 513 [27] M. Zakeri, A. Samimi, M. Shafiee Afarani, A. Salehirad, Effects of porosity and pore size  
514 distribution on mechanical strength reliability of industrial-scale catalyst during preparation  
515 and catalytic test steps, *Part. Sci. Technol.* 36 (2018) 96–103.  
516 <https://doi.org/10.1080/02726351.2016.1220437>.
- 517 [28] T. Pangestu, Y. Kurniawan, F.E. Soetaredjo, S.P. Santoso, W. Irawaty, M. Yuliana, S.B.  
518 Hartono, S. Ismadji, The synthesis of biodiesel using copper based metal-organic  
519 framework as a catalyst, *J. Environ. Chem. Eng.* 7 (2019) 103277.  
520 <https://doi.org/10.1016/j.jece.2019.103277>.
- 521 [29] N. Rahmat, N. Sadon, M.A. Yusof, Thermogravimetric Analysis (TGA) Profile at Different  
522 Calcination Conditions for Synthesis of PTES-SBA-15, *Am. J. Appl. Sci.* 14 (2017) 938–  
523 944. <https://doi.org/10.3844/ajassp.2017.938.944>.
- 524 [30] Y.Y. Margaretha, H.S. Prastyo, A. Ayucitra, S. Ismadji, Calcium oxide from pomacea sp.  
525 shell as a catalyst for biodiesel production, *Int. J. Energy Environ. Eng.* 3 (2012) 1–9.

- 526 <https://doi.org/10.1186/2251-6832-3-33>.
- 527 [31] A.M. Dehkoda, A.H. West, N. Ellis, Biochar based solid acid catalyst for biodiesel  
528 production, *Appl. Catal. A Gen.* 382 (2010) 197–204.  
529 <https://doi.org/10.1016/j.apcata.2010.04.051>.
- 530 [32] C. Samart, P. Sreetongkittikul, C. Sookman, Heterogeneous catalysis of transesterification  
531 of soybean oil using KI/mesoporous silica, *Fuel Process. Technol.* 90 (2009) 922–925.  
532 <https://doi.org/10.1016/j.fuproc.2009.03.017>.
- 533 [33] G. Baskar, S. Soumiya, Production of biodiesel from castor oil using iron (II) doped zinc  
534 oxide nanocatalyst, *Renew. Energy.* 98 (2016) 101–107.  
535 <https://doi.org/https://doi.org/10.1016/j.renene.2016.02.068>.
- 536 [34] B. Gurunathan, A. Ravi, Biodiesel production from waste cooking oil using copper doped  
537 zinc oxide nanocomposite as heterogeneous catalyst, *Bioresour. Technol.* 188 (2015) 124–  
538 127. <https://doi.org/https://doi.org/10.1016/j.biortech.2015.01.012>.
- 539 [35] J. Cai, Q.Y. Zhang, F.F. Wei, J.S. Huang, Y.M. Feng, H.T. Ma, Y. Zhang, Preparation of  
540 Copper (II) Containing Phosphomolybdic Acid Salt as Catalyst for the Synthesis of  
541 Biodiesel by Esterification, *J Oleo Sci.* 67 (2018) 427–432.  
542 <https://doi.org/10.5650/jos.ess17208>.
- 543 [36] C. Samart, C. Chaiya, P. Reubroycharoen, Biodiesel production by methanolysis of soybean  
544 oil using calcium supported on mesoporous silica catalyst, *Energy Convers. Manag.* 51  
545 (2010) 1428–1431. <https://doi.org/10.1016/j.enconman.2010.01.017>.
- 546 [37] W. Xie, H. Li, Alumina-supported potassium iodide as a heterogeneous catalyst for  
547 biodiesel production from soybean oil, *J. Mol. Catal. A Chem.* 255 (2006) 1–9.  
548 <https://doi.org/https://doi.org/10.1016/j.molcata.2006.03.061>.
- 549 [38] M. Farooq, A. Ramli, Biodiesel production from low FFA waste cooking oil using

550 heterogeneous catalyst derived from chicken bones, *Renew. Energy*. 76 (2015) 362–368.  
551 <https://doi.org/10.1016/j.renene.2014.11.042>.

552 [39] R. Alenezi, G.A. Leeke, J.M. Winterbottom, R.C.D. Santos, A.R. Khan, Esterification  
553 kinetics of free fatty acids with supercritical methanol for biodiesel production, *Energy*  
554 *Convers. Manag.* 51 (2010) 1055–1059. <https://doi.org/10.1016/j.enconman.2009.12.009>.

555 [40] M. Farooq, A. Ramli, D. Subbarao, Biodiesel production from waste cooking oil using  
556 bifunctional heterogeneous solid catalysts, *J. Clean. Prod.* 59 (2013) 131–140.  
557 <https://doi.org/10.1016/j.jclepro.2013.06.015>.

558 [41] I. Amalia Kartika, M. Yani, D. Ariono, P. Evon, L. Rigal, Biodiesel production from  
559 *Jatropha* seeds: Solvent extraction and in situ transesterification in a single step, *Fuel*. 106  
560 (2013) 111–117. <https://doi.org/10.1016/j.fuel.2013.01.021>.

561 [42] Z. Wei, C. Xu, B. Li, Application of waste eggshell as low-cost solid catalyst for biodiesel  
562 production, *Bioresour. Technol.* 100 (2009) 2883–2885.  
563 <https://doi.org/10.1016/j.biortech.2008.12.039>.

564 [43] A. Demirbas, Biodiesel from waste cooking oil via base-catalytic and supercritical methanol  
565 transesterification, *Energy Convers. Manag.* 50 (2009) 923–927.  
566 <https://doi.org/10.1016/j.enconman.2008.12.023>.

567 [44] I.A. Reşitoğlu, A. Keskin, M. Gürü, The optimization of the esterification reaction in  
568 biodiesel production from trap grease, *Energy Sources, Part A Recover. Util. Environ. Eff.*  
569 34 (2012) 1238–1248. <https://doi.org/10.1080/15567031003792395>.

570 [45] A. Hayyan, F.S. Mjalli, M.A. Hashim, M. Hayyan, I.M. AlNashef, S.M. Al-Zahrani, M.A.  
571 Al-Saadi, Ethanesulfonic acid-based esterification of industrial acidic crude palm oil for  
572 biodiesel production, *Bioresour. Technol.* 102 (2011) 9564–9570.  
573 <https://doi.org/10.1016/j.biortech.2011.07.074>.

- 574 [46] S.L. Lee, Y.C. Wong, Y.P. Tan, S.Y. Yew, Transesterification of palm oil to biodiesel by  
575 using waste obtuse horn shell-derived CaO catalyst, *Energy Convers. Manag.* 93 (2015)  
576 282–288. <https://doi.org/10.1016/j.enconman.2014.12.067>.
- 577 [47] W. Xie, T. Wang, Biodiesel production from soybean oil transesterification using tin oxide-  
578 supported WO<sub>3</sub> catalysts, *Fuel Process. Technol.* 109 (2013) 150–155.  
579 <https://doi.org/10.1016/j.fuproc.2012.09.053>.
- 580 [48] M. Kouzu, J.S. Hidaka, Transesterification of vegetable oil into biodiesel catalyzed by CaO:  
581 A review, *Fuel*. 93 (2012) 1–12. <https://doi.org/10.1016/j.fuel.2011.09.015>.
- 582 [49] D.M. Marinković, M. V. Stanković, A. V. Veličković, J.M. Avramović, M.R. Miladinović,  
583 O.O. Stamenković, V.B. Veljković, D.M. Jovanović, Calcium oxide as a promising  
584 heterogeneous catalyst for biodiesel production: Current state and perspectives, *Renew.*  
585 *Sustain. Energy Rev.* 56 (2016) 1387–1408. <https://doi.org/10.1016/j.rser.2015.12.007>.
- 586 [50] A.K. Endalew, Y. Kiros, R. Zanzi, Inorganic heterogeneous catalysts for biodiesel  
587 production from vegetable oils, *Biomass and Bioenergy*. 35 (2011) 3787–3809.  
588 <https://doi.org/10.1016/j.biombioe.2011.06.011>.
- 589

## 1 **Abstract**

2 To promote the use of low-quality oils in producing biodiesel, a bifunctional acid-base  
3 catalyst Fe/DS-HMS-NH<sub>2</sub> is fabricated using the two-step condensation technique. The obtained  
4 Fe/DS-HMS-NH<sub>2</sub> is of a doubled shell structure in spherical shape with a uniform size of 156 nm.  
5 Its hollow core (with a diameter of 86 nm) and two spatial shells with different active sites enables  
6 the esterification and transesterification reactions to be accomplished in a one-pot synthesis. The  
7 influences of four independent reaction variables on the yield of fatty acid methyl esters  $Y_F$  was  
8 studied, including catalyst loading  $m_c$ , reaction time  $t$ , reaction temperature  $T$ , and the methanol to  
9 degummed palm oil mass ratio  $r_{m/o}$ . The highest yield was obtained at 85.36% (w/w) when  $m_c =$   
10 6% (w/w),  $t = 4.5$  h,  $T = 60$  °C, and  $r_{m/o} = 6:1$ . The Fe/DS-HMS-NH<sub>2</sub> shows a good recyclability  
11 with  $Y_F > 80\%$  (w/w) up to three reaction cycles.

12 *Keywords: bifunctional catalyst; biodiesel; renewable energy; hollow mesoporous silica; iron*  
13 *impregnation; amine functionalization*

14 **1. Introduction<sup>1</sup>**

15 The global fuel demand is growing rapidly as it undergoes an extensive urbanization.  
16 Our heavy reliance on fossil fuel brings the risk of unstable market price and reduced fuel  
17 availability. The gas emission from fossil fuel combustion also causes environmental concerns.  
18 Therefore, developing an alternative fuel that is biodegradable, sustainable and with a low  
19 carbon emission is the most significant energy and environmental challenge for us in the  
20 coming decades [1,2]. Since 2006, the Indonesian government has been committed to reducing  
21 carbon emissions by replacing fossil fuels with biodiesel [3]. It is also declared that the use of  
22 biodiesel in diesel blend will be increased from B20 to B30 starting from 2020 [4], with a  
23 strategy to boost the domestic use of palm oil and lower down energy imports. Usually,  
24 biodiesel is obtained through the conventional transesterification process of refined oil [5].  
25 However, the technologies of utilizing non-refined oil, specifically the low-quality oil, have  
26 currently attracted extensive interests and are being developed. Various types of low-quality  
27 oil have been studied to produce high-quality biodiesel using sundry of technical routes,  
28 including the two steps acidic esterification followed by basic transesterification [6],

---

1

FFA	Free fatty acids
FAME	Fatty acid methyl esters
DPO	Degummed palm oil
CPO	Crude palm oil
SS-HMS-NH <sub>2</sub>	Single-shelled hollow mesoporous silica
DS-HMS-NH <sub>2</sub>	Double-shelled hollow mesoporous silica
Fe/DS-HMS-NH <sub>2</sub>	Iron (II) impregnated double-shelled hollow mesoporous silica

29 noncatalytic transesterification using alcohol under subcritical [7] and supercritical conditions  
30 [8], enzymatic transesterification [9] and solid-catalyzed transesterification [10]. Among the  
31 available routes, the use of heterogeneous (solid) catalysts has been attracting a growing  
32 interest in recent years, as it has the advantage of easier separation, tolerance to impurities  
33 (i.e., FFA, water and other minor compounds), and good reusability [11] which means  
34 minimal waste and toxic water production [12] and environmentally friendly [13]. Boey et al.  
35 (2011) and Lam et al. (2010) also stated that heterogeneous catalysts lower the product  
36 contamination level, and reduce the corrosion problem [14,15]. Various solid catalysts and  
37 their modifications have been reported, such as zirconia [16], silica impregnated with zinc  
38 stearate (ZS/Si) [17], heterogeneous KF/ZnO catalyst [18], heterogeneous Zn/I<sub>2</sub> catalyst [12].  
39 However, despite their insensitivity to impurities, these catalysts solely act as the mono  
40 functional catalysts, depending on their acidity nature and have the following disadvantages  
41 during the conversion of low-quality oil to biodiesel: (1) the reaction carried out in the  
42 presence of an acidic heterogeneous catalyst is slow, and at the same time, requires large  
43 amount of alcohol [19], meanwhile (2) the basic heterogeneous catalysts usually result in a  
44 lower biodiesel yield and purity, since this type of catalyst leaves the FFA unreacted during  
45 the reaction.

46 In this paper, we prepared and characterized a new class of heterogeneous catalyst,  
47 the double-shelled hollow mesoporous silica impregnated with divalent iron metal (Fe/DS-  
48 HMS-NH<sub>2</sub>), to be used as an acid-base bifunctional catalyst in the production of biodiesel  
49 from a low-quality oil. This catalyst enables a simple process of converting low-quality oil to  
50 biodiesel by combining the two processes of esterification and transesterification into a single-  
51 stage process. This is achieved by having double active surface layers that facilitate the two  
52 reactions to run simultaneously. The primary (inner) shell is designed to promote the

53 transesterification reaction by adding  $\text{-NH}_2$  as the basic site, while the outer layer is  
54 impregnated with the divalent iron (Fe (II)), which is selected as the impregnated metals due  
55 to its nature as a strong Lewis acid, and its ability to change the oxidation level and activate  
56 the substance during the process [20].

57 The synthesis, characterization and catalytic activity of the Fe/DS-HMS-NH<sub>2</sub> will be  
58 investigated in this paper. Its performance as an acid-base bifunctional catalyst for biodiesel  
59 preparation will be examined at various conditions, including catalyst loading  $m_c$  (% , w/w),  
60 reaction temperature  $T$  (°C), reaction time  $t$  (h), and the mass ratio of methanol to oil  $r_{m/o}$ . In  
61 this present research, degummed palm oil (DPO) is selected as the lipid material. With similar  
62 content of FFA and moisture as the crude palm oil (CPO), DPO is also classified as a low-  
63 quality oil, along with industrial fats, oils and greases, and other crude/waste lipids. Therefore,  
64 it is considered as a suitable raw material to determine the catalytic ability of Fe/DS-HMS-  
65 NH<sub>2</sub> in converting both FFA and triglycerides in DPO into biodiesel. We will also show that  
66 the Fe/DS-HMS-NH<sub>2</sub> can be regenerated and reused, which is regarded as an important feature  
67 for heterogeneous catalysts as it will reduce the cost for production and pollutant discharges  
68 [21,22]. The recyclability of the catalyst will be investigated at the operating condition giving  
69 the highest yield of fatty acid methyl esters (FAME)  $Y_F$ .

70

## 71 **2. Materials and methods**

### 72 **2.1 Materials**

73 CPO was collected from the local manufacturer in Indonesia. Prior to use, CPO was  
74 degummed using 1% (w/w) phosphoric acid (PA, 85% purity) at a temperature of 80 – 90°C  
75 for 30 min to reduce the phosphorus content. Several important characteristics of the  
76 degummed CPO (i.e., DPO), namely free fatty acid content, acid value, saponification value,

77 and moisture content were analyzed in accordance with the standard method of AOCS Ca 5a-  
78 40, Cd 3d-63, Cd 3d-25, and Ca 2e-84, respectively.

79 3-aminopropyl-triethoxysilane (APTES) was purchased from Fisher Scientific  
80 (Pittsburgh, USA), while other chemicals required for the fabrication of Fe/DS-HMS, namely  
81 iron (II) sulfate heptahydrate ( $\text{FeSO}_4 \cdot 7\text{H}_2\text{O}$ , 99.99% purity), tetraethylorthosilicate (TEOS),  
82 cetyltrimethylammonium bromide (CTAB), ethanol (98% purity), methanol (99,9% purity),  
83 hydrochloric acid (HCl, 37% purity), ammonium hydroxide solution ( $\text{NH}_4\text{OH}$ , 25% purity),  
84 and n-hexane (95% purity) were obtained from Merck (Merck, Germany). The FAMES  
85 standard (47885 U) containing 37 components FAME mix was procured from Supelco  
86 (Bellefonte, PA, USA). Ultra-high purity nitrogen gas (> 99.0% purity) was purchased from  
87 Aneka Gas Industry Pty. Ltd., Indonesia. All chemicals used in this study were of analytical  
88 grade and required no further purification.

89

## 90 **2.2 Preparation of DS-HMS-NH<sub>2</sub>**

91 In a typical synthesis, 0.14 g of CTAB, 20 ml of ethanol, 50 ml of deionized water and  
92 1 ml of  $\text{NH}_4\text{OH}$  solution were simultaneously introduced into a glass beaker and mixed for 15  
93 minutes at room temperature. Then 1 ml of TEOS was slowly added into the above solution  
94 and kept stirring for 24 hours. The precipitates were collected through centrifugation at 4500  
95 rpm for 30 min, triplicate ethanol washing, and drying at 120 °C overnight. After the  
96 calcination at 550°C for 6 h, the single shelled hollow mesoporous silica (SS-HMS-NH<sub>2</sub>) was  
97 obtained.

98 The outer shell of the particle was fabricated using a multilevel scheme based on SS-  
99 HMS-NH<sub>2</sub>. In a typical synthesis, 0.5 g CTAB, 18 ml deionized water, and 50 ml of ethanol  
100 were introduced into a beaker glass. Meanwhile, 0.063 g of SS-HMS-NH<sub>2</sub> was added into a

101 mixture of 4 ml deionized water and 8.5 ml of 25% (w/w)  $\text{NH}_4\text{OH}$  solution. The above two  
102 solutions were then combined and stirred for 15 min at 250 rpm, after which 100  $\mu\text{l}$  TEOS  
103 and 21  $\mu\text{l}$  APTES were slowly added into it and the mixture was kept stirring for 24 h to allow  
104 the condensation reaction of silica. Finally, the solid product was collected by centrifugation  
105 at 4500 rpm for 15 min, which was then repeatedly washed with 60 ml of ethanol and 4 ml of  
106 HCl, and oven-dried at 120°C. The dried product was calcined at 550 °C for 6 h to obtain  
107 double-shelled hollow mesoporous silica (DS-HMS-NH<sub>2</sub>).

108

### 109 **2.3 Iron (II) impregnation onto DS-HMS-NH<sub>2</sub> surface**

110 The impregnation of divalent iron onto the DS-HMS-NH<sub>2</sub> surface was achieved as  
111 follows to fabricate Fe/DS-HMS-NH<sub>2</sub> catalysts. In a typical synthesis, 0.1 g DS-HMS-NH<sub>2</sub>  
112 was mixed with 50 ml of deionized water under sonication for 30 minutes at room temperature.  
113 Meanwhile, two separate solutions were prepared: (1) 5 mg of  $\text{FeSO}_4 \cdot 7\text{H}_2\text{O}$  was dissolved in  
114 50 ml of deionized water, and (2) 0.2 g of CTAB was dissolved in 10 ml ethanol. Solution (1)  
115 and (2) were then added into the DS-HMS-NH<sub>2</sub> solution and stirred for 12 hours at ambient  
116 conditions. The Fe/DS-HMS-NH<sub>2</sub> precipitates were separated by a centrifugation at 4500 rpm  
117 for 15 min, and then dried at 120 °C for 12 h and calcined at 550 °C for 5 hours to obtain the  
118 Fe/DS-HMS-NH<sub>2</sub> powder.

119

### 120 **2.4. Catalytic activity of Fe/DS-HMS-NH<sub>2</sub> at various reaction conditions**

121 The *in-situ* esterification/transesterification reactions from DPO to FAME were carried  
122 out in a glass flask equipped with a reflux condenser and external heater under constant  
123 magnetic stirring (250 rpm) at various conditions. Specifically, the influence of four reaction  
124 parameters were investigated due to their relevance to industrial applications: catalyst loading

125  $m_c$  (% , w/w), reaction temperature  $T$  ( $^{\circ}\text{C}$ ), reaction time  $t$  (h), and the mass ratio of methanol  
 126 to DPO  $r_{m/o}$ . To determine the amount of Fe/DS-HMS-NH<sub>2</sub> catalyst that produces the  
 127 maximum FAME yield  $Y_F$ , a few reactions were carried out with different amounts of Fe/DS-  
 128 HMS-NH<sub>2</sub> ( $m_c = 2\%$ ,  $4\%$ ,  $6\%$ ,  $8\%$ , w/w) at the following condition:  $T = 60$   $^{\circ}\text{C}$ ,  $t = 4.5$  h and  
 129  $r_{m/o} = 10:1$ . Once the optimum catalyst loading is obtained, the catalytic activity of Fe/DS-  
 130 HMS-NH<sub>2</sub> was investigated within an experimental matrix defined by  $T = 40$   $^{\circ}\text{C}$ ,  $50$   $^{\circ}\text{C}$ ,  $60$   $^{\circ}\text{C}$ ,  
 131  $t = 0.5$  h,  $2.5$  h,  $4.5$  h, and  $r_{m/o} = 2:1$ ,  $6:1$ ,  $10:1$ . The experimental runs were designed in a  
 132 random order using face centered-central composite design (CCF-CCD) as listed in Table 1.  
 133 All the experimental runs were conducted with the same procedure.

134 **Table 1.** Experimental matrix at the optimum catalyst loading  $m_c = 6\%$  (w/w)

Run	Input Parameters			$Y_F$ (% , w/w)
	$T$ ( $^{\circ}\text{C}$ )	$t$ (h)	$r_{m/o}$	
1	60	4.5	10:1	$85.24 \pm 1.19$
2	40	0.5	10:1	$40.27 \pm 0.58$
3	40	2.5	6:1	$55.09 \pm 0.76$
4	50	4.5	6:1	$75.15 \pm 0.65$
5	50	2.5	10:1	$60.07 \pm 0.44$
6	40	0.5	2:1	$35.19 \pm 0.92$
7	40	4.5	10:1	$70.22 \pm 1.01$
8	50	2.5	2:1	$67.03 \pm 0.51$
9	60	4.5	2:1	$80.11 \pm 0.68$
10	50	2.5	6:1	$65.16 \pm 0.47$
11	50	2.5	6:1	$66.96 \pm 0.73$
12	50	2.5	6:1	$65.87 \pm 0.79$
13	50	0.5	6:1	$65.01 \pm 0.37$
14	60	4.5	6:1	$85.36 \pm 0.62$
15	50	2.5	6:1	$63.21 \pm 0.42$
16	60	0.5	10:1	$70.01 \pm 0.56$
17	50	2.5	6:1	$63.20 \pm 0.69$
18	50	2.5	6:1	$67.18 \pm 0.45$
19	60	0.5	2:1	$69.09 \pm 0.53$
20	40	4.5	2:1	$59.11 \pm 0.78$

135  
 136 After the reaction completed, Fe/DS-HMS-NH<sub>2</sub> catalyst was recovered by  
 137 centrifugation at 4500 rpm for 15 min, and calcination at 550  $^{\circ}\text{C}$  for 5 h. The liquid product

138 was subjected to a two-stage liquid-liquid extraction using methanol and n-hexane  
139 sequentially for purification. Then the FAME-rich phase was separated from the by-products  
140 (i.e., glycerol, excess methanol, soap, and the other unwanted materials) and evaporated under  
141 vacuum to obtain the final FAME product. As an evaluation of the catalytic activity of Fe/DS-  
142 HMS-NH<sub>2</sub>, the yield of FAME was calculated by the following equation:

$$Y_F (\%, \text{ w/w}) = \frac{m_F p_F}{m_s} \times 100 \quad (1)$$

143 Where  $m_F$  is the mass of the final FAME product (g),  $p_F$  is the FAME purity (% w/w)  
144 obtained from equation (2) shown in the next section, and  $m_s$  is the total mass of the DPO (g).  
145

## 146 **2.5 Characterization of Fe/DS-HMS-NH<sub>2</sub> catalyst and FAME**

147 The characterization of Fe/DS-HMS-NH<sub>2</sub> was conducted using field-emission  
148 scanning electron microscopy with energy dispersive X-Ray spectroscopy (FESEM/EDX),  
149 transmission electron microscopy (TEM), nitrogen sorption, and thermogravimetric analysis  
150 (TGA). The FESEM/EDX images were taken on a JEOL JSM-6500 F (Jeol Ltd., Japan)  
151 running at 15 kV with a working distance of 12.4 mm, while TEM was carried out on JEOL  
152 JEM-2100 with an accelerating voltage of 200 kV. Nitrogen sorption analysis was conducted  
153 at 77 K on a Micrometrics ASAP 2010 Sorption Analyzer. The sample was degassed at 423  
154 K prior to analysis. To determine the thermal stability and volatile component fraction of the  
155 Fe/DS-HMS-NH<sub>2</sub> catalyst, a TGA analysis was performed using TG/DTA Diamond  
156 instrument (Perkin-Elmer, Japan).

157 The final FAME product characteristics, including its kinematic viscosity (at 40°C),  
158 flashpoint, cetane number, acid value and calorific value were determined according to the  
159 standard methods of ASTM D445, ASTM D93, ASTM D613, ASTM D664, and ASTM D240,  
160 respectively. The purity of FAME ( $p_F$ ) in the final product was analyzed using a gas

161 chromatograph (Shimadzu GC-2014) equipped with a split/splitless injector and a flame  
162 ionization detector (FID). The stationary phase used for separation was the narrow bore non-  
163 polar DB-WAX column (30 m × 0.25 mm ID × 0.25 μm film thickness, Agilent Technology,  
164 CA), and the temperature profile for the analysis was in accordance with the study conducted  
165 by Harijaya et al. (2019) [23]. Methyl heptadecanoate (MH) was used as an internal standard,  
166 while an external FAME reference (47885 U, containing 37 components FAME standard mix)  
167 was used to obtain the FAME compositional profile.  $p_F$  is calculated by the following equation:

$$p_F (\%, w/w) = \left( \frac{\sum A_F - A_{MH}}{A_{MH}} \right) \left( \frac{V_{MH} C_{MH}}{m_F} \right) \times 100 \quad (2)$$

168 Where  $\sum A_F$  is the total peak area of FAME,  $A_{MH}$  is the corresponding area of methyl  
169 heptadecanoate (MH) peak,  $V_{MH}$  is the volume of MH solution (ml),  $C_{MH}$  is the actual  
170 concentration of MH solution (g/ml), and  $m_F$  is the actual mass of the final FAME product  
171 (g).

172

## 173 **2.6 Recyclability of Fe/DS-HMS-NH<sub>2</sub>**

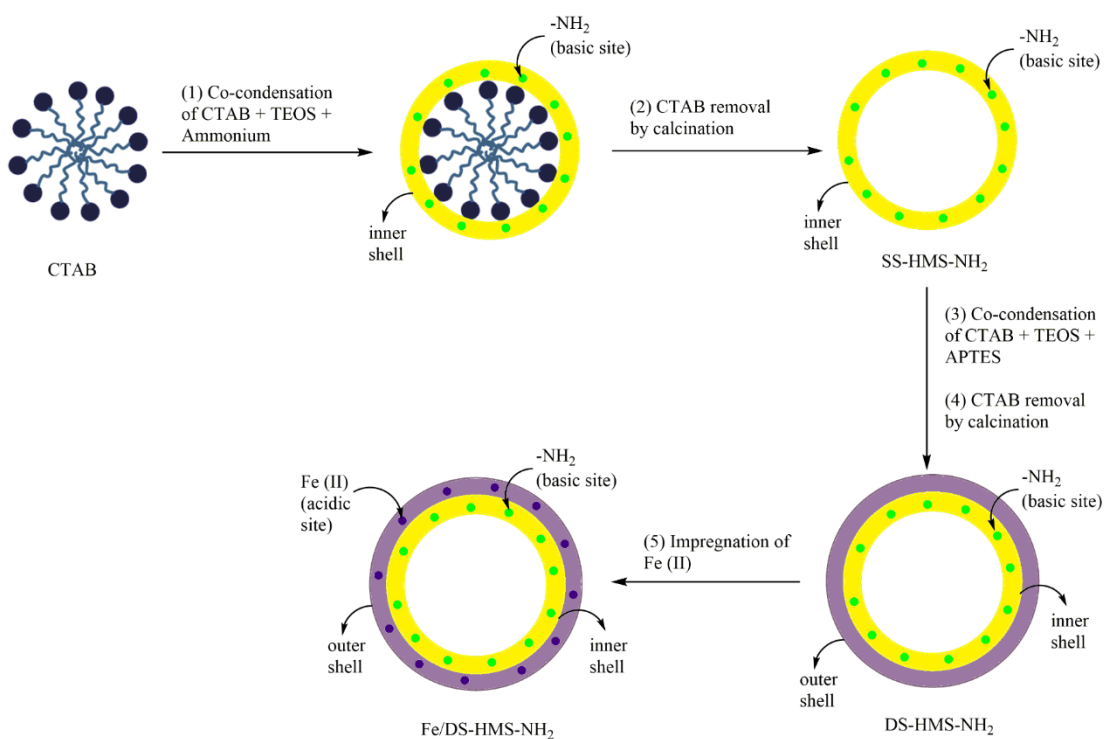
174 Fe/DS-HMS-NH<sub>2</sub> was repeatedly used for the transesterification process at the  
175 operating condition where the maximum yield of FAME was obtained. The recyclability of  
176 Fe/DS-HMS-NH<sub>2</sub> was determined by the number of repetitions until when the yield became  
177 lower than 80% (w/w). The purity and yield of FAME were analyzed according to the  
178 procedures in section 2.4-2.5. All experiments were carried out in triplicates to verify the  
179 results.

180

## 181 **3. Result and Discussions**

### 182 **3.1 The mechanism scheme of Fe/DS-HMS-NH<sub>2</sub> fabrication**

183 The Fe/DS-HMS-NH<sub>2</sub> was synthesized by a two-step co-condensation technique.  
 184 The mechanism scheme in Figure 1 illustrates the fabrication route: (1) firstly, TEOS and  
 185 CTAB undergo a co-condensation reaction along with the ammonium solution; (2) then  
 186 CTAB, the soft template of the core, is removed by calcination, and the SS-HMS-NH<sub>2</sub> is thus  
 187 formed; (3) TEOS, APTES, and CTAB undergo another co-condensation reaction on the outer  
 188 surface of the SS-HMS-NH<sub>2</sub> spheres; (4) DS-HMS-NH<sub>2</sub> nanosphere is obtained by removing  
 189 CTAB and APTES in calcination; (5) the divalent iron (Fe (II)) was incorporated onto the  
 190 surface of DS-HMS-NH<sub>2</sub> by a traditional wet impregnation technique, and the Fe/DS-HMS-  
 191 NH<sub>2</sub> nanosphere is obtained.



192  
 193 **Figure 1.** The mechanism scheme of Fe/DS-HMS-NH<sub>2</sub> fabrication.

194  
 195 **3.2 Characterization of Fe/DS-HMS-NH<sub>2</sub> catalysts**

196 Figure 2a, c–d present the SEM and TEM images of the Fe/DS-HMS-NH<sub>2</sub> catalyst  
197 synthesized by the co-condensation technique. The catalyst is spherical with a uniform size at  
198 *ca.* 156 nm (Figure 2a). Notably, Fe/DS-HMS-NH<sub>2</sub> is composed of two shell layers, indicated  
199 by the darker color of the inner shell in Figure 2c-d. Its hollow-core structure is clearly  
200 presented with the diameter of 86 nm (Figure 2d). The shell thicknesses of the inner and outer  
201 layer of Fe/DS-HMS-NH<sub>2</sub>, are 22 nm and 13 nm, respectively. The impregnation of Fe (II) on  
202 the surface of the silica layer was successful, evidenced from the EDX result showing a  
203 percentage of 2.87% (Figure 2b). Based on the fabrication procedure, it was reasonable to  
204 consider that the Fe (II) sites and basic amino sites were spatially isolated and located in  
205 different shells.

206 The textural properties of Fe/DS-HMS-NH<sub>2</sub> analyzed by the nitrogen sorption are  
207 presented in Table 2 and Figure 2e. The nitrogen adsorption and desorption isotherm of the  
208 catalyst exhibits a typical type-IV isotherm, indicating the presence of a mesoporous structure  
209 with worm-like capillary pores molded by the CTAB micelles. The pore size of the  
210 mesoporous structure is found to be 2.43 nm (Figure 2e (inset)). A steep increase of the  
211 nitrogen adsorption amount at  $p/p^0$  close to unity also suggests that there are macropores  
212 structure within the particle, corresponding to the hollow core. Similar adsorption and  
213 desorption profile also pointed out that the pores are highly accessible. The specific surface  
214 area  $S_{\text{BET}}$  obtained in this study was 782.84 m<sup>2</sup>/g, lower than the value 1100 – 1350 m<sup>2</sup>/g for  
215 a similar double shelled hollow mesoporous silica [22]. Such a discrepancy was likely due to  
216 the reason that it was strongly influenced by the shell thickness. Zhou et al. (2014) reported  
217 that when the thickness of hollow mesoporous silica nanoparticles (HMSN) increases from  
218 46 nm to 82 nm, the surface area of HMSN particles was declined from 986 m<sup>2</sup>/g to 614 m<sup>2</sup>/g

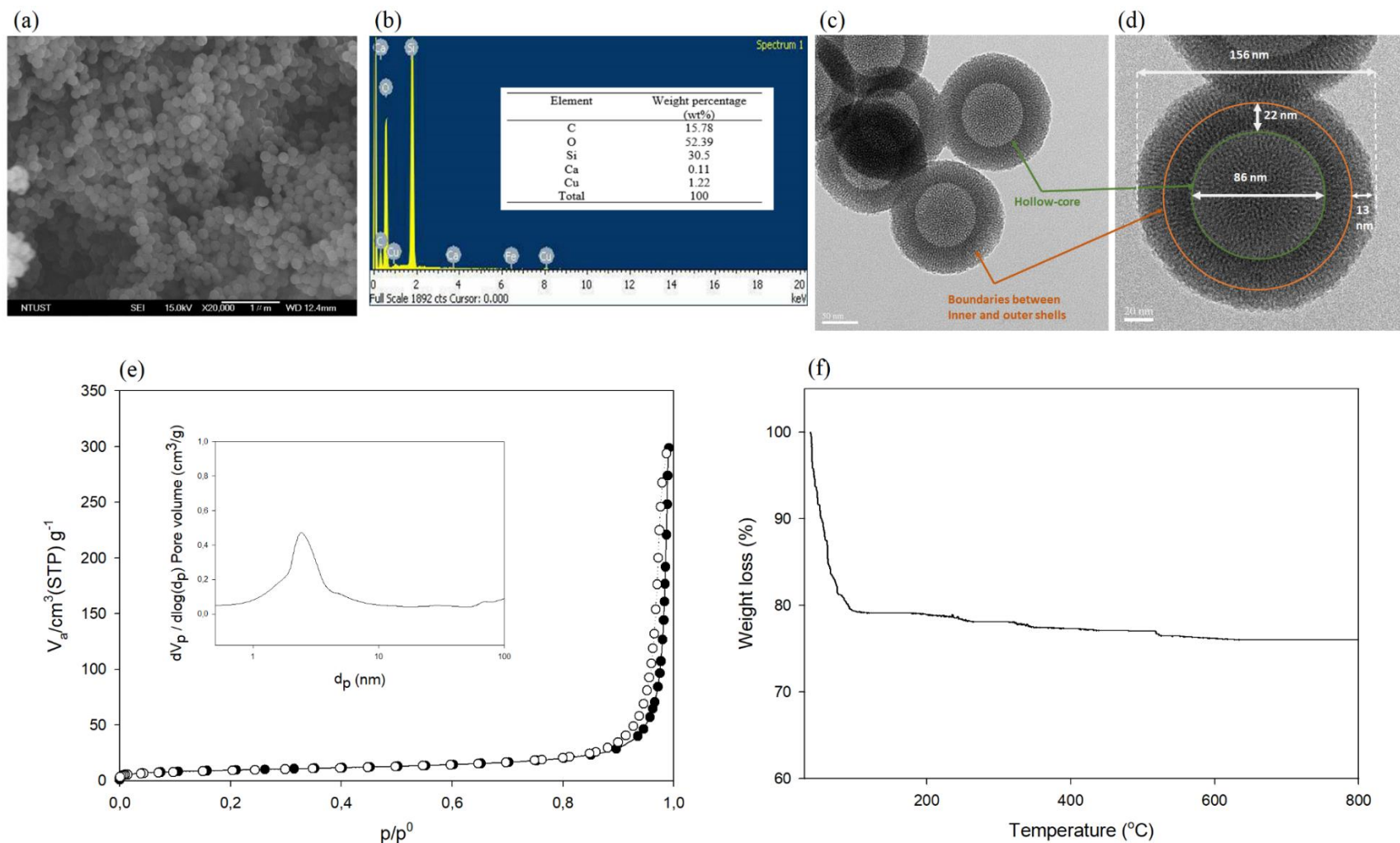
219 [24]. Zhou et al. (2014) and Cao et al. (2011) also observed that an increase in the particle  
 220 mass due to the addition of TEOS and CTAB in the synthesis of the second shell lowers the  
 221 surface area, since the amount of TEOS during the fabrication is directly proportional to the  
 222 thickness of the shell [24,25]. Meanwhile, the pore volume of Fe/DS-HMS-NH<sub>2</sub> (0.64 cm<sup>3</sup>/g)  
 223 was found to be slightly higher than that reported by You et al. (2018) (0.61 cm<sup>3</sup>/g) [22].  
 224 Based on its textural analysis, Fe/DS-HMS-NH<sub>2</sub> possesses comparable specific surface area  
 225 and pore volume with those of existing heterogeneous catalysts (i.e., HMS-Al@MS-NH<sub>2</sub> [22],  
 226 char-based catalyst [26],  $\gamma$ -alumina industrial-grade catalyst [27], and copper-based metal-  
 227 organic framework [28]), which usually range from 200 – 1300 cm<sup>2</sup>/g and 0.18 – 1.68 cm<sup>3</sup>/g  
 228 respectively.

229 **Table 2.** Textural properties of Fe/DS-HMS-NH<sub>2</sub>.

Material	$S_{\text{BET}}$ (cm <sup>2</sup> /g)	Pore volume (cm <sup>3</sup> /g)	Pore size (nm)
Fe/DS-HMS-NH <sub>2</sub>	782.84	0.64	2.43

230 To demonstrate the feasibility of Fe/DS-HMS-NH<sub>2</sub> for the reactions at an elevated  
 231 temperature, its thermal stability was investigated. The TGA profile in Figure 2f shows a 20%  
 232 decrease in weight up to the temperature of 100°C, attributed to the removal of free moisture  
 233 content. Further heating up to 800 °C does not significantly decrease the mass of Fe/DS-HMS-  
 234 NH<sub>2</sub>, suggesting that the catalyst is stable at high temperatures [29]. Therefore, our Fe/DS-  
 235 HMS-NH<sub>2</sub> can be considered as a promising heterogeneous catalyst for the *in-situ*  
 236 esterification/transesterification reaction.

237



239 **Figure 2.** (a) SEM image, (b) Elemental composition, (c) – (d) TEM images at various magnifications, (c) BJH pore size distribution  
 240 curve, (e) Nitrogen adsorption-desorption isotherm with BJH pore size distribution curve (inset), (f) Thermogravimetric profile of the  
 241 Fe/DS-HMS-NH<sub>2</sub> catalyst.

242 **3.3 The catalytic activity of Fe/DS-HMS-NH<sub>2</sub> in the *in-situ* esterification/transesterification**  
243 **of DPO**

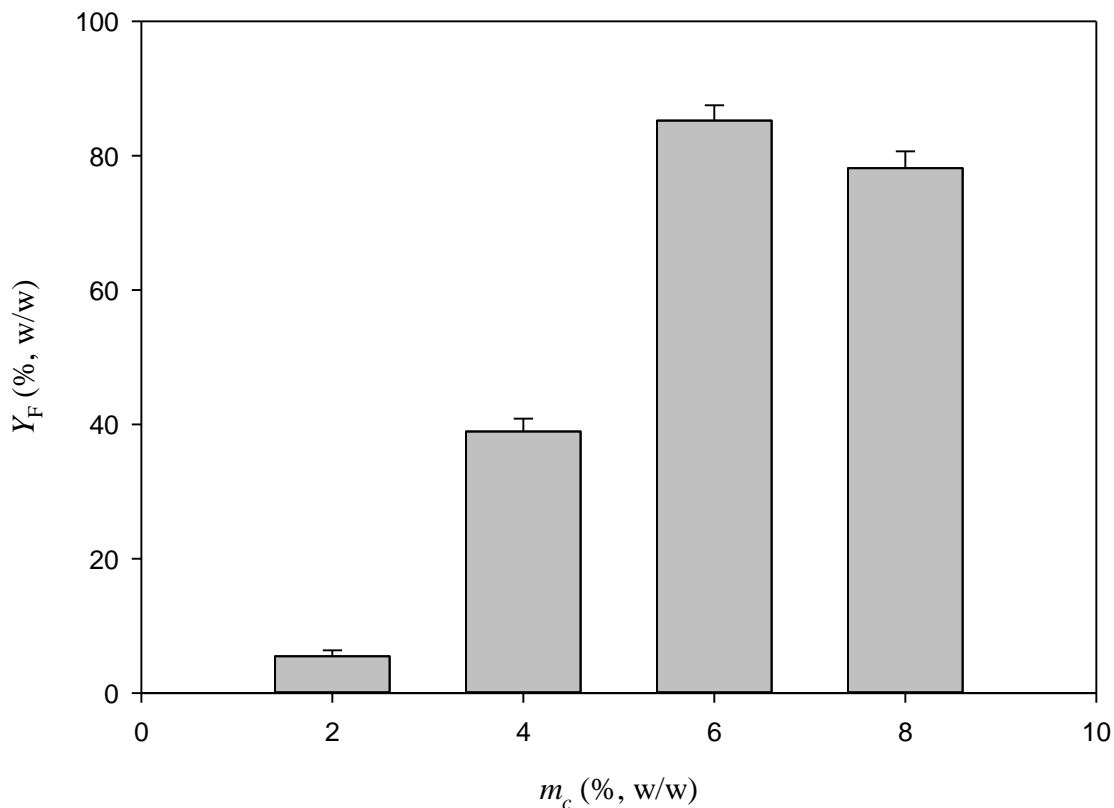
244 The characteristics of DPO as the raw material for biodiesel preparation are  
245 presented in Table 3. As homogenous catalysts are sensitive to impurities, the conversion of  
246 DPO to FAME for biodiesel production usually requires two reaction steps, namely acid-  
247 catalyzed esterification to lower the FFA content by converting them into FAME, and basic  
248 catalyzed transesterification to convert the acyl glycerides into FAME. However,  
249 heterogeneous catalysts can have good tolerance towards the FFA and water content in the  
250 lipid materials [10]; for Fe/DS-HMS-NH<sub>2</sub>, its two spatial shells with different active sites can  
251 facilitate the above two reactions in a one-pot process, and therefore efficient conversion from  
252 DPO to FAME is achieved in a single step.

253 **Table 3.** Characteristics of DPO.

Parameter	Value
FFA (% w/w)	5.54
Moisture Content (% w/w)	0.20
Saponification Value (mg KOH/g DPO)	234.08
Acid Value (mg KOH/g DPO)	12.04
Molecular weight (g/mol)	756.62

254  
255 Figure 3 presents the FAME yield obtained at various Fe/DS-HMS-NH<sub>2</sub> loadings  
256 at the condition of  $T = 60\text{ }^{\circ}\text{C}$ ,  $t = 4.5\text{ h}$  and  $r_{m/o} = 10:1$ . The results indicate that the yield of  
257 FAME is proportional to the number of active sites offered by the Fe/DS-HMS-NH<sub>2</sub> [30,31];  
258 therefore  $Y_F$  increases with  $m_c$  when the latter is within 6% (w/w). This agrees well with  
259 previous work on biodiesel production using different solid catalysts, e.g., pomacea sp. shell-  
260 based CaO [30], sulfonated biochar [31], and KI/mesoporous silica [32]. A maximum yield  
261 85.24% (w/w) is obtained when the catalyst loading  $m_c = 6\%$  (w/w). Further increase of the  
262 Fe/DS-HMS-NH<sub>2</sub> results in a reduced yield of FAME, which is probably due to the

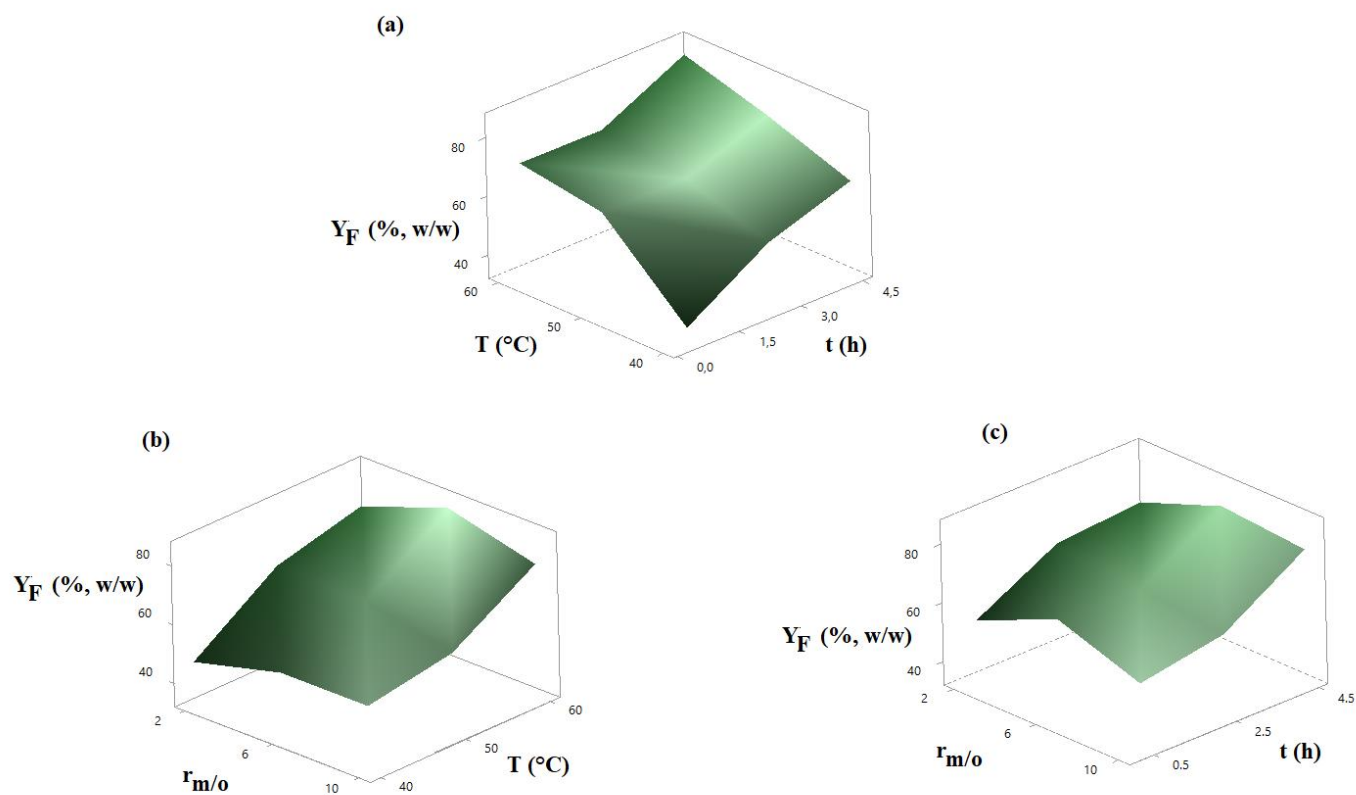
263 aggregation and inconsistent dispersity of the catalyst in the reaction system of an enhanced  
264 viscosity [33,34]. Cai et al. (2018) and Samart et al. (2010) also mentioned that excess catalyst  
265 may also disturbed the mixing between the reactants, due to stronger adsorption of the  
266 reactants to the catalyst [35,36].



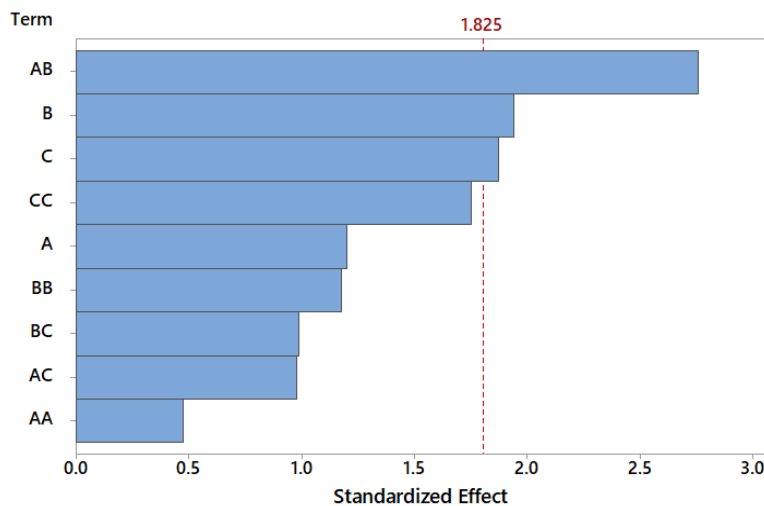
267 **Figure 3.** The yield of FAME at various Fe/DS-HMS-NH<sub>2</sub> loadings with the reaction  
268 condition of  $T = 60$  °C,  $t = 4.5$  h and  $r_{m/o} = 10:1$ .  
269  
270

271 At a constant catalyst loading  $m_c = 6\%$  (w/w), Figure 4 and Table 1 present the  
272 FAME yield  $Y_F$  at various reaction time  $t$ , temperature  $T$ , and mass ratio of methanol to DPO  
273  $r_{m/o}$ . The maximum  $Y_F = 85.36\%$  (w/w) (with a purity of 97.89% (w/w)) is obtained at the  
274 condition of  $T = 60$  °C,  $t = 4.5$  h,  $r_{m/o} = 6:1$ . This result indicates that Fe/DS-HMS-NH<sub>2</sub> is  
275 superior, specifically in terms of reaction time and temperature, compared with the existing  
276 catalysts reported in the literatures. Pal et al. (2011) mentioned that 94% (w/w) FAME yield

277 was achieved only after 24 h reaction using 7% Zn-doped mesoporous silica as the catalyst  
278 loading [17]. Long reaction time (8 h) were also reported by Xie and Li (2006) using alumina-  
279 supported KI [37]. Meanwhile, Omar and Amin (2011) stated that the transesterification of  
280 waste cooking oil over alkaline/zirconia catalyst requires high temperature (115.5°C) to  
281 achieve 79.7% (w/w) FAME yield [16].



283 **Figure 4.** The FAME yield  $Y_F$  (% w/w) at various (a)  $T$  and  $t$ , (b)  $T$  and  $r_{m/o}$ , and (c)  $t$  and  $r_{m/o}$ .  
284



285  
286  
287  
288  
289

**Figure 5.** Pareto chart of the standardized effect for the biodiesel preparation with Fe/DS-HMS-NH<sub>2</sub>, using  $Y_F$  as the response at a 95% confidence interval where  $A = T$ ,  $B = t$ ,  $C = r_{m/o}$ .

290

Based on the experimental results, the reaction time  $t$  was the most significant factor,

291

followed by  $r_{m/o}$  and  $T$ , which is supported by the Pareto chart of the standardized effect in

292

Figure 5 showing that  $t$ ,  $r_{m/o}$ , and the two-way interaction between  $t$  and  $T$  are the three

293

significant parameters in the reaction system. The effect of reaction temperature on the

294

production of biodiesel using Fe/DS-HMS-NH<sub>2</sub> is shown in Figure 4a–b. An increased

295

reaction temperature contributes to a higher yield, with the maximum achieved at 60°C, which

296

is related to the fact that both esterification and transesterification reaction are endothermic

297

and reversible [38,39]. At a higher reaction temperature, the kinetic energy and mobility of

298

reactant molecules increase, promoting the collisions between the molecules and Fe/DS-

299

HMS-NH<sub>2</sub> particles which then increases the reaction rate constant and shift the reaction

300

towards the product [38,40]. Moreover, the mass transfer of the reactant molecules through

301

the boundary layer of Fe/DS-HMS-NH<sub>2</sub> is also accelerated at an elevated temperature,

302

resulting in the faster diffusion of the reactants into the pore of catalyst; hence, improving the

303

FAME yield.

304                   Specifically, Figures 4a and c show a significant increase of the FAME yield by  
305 extending the duration of the biodiesel synthesis from 0.5 h to 4.5 h, at a constant temperature  
306 or mass ratio of methanol to DPO. Longer reaction time provides sufficient time for the  
307 reactants to reach the active sites of Fe/DS-HMS-NH<sub>2</sub> through adsorption and diffusion, and  
308 convert DPO into FAME [41]. Meanwhile, prolonged duration of reaction also gives the  
309 catalyst more time to adsorb the reactant and desorb the reaction product [28]. Wei et al. (2009)  
310 also mentioned that adsorption and desorption of reactants from the catalyst is the rate-  
311 determining step in the overall reaction [42]. Therefore, allowing longer contact between the  
312 reactant molecules and the catalyst ensures high conversions of FFA and acyl glycerides to  
313 FAME.

314                   Stoichiometrically, three moles of methanol are required to react with one mole of  
315 triglycerides in the transesterification reaction, while one mole of methanol is needed to react  
316 with one mole of free fatty acids in the esterification reaction [43,44]. Both reactions are  
317 known to be reversible; thus, the amount of methanol in the two reactions is usually provided  
318 in excess to shift the reaction equilibrium to the product side. As seen from Figure 4b–c,  
319 having excess methanol from  $r_{m/o} = 2:1$  to  $r_{m/o} = 6:1$  contributes to a higher FAME yield,  
320 while further addition up to  $r_{m/o} = 10:1$  has no improvement. While most studies agree that  
321 excess methanol is desirable to allow more frequent interactions between the lipid and  
322 methanol triggering the formation of FAME, Pangestu et al. (2019) found that excess  
323 methanol may also accelerate the production of glycerol despite the higher yield of FAME  
324 [28]. As the esterification and transesterification are both reversible, a higher concentration  
325 of glycerol in the reaction system may induce a reverse reaction to the reactant side, creating  
326 an equilibrium between the products and reactants [28]. Hayyan et al. (2011) also reported  
327 that an excessive amount of methanol causes higher solubility of glycerol in the FAME phase

328 that could lead to a complicated separation between biodiesel and glycerol [45]. Moreover,  
 329 from the techno-economic viewpoint, the higher mass ratio of methanol to DPO also increases  
 330 the material and processing cost [23,45]. Therefore, it can be concluded that the optimum  
 331 level is  $r_{m/o} = 6:1$ .

332 The fuel properties of the final FAME product are presented in Table 4. The  
 333 measurement results indicate that the product resulted in this study has a comparable  
 334 combustion and flow properties with those of the commercial biodiesel. The calorific value  
 335 (45.143 MJ/kg) is also within the range required in the common petrodiesel (42-46 MJ/kg).

336 **Table 4.** Fuel properties of the final FAME product

Properties	Methods	Unit	Final FAME product	ASTM D6751
Kinematic viscosity (at 40°C)	ASTM D445	mm <sup>2</sup> /s	2.64	1.9 – 6.0
Flashpoint	ASTM D93	°C	164.2	93 min
Cetane number	ASTM D613	-	55.7	47 min
Acid value	ASTM D664	mg KOH/g	0.24	0.5 max
Calorific value	ASTM D240	MJ/kg	45.143	-

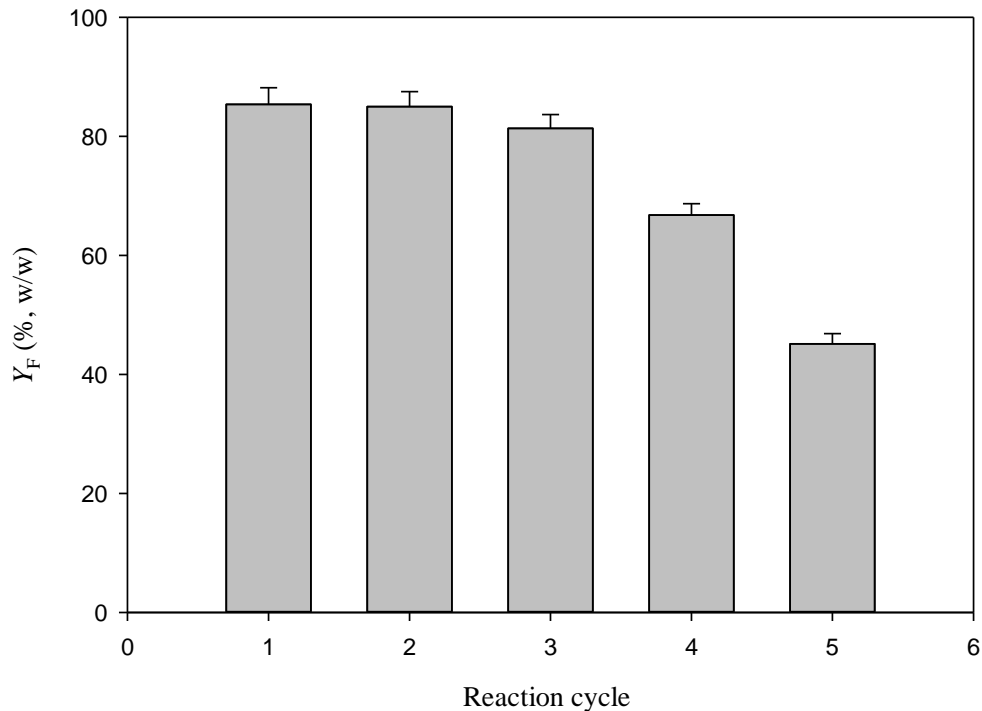
337

338 Meanwhile, its compositional profile is obtained by comparing the methyl ester  
 339 peaks in the chromatogram with those in the external FAME standard (47885 U, containing  
 340 37 components FAME standard mix). The 12 identified peaks are 3.05% myristoleic acid  
 341 methyl ester (C14:1), 2.37% cis-10-pentadecanoic acid methyl ester (C15:1), 35.78% palmitic  
 342 acid methyl ester (C16:0), 8.13% palmitoleic acid methyl ester (C16:1), 8.36% stearic acid  
 343 methyl ester (C18:0), 32.57% oleic acid methyl ester (C18:1n9c), 3.05% elaidic acid methyl  
 344 ester (C18:1n9t), 1.17% cis-8,11,14-eicosatrienoic acid methyl ester (C20:3n6), 2.48%  
 345 arachidonic acid methyl ester (C20:4n6), 0.52% cis-5,8,11,14,17-eicosapentaenoic acid  
 346 methyl ester (C20:5n3), 1.07% erucic acid methyl ester (C22:1n9), 1.45 % cis-13,16-  
 347 docosadienoic acid methyl ester (C22:2).

348

### 349 **3.4 Recyclability of Fe/DS-HMS-NH<sub>2</sub>**

350           An important feature of using heterogeneous catalysts for biodiesel preparation is  
351 its recyclability. In order to determine the recyclability of Fe/DS-HMS-NH<sub>2</sub>, several reaction  
352 cycles were conducted in series using the operating condition of  $m_c = 6\%$  (w/w),  $T = 60\text{ }^\circ\text{C}$ ,  $t$   
353  $= 4.5\text{ h}$ ,  $r_{m/o} = 6:1$ . Fe/DS-HMS-NH<sub>2</sub> was recovered following the method described in section  
354 2.4, while fresh methanol and DPO were used in every cycle. The catalytic ability of the  
355 recycled Fe/DS-HMS-NH<sub>2</sub> for *in-situ* esterification/transesterification process is presented in  
356 Figure 6. The result indicates that recycled Fe/DS-HMS-NH<sub>2</sub> can maintain a high yield of  
357 FAME above 80% (w/w) until the third cycle, close to the yield of fresh catalyst 85.36%  
358 (w/w). The purity of FAME for the first three cycles are 97.89%, 97.66% and 98.01% (w/w)  
359 respectively, higher than the commercial purity (96.5%, w/w). These results indicate that the  
360 catalytic activity of Fe/DS-HMS-NH<sub>2</sub> is maintained at a high level after regeneration. A  
361 significant drop in catalytic ability is observed from the forth cycle in Figure 6; similar  
362 performance has been reported for some other heterogeneous catalysts where three cycles  
363 seem to be an average number in term of their recyclability [46,47]. The catalytic deactivation  
364 of Fe/DS-HMS-NH<sub>2</sub> is generally due to the pore blockage caused by the contact between  
365 active sites on the catalyst surface and the deactivation-induced components, namely free  
366 glycerol, acyl glycerides, and biodiesel. Moreover, the high content of FFA in DPO also plays  
367 an important role in the deactivation of Fe/DS-HMS-NH<sub>2</sub> catalyst because FFA tends to  
368 neutralize the basic sites in the inner shell of Fe/DS-HMS-NH<sub>2</sub> [48], resulting in the  
369 generation of amine-carboxylate that induces the formation of emulsion.



370

371 **Figure 6.** Recyclability of Fe/DS-HMS-NH<sub>2</sub> in the *in-situ* esterification/transesterification  
 372 of DPO.

373

374 **3.5 The reaction mechanism of the *in-situ* esterification/transesterification of DPO using**  
 375 **Fe/DS-HMS-NH<sub>2</sub>**

376 In the preparation of biodiesel from DPO, Fe/DS-HMS-NH<sub>2</sub> acts as both acid and  
 377 base catalysts to facilitate the esterification of FFA and the transesterification of acyl  
 378 glycerides. The main steps for the reaction mechanism catalyzed by Fe/DS-HMS-NH<sub>2</sub> are the  
 379 formation of nucleophilic alkoxides, the nucleophilic attack on the electrophilic part of the  
 380 carbonyl group of the triglycerides, and electron delocalisation [49,50] as depicted in Figure  
 381 7. The detailed description is as follows:

382 **Step 1:** Acyl glycerides, FFA and methanol enter the surface of catalyst through the  
 383 adsorption process to reach the outer shell impregnated by the divalent iron. In this step, FFA

384 undergoes the electron delocalization to form a carbocation and a carbanion, where the latter  
385 binds to the iron embedded on the catalyst.

386 **Step 2:** The reaction continues as the methoxide anion of methanol attacks the carbocation,  
387 whereas the hydronium cation attaches to the hydroxyl group of FFA to form water.

388 **Step 3:** Through the electron delocalization of the carbon atom, the water is released from the  
389 complex with FAME and the iron-embedded catalyst, followed by the release of FAME from  
390 the catalyst.

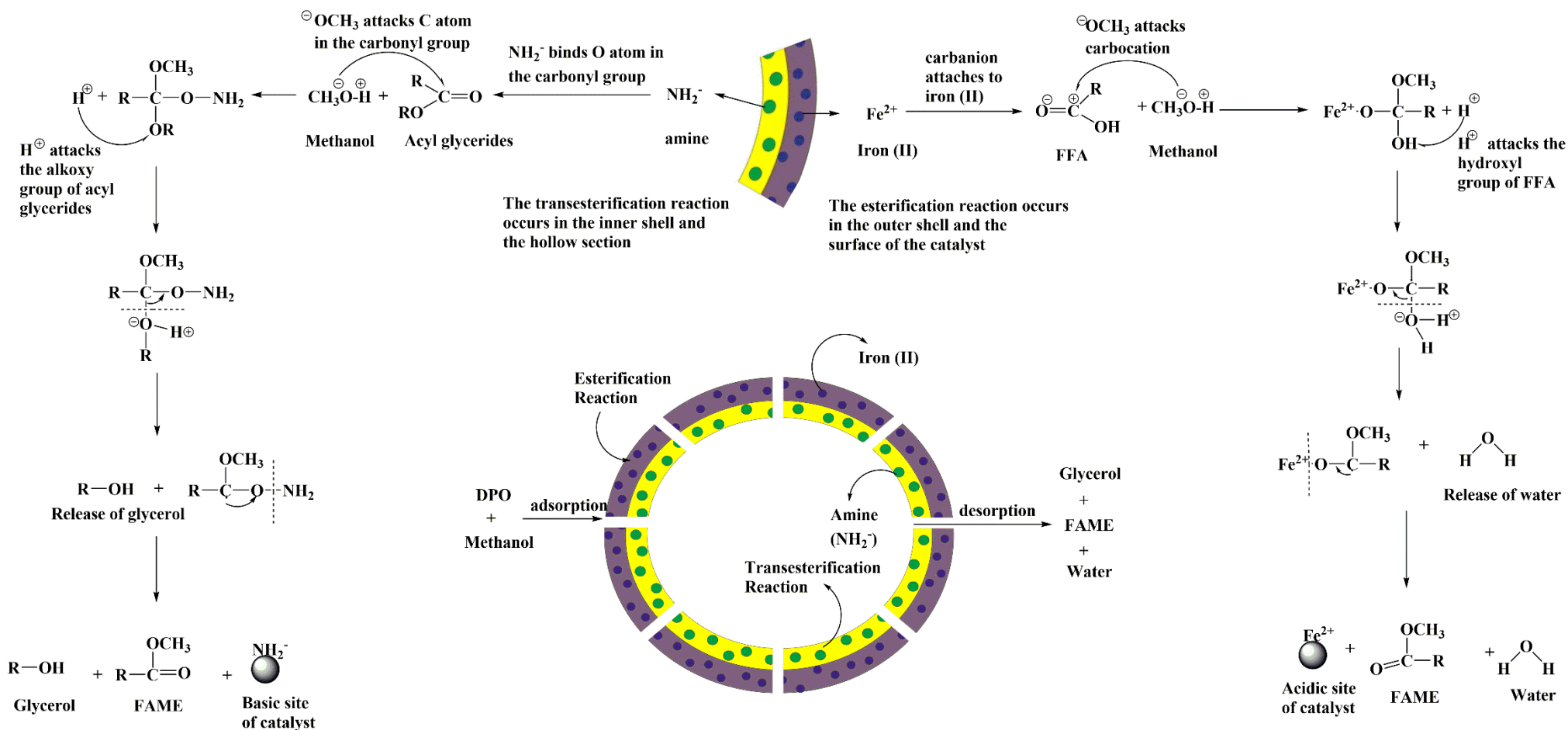
391 **Step 4:** The reaction continues when the acyl glycerides and methanol diffuse further to the  
392 amine-functionalized inner shell. The oxygen atom in the carbonyl group of acyl glycerides  
393 readily binds to the amine active sites.

394 **Step 5:** Subsequently, the methoxide anion of the methanol attacks the carbon atom in the  
395 carbonyl group of acyl glycerides, while the protonated  $H^+$  binds to the alkoxy group (RO-)  
396 of the acyl glycerides to form a complex of amine-functionalized catalyst with FAME and  
397 glycerol.

398 **Step 6:** Again, through the delocalization of oxygen in the complex, the glycerol and amine-  
399 functionalized catalyst are successively released from the complex.

400 **Step 7:** All three products, including FAME, glycerol, and water are then desorbed to the  
401 surface of the Fe/DS-HMS-NH<sub>2</sub> catalyst.

402



404 **Figure 7.** The reaction mechanism of the *in-situ* esterification/transesterification of DPO using Fe/DS-HMS-NH<sub>2</sub>.

405

## 406 **Conclusions**

407 Fe/DS-HMS-NH<sub>2</sub> is synthesized through the two-step condensation technique and  
408 successfully employed as a heterogeneous catalyst for preparing biodiesel from DPO, a lipid  
409 source with significant FFA and moisture content. The obtained Fe/DS-HMS-NH<sub>2</sub> has a  
410 uniform spherical shape with a particle size of 156 nm and hollow diameter of 86 nm. It is  
411 composed of two spatial silica shells with different active sites, and their thickness are 22 nm  
412 for the inner shell and 13 nm for the outer shell. Fe/DS-HMS-NH<sub>2</sub> has a specific surface area  
413 of 782.84 m<sup>2</sup>/g with a pore volume of 0.64 cm<sup>3</sup>/g, comparable with the existing solid catalysts.  
414 In the *in-situ* esterification/transesterification process using the Fe/DS-HMS-NH<sub>2</sub> catalyst,  
415 reaction time  $t$  is the variable with most significant influence on the yield of FAME  $Y_F$ ,  
416 followed by the reaction temperature  $T$  and the mass ratio of methanol to DPO  $r_{m/o}$ . The  
417 maximum  $Y_F$  is 85.36% (w/w), obtained at the following conditions:  $T = 60^\circ\text{C}$ ,  $t = 4.5$  h, and  
418  $r_{m/o} = 6:1$ , with a catalyst loading of 6% (w/w). Notably, Fe/DS-HMS-NH<sub>2</sub> catalyst shows a  
419 good recyclability, with the yield staying above 80% for three reaction cycles. Therefore,  
420 Fe/DS-HMS-NH<sub>2</sub> is a promising heterogeneous catalyst to obtain biodiesel from DPO or other  
421 lipid materials with high FFA and water content. Further study on (1) the extension of the  
422 catalyst lifetime by creating a technique suitable for its regeneration, and also (2) the design  
423 of a plausible route between the current research and its industrial application should be the  
424 main focus for future research expansion.

425

## 426 **Acknowledgments**

427 The authors acknowledge the funding supports from Widya Mandala Catholic University  
428 Surabaya, through the research grant no. 2263/WM01/N/2020. We also thank Professor  
429 Chun-Hu Chen, National Sun Yat Sen University, and Taiwan Tech (National Taiwan

430 University of Science and Technology) for providing the facility for the catalyst  
431 characterizations.

## 432 REFERENCES

- 433 [1] P. Agung, D. Hartono, A.A. Awiryra, Pengaruh Urbanisasi Terhadap Konsumsi Energi Dan  
434 Emisi CO<sub>2</sub>: Analisis Provinsi di Indonesia (The Effect of Urbanization on Energy  
435 Consumption and CO<sub>2</sub> Emissions: An Analysis of Provinces in Indonesia), *J. Ekon.*  
436 *Kuantitatif Terap.* 1 (2017) 9–17. <https://doi.org/10.24843/jekt.2017.v10.i01.p02>.
- 437 [2] A. Fitriyatus, A. Fauzi, B. Juanda, Prediction of Fuel Supply and Consumption in Indonesia  
438 with System Dynamics Model, *J. Ekon. Dan Pembang. Indones.* 17 (2018) 118–137.
- 439 [3] F.T.R. Silalahi, T.M. Simatupang, M.P. Siallagan, Biodiesel produced from palm oil in  
440 Indonesia: Current status and opportunities, *AIMS Energy.* 8 (2020) 81–101.  
441 <https://doi.org/10.3934/energy.2020.1.81>.
- 442 [4] F. Nangoy, B.C. Munthe, Indonesia President wants B30 in use by Jan 2020: cabinet  
443 secretary, Reuters. (2019).
- 444 [5] J.M. Marchetti, A summary of the available technologies for biodiesel production based on  
445 a comparison of different feedstock's properties, *Process Saf. Environ. Prot.* 90 (2012) 157–  
446 163. <https://doi.org/10.1016/j.psep.2011.06.010>.
- 447 [6] K. Suwannakarn, E. Lotero, K. Ngaosuwan, J.G. Goodwin Jr, Simultaneous free fatty acid  
448 esterification and triglyceride transesterification using a solid acid catalyst with in situ  
449 removal of water and unreacted methanol, *Ind. Eng. Chem. Res.* 48 (2009) 2810–2818.  
450 <https://doi.org/https://doi.org/10.1021/ie800889w>.
- 451 [7] Y.A. Tsigie, L.H. Huynh, S. Ismadji, A.M. Engida, Y.H. Ju, In situ biodiesel production  
452 from wet *Chlorella vulgaris* under subcritical condition, *Chem. Eng. J.* 213 (2012) 104–108.  
453 <https://doi.org/10.1016/j.cej.2012.09.112>.

- 454 [8] P.D. Patil, V.G. Gude, A. Mannarswamy, P. Cooke, N. Nirmalakhandan, P. Lammers, S.  
455 Deng, Comparison of direct transesterification of algal biomass under supercritical  
456 methanol and microwave irradiation conditions, *Fuel*. 97 (2012) 822–831.  
457 <https://doi.org/10.1016/j.fuel.2012.02.037>.
- 458 [9] A. Kumari, P. Mahapatra, V.K. Garlapati, R. Banerjee, Enzymatic transesterification of  
459 *Jatropha* oil, *Biotechnol Biofuels*. 2 (2009) 1. <https://doi.org/10.1186/1754-6834-2-1>.
- 460 [10] R. Mat, R.A. Samsudin, M. Mohamed, A. Johari, Solid catalysts and their application in  
461 biodiesel production, *Bull. Chem. React. Eng. Catal.* 7 (2012) 142–149.  
462 <https://doi.org/10.9767/bcrec.7.2.3047.142-149>.
- 463 [11] W. Suryaputra, I. Winata, N. Indraswati, S. Ismadji, Waste capiz (*Amusium cristatum*) shell  
464 as a new heterogeneous catalyst for biodiesel production, *Renew. Energy*. 50 (2013) 795–  
465 799. <https://doi.org/10.1016/j.renene.2012.08.060>.
- 466 [12] H. Li, W. Xie, Transesterification of Soybean Oil to Biodiesel with Zn/I<sub>2</sub> Catalyst, *Catal.*  
467 *Letters*. 107 (2006) 25–30. <https://doi.org/10.1007/s10562-005-9727-9>.
- 468 [13] A.A. Refaat, A.A. Refaat, Archive of SID Different techniques for the production of  
469 biodiesel from waste vegetable oil, *Int. J. Environ. Sci. Tech.* 7 (2010) 183–213.
- 470 [14] P.L. Boey, G.P. Maniam, S.A. Hamid, Performance of calcium oxide as a heterogeneous  
471 catalyst in biodiesel production: A review, *Chem. Eng. J.* 168 (2011) 15–22.  
472 <https://doi.org/10.1016/j.cej.2011.01.009>.
- 473 [15] M.K. Lam, K.T. Lee, A.R. Mohamed, Homogeneous, heterogeneous and enzymatic  
474 catalysis for transesterification of high free fatty acid oil (waste cooking oil) to biodiesel: A  
475 review, *Biotechnol. Adv.* 28 (2010) 500–518.  
476 <https://doi.org/10.1016/j.biotechadv.2010.03.002>.
- 477 [16] W.N.N.W. Omar, N.A.S. Amin, Biodiesel production from waste cooking oil over alkaline

478 modified zirconia catalyst, *Fuel Process. Technol.* 92 (2011) 2397–2405.  
479 <https://doi.org/10.1016/j.fuproc.2011.08.009>.

480 [17] N. Pal, M. Paul, A. Bhaumik, Highly ordered Zn-doped mesoporous silica: An efficient  
481 catalyst for transesterification reaction, *J. Solid State Chem.* 184 (2011) 1805–1812.  
482 <https://doi.org/10.1016/j.jssc.2011.05.033>.

483 [18] W. Xie, X. Huang, Synthesis of biodiesel from soybean oil using heterogeneous KF/ZnO  
484 catalyst, *Catal. Letters.* 107 (2006) 53–59. [https://doi.org/https://doi.org/10.1007/s10562-](https://doi.org/https://doi.org/10.1007/s10562-005-9731-0)  
485 [005-9731-0](https://doi.org/https://doi.org/10.1007/s10562-005-9731-0).

486 [19] S.M. Coman, V.I. Parvulescu, Heterogeneous Catalysis for Biodiesel Production, Role  
487 *Catal. Sustain. Prod. Bio-Fuels Bio-Chemicals.* (2013) 93–136.  
488 <https://doi.org/10.1016/B978-0-444-56330-9.00004-8>.

489 [20] J. Santos, J. Phillips, J.A. Dumesic, Metal-support interactions between iron and titania for  
490 catalysts prepared by thermal decomposition of iron pentacarbonyl and by impregnation, *J.*  
491 *Catal.* 81 (1983) 147–167. [https://doi.org/10.1016/0021-9517\(83\)90154-9](https://doi.org/10.1016/0021-9517(83)90154-9).

492 [21] D.D. Bala, M. Misra, D. Chidambaram, Solid-acid catalyzed biodiesel production, part I:  
493 biodiesel synthesis from low quality feedstock, *J. Clean. Prod.* 142 (2017) 4169–4177.  
494 <https://doi.org/10.1016/j.jclepro.2016.02.128>.

495 [22] C. You, C. Yu, X. Yang, Y. Li, H. Huo, Z. Wang, Y. Jiang, X. Xu, K. Lin, Double-shelled  
496 hollow mesoporous silica nanosphere as acid-base bifunctional catalyst for cascade  
497 reactions, *New J. Chem.* 42 (2018) 4095–4101. <https://doi.org/10.1039/C7NJ04670G>.

498 [23] F.H. Santosa, L. Laysandra, F.E. Soetaredjo, S.P. Santoso, S. Ismadji, M. Yuliana, A facile  
499 noncatalytic methyl ester production from waste chicken tallow using single step subcritical  
500 methanol: Optimization study, *Int. J. Energy Res.* 43 (2019) 8852–8863.  
501 <https://doi.org/10.1002/er.4844>.

- 502 [24] X. Zhou, X. Cheng, W. Feng, K. Qiu, L. Chen, W. Nie, Z. Yin, X. Mo, H. Wang, C. He,  
503 Synthesis of hollow mesoporous silica nanoparticles with tunable shell thickness and pore  
504 size using amphiphilic block copolymers as core templates, *Dalt. Trans.* 43 (2014) 11834–  
505 11842. <https://doi.org/10.1039/c4dt01138d>.
- 506 [25] S. Cao, Z. Zhao, X. Jin, W. Sheng, S. Li, Y. Ge, M. Dong, W. Wu, L. Fang, Unique double-  
507 shelled hollow silica microspheres: Template-guided self-assembly, tunable pore size, high  
508 thermal stability, and their application in removal of neutral red, *J. Mater. Chem.* 21 (2011)  
509 19124–19131. <https://doi.org/10.1039/c1jm13011k>.
- 510 [26] N.B. Klinghoffer, M.J. Castaldi, A. Nzihou, Catalyst Properties and Catalytic Performance  
511 of Char from Biomass Gasification, *Ind. Eng. Chem. Res.* 51 (2012) 13113–13122.  
512 <https://doi.org/10.1021/ie3014082>.
- 513 [27] M. Zakeri, A. Samimi, M. Shafiee Afarani, A. Salehirad, Effects of porosity and pore size  
514 distribution on mechanical strength reliability of industrial-scale catalyst during preparation  
515 and catalytic test steps, *Part. Sci. Technol.* 36 (2018) 96–103.  
516 <https://doi.org/10.1080/02726351.2016.1220437>.
- 517 [28] T. Pangestu, Y. Kurniawan, F.E. Soetaredjo, S.P. Santoso, W. Irawaty, M. Yuliana, S.B.  
518 Hartono, S. Ismadji, The synthesis of biodiesel using copper based metal-organic  
519 framework as a catalyst, *J. Environ. Chem. Eng.* 7 (2019) 103277.  
520 <https://doi.org/10.1016/j.jece.2019.103277>.
- 521 [29] N. Rahmat, N. Sadon, M.A. Yusof, Thermogravimetric Analysis (TGA) Profile at Different  
522 Calcination Conditions for Synthesis of PTES-SBA-15, *Am. J. Appl. Sci.* 14 (2017) 938–  
523 944. <https://doi.org/10.3844/ajassp.2017.938.944>.
- 524 [30] Y.Y. Margaretha, H.S. Prastyo, A. Ayucitra, S. Ismadji, Calcium oxide from pomacea sp.  
525 shell as a catalyst for biodiesel production, *Int. J. Energy Environ. Eng.* 3 (2012) 1–9.

- 526 <https://doi.org/10.1186/2251-6832-3-33>.
- 527 [31] A.M. Dehkoda, A.H. West, N. Ellis, Biochar based solid acid catalyst for biodiesel  
528 production, *Appl. Catal. A Gen.* 382 (2010) 197–204.  
529 <https://doi.org/10.1016/j.apcata.2010.04.051>.
- 530 [32] C. Samart, P. Sreetongkittikul, C. Sookman, Heterogeneous catalysis of transesterification  
531 of soybean oil using KI/mesoporous silica, *Fuel Process. Technol.* 90 (2009) 922–925.  
532 <https://doi.org/10.1016/j.fuproc.2009.03.017>.
- 533 [33] G. Baskar, S. Soumiya, Production of biodiesel from castor oil using iron (II) doped zinc  
534 oxide nanocatalyst, *Renew. Energy.* 98 (2016) 101–107.  
535 <https://doi.org/https://doi.org/10.1016/j.renene.2016.02.068>.
- 536 [34] B. Gurunathan, A. Ravi, Biodiesel production from waste cooking oil using copper doped  
537 zinc oxide nanocomposite as heterogeneous catalyst, *Bioresour. Technol.* 188 (2015) 124–  
538 127. <https://doi.org/https://doi.org/10.1016/j.biortech.2015.01.012>.
- 539 [35] J. Cai, Q.Y. Zhang, F.F. Wei, J.S. Huang, Y.M. Feng, H.T. Ma, Y. Zhang, Preparation of  
540 Copper (II) Containing Phosphomolybdic Acid Salt as Catalyst for the Synthesis of  
541 Biodiesel by Esterification, *J Oleo Sci.* 67 (2018) 427–432.  
542 <https://doi.org/10.5650/jos.ess17208>.
- 543 [36] C. Samart, C. Chaiya, P. Reubroycharoen, Biodiesel production by methanolysis of soybean  
544 oil using calcium supported on mesoporous silica catalyst, *Energy Convers. Manag.* 51  
545 (2010) 1428–1431. <https://doi.org/10.1016/j.enconman.2010.01.017>.
- 546 [37] W. Xie, H. Li, Alumina-supported potassium iodide as a heterogeneous catalyst for  
547 biodiesel production from soybean oil, *J. Mol. Catal. A Chem.* 255 (2006) 1–9.  
548 <https://doi.org/https://doi.org/10.1016/j.molcata.2006.03.061>.
- 549 [38] M. Farooq, A. Ramli, Biodiesel production from low FFA waste cooking oil using

550 heterogeneous catalyst derived from chicken bones, *Renew. Energy*. 76 (2015) 362–368.  
551 <https://doi.org/10.1016/j.renene.2014.11.042>.

552 [39] R. Alenezi, G.A. Leeke, J.M. Winterbottom, R.C.D. Santos, A.R. Khan, Esterification  
553 kinetics of free fatty acids with supercritical methanol for biodiesel production, *Energy*  
554 *Convers. Manag.* 51 (2010) 1055–1059. <https://doi.org/10.1016/j.enconman.2009.12.009>.

555 [40] M. Farooq, A. Ramli, D. Subbarao, Biodiesel production from waste cooking oil using  
556 bifunctional heterogeneous solid catalysts, *J. Clean. Prod.* 59 (2013) 131–140.  
557 <https://doi.org/10.1016/j.jclepro.2013.06.015>.

558 [41] I. Amalia Kartika, M. Yani, D. Ariono, P. Evon, L. Rigal, Biodiesel production from  
559 *Jatropha* seeds: Solvent extraction and in situ transesterification in a single step, *Fuel*. 106  
560 (2013) 111–117. <https://doi.org/10.1016/j.fuel.2013.01.021>.

561 [42] Z. Wei, C. Xu, B. Li, Application of waste eggshell as low-cost solid catalyst for biodiesel  
562 production, *Bioresour. Technol.* 100 (2009) 2883–2885.  
563 <https://doi.org/10.1016/j.biortech.2008.12.039>.

564 [43] A. Demirbas, Biodiesel from waste cooking oil via base-catalytic and supercritical methanol  
565 transesterification, *Energy Convers. Manag.* 50 (2009) 923–927.  
566 <https://doi.org/10.1016/j.enconman.2008.12.023>.

567 [44] I.A. Reşitoğlu, A. Keskin, M. Gürü, The optimization of the esterification reaction in  
568 biodiesel production from trap grease, *Energy Sources, Part A Recover. Util. Environ. Eff.*  
569 34 (2012) 1238–1248. <https://doi.org/10.1080/15567031003792395>.

570 [45] A. Hayyan, F.S. Mjalli, M.A. Hashim, M. Hayyan, I.M. AlNashef, S.M. Al-Zahrani, M.A.  
571 Al-Saadi, Ethanesulfonic acid-based esterification of industrial acidic crude palm oil for  
572 biodiesel production, *Bioresour. Technol.* 102 (2011) 9564–9570.  
573 <https://doi.org/10.1016/j.biortech.2011.07.074>.

- 574 [46] S.L. Lee, Y.C. Wong, Y.P. Tan, S.Y. Yew, Transesterification of palm oil to biodiesel by  
575 using waste obtuse horn shell-derived CaO catalyst, *Energy Convers. Manag.* 93 (2015)  
576 282–288. <https://doi.org/10.1016/j.enconman.2014.12.067>.
- 577 [47] W. Xie, T. Wang, Biodiesel production from soybean oil transesterification using tin oxide-  
578 supported WO<sub>3</sub> catalysts, *Fuel Process. Technol.* 109 (2013) 150–155.  
579 <https://doi.org/10.1016/j.fuproc.2012.09.053>.
- 580 [48] M. Kouzu, J.S. Hidaka, Transesterification of vegetable oil into biodiesel catalyzed by CaO:  
581 A review, *Fuel*. 93 (2012) 1–12. <https://doi.org/10.1016/j.fuel.2011.09.015>.
- 582 [49] D.M. Marinković, M. V. Stanković, A. V. Veličković, J.M. Avramović, M.R. Miladinović,  
583 O.O. Stamenković, V.B. Veljković, D.M. Jovanović, Calcium oxide as a promising  
584 heterogeneous catalyst for biodiesel production: Current state and perspectives, *Renew.*  
585 *Sustain. Energy Rev.* 56 (2016) 1387–1408. <https://doi.org/10.1016/j.rser.2015.12.007>.
- 586 [50] A.K. Endalew, Y. Kiros, R. Zanzi, Inorganic heterogeneous catalysts for biodiesel  
587 production from vegetable oils, *Biomass and Bioenergy*. 35 (2011) 3787–3809.  
588 <https://doi.org/10.1016/j.biombioe.2011.06.011>.
- 589

**Declaration of interests**

The authors declare that they have no known competing financial interests or personal relationships that could have appeared to influence the work reported in this paper.

The authors declare the following financial interests/personal relationships which may be considered as potential competing interests:

## **CREDIT AUTHOR STATEMENT**

- Stefanus Kevin Suryajaya - Conceptualization, methodology, investigation, software, writing – original draft
- Yohanes Ricky Mulyono - Conceptualization, methodology, investigation, software, writing – original draft
- Shella Permatasari Santoso - Conceptualization, data curation, supervision
- Maria Yuliana - Conceptualization, resources, visualization, writing-review and editing, supervision
- Alfin Kurniawan - Investigation, resources
- Aning Ayucitra - Investigation, validation
- Yueting Sun - Writing-review and editing
- Sandy Budi Hartono - Software, validation
- Felycia Edi Soetaredjo - Resources, visualization
- Suryadi Ismadji - Resources, validation



Maria Yuliana &lt;mariayuliana@ukwms.ac.id&gt;

---

**Your Submission RENE-D-20-04164R1**

1 message

---

**Renewable Energy** <em@editorialmanager.com>  
Reply-To: Renewable Energy <rene@elsevier.com>  
To: Maria Yuliana <mariayuliana@ukwms.ac.id>

Wed, Jan 20, 2021 at 12:44 AM

Ms. Ref. No.: RENE-D-20-04164R1

Title: IRON (II) IMPREGNATED DOUBLE-SHELLED HOLLOW MESOPOROUS SILICA AS ACID-BASE BIFUNCTIONAL CATALYST FOR THE CONVERSION OF LOW-QUALITY OIL TO METHYL ESTERS

Renewable Energy

Dear Dr. Yuliana,

The review of your paper is now complete; the Reviewers' reports are below. We kindly ask you to revise the paper considering the Reviewers' remarks and suggestions presented below. When this process is completed, the paper may be acceptable for publication in RENEWABLE ENERGY.

Once you have revised the paper accordingly, please submit it together with a detailed description of your response to these comments. Please, also include a separate copy of the revised paper in which you have marked the revisions made.

The revision will be due by: 18/02/2021

To submit a revision, please go to <https://www.editorialmanager.com/rene/> and login as an Author.

Your username is: [mariayuliana@ukwms.ac.id](mailto:mariayuliana@ukwms.ac.id)

If you need to retrieve password details, please go to: <https://www.editorialmanager.com/rene/l.asp?i=1113310&l=UBGAC2Z6>

NOTE: Upon submitting your revised manuscript, please upload the source files for your article. For additional details regarding acceptable file formats, please refer to the Guide for Authors at: <http://www.elsevier.com/journals/renewable-energy/0960-1481/guide-for-authors>

When submitting your revised paper, we ask that you include the following items:

Manuscript, Marked manuscript and Figure Source Files (mandatory)

We cannot accommodate PDF manuscript files for production purposes. We also ask that when submitting your revision you follow the journal formatting guidelines. Figures and tables may be embedded within the source file for the submission as long as they are of sufficient resolution for Production. For any figure that cannot be embedded within the source file (such as \*.PSD Photoshop files), the original figure needs to be uploaded separately. Refer to the Guide for Authors for additional information.

<http://www.elsevier.com/journals/renewable-energy/0960-1481/guide-for-authors>

Highlights (mandatory)

Highlights consist of a short collection of bullet points that convey the core findings of the article and should be submitted in a separate file in the online submission system. Please use 'Highlights' in the file name and include 3 to 5 bullet points (maximum 85 characters, including spaces, per bullet point). See the following website for more information

<http://www.elsevier.com/highlights>

On your Main Menu page, you will find a folder entitled "Submissions Needing Revision". Your submission record will be presented here.

Please note that this journal offers a new, free service called AudioSlides: brief, webcast-style presentations that are shown next to published articles on ScienceDirect (see also <http://www.elsevier.com/audioslides>). If your paper is accepted for publication, you will automatically receive an invitation to create an AudioSlides presentation.

Effective peer review is essential to uphold the quality and validity of individual articles, but also the overall integrity of the journal. We would like to remind you that for every article considered for publication, there are usually at least 2 reviews required for each review round, and it is critical that scientists wishing to publish their research also be willing to provide reviews to similarly enable the peer review of papers by other authors. Please accept any review assignment within your expertise area(s) we may address to you and undertake reviewing in the manner in which you would hope your own paper to be reviewed.

Renewable Energy features the Interactive Plot Viewer, see: <http://www.elsevier.com/interactiveplots>. Interactive Plots provide easy access to the data behind plots. To include one with your article, please prepare a .csv file with your plot data and test it online at <http://authortools.elsevier.com/interactiveplots/verification> before submission as supplementary material.

Renewable Energy features the Interactive Plot Viewer, see: <http://www.elsevier.com/interactiveplots>. Interactive Plots provide easy access to the data behind plots. To include one with your article, please prepare a .csv file with your plot data and test it online at <http://authortools.elsevier.com/interactiveplots/verification> before submission as supplementary material.

#### MethodsX file (optional)

If you have customized (a) research method(s) for the project presented in your Renewable Energy article, you are invited to submit this part of your work as MethodsX article alongside your revised research article. MethodsX is an independent journal that publishes the work you have done to develop research methods to your specific needs or setting. This is an opportunity to get full credit for the time and money you may have spent on developing research methods, and to increase the visibility and impact of your work.

How does it work?

- 1) Fill in the MethodsX article template: <https://www.elsevier.com/MethodsX-template>
- 2) Place all MethodsX files (including graphical abstract, figures and other relevant files) into a .zip file and upload this as a 'Method Details (MethodsX)' item alongside your revised Renewable Energy manuscript. Please ensure all of your relevant MethodsX documents are zipped into a single file.
- 3) If your Renewable Energy research article is accepted, your MethodsX article will automatically be transferred to MethodsX, where it will be reviewed and published as a separate article upon acceptance. MethodsX is a fully Open Access journal, the publication fee is only 520 US\$.

Questions? Please contact the MethodsX team at [methodsx@elsevier.com](mailto:methodsx@elsevier.com). Example MethodsX articles can be found here: <http://www.sciencedirect.com/science/journal/22150161>

Include interactive data visualizations in your publication and let your readers interact and engage more closely with your research. Follow the instructions here: <https://www.elsevier.com/authors/author-services/data-visualization> to find out about available data visualization options and how to include them with your article.

Thank you very much for expressing your interest in RENEWABLE ENERGY.

#### MethodsX file (optional)

We invite you to submit a method article alongside your research article. This is an opportunity to get full credit for the time and money you have spent on developing research methods, and to increase the visibility and impact of your work. If your research article is accepted, your method article will be automatically transferred over to the open access journal, MethodsX, where it will be editorially reviewed and published as a separate method article upon acceptance. Both articles will be linked on ScienceDirect. Please use the MethodsX template available here when preparing your article: <https://www.elsevier.com/MethodsX-template>. Open access fees apply.

Sincerely,

Soteris Kalogirou, D.Sc.  
Editor-in-Chief  
Renewable Energy

#### Data in Brief (optional):

We invite you to convert your supplementary data (or a part of it) into an additional journal publication in Data in Brief, a multi-disciplinary open access journal. Data in Brief articles are a fantastic way to describe supplementary data and associated metadata, or full raw datasets deposited in an external repository, which are otherwise unnoticed. A Data in Brief article (which will be reviewed, formatted, indexed, and given a DOI) will make your data easier to find, reproduce, and cite.

You can submit to Data in Brief via the Renewable Energy submission system when you upload your revised Renewable Energy manuscript. To do so, complete the template and follow the co-submission instructions found here: [www.elsevier.com/dib-template](http://www.elsevier.com/dib-template). If your Renewable Energy manuscript is accepted, your Data in Brief submission will automatically be transferred to Data in Brief for editorial review and publication.

Please note: an open access Article Publication Charge (APC) is payable by the author or research funder to cover the costs associated with publication in Data in Brief and ensure your data article is immediately and permanently free to access by all. For the current APC see: [www.elsevier.com/journals/data-in-brief/2352-3409/open-access-journal](http://www.elsevier.com/journals/data-in-brief/2352-3409/open-access-journal)

Please contact the Data in Brief editorial office at [dib-me@elsevier.com](mailto:dib-me@elsevier.com) or visit the Data in Brief homepage ([www.journals.elsevier.com/data-in-brief/](http://www.journals.elsevier.com/data-in-brief/)) if you have questions or need further information.

.....  
Note: While submitting the revised manuscript, please double check the author names provided in the submission so that authorship related changes are made in the revision stage. If your manuscript is accepted, any authorship change will involve approval from co-authors and respective editor handling the submission and this may cause a significant delay in publishing your manuscript.  
.....

Reviewers' comments:

%ATTACH\_FOR\_REVIEWER\_DEEP\_LINK INSTRUCTIONS%

Subject Editor:

- I understand Table 1 contains mainly the description of the experimental conditions tested in this research. However, it also contains experimental results (YF), thus I believe it would better located in section 3 (maybe section 3.3, before Figure 3) with the necessary arrangements in the text and renumbering of tables 2 and 3.
- Graphical abstract will not be readable at the required size.
- Image size: Please provide an image with a minimum of 531 × 1328 pixels (h × w) or proportionally more. The image should be readable at a size of 5 × 13 cm using a regular screen resolution of 96 dpi. Preferred file types: TIFF, EPS, PDF or MS Office files. You can view Example Graphical Abstracts on our information site (<https://www.elsevier.com/authors/tools-and-resources/graphical-abstract>).

Reviewer #1: Authors made sufficient revisions in the updated manuscript, now in the present format the research article can accept for the publication in this esteemed journal.

Reviewer #2: I would like to thank the authors for considering my previous comments. However, there are still two important comments which have not been properly addressed.

1. The Graphic Abstract needs to be revised to satisfy the journal's requirements.
2. When the authors benchmark the performance of different catalysts, it is better to compare those catalysts in a Table or Figure. Particularly, it is important to show the distinct role of the bifunctional catalyst to enhance the biodiesel yield, compared to the monofunctional catalyst.

For further assistance, please visit our customer support site at <http://help.elsevier.com/app/answers/list/p/7923> Here you can search for solutions on a range of topics, find answers to frequently asked questions and learn more about EM via interactive tutorials. You will also find our 24/7 support contact details should you need any further assistance from one of our customer support representatives.

---

In compliance with data protection regulations, you may request that we remove your personal registration details at any time. (Use the following URL: <https://www.editorialmanager.com/rene/login.asp?a=r>). Please contact the publication office if you have any questions.



Maria Yuliana &lt;mariayuliana@ukwms.ac.id&gt;

---

**Editor handles your revised submission RENE-D-20-04164R2**

1 message

---

**Renewable Energy** <em@editorialmanager.com>  
Reply-To: Renewable Energy <rene@elsevier.com>  
To: Maria Yuliana <mariayuliana@ukwms.ac.id>

Thu, Jan 21, 2021 at 6:15 PM

Ref.: Revision of RENE-D-20-04164R2

Title: IRON (II) IMPREGNATED DOUBLE-SHELLED HOLLOW MESOPOROUS SILICA AS ACID-BASE BIFUNCTIONAL CATALYST FOR THE CONVERSION OF LOW-QUALITY OIL TO METHYL ESTERS

Dear Dr. Yuliana,

Your revised submission "IRON (II) IMPREGNATED DOUBLE-SHELLED HOLLOW MESOPOROUS SILICA AS ACID-BASE BIFUNCTIONAL CATALYST FOR THE CONVERSION OF LOW-QUALITY OIL TO METHYL ESTERS" will be handled by Editor-in-Chief Soteris Kalogirou, D.Sc..

You may check the progress of your revision by logging into the Editorial Manager as an author at <https://www.editorialmanager.com/rene/>.

Thank you for submitting your revision to this journal.

Kind regards,

Editorial Manager  
Renewable Energy

For further assistance, please visit our customer support site at <http://help.elsevier.com/app/answers/list/p/7923>. Here you can search for solutions on a range of topics, find answers to frequently asked questions and learn more about EM via interactive tutorials. You will also find our 24/7 support contact details should you need any further assistance from one of our customer support representatives.

---

In compliance with data protection regulations, you may request that we remove your personal registration details at any time. (Use the following URL: <https://www.editorialmanager.com/rene/login.asp?a=r>). Please contact the publication office if you have any questions.

## Renewable Energy

# IRON (II) IMPREGNATED DOUBLE-SHELLED HOLLOW MESOPOROUS SILICA AS ACID-BASE BIFUNCTIONAL CATALYST FOR THE CONVERSION OF LOW-QUALITY OIL TO METHYL ESTERS

--Manuscript Draft--

<b>Manuscript Number:</b>	RENE-D-20-04164R2
<b>Article Type:</b>	Research Paper
<b>Keywords:</b>	bifunctional catalyst; biodiesel; renewable energy; hollow mesoporous silica; iron impregnation; amine functionalization
<b>Corresponding Author:</b>	Maria Yuliana, Ph.D. Widya Mandala Catholic University Surabaya: Universitas Katolik Widya Mandala Surabaya Surabaya, East Java INDONESIA
<b>First Author:</b>	Stefanus Kevin Suryajaya
<b>Order of Authors:</b>	Stefanus Kevin Suryajaya Yohanes Ricky Mulyono Shella Permatasari Santoso Maria Yuliana, Ph.D. Alfin Kurniawan Aning Ayucitra Yueting Sun Sandy Budi Hartono Felycia Edi Soetaredjo Suryadi Ismadji
<b>Abstract:</b>	<p>To promote the use of low-quality oils in producing biodiesel, a bifunctional acid-base catalyst Fe/DS-HMS-NH<sub>2</sub> is fabricated using the two-step condensation technique. The obtained Fe/DS-HMS-NH<sub>2</sub> is of a doubled shell structure in spherical shape with a uniform size of 156 nm. Its hollow core (with a diameter of 86 nm) and two spatial shells with different active sites enables the esterification and transesterification reactions to be accomplished in a one-pot synthesis. The influences of four independent reaction variables on the yield of fatty acid methyl esters YF was studied, including catalyst loading <math>m_c</math>, reaction time <math>t</math>, reaction temperature <math>T</math>, and the methanol to degummed palm oil mass ratio <math>rm/o</math>. The highest yield was obtained at 85.36% (w/w) when <math>m_c = 6\%</math> (w/w), <math>t = 4.5</math> h, <math>T = 60</math> oC, and <math>rm/o = 6:1</math>. The Fe/DS-HMS-NH<sub>2</sub> shows a good recyclability with YF &gt; 80% (w/w) up to three reaction cycles.</p>

# **IRON (II) IMPREGNATED DOUBLE-SHELLED HOLLOW MESOPOROUS SILICA AS ACID-BASE BIFUNCTIONAL CATALYST FOR THE CONVERSION OF LOW-QUALITY OIL TO METHYL ESTERS**

Stefanus Kevin Suryajaya<sup>1,a</sup>, Yohanes Ricky Mulyono<sup>1,a</sup>, Shella Permatasari Santoso<sup>1,2</sup>, Maria Yuliana<sup>1\*</sup>, Alfin Kurniawan<sup>3</sup>, Aning Ayucitra<sup>1</sup>, Yueting Sun<sup>4</sup>, Sandy Budi Hartono<sup>1</sup>, Felycia Edi Soetaredjo<sup>1,2</sup>, Suryadi Ismadji<sup>1,2</sup>

<sup>1</sup> Department of Chemical Engineering, Widya Mandala Catholic University Surabaya, Kalijudan 37, Surabaya 60114, Indonesia

<sup>2</sup> Department of Chemical Engineering, National Taiwan University of Science and Technology, 43, Keelung Rd., Sec. 4, Taipei 10607, Taiwan

<sup>3</sup> Department of Chemistry, National Sun Yat-Sen University, Kaohsiung 80424, Taiwan

<sup>4</sup> Department of Mechanical Engineering, University of Birmingham, Edgbaston, Birmingham B15 2TT, United Kingdom

<sup>a</sup> These authors contributed equally to this work

\*Corresponding authors: Tel. (62) 31 3891264; Fax. (62) 31 3891267; Email address: [mariayuliana@ukwms.ac.id](mailto:mariayuliana@ukwms.ac.id) (M. Yuliana)



Widya Mandala Catholic University Surabaya  
Engineering Faculty  
**CHEMICAL ENGINEERING DEPARTMENT**  
Jl. Kalijudan 37 Surabaya 60114; Phone: +62 313893933 Fax: +62 31 3891267  
Website: <http://www.ukwms.ac.id>

---

January 20, 2021

**Professor Soteris Kalogirou**

Editor-in-Chief

*Renewable Energy*

Dear Professor Kalogirou,

On behalf of my co-author, I am writing to submit the revised manuscript for publication consideration in *Renewable Energy*. The details of the manuscript are as follows:

Title of Manuscript: **IRON (II) IMPREGNATED DOUBLE-SHELLED HOLLOW MESOPOROUS SILICA AS ACID-BASE BIFUNCTIONAL CATALYST FOR THE CONVERSION OF LOW-QUALITY OIL TO METHYL ESTERS**

Authors: Stefanus Kevin Suryajaya ([sstefanuskevin@gmail.com](mailto:sstefanuskevin@gmail.com)), Yohanes Ricky Mulyono ([rickymulyono96@gmail.com](mailto:rickymulyono96@gmail.com)), Shella Permatasari Santoso ([shella\\_p5@yahoo.com](mailto:shella_p5@yahoo.com)), Maria Yuliana, Alfin Kurniawan ([alfin\\_kur@yahoo.com](mailto:alfin_kur@yahoo.com)), Aning Ayucitra ([aayucitra@yahoo.com](mailto:aayucitra@yahoo.com)), Yueting Sun ([y.sun.9@bham.ac.uk](mailto:y.sun.9@bham.ac.uk)), Sandy Budi Hartono ([sandy@ukwms.ac.id](mailto:sandy@ukwms.ac.id)), Felycia Edi Soetaredjo ([felyciae@yahoo.com](mailto:felyciae@yahoo.com)), Suryadi Ismadji ([suryadiismadji@yahoo.com](mailto:suryadiismadji@yahoo.com))

Corresponding author:

Maria Yuliana; Department of Chemical Engineering; Widya Mandala Catholic University Surabaya; Kalijudan 37, Surabaya 60114, Indonesia

Tel: (62) 31 3891264; Fax. (62) 31 3891267;

E-mail: [mariayuliana@ukwms.ac.id](mailto:mariayuliana@ukwms.ac.id)

Keywords: *bifunctional catalyst; biodiesel; renewable energy; hollow mesoporous silica; iron impregnation; amine functionalization*

Word counts: 4859 words (excluding abstract, tables, figures, and references)

We greatly appreciate the constructive comments and suggestions given by the editor and reviewers. We have addressed the major concerns of the reviewers and revised the manuscript accordingly. We also know of no conflicts of interest associated with this publication and there has been no significant financial support for this work that could have influenced its outcome. Furthermore, we have strictly prepared the manuscript in accordance with the journal and ethical guidelines.



Widya Mandala Catholic University Surabaya

Engineering Faculty

**CHEMICAL ENGINEERING DEPARTMENT**

Jl. Kalijudan 37 Surabaya 60114; Phone: +62 313893933 Fax: +62 31 3891267

Website: <http://www.ukwms.ac.id>

---

Thank you for your consideration. I am looking forward to hearing from your positive response.

Sincerely yours,

A handwritten signature in blue ink, consisting of a tall, thin vertical stroke followed by a series of loops and a horizontal line at the bottom.

Maria Yuliana



Widya Mandala Catholic University Surabaya  
Engineering Faculty

**CHEMICAL ENGINEERING DEPARTMENT**

Jl. Kalijudan 37 Surabaya 60114; Phone: +62 313893933 Fax: +62 31  
3891267

Website: <http://www.ukwms.ac.id>

---

Journal: *Renewable Energy*

Title: **Iron (II) impregnated double-shelled hollow mesoporous silica as acid-base bifunctional catalyst for the conversion of low-quality oil to methyl esters**

Dear Editor,

We appreciate your useful comments and suggestions on our manuscript. We have modified the manuscript accordingly, and detailed corrections are listed below:

Subject Editor

- 1) I understand Table 1 contains mainly the description of the experimental conditions tested in this research. However, it also contains experimental results (YF), thus I believe it would be better located in section 3 (maybe section 3.3, before Figure 3) with the necessary arrangements in the text and renumbering of tables 2 and 3.

*Response: We have moved Table 1 to section 3.3, and also made necessary arrangements in the text, as highlighted in p.7 line 132, p.11 line 205, p.12 line 227, p.14 line 243 and 251, p.15 line 265, p.16 line 271.*

- 2) Graphical abstract will not be readable at the required size. Image size: Please provide an image with a minimum of  $531 \times 1328$  pixels (h  $\times$  w) or proportionally more. The image should be readable at a size of  $5 \times 13$  cm using a regular screen resolution of 96 dpi. Preferred file types: TIFF, EPS, PDF or MS Office files.

*Response: We have revised the graphical abstract; the dimension is  $786 \times 1964$  pixels (h  $\times$  w), which is proportional to the mentioned pixels.*

Reviewer #1

- 1) Authors made sufficient revisions in the updated manuscript, now in the present format the research article can accept for the publication in this esteemed journal.

*Response: We would like to thank the reviewer for the thoughtful comments given previously to improve our manuscript.*

Reviewer #2

- 1) The Graphic Abstract needs to be revised to satisfy the journal's requirements.

*Response: We have revised the graphical abstract according to the requirements of the journal.*



Widya Mandala Catholic University Surabaya  
Engineering Faculty

**CHEMICAL ENGINEERING DEPARTMENT**

Jl. Kalijudan 37 Surabaya 60114; Phone: +62 313893933 Fax: +62 31  
3891267

Website: <http://www.ukwms.ac.id>

---

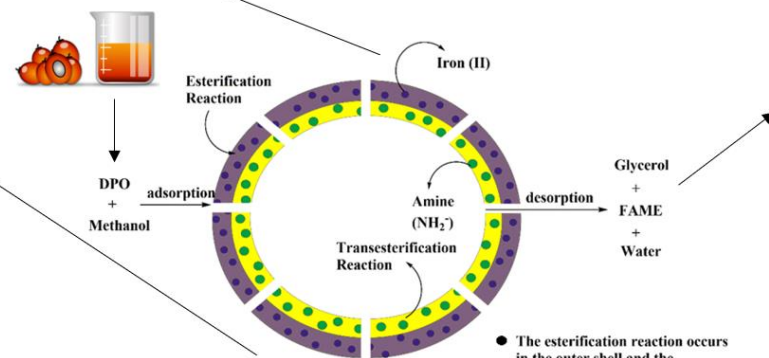
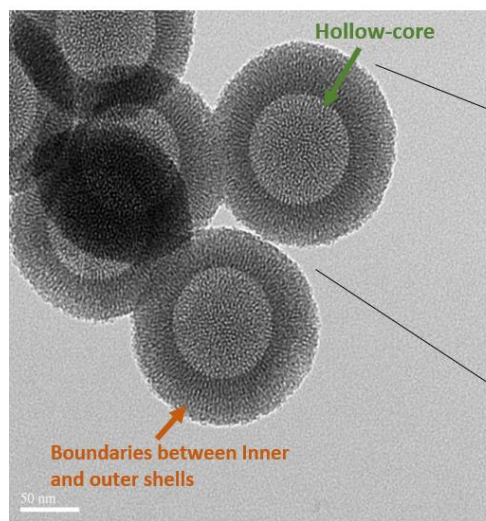
- 2) When the authors benchmark the performance of different catalysts, it is better to compare those catalysts in a Table or Figure. Particularly, it is important to show the distinct role of the bifunctional catalyst to enhance the biodiesel yield, compared to the monofunctional catalyst.

*Response: We have added a table in the text (Table 4, p.4 line 334) as well as a paragraph to briefly describe the distinct role of bifunctional catalyst to enhance the yield of FAME (p.19 line 324-333).*

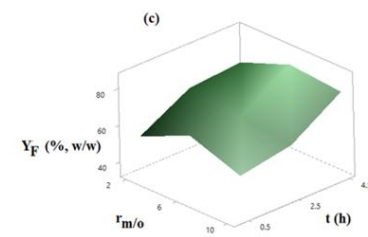
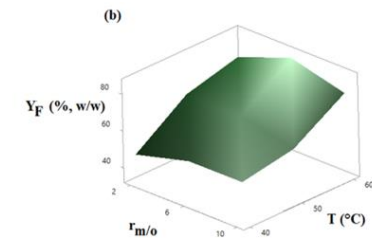
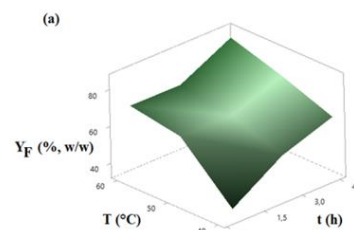
The manuscript has been resubmitted to your journal. We look forward to your positive response.

Sincerely yours,

Maria Yuliana



- The esterification reaction occurs in the outer shell and the surface of the catalyst
- The transesterification reaction occurs in the inner shell and the hollow section



- A novel acid-base bifunctional catalyst, Fe/DS-HMS-NH<sub>2</sub>, has been fabricated
- Fe/DS-HMS-NH<sub>2</sub> has been successfully employed to convert low-quality oil to FAME
- 85.36% of FAME yield was achieved from low-quality oil using Fe/DS-HMS-NH<sub>2</sub>
- The fuel properties of the final FAME product conform to ASTM D6751
- Fe/DS-HMS-NH<sub>2</sub> shows a good recyclability with FAME yield > 80% up to the third run

**1 Abstract**

2 To promote the use of low-quality oils in producing biodiesel, a bifunctional acid-base  
3 catalyst Fe/DS-HMS-NH<sub>2</sub> is fabricated using the two-step condensation technique. The obtained  
4 Fe/DS-HMS-NH<sub>2</sub> is of a doubled shell structure in spherical shape with a uniform size of 156 nm.  
5 Its hollow core (with a diameter of 86 nm) and two spatial shells with different active sites enables  
6 the esterification and transesterification reactions to be accomplished in a one-pot synthesis. The  
7 influences of four independent reaction variables on the yield of fatty acid methyl esters  $Y_F$  was  
8 studied, including catalyst loading  $m_c$ , reaction time  $t$ , reaction temperature  $T$ , and the methanol to  
9 degummed palm oil mass ratio  $r_{m/o}$ . The highest yield was obtained at 85.36% (w/w) when  $m_c =$   
10 6% (w/w),  $t = 4.5$  h,  $T = 60$  °C, and  $r_{m/o} = 6:1$ . The Fe/DS-HMS-NH<sub>2</sub> shows a good recyclability  
11 with  $Y_F > 80\%$  (w/w) up to three reaction cycles.

12 *Keywords: bifunctional catalyst; biodiesel; renewable energy; hollow mesoporous silica; iron*  
13 *impregnation; amine functionalization*

14 **1. Introduction<sup>1</sup>**

15           The global fuel demand is growing rapidly as it undergoes an extensive urbanization.  
16       Our heavy reliance on fossil fuel brings the risk of unstable market price and reduced fuel  
17       availability. The gas emission from fossil fuel combustion also causes environmental concerns.  
18       Therefore, developing an alternative fuel that is biodegradable, sustainable and with a low  
19       carbon emission is the most significant energy and environmental challenge for us in the  
20       coming decades [1,2]. Since 2006, the Indonesian government has been committed to reducing  
21       carbon emissions by replacing fossil fuels with biodiesel [3]. It is also declared that the use of  
22       biodiesel in diesel blend will be increased from B20 to B30 starting from 2020 [4], with a  
23       strategy to boost the domestic use of palm oil and lower down energy imports. Usually,  
24       biodiesel is obtained through the conventional transesterification process of refined oil [5].  
25       However, the technologies of utilizing non-refined oil, specifically the low-quality oil, have  
26       currently attracted extensive interests and are being developed. Various types of low-quality  
27       oil have been studied to produce high-quality biodiesel using sundry of technical routes,  
28       including the two steps acidic esterification followed by basic transesterification [6],

---

1

FFA	Free fatty acids
FAME	Fatty acid methyl esters
DPO	Degummed palm oil
CPO	Crude palm oil
SS-HMS-NH <sub>2</sub>	Single-shelled hollow mesoporous silica
DS-HMS-NH <sub>2</sub>	Double-shelled hollow mesoporous silica
Fe/DS-HMS-NH <sub>2</sub>	Iron (II) impregnated double-shelled hollow mesoporous silica

29 noncatalytic transesterification using alcohol under subcritical [7] and supercritical conditions  
30 [8], enzymatic transesterification [9] and solid-catalyzed transesterification [10]. Among the  
31 available routes, the use of heterogeneous (solid) catalysts has been attracting a growing  
32 interest in recent years, as it has the advantage of easier separation, tolerance to impurities  
33 (i.e., FFA, water and other minor compounds), and good reusability [11] which means  
34 minimal waste and toxic water production [12] and environmentally friendly [13]. Boey et al.  
35 (2011) and Lam et al. (2010) also stated that heterogeneous catalysts lower the product  
36 contamination level, and reduce the corrosion problem [14,15]. Various solid catalysts and  
37 their modifications have been reported, such as zirconia [16], silica impregnated with zinc  
38 stearate (ZS/Si) [17], heterogeneous KF/ZnO catalyst [18], heterogeneous Zn/I<sub>2</sub> catalyst [12].  
39 However, despite their insensitivity to impurities, these catalysts solely act as the mono  
40 functional catalysts, depending on their acidity nature and have the following disadvantages  
41 during the conversion of low-quality oil to biodiesel: (1) the reaction carried out in the  
42 presence of an acidic heterogeneous catalyst is slow, and at the same time, requires large  
43 amount of alcohol [19], meanwhile (2) the basic heterogeneous catalysts usually result in a  
44 lower biodiesel yield and purity, since this type of catalyst leaves the FFA unreacted during  
45 the reaction.

46 In this paper, we prepared and characterized a new class of heterogeneous catalyst,  
47 the double-shelled hollow mesoporous silica impregnated with divalent iron metal (Fe/DS-  
48 HMS-NH<sub>2</sub>), to be used as an acid-base bifunctional catalyst in the production of biodiesel  
49 from a low-quality oil. This catalyst enables a simple process of converting low-quality oil to  
50 biodiesel by combining the two processes of esterification and transesterification into a single-  
51 stage process. This is achieved by having double active surface layers that facilitate the two  
52 reactions to run simultaneously. The primary (inner) shell is designed to promote the

53 transesterification reaction by adding  $-\text{NH}_2$  as the basic site, while the outer layer is  
54 impregnated with the divalent iron (Fe (II)), which is selected as the impregnated metals due  
55 to its nature as a strong Lewis acid, and its ability to change the oxidation level and activate  
56 the substance during the process [20].

57 The synthesis, characterization and catalytic activity of the Fe/DS-HMS-NH<sub>2</sub> will be  
58 investigated in this paper. Its performance as an acid-base bifunctional catalyst for biodiesel  
59 preparation will be examined at various conditions, including catalyst loading  $m_c$  (% , w/w),  
60 reaction temperature  $T$  (°C), reaction time  $t$  (h), and the mass ratio of methanol to oil  $r_{m/o}$ . In  
61 this present research, degummed palm oil (DPO) is selected as the lipid material. With similar  
62 content of FFA and moisture as the crude palm oil (CPO), DPO is also classified as a low-  
63 quality oil, along with industrial fats, oils and greases, and other crude/waste lipids. Therefore,  
64 it is considered as a suitable raw material to determine the catalytic ability of Fe/DS-HMS-  
65 NH<sub>2</sub> in converting both FFA and triglycerides in DPO into biodiesel. We will also show that  
66 the Fe/DS-HMS-NH<sub>2</sub> can be regenerated and reused, which is regarded as an important feature  
67 for heterogeneous catalysts as it will reduce the cost for production and pollutant discharges  
68 [21,22]. The recyclability of the catalyst will be investigated at the operating condition giving  
69 the highest yield of fatty acid methyl esters (FAME)  $Y_F$ .

70

## 71 **2. Materials and methods**

### 72 **2.1 Materials**

73 CPO was collected from the local manufacturer in Indonesia. Prior to use, CPO was  
74 degummed using 1% (w/w) phosphoric acid (PA, 85% purity) at a temperature of 80 – 90°C  
75 for 30 min to reduce the phosphorus content. Several important characteristics of the  
76 degummed CPO (i.e., DPO), namely free fatty acid content, acid value, saponification value,

77 and moisture content were analyzed in accordance with the standard method of AOCS Ca 5a-  
78 40, Cd 3d-63, Cd 3d-25, and Ca 2e-84, respectively.

79 3-aminopropyl-triethoxysilane (APTES) was purchased from Fisher Scientific  
80 (Pittsburgh, USA), while other chemicals required for the fabrication of Fe/DS-HMS, namely  
81 iron (II) sulfate heptahydrate ( $\text{FeSO}_4 \cdot 7\text{H}_2\text{O}$ , 99.99% purity), tetraethylorthosilicate (TEOS),  
82 cetyltrimethylammonium bromide (CTAB), ethanol (98% purity), methanol (99,9% purity),  
83 hydrochloric acid (HCl, 37% purity), ammonium hydroxide solution ( $\text{NH}_4\text{OH}$ , 25% purity),  
84 and n-hexane (95% purity) were obtained from Merck (Merck, Germany). The FAMES  
85 standard (47885 U) containing 37 components FAME mix was procured from Supelco  
86 (Bellefonte, PA, USA). Ultra-high purity nitrogen gas (> 99.0% purity) was purchased from  
87 Aneka Gas Industry Pty. Ltd., Indonesia. All chemicals used in this study were of analytical  
88 grade and required no further purification.

89

## 90 **2.2 Preparation of DS-HMS-NH<sub>2</sub>**

91 In a typical synthesis, 0.14 g of CTAB, 20 ml of ethanol, 50 ml of deionized water and  
92 1 ml of  $\text{NH}_4\text{OH}$  solution were simultaneously introduced into a glass beaker and mixed for 15  
93 minutes at room temperature. Then 1 ml of TEOS was slowly added into the above solution  
94 and kept stirring for 24 hours. The precipitates were collected through centrifugation at 4500  
95 rpm for 30 min, triplicate ethanol washing, and drying at 120 °C overnight. After the  
96 calcination at 550°C for 6 h, the single shelled hollow mesoporous silica (SS-HMS-NH<sub>2</sub>) was  
97 obtained.

98 The outer shell of the particle was fabricated using a multilevel scheme based on SS-  
99 HMS-NH<sub>2</sub>. In a typical synthesis, 0.5 g CTAB, 18 ml deionized water, and 50 ml of ethanol  
100 were introduced into a beaker glass. Meanwhile, 0.063 g of SS-HMS-NH<sub>2</sub> was added into a

101 mixture of 4 ml deionized water and 8.5 ml of 25% (w/w)  $\text{NH}_4\text{OH}$  solution. The above two  
102 solutions were then combined and stirred for 15 min at 250 rpm, after which 100  $\mu\text{l}$  TEOS  
103 and 21  $\mu\text{l}$  APTES were slowly added into it and the mixture was kept stirring for 24 h to allow  
104 the condensation reaction of silica. Finally, the solid product was collected by centrifugation  
105 at 4500 rpm for 15 min, which was then repeatedly washed with 60 ml of ethanol and 4 ml of  
106 HCl, and oven-dried at 120°C. The dried product was calcined at 550 °C for 6 h to obtain  
107 double-shelled hollow mesoporous silica (DS-HMS-NH<sub>2</sub>).

108

### 109 **2.3 Iron (II) impregnation onto DS-HMS-NH<sub>2</sub> surface**

110 The impregnation of divalent iron onto the DS-HMS-NH<sub>2</sub> surface was achieved as  
111 follows to fabricate Fe/DS-HMS-NH<sub>2</sub> catalysts. In a typical synthesis, 0.1 g DS-HMS-NH<sub>2</sub>  
112 was mixed with 50 ml of deionized water under sonication for 30 minutes at room temperature.  
113 Meanwhile, two separate solutions were prepared: (1) 5 mg of  $\text{FeSO}_4 \cdot 7\text{H}_2\text{O}$  was dissolved in  
114 50 ml of deionized water, and (2) 0.2 g of CTAB was dissolved in 10 ml ethanol. Solution (1)  
115 and (2) were then added into the DS-HMS-NH<sub>2</sub> solution and stirred for 12 hours at ambient  
116 conditions. The Fe/DS-HMS-NH<sub>2</sub> precipitates were separated by a centrifugation at 4500 rpm  
117 for 15 min, and then dried at 120 °C for 12 h and calcined at 550 °C for 5 hours to obtain the  
118 Fe/DS-HMS-NH<sub>2</sub> powder.

119

### 120 **2.4. Catalytic activity of Fe/DS-HMS-NH<sub>2</sub> at various reaction conditions**

121 The *in-situ* esterification/transesterification reactions from DPO to FAME were carried  
122 out in a glass flask equipped with a reflux condenser and external heater under constant  
123 magnetic stirring (250 rpm) at various conditions. Specifically, the influence of four reaction  
124 parameters were investigated due to their relevance to industrial applications: catalyst loading

125  $m_c$  (% , w/w), reaction temperature  $T$  ( $^{\circ}\text{C}$ ), reaction time  $t$  (h), and the mass ratio of methanol  
126 to DPO  $r_{m/o}$ . To determine the amount of Fe/DS-HMS-NH<sub>2</sub> catalyst that produces the  
127 maximum FAME yield  $Y_F$ , a few reactions were carried out with different amounts of Fe/DS-  
128 HMS-NH<sub>2</sub> ( $m_c = 2\%$ ,  $4\%$ ,  $6\%$ ,  $8\%$ , w/w) at the following condition:  $T = 60$   $^{\circ}\text{C}$ ,  $t = 4.5$  h and  
129  $r_{m/o} = 10:1$ . Once the optimum catalyst loading is obtained, the catalytic activity of Fe/DS-  
130 HMS-NH<sub>2</sub> was investigated within an experimental matrix defined by  $T = 40$   $^{\circ}\text{C}$ ,  $50$   $^{\circ}\text{C}$ ,  $60$   $^{\circ}\text{C}$ ,  
131  $t = 0.5$  h,  $2.5$  h,  $4.5$  h, and  $r_{m/o} = 2:1$ ,  $6:1$ ,  $10:1$ . The experimental runs were designed in a  
132 random order using face centered-central composite design (CCF-CCD) as listed in [Table 3](#).  
133 All the experimental runs were conducted with the same procedure.

134 After the reaction completed, Fe/DS-HMS-NH<sub>2</sub> catalyst was recovered by  
135 centrifugation at 4500 rpm for 15 min, and calcination at 550  $^{\circ}\text{C}$  for 5 h. The liquid product  
136 was subjected to a two-stage liquid-liquid extraction using methanol and n-hexane  
137 sequentially for purification. Then the FAME-rich phase was separated from the by-products  
138 (i.e., glycerol, excess methanol, soap, and the other unwanted materials) and evaporated under  
139 vacuum to obtain the final FAME product. As an evaluation of the catalytic activity of Fe/DS-  
140 HMS-NH<sub>2</sub>, the yield of FAME was calculated by the following equation:

$$Y_F (\%, \text{ w/w}) = \frac{m_F p_F}{m_S} \times 100 \quad (1)$$

141 Where  $m_F$  is the mass of the final FAME product (g),  $p_F$  is the FAME purity (% , w/w)  
142 obtained from equation (2) shown in the next section, and  $m_S$  is the total mass of the DPO (g).

143

## 144 **2.5 Characterization of Fe/DS-HMS-NH<sub>2</sub> catalyst and FAME**

145 The characterization of Fe/DS-HMS-NH<sub>2</sub> was conducted using field-emission  
146 scanning electron microscopy with energy dispersive X-Ray spectroscopy (FESEM/EDX),  
147 transmission electron microscopy (TEM), nitrogen sorption, and thermogravimetric analysis

148 (TGA). The FESEM/EDX images were taken on a JEOL JSM-6500 F (Jeol Ltd., Japan)  
149 running at 15 kV with a working distance of 12.4 mm, while TEM was carried out on JEOL  
150 JEM-2100 with an accelerating voltage of 200 kV. Nitrogen sorption analysis was conducted  
151 at 77 K on a Micrometrics ASAP 2010 Sorption Analyzer. The sample was degassed at 423  
152 K prior to analysis. To determine the thermal stability and volatile component fraction of the  
153 Fe/DS-HMS-NH<sub>2</sub> catalyst, a TGA analysis was performed using TG/DTA Diamond  
154 instrument (Perkin-Elmer, Japan).

155 The final FAME product characteristics, including its kinematic viscosity (at 40°C),  
156 flashpoint, cetane number, acid value and calorific value were determined according to the  
157 standard methods of ASTM D445, ASTM D93, ASTM D613, ASTM D664, and ASTM D240,  
158 respectively. The purity of FAME ( $p_F$ ) in the final product was analyzed using a gas  
159 chromatograph (Shimadzu GC-2014) equipped with a split/splitless injector and a flame  
160 ionization detector (FID). The stationary phase used for separation was the narrow bore non-  
161 polar DB-WAX column (30 m × 0.25 mm ID × 0.25 μm film thickness, Agilent Technology,  
162 CA), and the temperature profile for the analysis was in accordance with the study conducted  
163 by Harijaya et al. (2019) [23]. Methyl heptadecanoate (MH) was used as an internal standard,  
164 while an external FAME reference (47885 U, containing 37 components FAME standard mix)  
165 was used to obtain the FAME compositional profile.  $p_F$  is calculated by the following equation:

$$p_F (\%, w/w) = \left( \frac{\sum A_F - A_{MH}}{A_{MH}} \right) \left( \frac{V_{MH} C_{MH}}{m_F} \right) \times 100 \quad (2)$$

166 Where  $\sum A_F$  is the total peak area of FAME,  $A_{MH}$  is the corresponding area of methyl  
167 heptadecanoate (MH) peak,  $V_{MH}$  is the volume of MH solution (ml),  $C_{MH}$  is the actual  
168 concentration of MH solution (g/ml), and  $m_F$  is the actual mass of the final FAME product  
169 (g).

170

## 171 **2.6 Recyclability of Fe/DS-HMS-NH<sub>2</sub>**

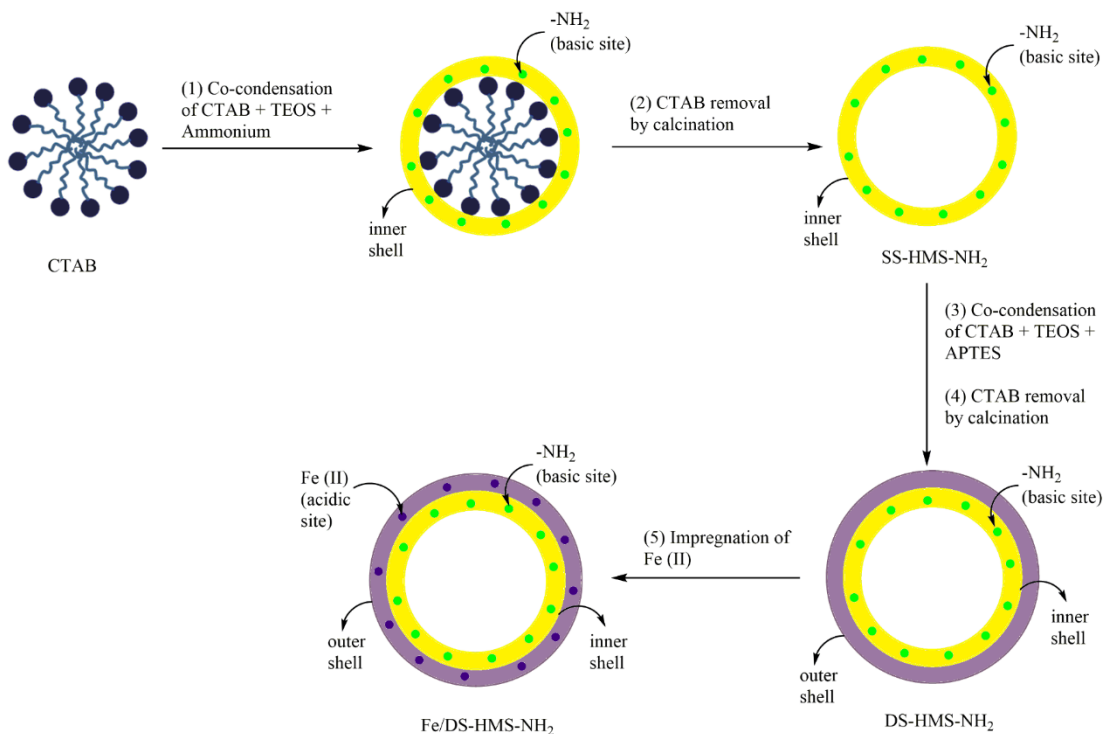
172 Fe/DS-HMS-NH<sub>2</sub> was repeatedly used for the transesterification process at the  
173 operating condition where the maximum yield of FAME was obtained. The recyclability of  
174 Fe/DS-HMS-NH<sub>2</sub> was determined by the number of repetitions until when the yield became  
175 lower than 80% (w/w). The purity and yield of FAME were analyzed according to the  
176 procedures in section 2.4-2.5. All experiments were carried out in triplicates to verify the  
177 results.

178

## 179 **3. Result and Discussions**

### 180 **3.1 The mechanism scheme of Fe/DS-HMS-NH<sub>2</sub> fabrication**

181 The Fe/DS-HMS-NH<sub>2</sub> was synthesized by a two-step co-condensation technique.  
182 The mechanism scheme in Figure 1 illustrates the fabrication route: (1) firstly, TEOS and  
183 CTAB undergo a co-condensation reaction along with the ammonium solution; (2) then  
184 CTAB, the soft template of the core, is removed by calcination, and the SS-HMS-NH<sub>2</sub> is thus  
185 formed; (3) TEOS, APTES, and CTAB undergo another co-condensation reaction on the outer  
186 surface of the SS-HMS-NH<sub>2</sub> spheres; (4) DS-HMS-NH<sub>2</sub> nanosphere is obtained by removing  
187 CTAB and APTES in calcination; (5) the divalent iron (Fe (II)) was incorporated onto the  
188 surface of DS-HMS-NH<sub>2</sub> by a traditional wet impregnation technique, and the Fe/DS-HMS-  
189 NH<sub>2</sub> nanosphere is obtained.



190

191

**Figure 1.** The mechanism scheme of Fe/DS-HMS-NH<sub>2</sub> fabrication.

192

### 193 3.2 Characterization of Fe/DS-HMS-NH<sub>2</sub> catalysts

194

Figure 2a, c–d present the SEM and TEM images of the Fe/DS-HMS-NH<sub>2</sub> catalyst

195

synthesized by the co-condensation technique. The catalyst is spherical with a uniform size at

196

*ca.* 156 nm (Figure 2a). Notably, Fe/DS-HMS-NH<sub>2</sub> is composed of two shell layers, indicated

197

by the darker color of the inner shell in Figure 2c-d. Its hollow-core structure is clearly

198

presented with the diameter of 86 nm (Figure 2d). The shell thicknesses of the inner and outer

199

layer of Fe/DS-HMS-NH<sub>2</sub>, are 22 nm and 13 nm, respectively. The impregnation of Fe (II) on

200

the surface of the silica layer was successful, evidenced from the EDX result showing a

201

percentage of 2.87% (Figure 2b). Based on the fabrication procedure, it was reasonable to

202 consider that the Fe (II) sites and basic amino sites were spatially isolated and located in  
203 different shells.

204 The textural properties of Fe/DS-HMS-NH<sub>2</sub> analyzed by the nitrogen sorption are  
205 presented in Table 1 and Figure 2e. The nitrogen adsorption and desorption isotherm of the  
206 catalyst exhibits a typical type-IV isotherm, indicating the presence of a mesoporous structure  
207 with worm-like capillary pores molded by the CTAB micelles. The pore size of the  
208 mesoporous structure is found to be 2.43 nm (Figure 2e (inset)). A steep increase of the  
209 nitrogen adsorption amount at  $p/p^0$  close to unity also suggests that there are macropores  
210 structure within the particle, corresponding to the hollow core. Similar adsorption and  
211 desorption profile also pointed out that the pores are highly accessible. The specific surface  
212 area  $S_{\text{BET}}$  obtained in this study was 782.84 m<sup>2</sup>/g, lower than the value 1100 – 1350 m<sup>2</sup>/g for  
213 a similar double shelled hollow mesoporous silica [22]. Such a discrepancy was likely due to  
214 the reason that it was strongly influenced by the shell thickness. Zhou et al. (2014) reported  
215 that when the thickness of hollow mesoporous silica nanoparticles (HMSN) increases from  
216 46 nm to 82 nm, the surface area of HMSN particles was declined from 986 m<sup>2</sup>/g to 614 m<sup>2</sup>/g  
217 [24]. Zhou et al. (2014) and Cao et al. (2011) also observed that an increase in the particle  
218 mass due to the addition of TEOS and CTAB in the synthesis of the second shell lowers the  
219 surface area, since the amount of TEOS during the fabrication is directly proportional to the  
220 thickness of the shell [24,25]. Meanwhile, the pore volume of Fe/DS-HMS-NH<sub>2</sub> (0.64 cm<sup>3</sup>/g)  
221 was found to be slightly higher than that reported by You et al. (2018) (0.61 cm<sup>3</sup>/g) [22].  
222 Based on its textural analysis, Fe/DS-HMS-NH<sub>2</sub> possesses comparable specific surface area  
223 and pore volume with those of existing heterogeneous catalysts (i.e., HMS-Al@MS-NH<sub>2</sub> [22],  
224 char-based catalyst [26],  $\gamma$ -alumina industrial-grade catalyst [27], and copper-based metal-

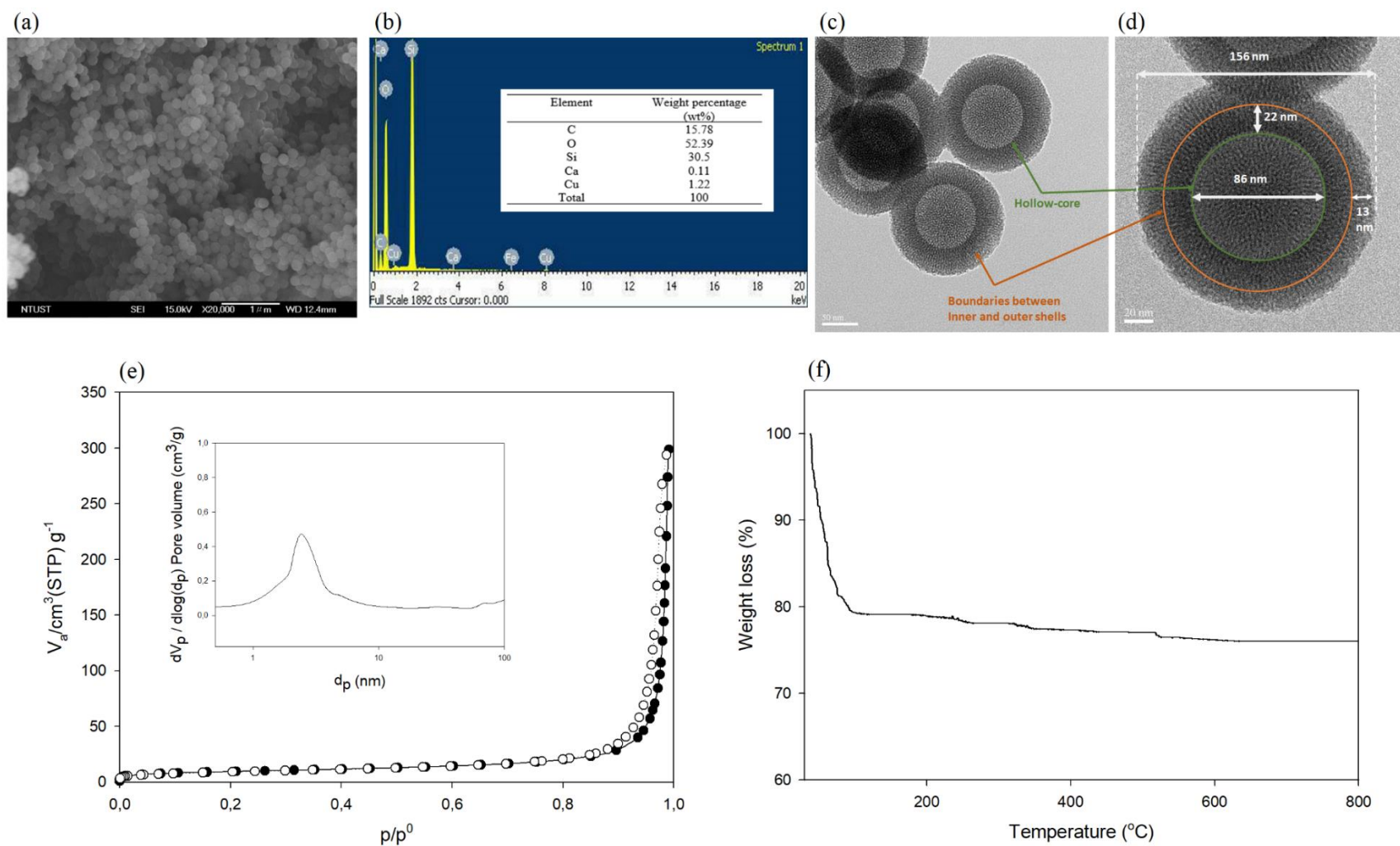
225 organic framework [28]), which usually range from 200 – 1300 cm<sup>2</sup>/g and 0.18 – 1.68 cm<sup>3</sup>/g  
226 respectively.

227 **Table 1.** Textural properties of Fe/DS-HMS-NH<sub>2</sub>.

Material	S <sub>BET</sub> (cm <sup>2</sup> /g)	Pore volume (cm <sup>3</sup> /g)	Pore size (nm)
Fe/DS-HMS-NH <sub>2</sub>	782.84	0.64	2.43

228 To demonstrate the feasibility of Fe/DS-HMS-NH<sub>2</sub> for the reactions at an elevated  
229 temperature, its thermal stability was investigated. The TGA profile in Figure 2f shows a 20%  
230 decrease in weight up to the temperature of 100°C, attributed to the removal of free moisture  
231 content. Further heating up to 800 °C does not significantly decrease the mass of Fe/DS-HMS-  
232 NH<sub>2</sub>, suggesting that the catalyst is stable at high temperatures [29]. Therefore, our Fe/DS-  
233 HMS-NH<sub>2</sub> can be considered as a promising heterogeneous catalyst for the *in-situ*  
234 esterification/transesterification reaction.

235



237 **Figure 2.** (a) SEM image, (b) Elemental composition, (c) – (d) TEM images at various magnifications, (c) BJH pore size distribution  
 238 curve, (e) Nitrogen adsorption-desorption isotherm with BJH pore size distribution curve (inset), (f) Thermogravimetric profile of the  
 239 Fe/DS-HMS-NH<sub>2</sub> catalyst.

240 **3.3 The catalytic activity of Fe/DS-HMS-NH<sub>2</sub> in the *in-situ* esterification/transesterification**  
241 **of DPO**

242 The characteristics of DPO as the raw material for biodiesel preparation are  
243 presented in Table 2. As homogenous catalysts are sensitive to impurities, the conversion of  
244 DPO to FAME for biodiesel production usually requires two reaction steps, namely acid-  
245 catalyzed esterification to lower the FFA content by converting them into FAME, and basic  
246 catalyzed transesterification to convert the acyl glycerides into FAME. However,  
247 heterogeneous catalysts can have good tolerance towards the FFA and water content in the  
248 lipid materials [10]; for Fe/DS-HMS-NH<sub>2</sub>, its two spatial shells with different active sites can  
249 facilitate the above two reactions in a one-pot process, and therefore efficient conversion from  
250 DPO to FAME is achieved in a single step.

251 **Table 2.** Characteristics of DPO.

Parameter	Value
FFA (% w/w)	5.54
Moisture Content (% w/w)	0.20
Saponification Value (mg KOH/g DPO)	234.08
Acid Value (mg KOH/g DPO)	12.04
Molecular weight (g/mol)	756.62

252  
253 Figure 3 presents the FAME yield obtained at various Fe/DS-HMS-NH<sub>2</sub> loadings  
254 at the condition of  $T = 60\text{ }^{\circ}\text{C}$ ,  $t = 4.5\text{ h}$  and  $r_{m/o} = 10:1$ . The results indicate that the yield of  
255 FAME is proportional to the number of active sites offered by the Fe/DS-HMS-NH<sub>2</sub> [30,31];  
256 therefore  $Y_F$  increases with  $m_c$  when the latter is within 6% (w/w). This agrees well with  
257 previous work on biodiesel production using different solid catalysts, e.g., pomacea sp. shell-  
258 based CaO [30], sulfonated biochar [31], and KI/mesoporous silica [32]. A maximum yield  
259 85.24% (w/w) is obtained when the catalyst loading  $m_c = 6\%$  (w/w). Further increase of the  
260 Fe/DS-HMS-NH<sub>2</sub> results in a reduced yield of FAME, which is probably due to the

261 aggregation and inconsistent dispersity of the catalyst in the reaction system of an enhanced  
 262 viscosity [33,34]. Cai et al. (2018) and Samart et al. (2010) also mentioned that excess catalyst  
 263 may also disturbed the mixing between the reactants, due to stronger adsorption of the  
 264 reactants to the catalyst [35,36].

265 **Table 3.** Experimental matrix at the optimum catalyst loading  $m_c = 6\%$  (w/w)

Run	Input Parameters			$Y_F$ (% , w/w)
	$T$ ( $^{\circ}\text{C}$ )	$t$ (h)	$r_{m/o}$	
1	60	4.5	10:1	$85.24 \pm 1.19$
2	40	0.5	10:1	$40.27 \pm 0.58$
3	40	2.5	6:1	$55.09 \pm 0.76$
4	50	4.5	6:1	$75.15 \pm 0.65$
5	50	2.5	10:1	$60.07 \pm 0.44$
6	40	0.5	2:1	$35.19 \pm 0.92$
7	40	4.5	10:1	$70.22 \pm 1.01$
8	50	2.5	2:1	$67.03 \pm 0.51$
9	60	4.5	2:1	$80.11 \pm 0.68$
10	50	2.5	6:1	$65.16 \pm 0.47$
11	50	2.5	6:1	$66.96 \pm 0.73$
12	50	2.5	6:1	$65.87 \pm 0.79$
13	50	0.5	6:1	$65.01 \pm 0.37$
14	60	4.5	6:1	$85.36 \pm 0.62$
15	50	2.5	6:1	$63.21 \pm 0.42$
16	60	0.5	10:1	$70.01 \pm 0.56$
17	50	2.5	6:1	$63.20 \pm 0.69$
18	50	2.5	6:1	$67.18 \pm 0.45$
19	60	0.5	2:1	$69.09 \pm 0.53$
20	40	4.5	2:1	$59.11 \pm 0.78$

266

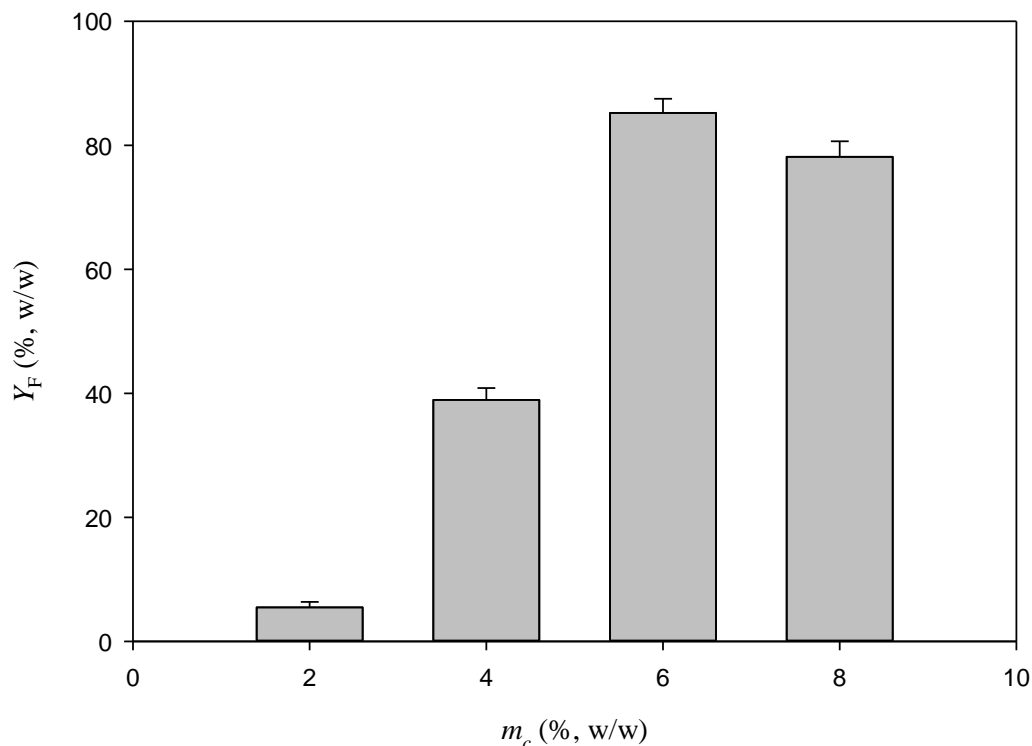
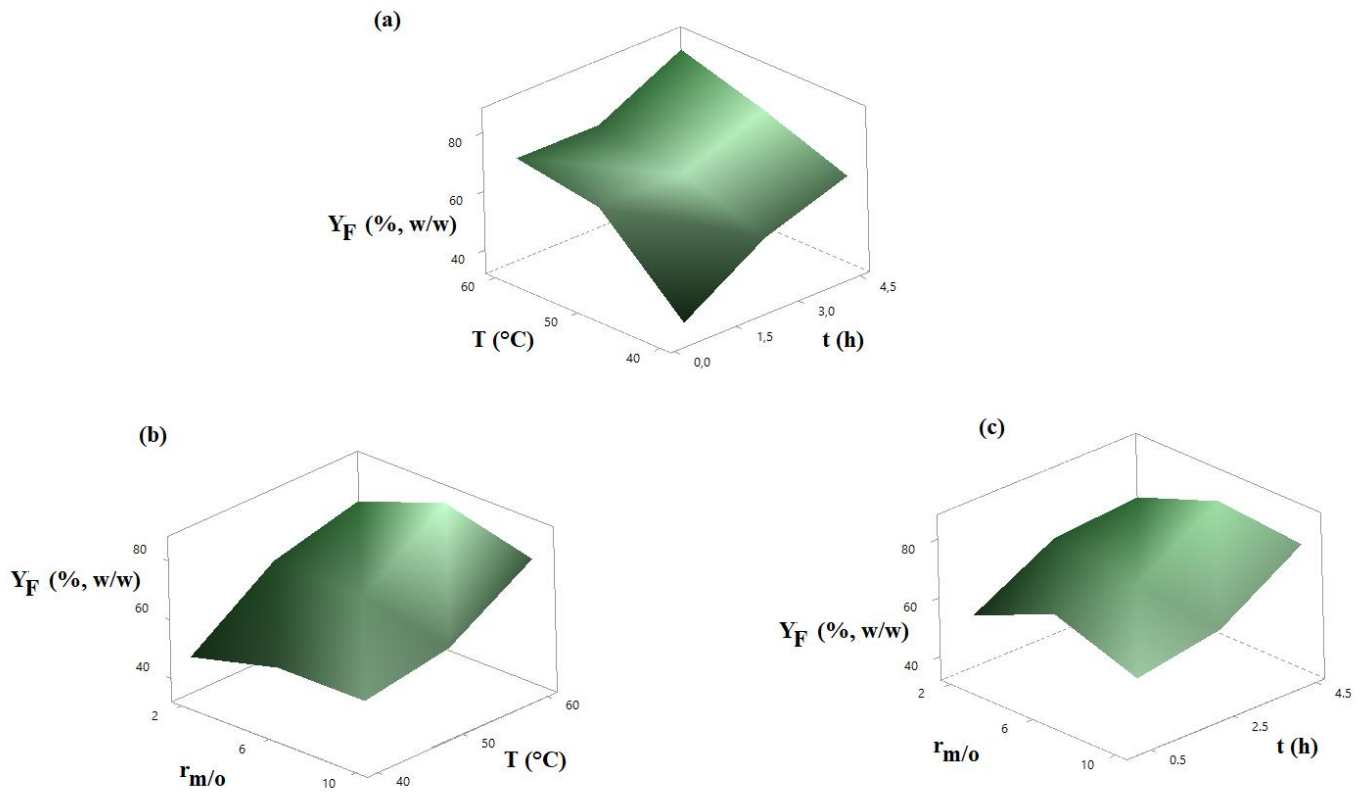


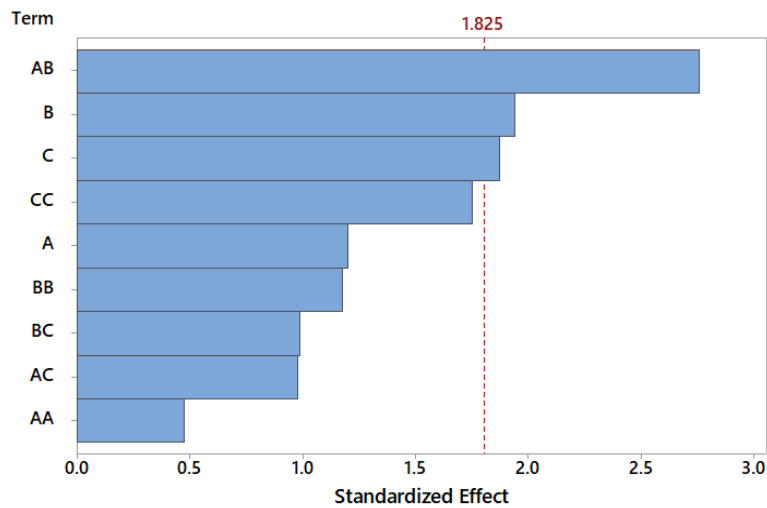
**Figure 3.** The yield of FAME at various Fe/DS-HMS-NH<sub>2</sub> loadings with the reaction condition of  $T = 60$  °C,  $t = 4.5$  h and  $r_{m/o} = 10:1$ .

267  
268  
269  
270

271 At a constant catalyst loading  $m_c = 6\%$  (w/w), Figure 4 and Table 3 present the  
272 FAME yield  $Y_F$  at various reaction time  $t$ , temperature  $T$ , and mass ratio of methanol to DPO  
273  $r_{m/o}$ . The maximum  $Y_F = 85.36\%$  (w/w) (with a purity of 97.89% (w/w)) is obtained at the  
274 condition of  $T = 60$  °C,  $t = 4.5$  h,  $r_{m/o} = 6:1$ . Based on the experimental results, the reaction  
275 time  $t$  was the most significant factor, followed by  $r_{m/o}$  and  $T$ , which is supported by the Pareto  
276 chart of the standardized effect in Figure 5 showing that  $t$ ,  $r_{m/o}$ , and the two-way interaction  
277 between  $t$  and  $T$  are the three significant parameters in the reaction system.



279 **Figure 4.** The FAME yield  $Y_F$  (% , w/w) at various (a)  $T$  and  $t$ , (b)  $T$  and  $r_{m/o}$ , and (c)  $t$  and  $r_{m/o}$ .  
 280



281 **Figure 5.** Pareto chart of the standardized effect for the biodiesel preparation with Fe/DS-  
 282 HMS-NH<sub>2</sub>, using  $Y_F$  as the response at a 95% confidence interval where A =  $T$ , B =  $t$ , C =  
 283  $r_{m/o}$ .  
 284  
 285

286           The effect of reaction temperature on the production of biodiesel using Fe/DS-  
287 HMS-NH<sub>2</sub> is shown in Figure 4a–b. An increased reaction temperature contributes to a higher  
288 yield, with the maximum achieved at 60°C, which is related to the fact that both esterification  
289 and transesterification reaction are endothermic and reversible [38,39]. At a higher reaction  
290 temperature, the kinetic energy and mobility of reactant molecules increase, promoting the  
291 collisions between the molecules and Fe/DS-HMS-NH<sub>2</sub> particles which then increases the  
292 reaction rate constant and shift the reaction towards the product [38,40]. Moreover, the mass  
293 transfer of the reactant molecules through the boundary layer of Fe/DS-HMS-NH<sub>2</sub> is also  
294 accelerated at an elevated temperature, resulting in the faster diffusion of the reactants into  
295 the pore of catalyst; hence, improving the FAME yield.

296           Specifically, Figures 4a and c show a significant increase of the FAME yield by  
297 extending the duration of the biodiesel synthesis from 0.5 h to 4.5 h, at a constant temperature  
298 or mass ratio of methanol to DPO. Longer reaction time provides sufficient time for the  
299 reactants to reach the active sites of Fe/DS-HMS-NH<sub>2</sub> through adsorption and diffusion, and  
300 convert DPO into FAME [41]. Meanwhile, prolonged duration of reaction also gives the  
301 catalyst more time to adsorb the reactant and desorb the reaction product [28]. Wei et al. (2009)  
302 also mentioned that adsorption and desorption of reactants from the catalyst is the rate-  
303 determining step in the overall reaction [42]. Therefore, allowing longer contact between the  
304 reactant molecules and the catalyst ensures high conversions of FFA and acyl glycerides to  
305 FAME.

306           Stoichiometrically, three moles of methanol are required to react with one mole of  
307 triglycerides in the transesterification reaction, while one mole of methanol is needed to react  
308 with one mole of free fatty acids in the esterification reaction [43,44]. Both reactions are  
309 known to be reversible; thus, the amount of methanol in the two reactions is usually provided

310 in excess to shift the reaction equilibrium to the product side. As seen from Figure 4b–c,  
311 having excess methanol from  $r_{m/o} = 2:1$  to  $r_{m/o} = 6:1$  contributes to a higher FAME yield,  
312 while further addition up to  $r_{m/o} = 10:1$  has no improvement. While most studies agree that  
313 excess methanol is desirable to allow more frequent interactions between the lipid and  
314 methanol triggering the formation of FAME, Pangestu et al. (2019) found that excess  
315 methanol may also accelerate the production of glycerol despite the higher yield of FAME  
316 [28]. As the esterification and transesterification are both reversible, a higher concentration  
317 of glycerol in the reaction system may induce a reverse reaction to the reactant side, creating  
318 an equilibrium between the products and reactants [28]. Hayyan et al. (2011) also reported  
319 that an excessive amount of methanol causes higher solubility of glycerol in the FAME phase  
320 that could lead to a complicated separation between biodiesel and glycerol [45]. Moreover,  
321 from the techno-economic viewpoint, the higher mass ratio of methanol to DPO also increases  
322 the material and processing cost [23,45]. Therefore, it can be concluded that the optimum  
323 level is  $r_{m/o} = 6:1$ .

324 A comparison of the FAME yield produced using Fe/DS-HMS-NH<sub>2</sub> with other  
325 existing catalysts is given in Table 4. It is notable that although the value of  $Y_F$  is higher when  
326 the refined feedstock is used as the reactant, the reaction time and the mass ratio of methanol  
327 to oil used in this study are lower. Moreover, among the studies using low-quality oil as raw  
328 lipid material, Fe/DS-HMS-NH<sub>2</sub> shows a higher catalytic activity compared with the other  
329 catalysts reported by Omar and Amin (2011), and Bala et al. (2017). This shows that Fe/DS-  
330 HMS-NH<sub>2</sub>, as a bifunctional catalyst, is able to enhance the yield of biodiesel at a comparable  
331 operating condition, which is due to its ability to convert not only triglycerides but also FFA  
332 into FAME in a one-pot system. The analysis result of the final FAME product shows that the  
333 conversion of FFA after reaction reaches 95.6%.

334  
335

**Table 4.** The comparison of catalytic activity of several heterogeneous catalysts for biodiesel production

Catalyst	Reactants	Operating condition	Yield (%)	References
Mesoporous zinc-doped silica	Cyanoacetate ester	$T = 60^{\circ}\text{C}$ , $t = 24$ h, $r_{m/o} = 10:1$ , $m_c = 7\%$ (w/w)	94.0	[17]
Alumina-supported KI	Refined soybean oil	$t = 8$ h, $r_{m/o} = 15:1$ , $m_c = 2.5\%$ (w/w)	96.0	[37]
Sr/ZrO <sub>2</sub>	Waste cooking oil	$T = 115.5^{\circ}\text{C}$ , $t = 169$ min, $r_{m/o} = 29:1$ (mol/mol), $m_c = 2.7\%$ (w/w)	79.7	[16]
Phosphotungstic acid-loaded KIT-5	Waste cooking oil	$T = 70^{\circ}\text{C}$ , $t = 4$ h, $r_{m/o} = 2:1$ (v/v), $m_c = 26.5\%$ (w/w)	83	[21]
Fe/DS-HMS-NH <sub>2</sub>	DPO	$T = 60^{\circ}\text{C}$ , $t = 4.5$ h, $r_{m/o} = 6:1$ (v/v), $m_c = 6\%$ (w/w)	85.36	This study

336

337 The fuel properties of the final FAME product are presented in Table 5. The  
338 measurement results indicate that the product resulted in this study has comparable  
339 combustion and flow properties with those of the commercial biodiesel. The calorific value  
340 (45.143 MJ/kg) is also within the range required in the common petrodiesel (42-46 MJ/kg).

341 **Table 5.** Fuel properties of the final FAME product

Properties	Methods	Unit	Final FAME product	ASTM D6751
Kinematic viscosity (at 40°C)	ASTM D445	mm <sup>2</sup> /s	2.64	1.9 – 6.0
Flashpoint	ASTM D93	°C	164.2	93 min
Cetane number	ASTM D613	-	55.7	47 min
Acid value	ASTM D664	mg KOH/g	0.24	0.5 max
Calorific value	ASTM D240	MJ/kg	45.143	-

342

343 Meanwhile, its compositional profile is obtained by comparing the methyl ester  
344 peaks in the chromatogram with those in the external FAME standard (47885 U, containing  
345 37 components FAME standard mix). The 12 identified peaks are 3.05% myristoleic acid  
346 methyl ester (C14:1), 2.37% cis-10-pentadecanoic acid methyl ester (C15:1), 35.78% palmitic  
347 acid methyl ester (C16:0), 8.13% palmitoleic acid methyl ester (C16:1), 8.36% stearic acid

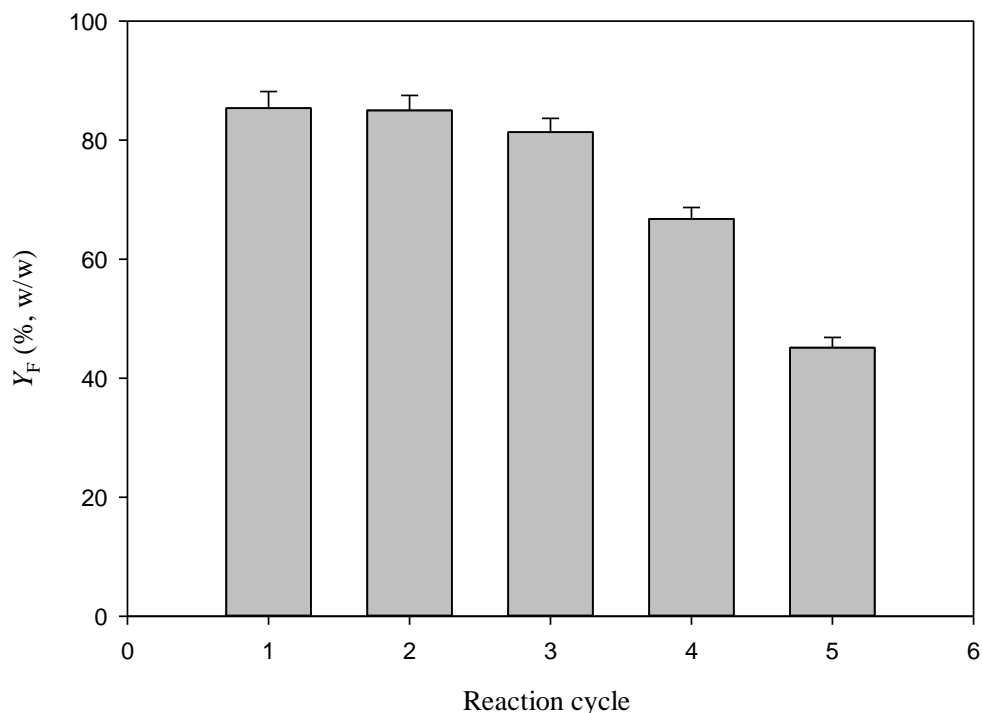
348 methyl ester (C18:0), 32.57% oleic acid methyl ester (C18:1n9c), 3.05% elaidic acid methyl  
349 ester (C18:1n9t), 1.17% cis-8,11,14-eicosatrienoic acid methyl ester (C20:3n6), 2.48%  
350 arachidonic acid methyl ester (C20:4n6), 0.52% cis-5,8,11,14,17-eicosapentaenoic acid  
351 methyl ester (C20:5n3), 1.07% erucic acid methyl ester (C22:1n9), 1.45 % cis-13,16-  
352 docosadienoic acid methyl ester (C22:2).

353

### 354 **3.4 Recyclability of Fe/DS-HMS-NH<sub>2</sub>**

355 An important feature of using heterogeneous catalysts for biodiesel preparation is  
356 its recyclability. In order to determine the recyclability of Fe/DS-HMS-NH<sub>2</sub>, several reaction  
357 cycles were conducted in series using the operating condition of  $m_c = 6\%$  (w/w),  $T = 60\text{ }^\circ\text{C}$ ,  $t$   
358  $= 4.5\text{ h}$ ,  $r_{m/o} = 6:1$ . Fe/DS-HMS-NH<sub>2</sub> was recovered following the method described in section  
359 2.4, while fresh methanol and DPO were used in every cycle. The catalytic ability of the  
360 recycled Fe/DS-HMS-NH<sub>2</sub> for *in-situ* esterification/transesterification process is presented in  
361 Figure 6. The result indicates that recycled Fe/DS-HMS-NH<sub>2</sub> can maintain a high yield of  
362 FAME above 80% (w/w) until the third cycle, close to the yield of fresh catalyst 85.36%  
363 (w/w). The purity of FAME for the first three cycles are 97.89%, 97.66% and 98.01% (w/w)  
364 respectively, higher than the commercial purity (96.5%, w/w). These results indicate that the  
365 catalytic activity of Fe/DS-HMS-NH<sub>2</sub> is maintained at a high level after regeneration. A  
366 significant drop in catalytic ability is observed from the forth cycle in Figure 6; similar  
367 performance has been reported for some other heterogeneous catalysts where three cycles  
368 seem to be an average number in term of their recyclability [46,47]. The catalytic deactivation  
369 of Fe/DS-HMS-NH<sub>2</sub> is generally due to the pore blockage caused by the contact between  
370 active sites on the catalyst surface and the deactivation-induced components, namely free  
371 glycerol, acyl glycerides, and biodiesel. Moreover, the high content of FFA in DPO also plays

372 an important role in the deactivation of Fe/DS-HMS-NH<sub>2</sub> catalyst because FFA tends to  
373 neutralize the basic sites in the inner shell of Fe/DS-HMS-NH<sub>2</sub> [48], resulting in the  
374 generation of amine-carboxylate that induces the formation of emulsion.



375  
376 **Figure 6.** Recyclability of Fe/DS-HMS-NH<sub>2</sub> in the *in-situ* esterification/transesterification  
377 of DPO.  
378

### 379 **3.5 The reaction mechanism of the *in-situ* esterification/transesterification of DPO using** 380 **Fe/DS-HMS-NH<sub>2</sub>**

381 In the preparation of biodiesel from DPO, Fe/DS-HMS-NH<sub>2</sub> acts as both acid and  
382 base catalysts to facilitate the esterification of FFA and the transesterification of acyl  
383 glycerides. The main steps for the reaction mechanism catalyzed by Fe/DS-HMS-NH<sub>2</sub> are the  
384 formation of nucleophilic alkoxides, the nucleophilic attack on the electrophilic part of the  
385 carbonyl group of the triglycerides, and electron delocalisation [49,50] as depicted in Figure  
386 7. The detailed description is as follows:

387 **Step 1:** Acyl glycerides, FFA and methanol enter the surface of catalyst through the  
388 adsorption process to reach the outer shell impregnated by the divalent iron. In this step, FFA  
389 undergoes the electron delocalization to form a carbocation and a carbanion, where the latter  
390 binds to the iron embedded on the catalyst.

391 **Step 2:** The reaction continues as the methoxide anion of methanol attacks the carbocation,  
392 whereas the hydronium cation attaches to the hydroxyl group of FFA to form water.

393 **Step 3:** Through the electron delocalization of the carbon atom, the water is released from the  
394 complex with FAME and the iron-embedded catalyst, followed by the release of FAME from  
395 the catalyst.

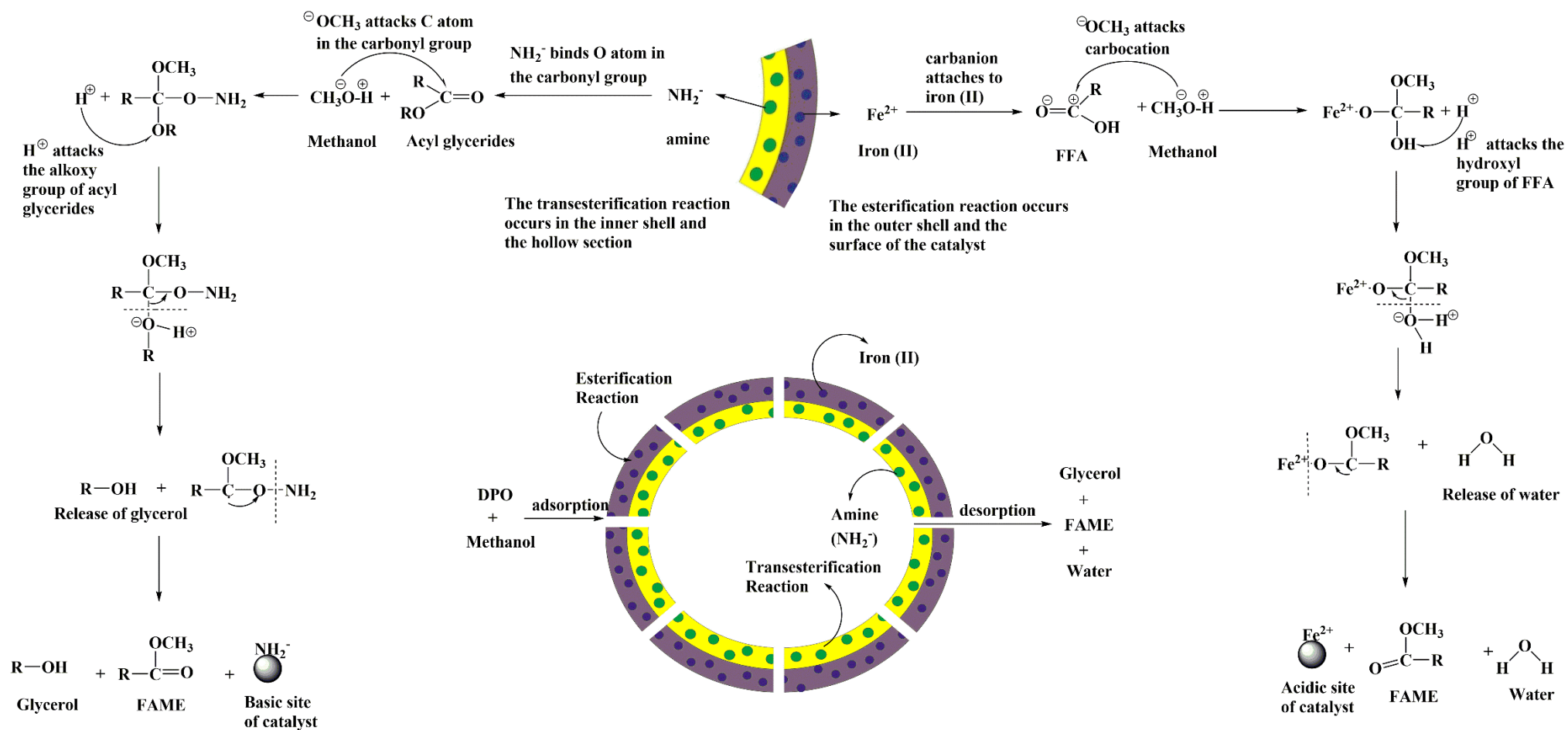
396 **Step 4:** The reaction continues when the acyl glycerides and methanol diffuse further to the  
397 amine-functionalized inner shell. The oxygen atom in the carbonyl group of acyl glycerides  
398 readily binds to the amine active sites.

399 **Step 5:** Subsequently, the methoxide anion of the methanol attacks the carbon atom in the  
400 carbonyl group of acyl glycerides, while the protonated  $H^+$  binds to the alkoxy group (RO-)  
401 of the acyl glycerides to form a complex of amine-functionalized catalyst with FAME and  
402 glycerol.

403 **Step 6:** Again, through the delocalization of oxygen in the complex, the glycerol and amine-  
404 functionalized catalyst are successively released from the complex.

405 **Step 7:** All three products, including FAME, glycerol, and water are then desorbed to the  
406 surface of the Fe/DS-HMS-NH<sub>2</sub> catalyst.

407



409

**Figure 7.** The reaction mechanism of the *in-situ* esterification/transesterification of DPO using Fe/DS-HMS-NH<sub>2</sub>.

410

## 411 **Conclusions**

412 Fe/DS-HMS-NH<sub>2</sub> is synthesized through the two-step condensation technique and  
413 successfully employed as a heterogeneous catalyst for preparing biodiesel from DPO, a lipid  
414 source with significant FFA and moisture content. The obtained Fe/DS-HMS-NH<sub>2</sub> has a  
415 uniform spherical shape with a particle size of 156 nm and hollow diameter of 86 nm. It is  
416 composed of two spatial silica shells with different active sites, and their thickness are 22 nm  
417 for the inner shell and 13 nm for the outer shell. Fe/DS-HMS-NH<sub>2</sub> has a specific surface area  
418 of 782.84 m<sup>2</sup>/g with a pore volume of 0.64 cm<sup>3</sup>/g, comparable with the existing solid catalysts.  
419 In the *in-situ* esterification/transesterification process using the Fe/DS-HMS-NH<sub>2</sub> catalyst,  
420 reaction time  $t$  is the variable with most significant influence on the yield of FAME  $Y_F$ ,  
421 followed by the reaction temperature  $T$  and the mass ratio of methanol to DPO  $r_{m/o}$ . The  
422 maximum  $Y_F$  is 85.36% (w/w), obtained at the following conditions:  $T = 60^\circ\text{C}$ ,  $t = 4.5$  h, and  
423  $r_{m/o} = 6:1$ , with a catalyst loading of 6% (w/w). Notably, Fe/DS-HMS-NH<sub>2</sub> catalyst shows a  
424 good recyclability, with the yield staying above 80% for three reaction cycles. Therefore,  
425 Fe/DS-HMS-NH<sub>2</sub> is a promising heterogeneous catalyst to obtain biodiesel from DPO or other  
426 lipid materials with high FFA and water content. Further study on (1) the extension of the  
427 catalyst lifetime by creating a technique suitable for its regeneration, and also (2) the design  
428 of a plausible route between the current research and its industrial application should be the  
429 main focus for future research expansion.

430

## 431 **Acknowledgments**

432 The authors acknowledge the funding supports from Widya Mandala Catholic University  
433 Surabaya and Indonesian Ministry of Research and Technology, through the research grant  
434 no. 2263/WM01/N/2020 and 130B/WM01.5/N/2020, respectively. We also thank Professor

435 Chun-Hu Chen, National Sun Yat Sen University, and Taiwan Tech (National Taiwan  
436 University of Science and Technology) for providing the facility for the catalyst  
437 characterizations.

438

## 439 REFERENCES

- 440 [1] P. Agung, D. Hartono, A.A. Awirya, Pengaruh Urbanisasi Terhadap Konsumsi Energi Dan  
441 Emisi CO<sub>2</sub>: Analisis Provinsi di Indonesia (The Effect of Urbanization on Energy  
442 Consumption and CO<sub>2</sub> Emissions: An Analysis of Provinces in Indonesia), *J. Ekon.*  
443 *Kuantitatif Terap.* 1 (2017) 9–17. <https://doi.org/10.24843/jekt.2017.v10.i01.p02>.
- 444 [2] A. Fitriyatus, A. Fauzi, B. Juanda, Prediction of Fuel Supply and Consumption in Indonesia  
445 with System Dynamics Model, *J. Ekon. Dan Pembang. Indones.* 17 (2018) 118–137.
- 446 [3] F.T.R. Silalahi, T.M. Simatupang, M.P. Siallagan, Biodiesel produced from palm oil in  
447 Indonesia: Current status and opportunities, *AIMS Energy.* 8 (2020) 81–101.  
448 <https://doi.org/10.3934/energy.2020.1.81>.
- 449 [4] F. Nangoy, B.C. Munthe, Indonesia President wants B30 in use by Jan 2020: cabinet  
450 secretary, Reuters. (2019).
- 451 [5] J.M. Marchetti, A summary of the available technologies for biodiesel production based on  
452 a comparison of different feedstock's properties, *Process Saf. Environ. Prot.* 90 (2012) 157–  
453 163. <https://doi.org/10.1016/j.psep.2011.06.010>.
- 454 [6] K. Suwannakarn, E. Lotero, K. Ngaosuwan, J.G. Goodwin Jr, Simultaneous free fatty acid  
455 esterification and triglyceride transesterification using a solid acid catalyst with in situ  
456 removal of water and unreacted methanol, *Ind. Eng. Chem. Res.* 48 (2009) 2810–2818.  
457 <https://doi.org/https://doi.org/10.1021/ie800889w>.
- 458 [7] Y.A. Tsigie, L.H. Huynh, S. Ismadji, A.M. Engida, Y.H. Ju, In situ biodiesel production

- 459 from wet *Chlorella vulgaris* under subcritical condition, *Chem. Eng. J.* 213 (2012) 104–108.  
460 <https://doi.org/10.1016/j.cej.2012.09.112>.
- 461 [8] P.D. Patil, V.G. Gude, A. Mannarswamy, P. Cooke, N. Nirmalakhandan, P. Lammers, S.  
462 Deng, Comparison of direct transesterification of algal biomass under supercritical  
463 methanol and microwave irradiation conditions, *Fuel.* 97 (2012) 822–831.  
464 <https://doi.org/10.1016/j.fuel.2012.02.037>.
- 465 [9] A. Kumari, P. Mahapatra, V.K. Garlapati, R. Banerjee, Enzymatic transesterification of  
466 *Jatropha* oil, *Biotechnol Biofuels.* 2 (2009) 1. <https://doi.org/10.1186/1754-6834-2-1>.
- 467 [10] R. Mat, R.A. Samsudin, M. Mohamed, A. Johari, Solid catalysts and their application in  
468 biodiesel production, *Bull. Chem. React. Eng. Catal.* 7 (2012) 142–149.  
469 <https://doi.org/10.9767/bcrec.7.2.3047.142-149>.
- 470 [11] W. Suryaputra, I. Winata, N. Indraswati, S. Ismadji, Waste capiz (*Amusium cristatum*) shell  
471 as a new heterogeneous catalyst for biodiesel production, *Renew. Energy.* 50 (2013) 795–  
472 799. <https://doi.org/10.1016/j.renene.2012.08.060>.
- 473 [12] H. Li, W. Xie, Transesterification of Soybean Oil to Biodiesel with Zn/I<sub>2</sub> Catalyst, *Catal.*  
474 *Letters.* 107 (2006) 25–30. <https://doi.org/10.1007/s10562-005-9727-9>.
- 475 [13] A.A. Refaat, A.A. Refaat, Archive of SID Different techniques for the production of  
476 biodiesel from waste vegetable oil, *Int. J. Environ. Sci. Tech.* 7 (2010) 183–213.
- 477 [14] P.L. Boey, G.P. Maniam, S.A. Hamid, Performance of calcium oxide as a heterogeneous  
478 catalyst in biodiesel production: A review, *Chem. Eng. J.* 168 (2011) 15–22.  
479 <https://doi.org/10.1016/j.cej.2011.01.009>.
- 480 [15] M.K. Lam, K.T. Lee, A.R. Mohamed, Homogeneous, heterogeneous and enzymatic  
481 catalysis for transesterification of high free fatty acid oil (waste cooking oil) to biodiesel: A  
482 review, *Biotechnol. Adv.* 28 (2010) 500–518.

- 483 <https://doi.org/10.1016/j.biotechadv.2010.03.002>.
- 484 [16] W.N.N.W. Omar, N.A.S. Amin, Biodiesel production from waste cooking oil over alkaline  
485 modified zirconia catalyst, *Fuel Process. Technol.* 92 (2011) 2397–2405.  
486 <https://doi.org/10.1016/j.fuproc.2011.08.009>.
- 487 [17] N. Pal, M. Paul, A. Bhaumik, Highly ordered Zn-doped mesoporous silica: An efficient  
488 catalyst for transesterification reaction, *J. Solid State Chem.* 184 (2011) 1805–1812.  
489 <https://doi.org/10.1016/j.jssc.2011.05.033>.
- 490 [18] W. Xie, X. Huang, Synthesis of biodiesel from soybean oil using heterogeneous KF/ZnO  
491 catalyst, *Catal. Letters.* 107 (2006) 53–59. [https://doi.org/https://doi.org/10.1007/s10562-](https://doi.org/https://doi.org/10.1007/s10562-005-9731-0)  
492 [005-9731-0](https://doi.org/https://doi.org/10.1007/s10562-005-9731-0).
- 493 [19] S.M. Coman, V.I. Parvulescu, Heterogeneous Catalysis for Biodiesel Production, *Role*  
494 *Catal. Sustain. Prod. Bio-Fuels Bio-Chemicals.* (2013) 93–136.  
495 <https://doi.org/10.1016/B978-0-444-56330-9.00004-8>.
- 496 [20] J. Santos, J. Phillips, J.A. Dumesic, Metal-support interactions between iron and titania for  
497 catalysts prepared by thermal decomposition of iron pentacarbonyl and by impregnation, *J.*  
498 *Catal.* 81 (1983) 147–167. [https://doi.org/10.1016/0021-9517\(83\)90154-9](https://doi.org/10.1016/0021-9517(83)90154-9).
- 499 [21] D.D. Bala, M. Misra, D. Chidambaram, Solid-acid catalyzed biodiesel production, part I:  
500 biodiesel synthesis from low quality feedstock, *J. Clean. Prod.* 142 (2017) 4169–4177.  
501 <https://doi.org/10.1016/j.jclepro.2016.02.128>.
- 502 [22] C. You, C. Yu, X. Yang, Y. Li, H. Huo, Z. Wang, Y. Jiang, X. Xu, K. Lin, Double-shelled  
503 hollow mesoporous silica nanosphere as acid-base bifunctional catalyst for cascade  
504 reactions, *New J. Chem.* 42 (2018) 4095–4101. <https://doi.org/10.1039/C7NJ04670G>.
- 505 [23] F.H. Santosa, L. Laysandra, F.E. Soetaredjo, S.P. Santoso, S. Ismadji, M. Yuliana, A facile  
506 noncatalytic methyl ester production from waste chicken tallow using single step subcritical

- 507           methanol: Optimization study, *Int. J. Energy Res.* 43 (2019) 8852–8863.  
508           <https://doi.org/10.1002/er.4844>.
- 509 [24] X. Zhou, X. Cheng, W. Feng, K. Qiu, L. Chen, W. Nie, Z. Yin, X. Mo, H. Wang, C. He,  
510           Synthesis of hollow mesoporous silica nanoparticles with tunable shell thickness and pore  
511           size using amphiphilic block copolymers as core templates, *Dalt. Trans.* 43 (2014) 11834–  
512           11842. <https://doi.org/10.1039/c4dt01138d>.
- 513 [25] S. Cao, Z. Zhao, X. Jin, W. Sheng, S. Li, Y. Ge, M. Dong, W. Wu, L. Fang, Unique double-  
514           shelled hollow silica microspheres: Template-guided self-assembly, tunable pore size, high  
515           thermal stability, and their application in removal of neutral red, *J. Mater. Chem.* 21 (2011)  
516           19124–19131. <https://doi.org/10.1039/c1jm13011k>.
- 517 [26] N.B. Klinghoffer, M.J. Castaldi, A. Nzihou, Catalyst Properties and Catalytic Performance  
518           of Char from Biomass Gasification, *Ind. Eng. Chem. Res.* 51 (2012) 13113–13122.  
519           <https://doi.org/10.1021/ie3014082>.
- 520 [27] M. Zakeri, A. Samimi, M. Shafiee Afarani, A. Salehirad, Effects of porosity and pore size  
521           distribution on mechanical strength reliability of industrial-scale catalyst during preparation  
522           and catalytic test steps, *Part. Sci. Technol.* 36 (2018) 96–103.  
523           <https://doi.org/10.1080/02726351.2016.1220437>.
- 524 [28] T. Pangestu, Y. Kurniawan, F.E. Soetaredjo, S.P. Santoso, W. Irawaty, M. Yuliana, S.B.  
525           Hartono, S. Ismadji, The synthesis of biodiesel using copper based metal-organic  
526           framework as a catalyst, *J. Environ. Chem. Eng.* 7 (2019) 103277.  
527           <https://doi.org/10.1016/j.jece.2019.103277>.
- 528 [29] N. Rahmat, N. Sadon, M.A. Yusof, Thermogravimetric Analysis (TGA) Profile at Different  
529           Calcination Conditions for Synthesis of PTES-SBA-15, *Am. J. Appl. Sci.* 14 (2017) 938–  
530           944. <https://doi.org/10.3844/ajassp.2017.938.944>.

- 531 [30] Y.Y. Margaretha, H.S. Prastyo, A. Ayucitra, S. Ismadji, Calcium oxide from pomacea sp.  
532 shell as a catalyst for biodiesel production, *Int. J. Energy Environ. Eng.* 3 (2012) 1–9.  
533 <https://doi.org/10.1186/2251-6832-3-33>.
- 534 [31] A.M. Dekhoda, A.H. West, N. Ellis, Biochar based solid acid catalyst for biodiesel  
535 production, *Appl. Catal. A Gen.* 382 (2010) 197–204.  
536 <https://doi.org/10.1016/j.apcata.2010.04.051>.
- 537 [32] C. Samart, P. Sreetongkittikul, C. Sookman, Heterogeneous catalysis of transesterification  
538 of soybean oil using KI/mesoporous silica, *Fuel Process. Technol.* 90 (2009) 922–925.  
539 <https://doi.org/10.1016/j.fuproc.2009.03.017>.
- 540 [33] G. Baskar, S. Soumiya, Production of biodiesel from castor oil using iron (II) doped zinc  
541 oxide nanocatalyst, *Renew. Energy.* 98 (2016) 101–107.  
542 <https://doi.org/https://doi.org/10.1016/j.renene.2016.02.068>.
- 543 [34] B. Gurunathan, A. Ravi, Biodiesel production from waste cooking oil using copper doped  
544 zinc oxide nanocomposite as heterogeneous catalyst, *Bioresour. Technol.* 188 (2015) 124–  
545 127. <https://doi.org/https://doi.org/10.1016/j.biortech.2015.01.012>.
- 546 [35] J. Cai, Q.Y. Zhang, F.F. Wei, J.S. Huang, Y.M. Feng, H.T. Ma, Y. Zhang, Preparation of  
547 Copper (II) Containing Phosphomolybdic Acid Salt as Catalyst for the Synthesis of  
548 Biodiesel by Esterification, *J Oleo Sci.* 67 (2018) 427–432.  
549 <https://doi.org/10.5650/jos.ess17208>.
- 550 [36] C. Samart, C. Chaiya, P. Reubroycharoen, Biodiesel production by methanolysis of soybean  
551 oil using calcium supported on mesoporous silica catalyst, *Energy Convers. Manag.* 51  
552 (2010) 1428–1431. <https://doi.org/10.1016/j.enconman.2010.01.017>.
- 553 [37] W. Xie, H. Li, Alumina-supported potassium iodide as a heterogeneous catalyst for  
554 biodiesel production from soybean oil, *J. Mol. Catal. A Chem.* 255 (2006) 1–9.

555 <https://doi.org/https://doi.org/10.1016/j.molcata.2006.03.061>.

556 [38] M. Farooq, A. Ramli, Biodiesel production from low FFA waste cooking oil using  
557 heterogeneous catalyst derived from chicken bones, *Renew. Energy*. 76 (2015) 362–368.  
558 <https://doi.org/10.1016/j.renene.2014.11.042>.

559 [39] R. Alenezi, G.A. Leeke, J.M. Winterbottom, R.C.D. Santos, A.R. Khan, Esterification  
560 kinetics of free fatty acids with supercritical methanol for biodiesel production, *Energy*  
561 *Convers. Manag.* 51 (2010) 1055–1059. <https://doi.org/10.1016/j.enconman.2009.12.009>.

562 [40] M. Farooq, A. Ramli, D. Subbarao, Biodiesel production from waste cooking oil using  
563 bifunctional heterogeneous solid catalysts, *J. Clean. Prod.* 59 (2013) 131–140.  
564 <https://doi.org/10.1016/j.jclepro.2013.06.015>.

565 [41] I. Amalia Kartika, M. Yani, D. Ariono, P. Evon, L. Rigal, Biodiesel production from  
566 jatropha seeds: Solvent extraction and in situ transesterification in a single step, *Fuel*. 106  
567 (2013) 111–117. <https://doi.org/10.1016/j.fuel.2013.01.021>.

568 [42] Z. Wei, C. Xu, B. Li, Application of waste eggshell as low-cost solid catalyst for biodiesel  
569 production, *Bioresour. Technol.* 100 (2009) 2883–2885.  
570 <https://doi.org/10.1016/j.biortech.2008.12.039>.

571 [43] A. Demirbas, Biodiesel from waste cooking oil via base-catalytic and supercritical methanol  
572 transesterification, *Energy Convers. Manag.* 50 (2009) 923–927.  
573 <https://doi.org/10.1016/j.enconman.2008.12.023>.

574 [44] I.A. Reşitoğlu, A. Keskin, M. Gürü, The optimization of the esterification reaction in  
575 biodiesel production from trap grease, *Energy Sources, Part A Recover. Util. Environ. Eff.*  
576 34 (2012) 1238–1248. <https://doi.org/10.1080/15567031003792395>.

577 [45] A. Hayyan, F.S. Mjalli, M.A. Hashim, M. Hayyan, I.M. AlNashef, S.M. Al-Zahrani, M.A.  
578 Al-Saadi, Ethanesulfonic acid-based esterification of industrial acidic crude palm oil for

579 biodiesel production, *Bioresour Technol.* 102 (2011) 9564–9570.  
580 <https://doi.org/10.1016/j.biortech.2011.07.074>.

581 [46] S.L. Lee, Y.C. Wong, Y.P. Tan, S.Y. Yew, Transesterification of palm oil to biodiesel by  
582 using waste obtuse horn shell-derived CaO catalyst, *Energy Convers. Manag.* 93 (2015)  
583 282–288. <https://doi.org/10.1016/j.enconman.2014.12.067>.

584 [47] W. Xie, T. Wang, Biodiesel production from soybean oil transesterification using tin oxide-  
585 supported WO<sub>3</sub> catalysts, *Fuel Process. Technol.* 109 (2013) 150–155.  
586 <https://doi.org/10.1016/j.fuproc.2012.09.053>.

587 [48] M. Kouzu, J.S. Hidaka, Transesterification of vegetable oil into biodiesel catalyzed by CaO:  
588 A review, *Fuel*. 93 (2012) 1–12. <https://doi.org/10.1016/j.fuel.2011.09.015>.

589 [49] D.M. Marinković, M. V. Stanković, A. V. Veličković, J.M. Avramović, M.R. Miladinović,  
590 O.O. Stamenković, V.B. Veljković, D.M. Jovanović, Calcium oxide as a promising  
591 heterogeneous catalyst for biodiesel production: Current state and perspectives, *Renew.*  
592 *Sustain. Energy Rev.* 56 (2016) 1387–1408. <https://doi.org/10.1016/j.rser.2015.12.007>.

593 [50] A.K. Endalew, Y. Kiros, R. Zanzi, Inorganic heterogeneous catalysts for biodiesel  
594 production from vegetable oils, *Biomass and Bioenergy*. 35 (2011) 3787–3809.  
595 <https://doi.org/10.1016/j.biombioe.2011.06.011>.

596

## 1 **Abstract**

2 To promote the use of low-quality oils in producing biodiesel, a bifunctional acid-base  
3 catalyst Fe/DS-HMS-NH<sub>2</sub> is fabricated using the two-step condensation technique. The obtained  
4 Fe/DS-HMS-NH<sub>2</sub> is of a doubled shell structure in spherical shape with a uniform size of 156 nm.  
5 Its hollow core (with a diameter of 86 nm) and two spatial shells with different active sites enables  
6 the esterification and transesterification reactions to be accomplished in a one-pot synthesis. The  
7 influences of four independent reaction variables on the yield of fatty acid methyl esters  $Y_F$  was  
8 studied, including catalyst loading  $m_c$ , reaction time  $t$ , reaction temperature  $T$ , and the methanol to  
9 degummed palm oil mass ratio  $r_{m/o}$ . The highest yield was obtained at 85.36% (w/w) when  $m_c =$   
10 6% (w/w),  $t = 4.5$  h,  $T = 60$  °C, and  $r_{m/o} = 6:1$ . The Fe/DS-HMS-NH<sub>2</sub> shows a good recyclability  
11 with  $Y_F > 80\%$  (w/w) up to three reaction cycles.

12 *Keywords: bifunctional catalyst; biodiesel; renewable energy; hollow mesoporous silica; iron*  
13 *impregnation; amine functionalization*

14 **1. Introduction<sup>1</sup>**

15           The global fuel demand is growing rapidly as it undergoes an extensive urbanization.  
16       Our heavy reliance on fossil fuel brings the risk of unstable market price and reduced fuel  
17       availability. The gas emission from fossil fuel combustion also causes environmental concerns.  
18       Therefore, developing an alternative fuel that is biodegradable, sustainable and with a low  
19       carbon emission is the most significant energy and environmental challenge for us in the  
20       coming decades [1,2]. Since 2006, the Indonesian government has been committed to reducing  
21       carbon emissions by replacing fossil fuels with biodiesel [3]. It is also declared that the use of  
22       biodiesel in diesel blend will be increased from B20 to B30 starting from 2020 [4], with a  
23       strategy to boost the domestic use of palm oil and lower down energy imports. Usually,  
24       biodiesel is obtained through the conventional transesterification process of refined oil [5].  
25       However, the technologies of utilizing non-refined oil, specifically the low-quality oil, have  
26       currently attracted extensive interests and are being developed. Various types of low-quality  
27       oil have been studied to produce high-quality biodiesel using sundry of technical routes,  
28       including the two steps acidic esterification followed by basic transesterification [6],

---

1

FFA	Free fatty acids
FAME	Fatty acid methyl esters
DPO	Degummed palm oil
CPO	Crude palm oil
SS-HMS-NH <sub>2</sub>	Single-shelled hollow mesoporous silica
DS-HMS-NH <sub>2</sub>	Double-shelled hollow mesoporous silica
Fe/DS-HMS-NH <sub>2</sub>	Iron (II) impregnated double-shelled hollow mesoporous silica

29 noncatalytic transesterification using alcohol under subcritical [7] and supercritical conditions  
30 [8], enzymatic transesterification [9] and solid-catalyzed transesterification [10]. Among the  
31 available routes, the use of heterogeneous (solid) catalysts has been attracting a growing  
32 interest in recent years, as it has the advantage of easier separation, tolerance to impurities  
33 (i.e., FFA, water and other minor compounds), and good reusability [11] which means  
34 minimal waste and toxic water production [12] and environmentally friendly [13]. Boey et al.  
35 (2011) and Lam et al. (2010) also stated that heterogeneous catalysts lower the product  
36 contamination level, and reduce the corrosion problem [14,15]. Various solid catalysts and  
37 their modifications have been reported, such as zirconia [16], silica impregnated with zinc  
38 stearate (ZS/Si) [17], heterogeneous KF/ZnO catalyst [18], heterogeneous Zn/I<sub>2</sub> catalyst [12].  
39 However, despite their insensitivity to impurities, these catalysts solely act as the mono  
40 functional catalysts, depending on their acidity nature and have the following disadvantages  
41 during the conversion of low-quality oil to biodiesel: (1) the reaction carried out in the  
42 presence of an acidic heterogeneous catalyst is slow, and at the same time, requires large  
43 amount of alcohol [19], meanwhile (2) the basic heterogeneous catalysts usually result in a  
44 lower biodiesel yield and purity, since this type of catalyst leaves the FFA unreacted during  
45 the reaction.

46 In this paper, we prepared and characterized a new class of heterogeneous catalyst,  
47 the double-shelled hollow mesoporous silica impregnated with divalent iron metal (Fe/DS-  
48 HMS-NH<sub>2</sub>), to be used as an acid-base bifunctional catalyst in the production of biodiesel  
49 from a low-quality oil. This catalyst enables a simple process of converting low-quality oil to  
50 biodiesel by combining the two processes of esterification and transesterification into a single-  
51 stage process. This is achieved by having double active surface layers that facilitate the two  
52 reactions to run simultaneously. The primary (inner) shell is designed to promote the

53 transesterification reaction by adding  $-\text{NH}_2$  as the basic site, while the outer layer is  
54 impregnated with the divalent iron (Fe (II)), which is selected as the impregnated metals due  
55 to its nature as a strong Lewis acid, and its ability to change the oxidation level and activate  
56 the substance during the process [20].

57           The synthesis, characterization and catalytic activity of the Fe/DS-HMS-NH<sub>2</sub> will be  
58 investigated in this paper. Its performance as an acid-base bifunctional catalyst for biodiesel  
59 preparation will be examined at various conditions, including catalyst loading  $m_c$  (% , w/w),  
60 reaction temperature  $T$  (°C), reaction time  $t$  (h), and the mass ratio of methanol to oil  $r_{m/o}$ . In  
61 this present research, degummed palm oil (DPO) is selected as the lipid material. With similar  
62 content of FFA and moisture as the crude palm oil (CPO), DPO is also classified as a low-  
63 quality oil, along with industrial fats, oils and greases, and other crude/waste lipids. Therefore,  
64 it is considered as a suitable raw material to determine the catalytic ability of Fe/DS-HMS-  
65 NH<sub>2</sub> in converting both FFA and triglycerides in DPO into biodiesel. We will also show that  
66 the Fe/DS-HMS-NH<sub>2</sub> can be regenerated and reused, which is regarded as an important feature  
67 for heterogeneous catalysts as it will reduce the cost for production and pollutant discharges  
68 [21,22]. The recyclability of the catalyst will be investigated at the operating condition giving  
69 the highest yield of fatty acid methyl esters (FAME)  $Y_F$ .

70

## 71 **2. Materials and methods**

### 72 **2.1 Materials**

73           CPO was collected from the local manufacturer in Indonesia. Prior to use, CPO was  
74 degummed using 1% (w/w) phosphoric acid (PA, 85% purity) at a temperature of 80 – 90°C  
75 for 30 min to reduce the phosphorus content. Several important characteristics of the  
76 degummed CPO (i.e., DPO), namely free fatty acid content, acid value, saponification value,

77 and moisture content were analyzed in accordance with the standard method of AOCS Ca 5a-  
78 40, Cd 3d-63, Cd 3d-25, and Ca 2e-84, respectively.

79 3-aminopropyl-triethoxysilane (APTES) was purchased from Fisher Scientific  
80 (Pittsburgh, USA), while other chemicals required for the fabrication of Fe/DS-HMS, namely  
81 iron (II) sulfate heptahydrate ( $\text{FeSO}_4 \cdot 7\text{H}_2\text{O}$ , 99.99% purity), tetraethylorthosilicate (TEOS),  
82 cetyltrimethylammonium bromide (CTAB), ethanol (98% purity), methanol (99,9% purity),  
83 hydrochloric acid (HCl, 37% purity), ammonium hydroxide solution ( $\text{NH}_4\text{OH}$ , 25% purity),  
84 and n-hexane (95% purity) were obtained from Merck (Merck, Germany). The FAMES  
85 standard (47885 U) containing 37 components FAME mix was procured from Supelco  
86 (Bellefonte, PA, USA). Ultra-high purity nitrogen gas (> 99.0% purity) was purchased from  
87 Aneka Gas Industry Pty. Ltd., Indonesia. All chemicals used in this study were of analytical  
88 grade and required no further purification.

89

## 90 **2.2 Preparation of DS-HMS-NH<sub>2</sub>**

91 In a typical synthesis, 0.14 g of CTAB, 20 ml of ethanol, 50 ml of deionized water and  
92 1 ml of  $\text{NH}_4\text{OH}$  solution were simultaneously introduced into a glass beaker and mixed for 15  
93 minutes at room temperature. Then 1 ml of TEOS was slowly added into the above solution  
94 and kept stirring for 24 hours. The precipitates were collected through centrifugation at 4500  
95 rpm for 30 min, triplicate ethanol washing, and drying at 120 °C overnight. After the  
96 calcination at 550°C for 6 h, the single shelled hollow mesoporous silica (SS-HMS-NH<sub>2</sub>) was  
97 obtained.

98 The outer shell of the particle was fabricated using a multilevel scheme based on SS-  
99 HMS-NH<sub>2</sub>. In a typical synthesis, 0.5 g CTAB, 18 ml deionized water, and 50 ml of ethanol  
100 were introduced into a beaker glass. Meanwhile, 0.063 g of SS-HMS-NH<sub>2</sub> was added into a

101 mixture of 4 ml deionized water and 8.5 ml of 25% (w/w)  $\text{NH}_4\text{OH}$  solution. The above two  
102 solutions were then combined and stirred for 15 min at 250 rpm, after which 100  $\mu\text{l}$  TEOS  
103 and 21  $\mu\text{l}$  APTES were slowly added into it and the mixture was kept stirring for 24 h to allow  
104 the condensation reaction of silica. Finally, the solid product was collected by centrifugation  
105 at 4500 rpm for 15 min, which was then repeatedly washed with 60 ml of ethanol and 4 ml of  
106 HCl, and oven-dried at 120°C. The dried product was calcined at 550 °C for 6 h to obtain  
107 double-shelled hollow mesoporous silica (DS-HMS-NH<sub>2</sub>).

108

### 109 **2.3 Iron (II) impregnation onto DS-HMS-NH<sub>2</sub> surface**

110 The impregnation of divalent iron onto the DS-HMS-NH<sub>2</sub> surface was achieved as  
111 follows to fabricate Fe/DS-HMS-NH<sub>2</sub> catalysts. In a typical synthesis, 0.1 g DS-HMS-NH<sub>2</sub>  
112 was mixed with 50 ml of deionized water under sonication for 30 minutes at room temperature.  
113 Meanwhile, two separate solutions were prepared: (1) 5 mg of  $\text{FeSO}_4 \cdot 7\text{H}_2\text{O}$  was dissolved in  
114 50 ml of deionized water, and (2) 0.2 g of CTAB was dissolved in 10 ml ethanol. Solution (1)  
115 and (2) were then added into the DS-HMS-NH<sub>2</sub> solution and stirred for 12 hours at ambient  
116 conditions. The Fe/DS-HMS-NH<sub>2</sub> precipitates were separated by a centrifugation at 4500 rpm  
117 for 15 min, and then dried at 120 °C for 12 h and calcined at 550 °C for 5 hours to obtain the  
118 Fe/DS-HMS-NH<sub>2</sub> powder.

119

### 120 **2.4. Catalytic activity of Fe/DS-HMS-NH<sub>2</sub> at various reaction conditions**

121 The *in-situ* esterification/transesterification reactions from DPO to FAME were carried  
122 out in a glass flask equipped with a reflux condenser and external heater under constant  
123 magnetic stirring (250 rpm) at various conditions. Specifically, the influence of four reaction  
124 parameters were investigated due to their relevance to industrial applications: catalyst loading

125  $m_c$  (% , w/w), reaction temperature  $T$  ( $^{\circ}\text{C}$ ), reaction time  $t$  (h), and the mass ratio of methanol  
126 to DPO  $r_{m/o}$ . To determine the amount of Fe/DS-HMS-NH<sub>2</sub> catalyst that produces the  
127 maximum FAME yield  $Y_F$ , a few reactions were carried out with different amounts of Fe/DS-  
128 HMS-NH<sub>2</sub> ( $m_c = 2\%$ , 4%, 6%, 8%, w/w) at the following condition:  $T = 60$   $^{\circ}\text{C}$ ,  $t = 4.5$  h and  
129  $r_{m/o} = 10:1$ . Once the optimum catalyst loading is obtained, the catalytic activity of Fe/DS-  
130 HMS-NH<sub>2</sub> was investigated within an experimental matrix defined by  $T = 40$   $^{\circ}\text{C}$ , 50  $^{\circ}\text{C}$ , 60  $^{\circ}\text{C}$ ,  
131  $t = 0.5$  h, 2.5 h, 4.5 h, and  $r_{m/o} = 2:1$ , 6:1, 10:1. The experimental runs were designed in a  
132 random order using face centered-central composite design (CCF-CCD) as listed in Table 3.  
133 All the experimental runs were conducted with the same procedure.

134 After the reaction completed, Fe/DS-HMS-NH<sub>2</sub> catalyst was recovered by  
135 centrifugation at 4500 rpm for 15 min, and calcination at 550  $^{\circ}\text{C}$  for 5 h. The liquid product  
136 was subjected to a two-stage liquid-liquid extraction using methanol and n-hexane  
137 sequentially for purification. Then the FAME-rich phase was separated from the by-products  
138 (i.e., glycerol, excess methanol, soap, and the other unwanted materials) and evaporated under  
139 vacuum to obtain the final FAME product. As an evaluation of the catalytic activity of Fe/DS-  
140 HMS-NH<sub>2</sub>, the yield of FAME was calculated by the following equation:

$$Y_F (\%, \text{ w/w}) = \frac{m_F p_F}{m_S} \times 100 \quad (1)$$

141 Where  $m_F$  is the mass of the final FAME product (g),  $p_F$  is the FAME purity (% , w/w)  
142 obtained from equation (2) shown in the next section, and  $m_S$  is the total mass of the DPO (g).

143

## 144 **2.5 Characterization of Fe/DS-HMS-NH<sub>2</sub> catalyst and FAME**

145 The characterization of Fe/DS-HMS-NH<sub>2</sub> was conducted using field-emission  
146 scanning electron microscopy with energy dispersive X-Ray spectroscopy (FESEM/EDX),  
147 transmission electron microscopy (TEM), nitrogen sorption, and thermogravimetric analysis

148 (TGA). The FESEM/EDX images were taken on a JEOL JSM-6500 F (Jeol Ltd., Japan)  
149 running at 15 kV with a working distance of 12.4 mm, while TEM was carried out on JEOL  
150 JEM-2100 with an accelerating voltage of 200 kV. Nitrogen sorption analysis was conducted  
151 at 77 K on a Micrometrics ASAP 2010 Sorption Analyzer. The sample was degassed at 423  
152 K prior to analysis. To determine the thermal stability and volatile component fraction of the  
153 Fe/DS-HMS-NH<sub>2</sub> catalyst, a TGA analysis was performed using TG/DTA Diamond  
154 instrument (Perkin-Elmer, Japan).

155 The final FAME product characteristics, including its kinematic viscosity (at 40°C),  
156 flashpoint, cetane number, acid value and calorific value were determined according to the  
157 standard methods of ASTM D445, ASTM D93, ASTM D613, ASTM D664, and ASTM D240,  
158 respectively. The purity of FAME ( $p_F$ ) in the final product was analyzed using a gas  
159 chromatograph (Shimadzu GC-2014) equipped with a split/splitless injector and a flame  
160 ionization detector (FID). The stationary phase used for separation was the narrow bore non-  
161 polar DB-WAX column (30 m × 0.25 mm ID × 0.25 μm film thickness, Agilent Technology,  
162 CA), and the temperature profile for the analysis was in accordance with the study conducted  
163 by Harijaya et al. (2019) [23]. Methyl heptadecanoate (MH) was used as an internal standard,  
164 while an external FAME reference (47885 U, containing 37 components FAME standard mix)  
165 was used to obtain the FAME compositional profile.  $p_F$  is calculated by the following equation:

$$p_F (\%, w/w) = \left( \frac{\sum A_F - A_{MH}}{A_{MH}} \right) \left( \frac{V_{MH} C_{MH}}{m_F} \right) \times 100 \quad (2)$$

166 Where  $\sum A_F$  is the total peak area of FAME,  $A_{MH}$  is the corresponding area of methyl  
167 heptadecanoate (MH) peak,  $V_{MH}$  is the volume of MH solution (ml),  $C_{MH}$  is the actual  
168 concentration of MH solution (g/ml), and  $m_F$  is the actual mass of the final FAME product  
169 (g).

170

## 171 **2.6 Recyclability of Fe/DS-HMS-NH<sub>2</sub>**

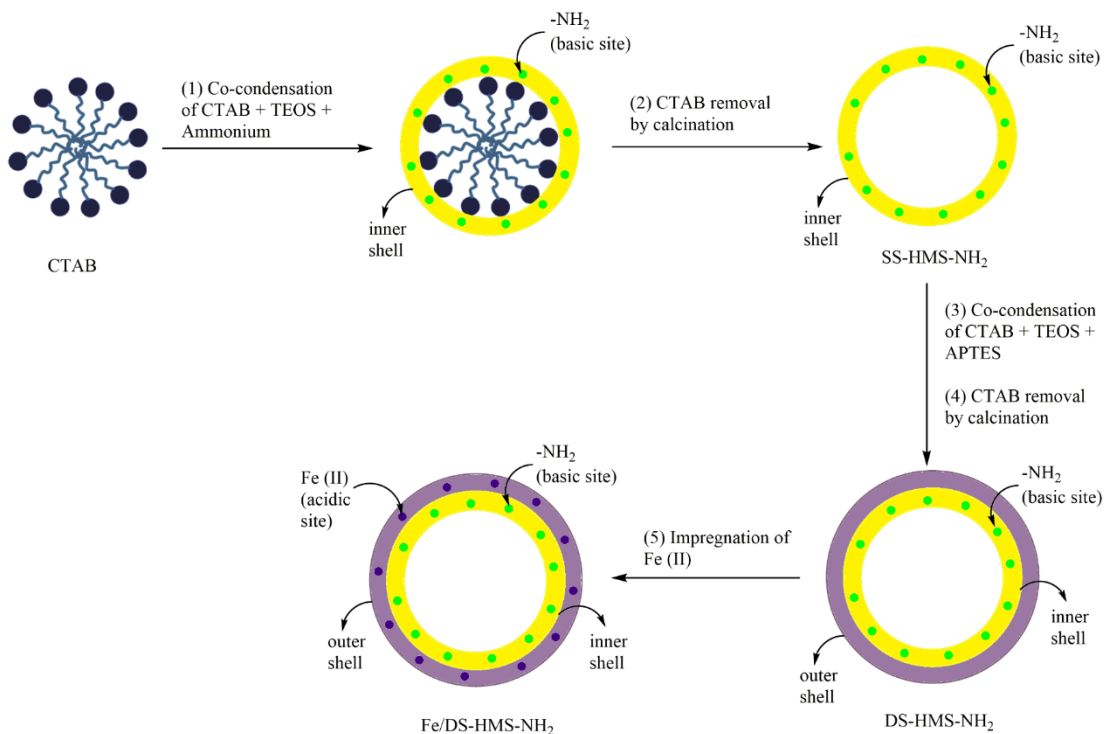
172 Fe/DS-HMS-NH<sub>2</sub> was repeatedly used for the transesterification process at the  
173 operating condition where the maximum yield of FAME was obtained. The recyclability of  
174 Fe/DS-HMS-NH<sub>2</sub> was determined by the number of repetitions until when the yield became  
175 lower than 80% (w/w). The purity and yield of FAME were analyzed according to the  
176 procedures in section 2.4-2.5. All experiments were carried out in triplicates to verify the  
177 results.

178

## 179 **3. Result and Discussions**

### 180 **3.1 The mechanism scheme of Fe/DS-HMS-NH<sub>2</sub> fabrication**

181 The Fe/DS-HMS-NH<sub>2</sub> was synthesized by a two-step co-condensation technique.  
182 The mechanism scheme in Figure 1 illustrates the fabrication route: (1) firstly, TEOS and  
183 CTAB undergo a co-condensation reaction along with the ammonium solution; (2) then  
184 CTAB, the soft template of the core, is removed by calcination, and the SS-HMS-NH<sub>2</sub> is thus  
185 formed; (3) TEOS, APTES, and CTAB undergo another co-condensation reaction on the outer  
186 surface of the SS-HMS-NH<sub>2</sub> spheres; (4) DS-HMS-NH<sub>2</sub> nanosphere is obtained by removing  
187 CTAB and APTES in calcination; (5) the divalent iron (Fe (II)) was incorporated onto the  
188 surface of DS-HMS-NH<sub>2</sub> by a traditional wet impregnation technique, and the Fe/DS-HMS-  
189 NH<sub>2</sub> nanosphere is obtained.



190

191

**Figure 1.** The mechanism scheme of Fe/DS-HMS-NH<sub>2</sub> fabrication.

192

### 193 3.2 Characterization of Fe/DS-HMS-NH<sub>2</sub> catalysts

194

Figure 2a, c–d present the SEM and TEM images of the Fe/DS-HMS-NH<sub>2</sub> catalyst

195

synthesized by the co-condensation technique. The catalyst is spherical with a uniform size at

196

*ca.* 156 nm (Figure 2a). Notably, Fe/DS-HMS-NH<sub>2</sub> is composed of two shell layers, indicated

197

by the darker color of the inner shell in Figure 2c-d. Its hollow-core structure is clearly

198

presented with the diameter of 86 nm (Figure 2d). The shell thicknesses of the inner and outer

199

layer of Fe/DS-HMS-NH<sub>2</sub>, are 22 nm and 13 nm, respectively. The impregnation of Fe (II) on

200

the surface of the silica layer was successful, evidenced from the EDX result showing a

201

percentage of 2.87% (Figure 2b). Based on the fabrication procedure, it was reasonable to

202 consider that the Fe (II) sites and basic amino sites were spatially isolated and located in  
203 different shells.

204 The textural properties of Fe/DS-HMS-NH<sub>2</sub> analyzed by the nitrogen sorption are  
205 presented in Table 1 and Figure 2e. The nitrogen adsorption and desorption isotherm of the  
206 catalyst exhibits a typical type-IV isotherm, indicating the presence of a mesoporous structure  
207 with worm-like capillary pores molded by the CTAB micelles. The pore size of the  
208 mesoporous structure is found to be 2.43 nm (Figure 2e (inset)). A steep increase of the  
209 nitrogen adsorption amount at  $p/p^0$  close to unity also suggests that there are macropores  
210 structure within the particle, corresponding to the hollow core. Similar adsorption and  
211 desorption profile also pointed out that the pores are highly accessible. The specific surface  
212 area  $S_{\text{BET}}$  obtained in this study was 782.84 m<sup>2</sup>/g, lower than the value 1100 – 1350 m<sup>2</sup>/g for  
213 a similar double shelled hollow mesoporous silica [22]. Such a discrepancy was likely due to  
214 the reason that it was strongly influenced by the shell thickness. Zhou et al. (2014) reported  
215 that when the thickness of hollow mesoporous silica nanoparticles (HMSN) increases from  
216 46 nm to 82 nm, the surface area of HMSN particles was declined from 986 m<sup>2</sup>/g to 614 m<sup>2</sup>/g  
217 [24]. Zhou et al. (2014) and Cao et al. (2011) also observed that an increase in the particle  
218 mass due to the addition of TEOS and CTAB in the synthesis of the second shell lowers the  
219 surface area, since the amount of TEOS during the fabrication is directly proportional to the  
220 thickness of the shell [24,25]. Meanwhile, the pore volume of Fe/DS-HMS-NH<sub>2</sub> (0.64 cm<sup>3</sup>/g)  
221 was found to be slightly higher than that reported by You et al. (2018) (0.61 cm<sup>3</sup>/g) [22].  
222 Based on its textural analysis, Fe/DS-HMS-NH<sub>2</sub> possesses comparable specific surface area  
223 and pore volume with those of existing heterogeneous catalysts (i.e., HMS-Al@MS-NH<sub>2</sub> [22],  
224 char-based catalyst [26],  $\gamma$ -alumina industrial-grade catalyst [27], and copper-based metal-

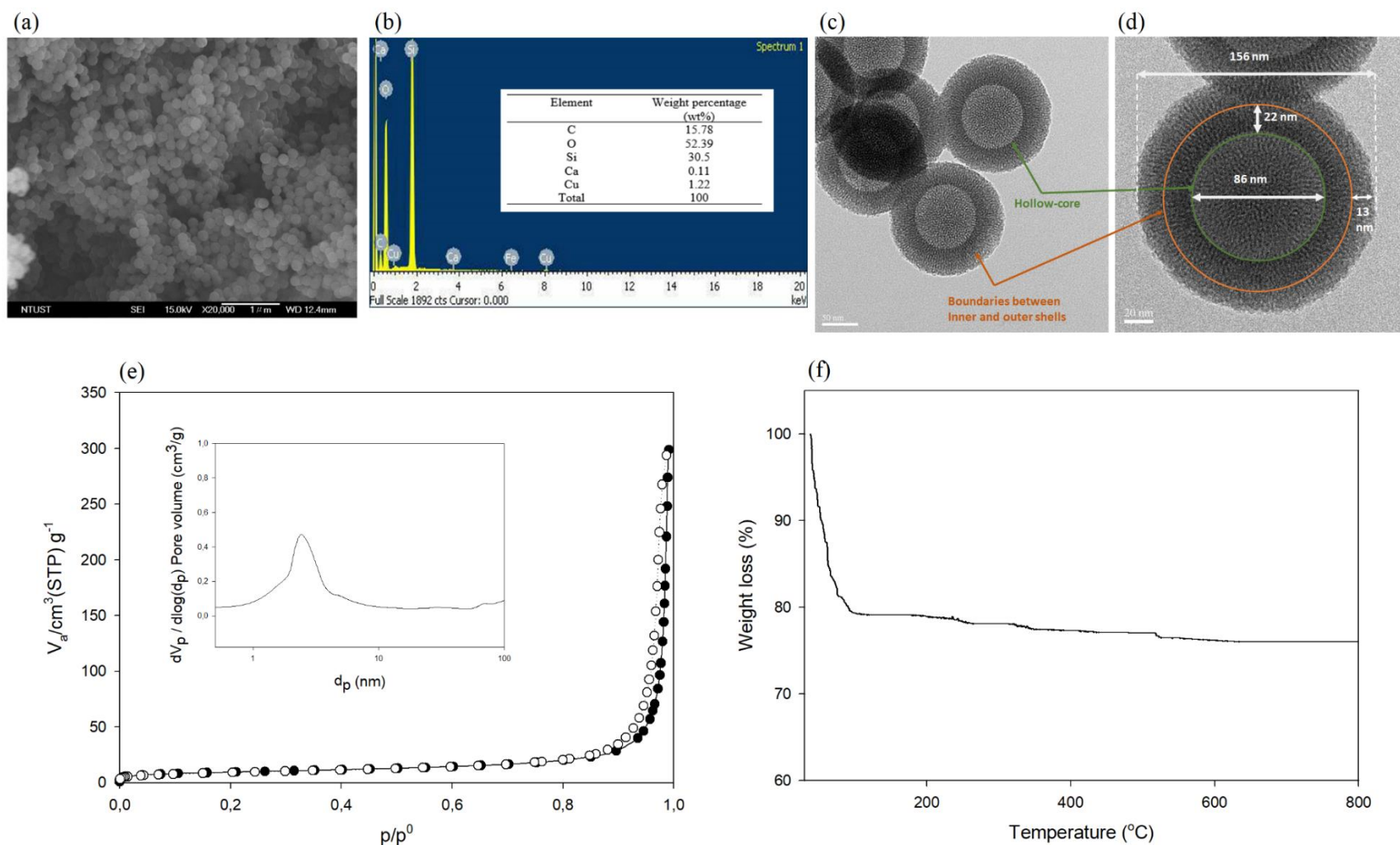
225 organic framework [28]), which usually range from 200 – 1300 cm<sup>2</sup>/g and 0.18 – 1.68 cm<sup>3</sup>/g  
226 respectively.

227 **Table 1.** Textural properties of Fe/DS-HMS-NH<sub>2</sub>.

Material	S <sub>BET</sub> (cm <sup>2</sup> /g)	Pore volume (cm <sup>3</sup> /g)	Pore size (nm)
Fe/DS-HMS-NH <sub>2</sub>	782.84	0.64	2.43

228 To demonstrate the feasibility of Fe/DS-HMS-NH<sub>2</sub> for the reactions at an elevated  
229 temperature, its thermal stability was investigated. The TGA profile in Figure 2f shows a 20%  
230 decrease in weight up to the temperature of 100°C, attributed to the removal of free moisture  
231 content. Further heating up to 800 °C does not significantly decrease the mass of Fe/DS-HMS-  
232 NH<sub>2</sub>, suggesting that the catalyst is stable at high temperatures [29]. Therefore, our Fe/DS-  
233 HMS-NH<sub>2</sub> can be considered as a promising heterogeneous catalyst for the *in-situ*  
234 esterification/transesterification reaction.

235



237 **Figure 2.** (a) SEM image, (b) Elemental composition, (c) – (d) TEM images at various magnifications, (c) BJH pore size distribution  
 238 curve, (e) Nitrogen adsorption-desorption isotherm with BJH pore size distribution curve (inset), (f) Thermogravimetric profile of the  
 239 Fe/DS-HMS-NH<sub>2</sub> catalyst.

240 **3.3 The catalytic activity of Fe/DS-HMS-NH<sub>2</sub> in the *in-situ* esterification/transesterification**  
241 **of DPO**

242 The characteristics of DPO as the raw material for biodiesel preparation are  
243 presented in Table 2. As homogenous catalysts are sensitive to impurities, the conversion of  
244 DPO to FAME for biodiesel production usually requires two reaction steps, namely acid-  
245 catalyzed esterification to lower the FFA content by converting them into FAME, and basic  
246 catalyzed transesterification to convert the acyl glycerides into FAME. However,  
247 heterogeneous catalysts can have good tolerance towards the FFA and water content in the  
248 lipid materials [10]; for Fe/DS-HMS-NH<sub>2</sub>, its two spatial shells with different active sites can  
249 facilitate the above two reactions in a one-pot process, and therefore efficient conversion from  
250 DPO to FAME is achieved in a single step.

251 **Table 2.** Characteristics of DPO.

Parameter	Value
FFA (% w/w)	5.54
Moisture Content (% w/w)	0.20
Saponification Value (mg KOH/g DPO)	234.08
Acid Value (mg KOH/g DPO)	12.04
Molecular weight (g/mol)	756.62

252  
253 Figure 3 presents the FAME yield obtained at various Fe/DS-HMS-NH<sub>2</sub> loadings  
254 at the condition of  $T = 60$  °C,  $t = 4.5$  h and  $r_{m/o} = 10:1$ . The results indicate that the yield of  
255 FAME is proportional to the number of active sites offered by the Fe/DS-HMS-NH<sub>2</sub> [30,31];  
256 therefore  $Y_F$  increases with  $m_c$  when the latter is within 6% (w/w). This agrees well with  
257 previous work on biodiesel production using different solid catalysts, e.g., pomacea sp. shell-  
258 based CaO [30], sulfonated biochar [31], and KI/mesoporous silica [32]. A maximum yield  
259 85.24% (w/w) is obtained when the catalyst loading  $m_c = 6\%$  (w/w). Further increase of the  
260 Fe/DS-HMS-NH<sub>2</sub> results in a reduced yield of FAME, which is probably due to the

261 aggregation and inconsistent dispersity of the catalyst in the reaction system of an enhanced  
 262 viscosity [33,34]. Cai et al. (2018) and Samart et al. (2010) also mentioned that excess catalyst  
 263 may also disturbed the mixing between the reactants, due to stronger adsorption of the  
 264 reactants to the catalyst [35,36].

265 **Table 3.** Experimental matrix at the optimum catalyst loading  $m_c = 6\%$  (w/w)

Run	Input Parameters			$Y_F$ (% , w/w)
	$T$ ( $^{\circ}\text{C}$ )	$t$ (h)	$r_{m/o}$	
1	60	4.5	10:1	$85.24 \pm 1.19$
2	40	0.5	10:1	$40.27 \pm 0.58$
3	40	2.5	6:1	$55.09 \pm 0.76$
4	50	4.5	6:1	$75.15 \pm 0.65$
5	50	2.5	10:1	$60.07 \pm 0.44$
6	40	0.5	2:1	$35.19 \pm 0.92$
7	40	4.5	10:1	$70.22 \pm 1.01$
8	50	2.5	2:1	$67.03 \pm 0.51$
9	60	4.5	2:1	$80.11 \pm 0.68$
10	50	2.5	6:1	$65.16 \pm 0.47$
11	50	2.5	6:1	$66.96 \pm 0.73$
12	50	2.5	6:1	$65.87 \pm 0.79$
13	50	0.5	6:1	$65.01 \pm 0.37$
14	60	4.5	6:1	$85.36 \pm 0.62$
15	50	2.5	6:1	$63.21 \pm 0.42$
16	60	0.5	10:1	$70.01 \pm 0.56$
17	50	2.5	6:1	$63.20 \pm 0.69$
18	50	2.5	6:1	$67.18 \pm 0.45$
19	60	0.5	2:1	$69.09 \pm 0.53$
20	40	4.5	2:1	$59.11 \pm 0.78$

266

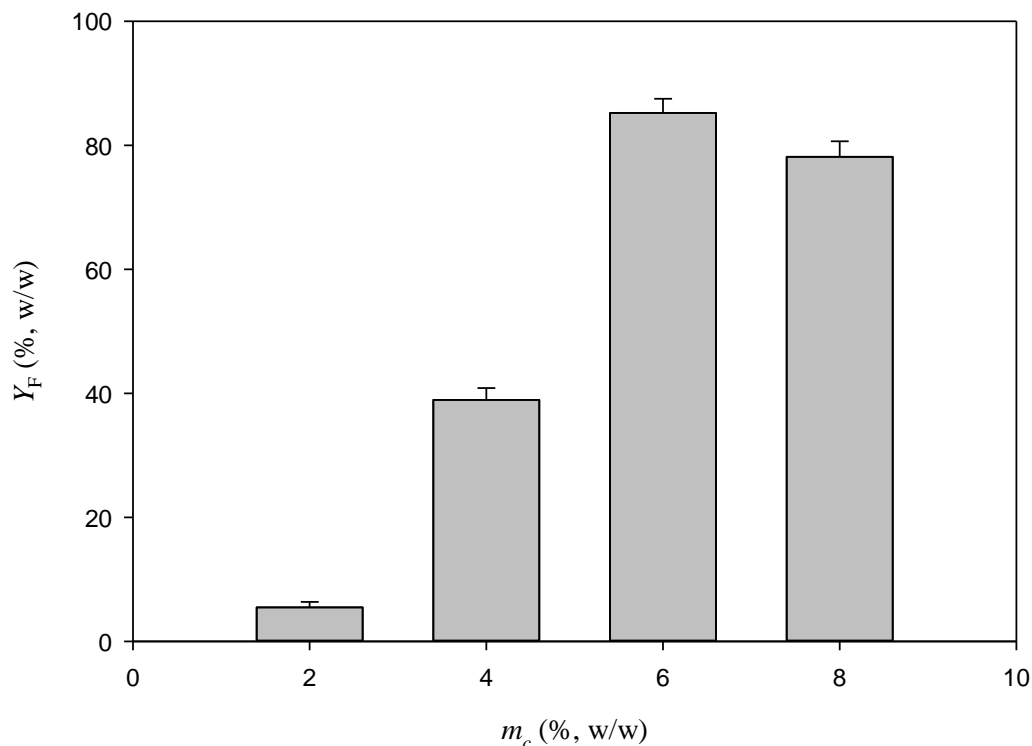
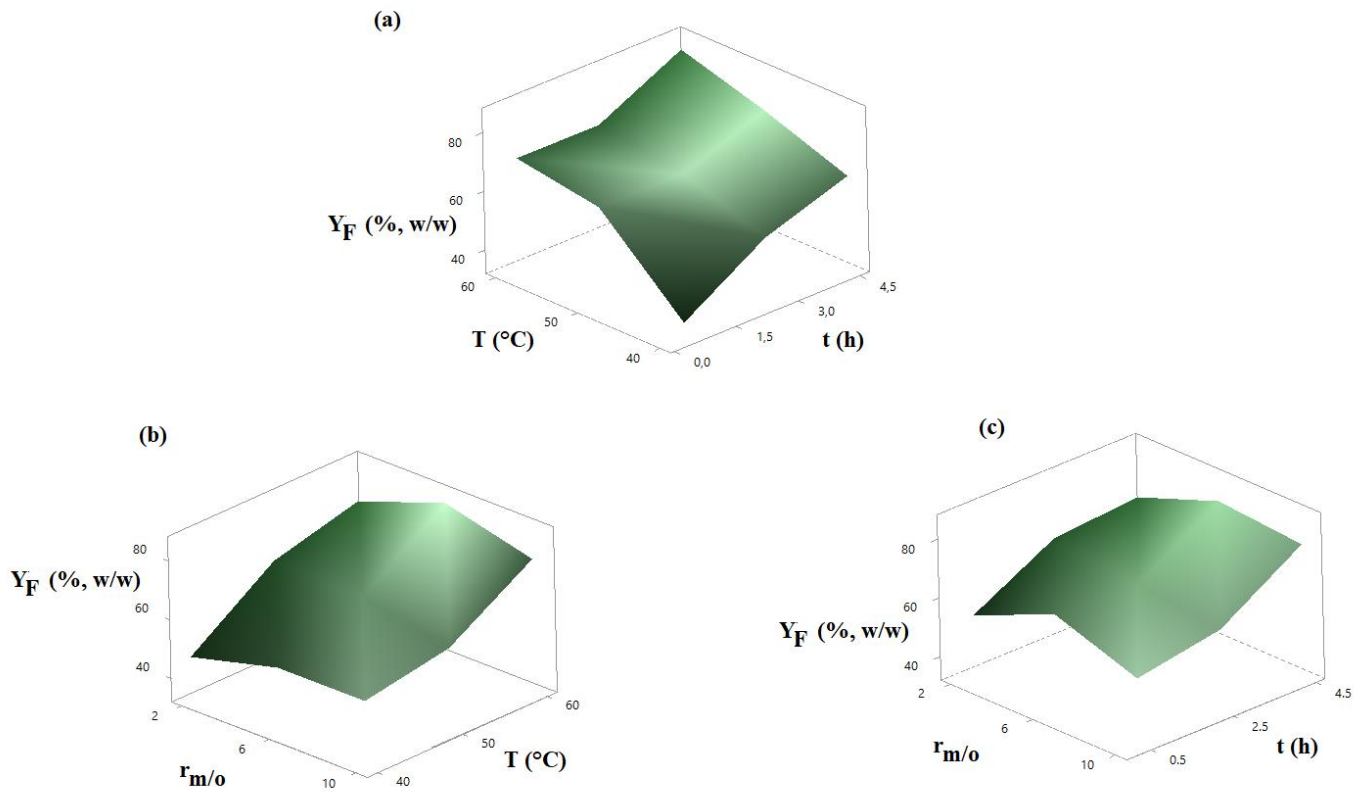


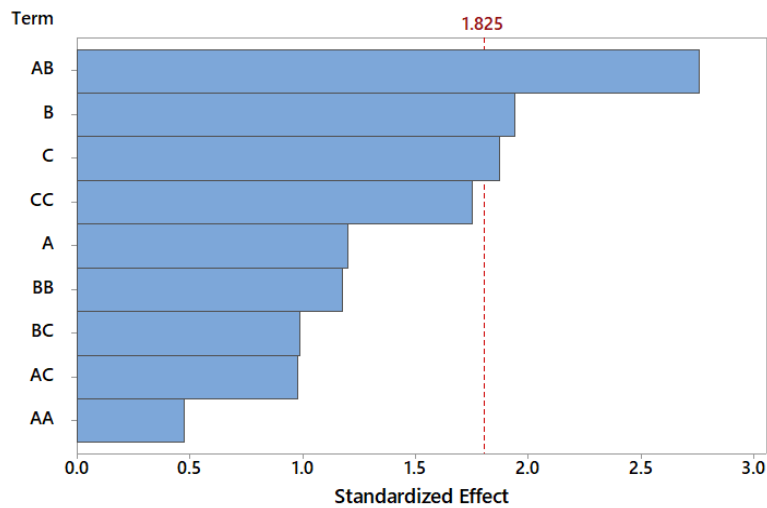
**Figure 3.** The yield of FAME at various Fe/DS-HMS-NH<sub>2</sub> loadings with the reaction condition of  $T = 60$  °C,  $t = 4.5$  h and  $r_{m/o} = 10:1$ .

267  
268  
269  
270

271 At a constant catalyst loading  $m_c = 6\%$  (w/w), Figure 4 and Table 3 present the  
272 FAME yield  $Y_F$  at various reaction time  $t$ , temperature  $T$ , and mass ratio of methanol to DPO  
273  $r_{m/o}$ . The maximum  $Y_F = 85.36\%$  (w/w) (with a purity of 97.89% (w/w)) is obtained at the  
274 condition of  $T = 60$  °C,  $t = 4.5$  h,  $r_{m/o} = 6:1$ . Based on the experimental results, the reaction  
275 time  $t$  was the most significant factor, followed by  $r_{m/o}$  and  $T$ , which is supported by the Pareto  
276 chart of the standardized effect in Figure 5 showing that  $t$ ,  $r_{m/o}$ , and the two-way interaction  
277 between  $t$  and  $T$  are the three significant parameters in the reaction system.



279 **Figure 4.** The FAME yield  $Y_F$  (% , w/w) at various (a)  $T$  and  $t$ , (b)  $T$  and  $r_{m/o}$ , and (c)  $t$  and  $r_{m/o}$ .  
 280



281 **Figure 5.** Pareto chart of the standardized effect for the biodiesel preparation with Fe/DS-  
 282 HMS-NH<sub>2</sub>, using  $Y_F$  as the response at a 95% confidence interval where A =  $T$ , B =  $t$ , C =  
 283  $r_{m/o}$ .  
 284  
 285

286           The effect of reaction temperature on the production of biodiesel using Fe/DS-  
287 HMS-NH<sub>2</sub> is shown in Figure 4a–b. An increased reaction temperature contributes to a higher  
288 yield, with the maximum achieved at 60°C, which is related to the fact that both esterification  
289 and transesterification reaction are endothermic and reversible [38,39]. At a higher reaction  
290 temperature, the kinetic energy and mobility of reactant molecules increase, promoting the  
291 collisions between the molecules and Fe/DS-HMS-NH<sub>2</sub> particles which then increases the  
292 reaction rate constant and shift the reaction towards the product [38,40]. Moreover, the mass  
293 transfer of the reactant molecules through the boundary layer of Fe/DS-HMS-NH<sub>2</sub> is also  
294 accelerated at an elevated temperature, resulting in the faster diffusion of the reactants into  
295 the pore of catalyst; hence, improving the FAME yield.

296           Specifically, Figures 4a and c show a significant increase of the FAME yield by  
297 extending the duration of the biodiesel synthesis from 0.5 h to 4.5 h, at a constant temperature  
298 or mass ratio of methanol to DPO. Longer reaction time provides sufficient time for the  
299 reactants to reach the active sites of Fe/DS-HMS-NH<sub>2</sub> through adsorption and diffusion, and  
300 convert DPO into FAME [41]. Meanwhile, prolonged duration of reaction also gives the  
301 catalyst more time to adsorb the reactant and desorb the reaction product [28]. Wei et al. (2009)  
302 also mentioned that adsorption and desorption of reactants from the catalyst is the rate-  
303 determining step in the overall reaction [42]. Therefore, allowing longer contact between the  
304 reactant molecules and the catalyst ensures high conversions of FFA and acyl glycerides to  
305 FAME.

306           Stoichiometrically, three moles of methanol are required to react with one mole of  
307 triglycerides in the transesterification reaction, while one mole of methanol is needed to react  
308 with one mole of free fatty acids in the esterification reaction [43,44]. Both reactions are  
309 known to be reversible; thus, the amount of methanol in the two reactions is usually provided

310 in excess to shift the reaction equilibrium to the product side. As seen from Figure 4b–c,  
311 having excess methanol from  $r_{m/o} = 2:1$  to  $r_{m/o} = 6:1$  contributes to a higher FAME yield,  
312 while further addition up to  $r_{m/o} = 10:1$  has no improvement. While most studies agree that  
313 excess methanol is desirable to allow more frequent interactions between the lipid and  
314 methanol triggering the formation of FAME, Pangestu et al. (2019) found that excess  
315 methanol may also accelerate the production of glycerol despite the higher yield of FAME  
316 [28]. As the esterification and transesterification are both reversible, a higher concentration  
317 of glycerol in the reaction system may induce a reverse reaction to the reactant side, creating  
318 an equilibrium between the products and reactants [28]. Hayyan et al. (2011) also reported  
319 that an excessive amount of methanol causes higher solubility of glycerol in the FAME phase  
320 that could lead to a complicated separation between biodiesel and glycerol [45]. Moreover,  
321 from the techno-economic viewpoint, the higher mass ratio of methanol to DPO also increases  
322 the material and processing cost [23,45]. Therefore, it can be concluded that the optimum  
323 level is  $r_{m/o} = 6:1$ .

324 A comparison of the FAME yield produced using Fe/DS-HMS-NH<sub>2</sub> with other  
325 existing catalysts is given in Table 4. It is notable that although the value of  $Y_F$  is higher when  
326 the refined feedstock is used as the reactant, the reaction time and the mass ratio of methanol  
327 to oil used in this study are lower. Moreover, among the studies using low-quality oil as raw  
328 lipid material, Fe/DS-HMS-NH<sub>2</sub> shows a higher catalytic activity compared with the other  
329 catalysts reported by Omar and Amin (2011), and Bala et al. (2017). This shows that Fe/DS-  
330 HMS-NH<sub>2</sub>, as a bifunctional catalyst, is able to enhance the yield of biodiesel at a comparable  
331 operating condition, which is due to its ability to convert not only triglycerides but also FFA  
332 into FAME in a one-pot system. The analysis result of the final FAME product shows that the  
333 conversion of FFA after reaction reaches 95.6%.

334 **Table 4.** The comparison of catalytic activity of several heterogeneous catalysts  
 335 for biodiesel production

Catalyst	Reactants	Operating condition	Yield (%)	References
Mesoporous zinc-doped silica	Cyanoacetate ester	$T = 60^{\circ}\text{C}$ , $t = 24$ h, $r_{m/o} = 10:1$ , $m_c = 7\%$ (w/w)	94.0	[17]
Alumina-supported KI	Refined soybean oil	$t = 8$ h, $r_{m/o} = 15:1$ , $m_c = 2.5\%$ (w/w)	96.0	[37]
Sr/ZrO <sub>2</sub>	Waste cooking oil	$T = 115.5^{\circ}\text{C}$ , $t = 169$ min, $r_{m/o} = 29:1$ (mol/mol), $m_c = 2.7\%$ (w/w)	79.7	[16]
Phosphotungstic acid-loaded KIT-5	Waste cooking oil	$T = 70^{\circ}\text{C}$ , $t = 4$ h, $r_{m/o} = 2:1$ (v/v), $m_c = 26.5\%$ (w/w)	83	[21]
Fe/DS-HMS-NH <sub>2</sub>	DPO	$T = 60^{\circ}\text{C}$ , $t = 4.5$ h, $r_{m/o} = 6:1$ (v/v), $m_c = 6\%$ (w/w)	85.36	This study

336  
 337 The fuel properties of the final FAME product are presented in Table 5. The  
 338 measurement results indicate that the product resulted in this study has comparable  
 339 combustion and flow properties with those of the commercial biodiesel. The calorific value  
 340 (45.143 MJ/kg) is also within the range required in the common petrodiesel (42-46 MJ/kg).

341 **Table 5.** Fuel properties of the final FAME product

Properties	Methods	Unit	Final FAME product	ASTM D6751
Kinematic viscosity (at 40°C)	ASTM D445	mm <sup>2</sup> /s	2.64	1.9 – 6.0
Flashpoint	ASTM D93	°C	164.2	93 min
Cetane number	ASTM D613	-	55.7	47 min
Acid value	ASTM D664	mg KOH/g	0.24	0.5 max
Calorific value	ASTM D240	MJ/kg	45.143	-

342  
 343 Meanwhile, its compositional profile is obtained by comparing the methyl ester  
 344 peaks in the chromatogram with those in the external FAME standard (47885 U, containing  
 345 37 components FAME standard mix). The 12 identified peaks are 3.05% myristoleic acid  
 346 methyl ester (C14:1), 2.37% cis-10-pentadecanoic acid methyl ester (C15:1), 35.78% palmitic  
 347 acid methyl ester (C16:0), 8.13% palmitoleic acid methyl ester (C16:1), 8.36% stearic acid

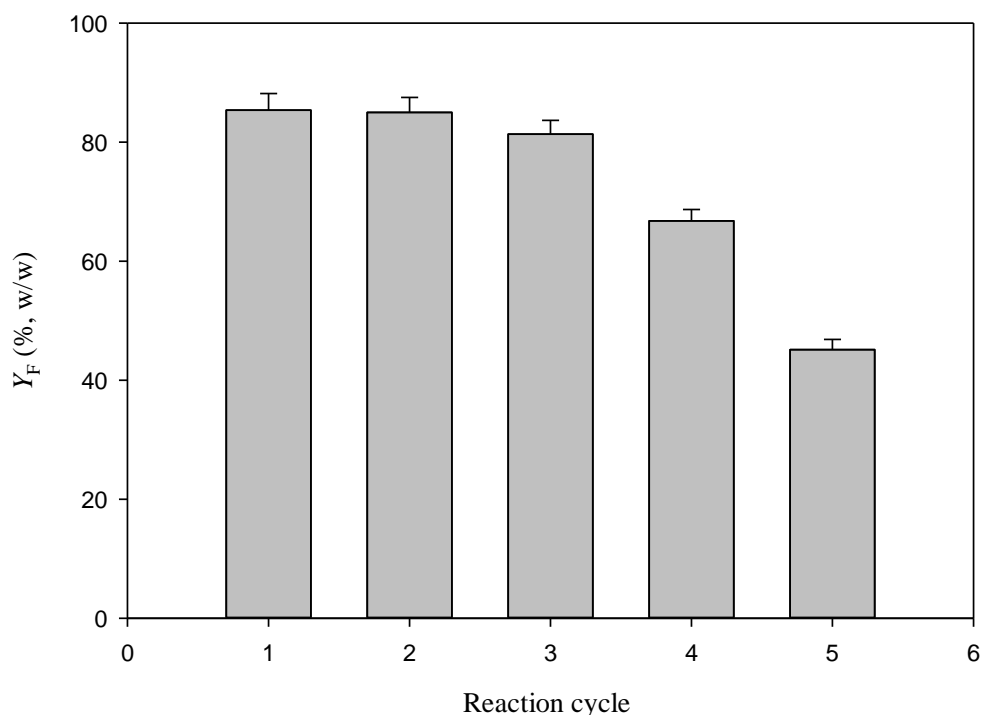
348 methyl ester (C18:0), 32.57% oleic acid methyl ester (C18:1n9c), 3.05% elaidic acid methyl  
349 ester (C18:1n9t), 1.17% cis-8,11,14-eicosatrienoic acid methyl ester (C20:3n6), 2.48%  
350 arachidonic acid methyl ester (C20:4n6), 0.52% cis-5,8,11,14,17-eicosapentaenoic acid  
351 methyl ester (C20:5n3), 1.07% erucic acid methyl ester (C22:1n9), 1.45 % cis-13,16-  
352 docosadienoic acid methyl ester (C22:2).

353

### 354 **3.4 Recyclability of Fe/DS-HMS-NH<sub>2</sub>**

355 An important feature of using heterogeneous catalysts for biodiesel preparation is  
356 its recyclability. In order to determine the recyclability of Fe/DS-HMS-NH<sub>2</sub>, several reaction  
357 cycles were conducted in series using the operating condition of  $m_c = 6\%$  (w/w),  $T = 60\text{ }^\circ\text{C}$ ,  $t$   
358  $= 4.5\text{ h}$ ,  $r_{m/o} = 6:1$ . Fe/DS-HMS-NH<sub>2</sub> was recovered following the method described in section  
359 2.4, while fresh methanol and DPO were used in every cycle. The catalytic ability of the  
360 recycled Fe/DS-HMS-NH<sub>2</sub> for *in-situ* esterification/transesterification process is presented in  
361 Figure 6. The result indicates that recycled Fe/DS-HMS-NH<sub>2</sub> can maintain a high yield of  
362 FAME above 80% (w/w) until the third cycle, close to the yield of fresh catalyst 85.36%  
363 (w/w). The purity of FAME for the first three cycles are 97.89%, 97.66% and 98.01% (w/w)  
364 respectively, higher than the commercial purity (96.5%, w/w). These results indicate that the  
365 catalytic activity of Fe/DS-HMS-NH<sub>2</sub> is maintained at a high level after regeneration. A  
366 significant drop in catalytic ability is observed from the forth cycle in Figure 6; similar  
367 performance has been reported for some other heterogeneous catalysts where three cycles  
368 seem to be an average number in term of their recyclability [46,47]. The catalytic deactivation  
369 of Fe/DS-HMS-NH<sub>2</sub> is generally due to the pore blockage caused by the contact between  
370 active sites on the catalyst surface and the deactivation-induced components, namely free  
371 glycerol, acyl glycerides, and biodiesel. Moreover, the high content of FFA in DPO also plays

372 an important role in the deactivation of Fe/DS-HMS-NH<sub>2</sub> catalyst because FFA tends to  
373 neutralize the basic sites in the inner shell of Fe/DS-HMS-NH<sub>2</sub> [48], resulting in the  
374 generation of amine-carboxylate that induces the formation of emulsion.



375  
376 **Figure 6.** Recyclability of Fe/DS-HMS-NH<sub>2</sub> in the *in-situ* esterification/transesterification  
377 of DPO.  
378

### 379 **3.5 The reaction mechanism of the *in-situ* esterification/transesterification of DPO using** 380 **Fe/DS-HMS-NH<sub>2</sub>**

381 In the preparation of biodiesel from DPO, Fe/DS-HMS-NH<sub>2</sub> acts as both acid and  
382 base catalysts to facilitate the esterification of FFA and the transesterification of acyl  
383 glycerides. The main steps for the reaction mechanism catalyzed by Fe/DS-HMS-NH<sub>2</sub> are the  
384 formation of nucleophilic alkoxides, the nucleophilic attack on the electrophilic part of the  
385 carbonyl group of the triglycerides, and electron delocalisation [49,50] as depicted in Figure  
386 7. The detailed description is as follows:

387 **Step 1:** Acyl glycerides, FFA and methanol enter the surface of catalyst through the  
388 adsorption process to reach the outer shell impregnated by the divalent iron. In this step, FFA  
389 undergoes the electron delocalization to form a carbocation and a carbanion, where the latter  
390 binds to the iron embedded on the catalyst.

391 **Step 2:** The reaction continues as the methoxide anion of methanol attacks the carbocation,  
392 whereas the hydronium cation attaches to the hydroxyl group of FFA to form water.

393 **Step 3:** Through the electron delocalization of the carbon atom, the water is released from the  
394 complex with FAME and the iron-embedded catalyst, followed by the release of FAME from  
395 the catalyst.

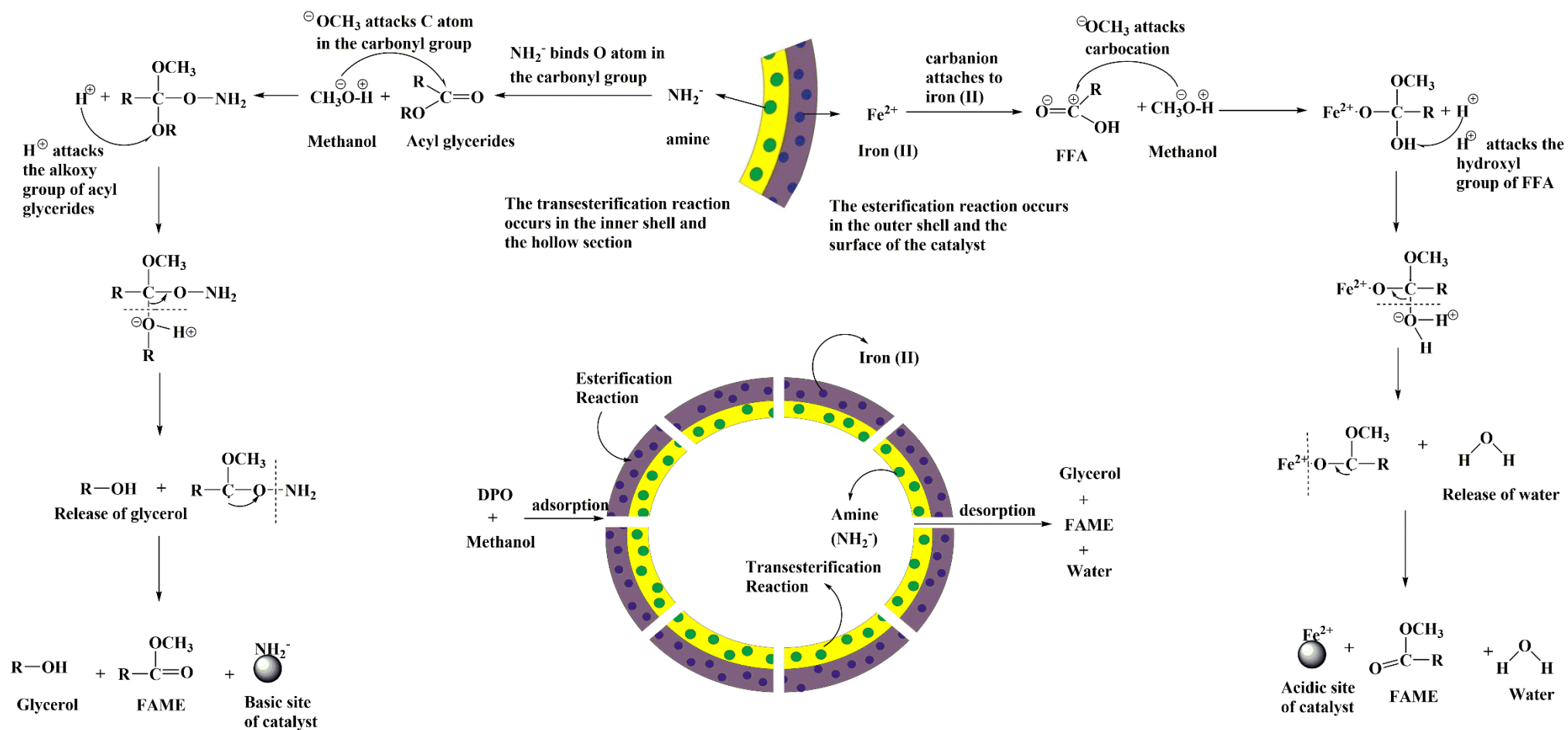
396 **Step 4:** The reaction continues when the acyl glycerides and methanol diffuse further to the  
397 amine-functionalized inner shell. The oxygen atom in the carbonyl group of acyl glycerides  
398 readily binds to the amine active sites.

399 **Step 5:** Subsequently, the methoxide anion of the methanol attacks the carbon atom in the  
400 carbonyl group of acyl glycerides, while the protonated  $H^+$  binds to the alkoxy group (RO-)  
401 of the acyl glycerides to form a complex of amine-functionalized catalyst with FAME and  
402 glycerol.

403 **Step 6:** Again, through the delocalization of oxygen in the complex, the glycerol and amine-  
404 functionalized catalyst are successively released from the complex.

405 **Step 7:** All three products, including FAME, glycerol, and water are then desorbed to the  
406 surface of the Fe/DS-HMS-NH<sub>2</sub> catalyst.

407



409 **Figure 7.** The reaction mechanism of the *in-situ* esterification/transesterification of DPO using Fe/DS-HMS-NH<sub>2</sub>.

410

## 411 **Conclusions**

412 Fe/DS-HMS-NH<sub>2</sub> is synthesized through the two-step condensation technique and  
413 successfully employed as a heterogeneous catalyst for preparing biodiesel from DPO, a lipid  
414 source with significant FFA and moisture content. The obtained Fe/DS-HMS-NH<sub>2</sub> has a  
415 uniform spherical shape with a particle size of 156 nm and hollow diameter of 86 nm. It is  
416 composed of two spatial silica shells with different active sites, and their thickness are 22 nm  
417 for the inner shell and 13 nm for the outer shell. Fe/DS-HMS-NH<sub>2</sub> has a specific surface area  
418 of 782.84 m<sup>2</sup>/g with a pore volume of 0.64 cm<sup>3</sup>/g, comparable with the existing solid catalysts.  
419 In the *in-situ* esterification/transesterification process using the Fe/DS-HMS-NH<sub>2</sub> catalyst,  
420 reaction time  $t$  is the variable with most significant influence on the yield of FAME  $Y_F$ ,  
421 followed by the reaction temperature  $T$  and the mass ratio of methanol to DPO  $r_{m/o}$ . The  
422 maximum  $Y_F$  is 85.36% (w/w), obtained at the following conditions:  $T = 60^\circ\text{C}$ ,  $t = 4.5$  h, and  
423  $r_{m/o} = 6:1$ , with a catalyst loading of 6% (w/w). Notably, Fe/DS-HMS-NH<sub>2</sub> catalyst shows a  
424 good recyclability, with the yield staying above 80% for three reaction cycles. Therefore,  
425 Fe/DS-HMS-NH<sub>2</sub> is a promising heterogeneous catalyst to obtain biodiesel from DPO or other  
426 lipid materials with high FFA and water content. Further study on (1) the extension of the  
427 catalyst lifetime by creating a technique suitable for its regeneration, and also (2) the design  
428 of a plausible route between the current research and its industrial application should be the  
429 main focus for future research expansion.

430

## 431 **Acknowledgments**

432 The authors acknowledge the funding supports from Widya Mandala Catholic University  
433 Surabaya and Indonesian Ministry of Research and Technology, through the research grant  
434 no. 2263/WM01/N/2020 and 130B/WM01.5/N/2020, respectively. We also thank Professor

435 Chun-Hu Chen, National Sun Yat Sen University, and Taiwan Tech (National Taiwan  
436 University of Science and Technology) for providing the facility for the catalyst  
437 characterizations.

438

## 439 REFERENCES

- 440 [1] P. Agung, D. Hartono, A.A. Awirya, Pengaruh Urbanisasi Terhadap Konsumsi Energi Dan  
441 Emisi CO<sub>2</sub>: Analisis Provinsi di Indonesia (The Effect of Urbanization on Energy  
442 Consumption and CO<sub>2</sub> Emissions: An Analysis of Provinces in Indonesia), *J. Ekon.*  
443 *Kuantitatif Terap.* 1 (2017) 9–17. <https://doi.org/10.24843/jekt.2017.v10.i01.p02>.
- 444 [2] A. Fitriyatus, A. Fauzi, B. Juanda, Prediction of Fuel Supply and Consumption in Indonesia  
445 with System Dynamics Model, *J. Ekon. Dan Pembang. Indones.* 17 (2018) 118–137.
- 446 [3] F.T.R. Silalahi, T.M. Simatupang, M.P. Siallagan, Biodiesel produced from palm oil in  
447 Indonesia: Current status and opportunities, *AIMS Energy.* 8 (2020) 81–101.  
448 <https://doi.org/10.3934/energy.2020.1.81>.
- 449 [4] F. Nangoy, B.C. Munthe, Indonesia President wants B30 in use by Jan 2020: cabinet  
450 secretary, Reuters. (2019).
- 451 [5] J.M. Marchetti, A summary of the available technologies for biodiesel production based on  
452 a comparison of different feedstock's properties, *Process Saf. Environ. Prot.* 90 (2012) 157–  
453 163. <https://doi.org/10.1016/j.psep.2011.06.010>.
- 454 [6] K. Suwannakarn, E. Lotero, K. Ngaosuwan, J.G. Goodwin Jr, Simultaneous free fatty acid  
455 esterification and triglyceride transesterification using a solid acid catalyst with in situ  
456 removal of water and unreacted methanol, *Ind. Eng. Chem. Res.* 48 (2009) 2810–2818.  
457 <https://doi.org/https://doi.org/10.1021/ie800889w>.
- 458 [7] Y.A. Tsigie, L.H. Huynh, S. Ismadji, A.M. Engida, Y.H. Ju, In situ biodiesel production

- 459 from wet *Chlorella vulgaris* under subcritical condition, *Chem. Eng. J.* 213 (2012) 104–108.  
460 <https://doi.org/10.1016/j.cej.2012.09.112>.
- 461 [8] P.D. Patil, V.G. Gude, A. Mannarswamy, P. Cooke, N. Nirmalakhandan, P. Lammers, S.  
462 Deng, Comparison of direct transesterification of algal biomass under supercritical  
463 methanol and microwave irradiation conditions, *Fuel.* 97 (2012) 822–831.  
464 <https://doi.org/10.1016/j.fuel.2012.02.037>.
- 465 [9] A. Kumari, P. Mahapatra, V.K. Garlapati, R. Banerjee, Enzymatic transesterification of  
466 *Jatropha* oil, *Biotechnol Biofuels.* 2 (2009) 1. <https://doi.org/10.1186/1754-6834-2-1>.
- 467 [10] R. Mat, R.A. Samsudin, M. Mohamed, A. Johari, Solid catalysts and their application in  
468 biodiesel production, *Bull. Chem. React. Eng. Catal.* 7 (2012) 142–149.  
469 <https://doi.org/10.9767/bcrec.7.2.3047.142-149>.
- 470 [11] W. Suryaputra, I. Winata, N. Indraswati, S. Ismadji, Waste capiz (*Amusium cristatum*) shell  
471 as a new heterogeneous catalyst for biodiesel production, *Renew. Energy.* 50 (2013) 795–  
472 799. <https://doi.org/10.1016/j.renene.2012.08.060>.
- 473 [12] H. Li, W. Xie, Transesterification of Soybean Oil to Biodiesel with Zn/I<sub>2</sub> Catalyst, *Catal.*  
474 *Letters.* 107 (2006) 25–30. <https://doi.org/10.1007/s10562-005-9727-9>.
- 475 [13] A.A. Refaat, A.A. Refaat, Archive of SID Different techniques for the production of  
476 biodiesel from waste vegetable oil, *Int. J. Environ. Sci. Tech.* 7 (2010) 183–213.
- 477 [14] P.L. Boey, G.P. Maniam, S.A. Hamid, Performance of calcium oxide as a heterogeneous  
478 catalyst in biodiesel production: A review, *Chem. Eng. J.* 168 (2011) 15–22.  
479 <https://doi.org/10.1016/j.cej.2011.01.009>.
- 480 [15] M.K. Lam, K.T. Lee, A.R. Mohamed, Homogeneous, heterogeneous and enzymatic  
481 catalysis for transesterification of high free fatty acid oil (waste cooking oil) to biodiesel: A  
482 review, *Biotechnol. Adv.* 28 (2010) 500–518.

- 483 <https://doi.org/10.1016/j.biotechadv.2010.03.002>.
- 484 [16] W.N.N.W. Omar, N.A.S. Amin, Biodiesel production from waste cooking oil over alkaline  
485 modified zirconia catalyst, *Fuel Process. Technol.* 92 (2011) 2397–2405.  
486 <https://doi.org/10.1016/j.fuproc.2011.08.009>.
- 487 [17] N. Pal, M. Paul, A. Bhaumik, Highly ordered Zn-doped mesoporous silica: An efficient  
488 catalyst for transesterification reaction, *J. Solid State Chem.* 184 (2011) 1805–1812.  
489 <https://doi.org/10.1016/j.jssc.2011.05.033>.
- 490 [18] W. Xie, X. Huang, Synthesis of biodiesel from soybean oil using heterogeneous KF/ZnO  
491 catalyst, *Catal. Letters.* 107 (2006) 53–59. [https://doi.org/https://doi.org/10.1007/s10562-](https://doi.org/https://doi.org/10.1007/s10562-005-9731-0)  
492 [005-9731-0](https://doi.org/https://doi.org/10.1007/s10562-005-9731-0).
- 493 [19] S.M. Coman, V.I. Parvulescu, Heterogeneous Catalysis for Biodiesel Production, *Role*  
494 *Catal. Sustain. Prod. Bio-Fuels Bio-Chemicals.* (2013) 93–136.  
495 <https://doi.org/10.1016/B978-0-444-56330-9.00004-8>.
- 496 [20] J. Santos, J. Phillips, J.A. Dumesic, Metal-support interactions between iron and titania for  
497 catalysts prepared by thermal decomposition of iron pentacarbonyl and by impregnation, *J.*  
498 *Catal.* 81 (1983) 147–167. [https://doi.org/10.1016/0021-9517\(83\)90154-9](https://doi.org/10.1016/0021-9517(83)90154-9).
- 499 [21] D.D. Bala, M. Misra, D. Chidambaram, Solid-acid catalyzed biodiesel production, part I:  
500 biodiesel synthesis from low quality feedstock, *J. Clean. Prod.* 142 (2017) 4169–4177.  
501 <https://doi.org/10.1016/j.jclepro.2016.02.128>.
- 502 [22] C. You, C. Yu, X. Yang, Y. Li, H. Huo, Z. Wang, Y. Jiang, X. Xu, K. Lin, Double-shelled  
503 hollow mesoporous silica nanosphere as acid-base bifunctional catalyst for cascade  
504 reactions, *New J. Chem.* 42 (2018) 4095–4101. <https://doi.org/10.1039/C7NJ04670G>.
- 505 [23] F.H. Santosa, L. Laysandra, F.E. Soetaredjo, S.P. Santoso, S. Ismadji, M. Yuliana, A facile  
506 noncatalytic methyl ester production from waste chicken tallow using single step subcritical

- 507           methanol: Optimization study, *Int. J. Energy Res.* 43 (2019) 8852–8863.  
508           <https://doi.org/10.1002/er.4844>.
- 509 [24] X. Zhou, X. Cheng, W. Feng, K. Qiu, L. Chen, W. Nie, Z. Yin, X. Mo, H. Wang, C. He,  
510           Synthesis of hollow mesoporous silica nanoparticles with tunable shell thickness and pore  
511           size using amphiphilic block copolymers as core templates, *Dalt. Trans.* 43 (2014) 11834–  
512           11842. <https://doi.org/10.1039/c4dt01138d>.
- 513 [25] S. Cao, Z. Zhao, X. Jin, W. Sheng, S. Li, Y. Ge, M. Dong, W. Wu, L. Fang, Unique double-  
514           shelled hollow silica microspheres: Template-guided self-assembly, tunable pore size, high  
515           thermal stability, and their application in removal of neutral red, *J. Mater. Chem.* 21 (2011)  
516           19124–19131. <https://doi.org/10.1039/c1jm13011k>.
- 517 [26] N.B. Klinghoffer, M.J. Castaldi, A. Nzihou, Catalyst Properties and Catalytic Performance  
518           of Char from Biomass Gasification, *Ind. Eng. Chem. Res.* 51 (2012) 13113–13122.  
519           <https://doi.org/10.1021/ie3014082>.
- 520 [27] M. Zakeri, A. Samimi, M. Shafiee Afarani, A. Salehirad, Effects of porosity and pore size  
521           distribution on mechanical strength reliability of industrial-scale catalyst during preparation  
522           and catalytic test steps, *Part. Sci. Technol.* 36 (2018) 96–103.  
523           <https://doi.org/10.1080/02726351.2016.1220437>.
- 524 [28] T. Pangestu, Y. Kurniawan, F.E. Soetaredjo, S.P. Santoso, W. Irawaty, M. Yuliana, S.B.  
525           Hartono, S. Ismadji, The synthesis of biodiesel using copper based metal-organic  
526           framework as a catalyst, *J. Environ. Chem. Eng.* 7 (2019) 103277.  
527           <https://doi.org/10.1016/j.jece.2019.103277>.
- 528 [29] N. Rahmat, N. Sadon, M.A. Yusof, Thermogravimetric Analysis (TGA) Profile at Different  
529           Calcination Conditions for Synthesis of PTES-SBA-15, *Am. J. Appl. Sci.* 14 (2017) 938–  
530           944. <https://doi.org/10.3844/ajassp.2017.938.944>.

- 531 [30] Y.Y. Margaretha, H.S. Prastyo, A. Ayucitra, S. Ismadji, Calcium oxide from pomacea sp.  
532 shell as a catalyst for biodiesel production, *Int. J. Energy Environ. Eng.* 3 (2012) 1–9.  
533 <https://doi.org/10.1186/2251-6832-3-33>.
- 534 [31] A.M. Dekhoda, A.H. West, N. Ellis, Biochar based solid acid catalyst for biodiesel  
535 production, *Appl. Catal. A Gen.* 382 (2010) 197–204.  
536 <https://doi.org/10.1016/j.apcata.2010.04.051>.
- 537 [32] C. Samart, P. Sreetongkittikul, C. Sookman, Heterogeneous catalysis of transesterification  
538 of soybean oil using KI/mesoporous silica, *Fuel Process. Technol.* 90 (2009) 922–925.  
539 <https://doi.org/10.1016/j.fuproc.2009.03.017>.
- 540 [33] G. Baskar, S. Soumiya, Production of biodiesel from castor oil using iron (II) doped zinc  
541 oxide nanocatalyst, *Renew. Energy.* 98 (2016) 101–107.  
542 <https://doi.org/https://doi.org/10.1016/j.renene.2016.02.068>.
- 543 [34] B. Gurunathan, A. Ravi, Biodiesel production from waste cooking oil using copper doped  
544 zinc oxide nanocomposite as heterogeneous catalyst, *Bioresour. Technol.* 188 (2015) 124–  
545 127. <https://doi.org/https://doi.org/10.1016/j.biortech.2015.01.012>.
- 546 [35] J. Cai, Q.Y. Zhang, F.F. Wei, J.S. Huang, Y.M. Feng, H.T. Ma, Y. Zhang, Preparation of  
547 Copper (II) Containing Phosphomolybdic Acid Salt as Catalyst for the Synthesis of  
548 Biodiesel by Esterification, *J Oleo Sci.* 67 (2018) 427–432.  
549 <https://doi.org/10.5650/jos.ess17208>.
- 550 [36] C. Samart, C. Chaiya, P. Reubroycharoen, Biodiesel production by methanolysis of soybean  
551 oil using calcium supported on mesoporous silica catalyst, *Energy Convers. Manag.* 51  
552 (2010) 1428–1431. <https://doi.org/10.1016/j.enconman.2010.01.017>.
- 553 [37] W. Xie, H. Li, Alumina-supported potassium iodide as a heterogeneous catalyst for  
554 biodiesel production from soybean oil, *J. Mol. Catal. A Chem.* 255 (2006) 1–9.

- 555 <https://doi.org/https://doi.org/10.1016/j.molcata.2006.03.061>.
- 556 [38] M. Farooq, A. Ramli, Biodiesel production from low FFA waste cooking oil using  
557 heterogeneous catalyst derived from chicken bones, *Renew. Energy*. 76 (2015) 362–368.  
558 <https://doi.org/10.1016/j.renene.2014.11.042>.
- 559 [39] R. Alenezi, G.A. Leeke, J.M. Winterbottom, R.C.D. Santos, A.R. Khan, Esterification  
560 kinetics of free fatty acids with supercritical methanol for biodiesel production, *Energy*  
561 *Convers. Manag.* 51 (2010) 1055–1059. <https://doi.org/10.1016/j.enconman.2009.12.009>.
- 562 [40] M. Farooq, A. Ramli, D. Subbarao, Biodiesel production from waste cooking oil using  
563 bifunctional heterogeneous solid catalysts, *J. Clean. Prod.* 59 (2013) 131–140.  
564 <https://doi.org/10.1016/j.jclepro.2013.06.015>.
- 565 [41] I. Amalia Kartika, M. Yani, D. Ariono, P. Evon, L. Rigal, Biodiesel production from  
566 jatropha seeds: Solvent extraction and in situ transesterification in a single step, *Fuel*. 106  
567 (2013) 111–117. <https://doi.org/10.1016/j.fuel.2013.01.021>.
- 568 [42] Z. Wei, C. Xu, B. Li, Application of waste eggshell as low-cost solid catalyst for biodiesel  
569 production, *Bioresour. Technol.* 100 (2009) 2883–2885.  
570 <https://doi.org/10.1016/j.biortech.2008.12.039>.
- 571 [43] A. Demirbas, Biodiesel from waste cooking oil via base-catalytic and supercritical methanol  
572 transesterification, *Energy Convers. Manag.* 50 (2009) 923–927.  
573 <https://doi.org/10.1016/j.enconman.2008.12.023>.
- 574 [44] I.A. Reşitoğlu, A. Keskin, M. Gürü, The optimization of the esterification reaction in  
575 biodiesel production from trap grease, *Energy Sources, Part A Recover. Util. Environ. Eff.*  
576 34 (2012) 1238–1248. <https://doi.org/10.1080/15567031003792395>.
- 577 [45] A. Hayyan, F.S. Mjalli, M.A. Hashim, M. Hayyan, I.M. AlNashef, S.M. Al-Zahrani, M.A.  
578 Al-Saadi, Ethanesulfonic acid-based esterification of industrial acidic crude palm oil for

- 579 biodiesel production, *Bioresour Technol.* 102 (2011) 9564–9570.  
580 <https://doi.org/10.1016/j.biortech.2011.07.074>.
- 581 [46] S.L. Lee, Y.C. Wong, Y.P. Tan, S.Y. Yew, Transesterification of palm oil to biodiesel by  
582 using waste obtuse horn shell-derived CaO catalyst, *Energy Convers. Manag.* 93 (2015)  
583 282–288. <https://doi.org/10.1016/j.enconman.2014.12.067>.
- 584 [47] W. Xie, T. Wang, Biodiesel production from soybean oil transesterification using tin oxide-  
585 supported WO<sub>3</sub> catalysts, *Fuel Process. Technol.* 109 (2013) 150–155.  
586 <https://doi.org/10.1016/j.fuproc.2012.09.053>.
- 587 [48] M. Kouzu, J.S. Hidaka, Transesterification of vegetable oil into biodiesel catalyzed by CaO:  
588 A review, *Fuel*. 93 (2012) 1–12. <https://doi.org/10.1016/j.fuel.2011.09.015>.
- 589 [49] D.M. Marinković, M. V. Stanković, A. V. Veličković, J.M. Avramović, M.R. Miladinović,  
590 O.O. Stamenković, V.B. Veljković, D.M. Jovanović, Calcium oxide as a promising  
591 heterogeneous catalyst for biodiesel production: Current state and perspectives, *Renew.*  
592 *Sustain. Energy Rev.* 56 (2016) 1387–1408. <https://doi.org/10.1016/j.rser.2015.12.007>.
- 593 [50] A.K. Endalew, Y. Kiros, R. Zanzi, Inorganic heterogeneous catalysts for biodiesel  
594 production from vegetable oils, *Biomass and Bioenergy*. 35 (2011) 3787–3809.  
595 <https://doi.org/10.1016/j.biombioe.2011.06.011>.

596

## **CREDIT AUTHOR STATEMENT**

- Stefanus Kevin Suryajaya - Conceptualization, methodology, investigation, software, writing – original draft
- Yohanes Ricky Mulyono - Conceptualization, methodology, investigation, software, writing – original draft
- Shella Permatasari Santoso - Conceptualization, data curation, supervision
- Maria Yuliana - Conceptualization, resources, visualization, writing-review and editing, supervision
- Alfin Kurniawan - Investigation, resources
- Aning Ayucitra - Investigation, validation
- Yueting Sun - Writing-review and editing
- Sandy Budi Hartono - Software, validation
- Felycia Edi Soetaredjo - Resources, visualization
- Suryadi Ismadji - Resources, validation

**Declaration of interests**

The authors declare that they have no known competing financial interests or personal relationships that could have appeared to influence the work reported in this paper.

The authors declare the following financial interests/personal relationships which may be considered as potential competing interests:



Maria Yuliana &lt;mariayuliana@ukwms.ac.id&gt;

---

**Your Submission RENE-D-20-04164R2**

1 message

---

**Renewable Energy** <em@editorialmanager.com>  
Reply-To: Renewable Energy <rene@elsevier.com>  
To: Maria Yuliana <mariayuliana@ukwms.ac.id>

Fri, Jan 22, 2021 at 7:33 PM

Ms. Ref. No.: RENE-D-20-04164R2

Title: IRON (II) IMPREGNATED DOUBLE-SHELLED HOLLOW MESOPOROUS SILICA AS ACID-BASE BIFUNCTIONAL CATALYST FOR THE CONVERSION OF LOW-QUALITY OIL TO METHYL ESTERS

Renewable Energy

Dear Dr. Yuliana,

I am pleased to inform you that your paper "IRON (II) IMPREGNATED DOUBLE-SHELLED HOLLOW MESOPOROUS SILICA AS ACID-BASE BIFUNCTIONAL CATALYST FOR THE CONVERSION OF LOW-QUALITY OIL TO METHYL ESTERS" has been accepted for publication in Renewable Energy.

Your accepted manuscript will now be transferred to our production department and work will begin on creation of the proof. If we need any additional information to create the proof, we will let you know. If not, you will be contacted again in the next few days with a request to approve the proof and to complete a number of online forms that are required for publication.

Effective peer review is essential to uphold the quality and validity of individual articles, but also the overall integrity of the journal. We would like to remind you that for every article considered for publication, there are usually at least 2 reviews required for each review round, and it is critical that scientists wishing to publish their research also be willing to provide reviews to similarly enable the peer review of papers by other authors. Please accept any review assignment within your expertise area(s) we may address to you and undertake reviewing in the manner in which you would hope your own paper to be reviewed.

Thank you very much for expressing your interest in Renewable Energy.

Sincerely,  
Soteris Kalogirou, D.Sc.  
Editor-in-Chief  
Renewable Energy

---

In compliance with data protection regulations, you may request that we remove your personal registration details at any time. (Use the following URL: <https://www.editorialmanager.com/rene/login.asp?a=r>). Please contact the publication office if you have any questions.

---

**Share your article [RENE\_14846] published in Renewable Energy**

9 messages

**Elsevier - Article Status** <Article\_Status@elsevier.com>

Sun, Jan 31, 2021 at 5:05 PM

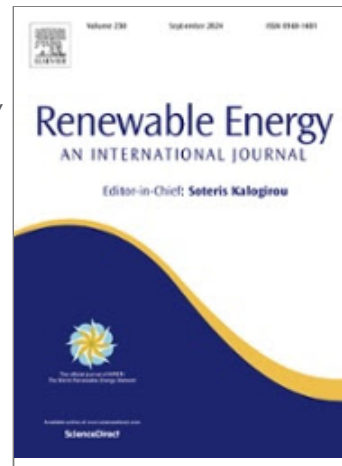
To: mariayuliana@ukwms.ac.id

**ELSEVIER****Share your article!**

Dear Dr. Yuliana,

We are pleased to let you know that the final version of your article *IRON (II) IMPREGNATED DOUBLE-SHELLED HOLLOW MESOPOROUS SILICA AS ACID-BASE BIFUNCTIONAL CATALYST FOR THE CONVERSION OF LOW-QUALITY OIL TO METHYL ESTERS* is now available online, containing full bibliographic details.

To help you access and share this work, we have created a Share Link – a personalized URL providing **50 days' free access** to your article. Anyone clicking on this link before March 22, 2021 will be taken directly to the final version of your article on ScienceDirect, which they are welcome to read or download. No sign up, registration or fees are required.



Your personalized Share Link:  
<https://authors.elsevier.com/a/1cVcS3QJ-dhnos>

Click on the icons below to share with your network:



We encourage you to use this Share Link to download a copy of the article for your own archive. The URL is also a quick and easy way to share your work with colleagues, co-authors and friends. And you are welcome to add the Share Link to your homepage or social media profiles, such as Facebook and Twitter.

You can find out more about Share Links on [Elsevier.com](https://www.elsevier.com).

Did you know, as an author, you can use your article for a wide range of scholarly, non-commercial purposes, and share and post your article online in a variety of ways? For more information visit [www.elsevier.com/sharing-articles](https://www.elsevier.com/sharing-articles).

Kind regards,  
Elsevier Researcher Support

**Increase your article's impact**Our [Get Noticed](#) guide contains a range of practical tips and advice to help you maximize visibility of your